REPORT DOCUMENTATION PAGE

Form Approved OMB No. 0704-188

1. AGENCY USE ONLY *(Leave blank)*	2. REPORT DATE	3. REPORT TYPE AND DATES COVERED
		FINAL 4/28/89-PRESENT

4. TITLE AND SUBTITLE
Some Strip Contributions to Transducer Design and Analysis

5. FUNDING NUMBERS
C- N00014-93-D-6032
PE- 63504N
TA- S0223
WU- DN780-137

6. AUTHOR(S)
David L. Carson *
Alan K. Walden

7. PERFORMING ORGANIZATION NAME(S) AND ADDRESS(ES)
NAVAL RESEARCH LABORATORY
UNDERWATER SOUND REFERENCE DETACHMENT
P.O. BOX 568337
ORLANDO, FL 32856-8337

8. PERFORMING ORGANIZATION REPORT NUMBER
NRL/PU/5917--95-292

9. SPONSORING/MONITORING AGENCY NAME(S) AND ADDRESS(ES)
NAVAL SEA SYSTEMS COMMAND
WASHINGTON, DC 20362-5101

10.SPONSORING/MONITORING AGENCY REPORT NUMBER

11. SUPPLEMENTARY NOTES
* TEXAS RESEARCH INSTITUTE, INC, 9063 BEE CAVES ROAD, AUSTIN, TX 78733-6201

12a. DISTRIBUTION/AVAILABILITY STATEMENT
APPROVED FOR PUBLIC RELEASE; DISTRIBUTION UNLIMITED

12b. DISTRIBUTION CODE

13. ABSTRACT *(Maximum 200 words)*

This book explains certain transducer design developments resulting from the Sonar Transducer Reliability Improvement Program, such as the Simplified Guidance Model for k_{33}-mode transducer elements. The model's usefulness in understanding and explaining certain transducer design techniques for a 33-mode projector element and array is discussed. The model is augmented and applied such that it may be used 1) as an educational tool to help inexperienced transducer design engineers acquire some subject knowledge, skills and insight; and 2) to illustrate some pertinent design and analysis aids. Section 2 establishes a basis for developing these design and analysis tools by providing one illustration of a systematic General Design Approach. In Section 3, one aspect of this approach is further clarified with a specific example. Section 4 considers the design options available to the engineer when all of the transducer design parameters except the ceramic stack assembly and the fiberglass tuning ring are fixed. In Section 5, the model is augmented to include the entire transducer and applied to derive and illustrate certain design aids. Appendix A contains many derivations used in the main text. Appendix B presents computer program predictions for selected examples in Section 5.

14. SUBJECT TERMS	15. NUMBER OF PAGES
Sonar transducers, Tonpilz transducers, k_{33}-mode transducers, Piezoelectric ceramic, Ceramic stack assembly, Design optimization	16. PRICE CODE

17. SECURITY CLASSIFICATION OF REPORT	18. SECURITY CLASSIFICATION OF THIS PAGE	19. SECURITY CLASSIFICATION OF ABSTRACT	20. LIMITATION OF ABSTRACT
UNCLASSIFIED	UNCLASSIFIED	UNCLASSIFIED	UL

NSN 7540-01-280-5500
Standard Form 298 (Rev 2-89)
Prescribed by ANSI Std 239-18
298-102

BLANK PAGE

Naval Research Laboratory
Underwater Sound Reference Detachment
P.O. Box 568337, Orlando, FL 32856-8337

NRL/FR/5917--95-292

SOME STRIP CONTRIBUTIONS TO TRANSDUCER DESIGN AND ANALYSIS

DAVID L. CARSON
Texas Research Institute
Austin, TX

ALAN K. WALDEN
Naval Research Laboratory
Underwater Sound Reference Detachment
Orlando, FL

June 23, 1995

CONTENTS

FIGURES

Appendix B:

TABLES

LIST OF SYMBOLS

a	=	radius of circular piston
A_c	=	electroded area of one side of a ceramic ring
A_f	=	area of one side of the fiberglass tuning ring
C	=	compliance of the ceramic stack in short circuit configuration
C'	=	compliance of the ceramic stack in open circuit configuration
C_e	=	effective compliance of the ceramic stack assembly in short circuit configuration
C_e'	=	effective compliance of the ceramic stack assembly in open circuit configuration
C_F	=	compliance of the fiberglass tuning ring
C_T	=	low frequency capacitance of one ceramic ring
d_{33}	=	piezoelectric charge coefficient
E, E_i	=	applied electrical voltage
ε	=	electric field
ε_o	=	permittivity of free space
ε_3^T	=	dielectric constant of ceramic
f_r	=	force on the radiating face
f	=	linear frequency
f_L	=	lower frequency end point used in the Fixed End Point Analysis
f_U	=	upper frequency end point used in the Fixed End Point Analysis
f_m	=	in-air resonance frequency
f_n	=	in-air anti-resonance frequency
f_e	=	in-water resonance frequency
F_H	=	force at the interface between the fiberglass washer and the radiating head assembly
g_{33}	=	piezoelectric voltage coefficient
$H_1(x)$	=	Struve function of the first order
I, I_i	=	input electrical current
$J_1(x)$	=	Bessel function of the first order
k	=	Acoustic wavenumber

K_{33} = piezoelectric coupling coefficient

L = length of the ceramic stack

l_c = length of one ceramic ring

l_f = thickness of the fiberglass tuning rings

m = effective mass of the head mass assembly which includes the effect of radiation loading

m_H = mass of the radiating head assembly

m_T = mass of the tail assembly

N = number of ceramic rings in the ceramic stack assembly

P_a = radiated acoustic power

P_e = input electrical power

R = radiation resistance

r = the constant of proportionality for the radiation resistance assuming a linear ω dependence

S_{33}^D = elastic constant measured in short circuit configuration with constant charge density

S_{33}^E = elastic constant measured in open circuit configuration with constant voltage

V_H = transducer head velocity

X = radiation reactance

x = the constant of proportionality for the radiation reactance assuming a linear ω dependence

Z_{ec} = mechanical impedance of the transducer in the short circuit configuration

Z_{ic} = mechanical impedance of the transducer in the open circuit configuration

Z_H = mechanical impedance presented into the CSA by the head mass assembly

Z_i = input electrical impedance

Z_r = transducer radiation impedance

Z_T = mechanical impedance presented into the CSA by the tail mass assembly

ω = angular frequency, $2\pi f$

ω_m = in-air angular resonance frequency

ω_n = in-air angular anti-resonance frequency

ω_{e0} = angular frequency at which the in-water phase between E and V_H is 0 degrees

ω_{i90} = angular frequency at which the in-water phase between E and V_H is 90 degrees

ω_{ev} = voltage velocity control angular frequency

ω_{iv} = current velocity control angular frequency

ω_i = in-water angular anti-resonance frequency

ω_e = in-water angular resonance frequency

ω_L = lower angular frequency end point used in the Fixed End Point Analysis

ω_U = upper angular frequency end point used in the Fixed End Point Analysis

SOME STRIP CONTRIBUTIONS TO TRANSDUCER DESIGN AND ANALYSIS

1.0 INTRODUCTION

Certain developments in the Sonar Transducer Reliability Improvement Program (STRIP) have applications beyond those already used and documented in the STRIP progress reports. One such development was the Simplified Guidance Model (SGM) for k_{33} mode longitudinal vibrator transducer elements [1]. For example, the SGM can be used to deduce, understand, and explain certain transducer design aids and design techniques which then may be used as tools for reducing the cost and time required to complete a 33-mode longitudinal vibrator projector element and array design. There may not be many more totally new large budget k_{33} mode transducer array design developments, but there probably will be major design modifications of present fleet arrays of these types of elements. There will also be important problems to solve concerning reproducibility and reliability of present fleet arrays of k_{33} mode transducers. Thus, there exists a continuing need to be able to effectively and efficiently modify existing sonar transducer array designs.

At the same time, there is a need to efficiently and effectively educate new sonar transducer array engineers. It is important not to lose the knowledge, skill, and insight base that resides with the engineers who are presently able to solve problems and supervise the procurement of reliable near replicas of present k_{33} mode transducers. Without a proper transfer of design and analysis skills, the Navy might find itself in the position of "reinventing the wheel" in this area. Much of the expertise developed by the present transducer array engineers was gained by studying performance predictions made using elaborate computer programs. The SGM may be augmented in such a way that, using only paper and pencil, an engineer may obtain much of the same insight and information as was gained from the elaborate, expensive computer-aided calculations. The same augmented SGM could be easily programmed on a personal computer as an inexpensive teaching aid. In fact, Appendix B presents such computer program prediction results for three selected examples taken from Sec. 5 and concludes that:

a. The corresponding derivations and design insights of Sec. 5 were fully consistent with subject computer predictions. This provided a strong indication that there were no significant errors in the associated "pencil and paper" derivations of Sec. 5.

b. The predictions provided additional clarity and understanding concerning the "design aid insights" as originally developed from the "pencil and paper" derivations of Sec. 5.

The goal of this document is to augment and apply the SGM in such a way as to be useful in satisfying all of the above indicated future needs. Some specific objectives are: 1) Augment the SGM so that it may be used as an educational tool to help new transducer array engineers acquire some of the

Manuscript approved 31 July 1995

subject knowledge, skills, and insight; and 2) Apply the augmented SGM to derive and illustrate some of the pertinent design and analysis aids.

In Sec. 2, a basis is established for developing these design and analysis tools by providing one specific illustration of a systematic General Design Approach (GDA). In Sec. 3, one aspect of the GDA; namely, the Trial Design Generation Scheme (TDGS), is further clarified with a specific example. Then, in the context of this GDA, the design and analysis aid tools are developed and explained. In Sec. 4, we consider the design options available to the engineer when all of the transducer design parameters except those for the ceramic stack assembly and a fiberglass tuning ring are fixed. Finally, in Sec. 5, the SGM is augmented to include the entire transducer and applied to derive and illustrate certain design and analysis aids. To keep the train of thought in the discussion fairly well focused, many of the derivations were placed in an Appendix A. Also, Appendix B presents computer program prediction results for three selected examples taken from Sec. 5.

2.0 GENERAL DESIGN APPROACH

The General Design Approach (GDA) is a three-step iterative procedure for projector transducer element and array design as suggested by Fig. 2-1.

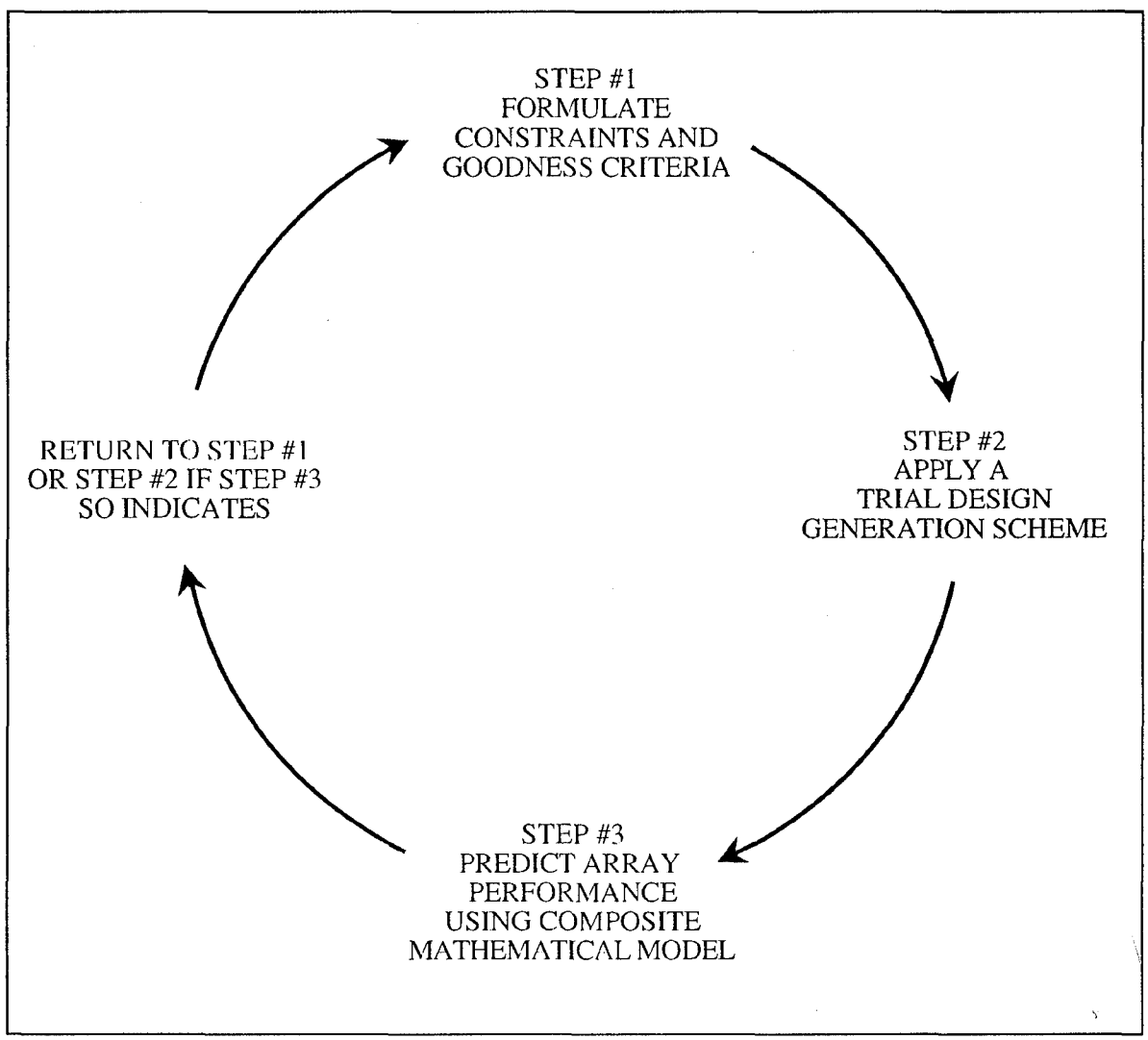

Fig. 2-1 — The general design approach is a three step iterative procedure for projector transducer element and array design

In Step 1 of Fig. 2-1 the design engineer attempts to specify all important design constraints and goodness (desired performance) criteria for the array, including those for the transducer element. Step 1 is neither simple nor unalterable. For example, each iteration through these three steps provides new understanding, and, thus, often indicates a need for further modification of the array design constraints and goodness criteria. In Step 2, the Trial Design Generation Scheme (TDGS) is developed. The TDGS is a systematic, practical scheme for developing trial transducer array element designs which reflect and satisfy the array constraints and goodness criteria of Step 1. The TDGS may include various approximations which facilitate the rapid, if not yet complete, attainment of specific transducer element

performance characteristics. The STRIP has developed a number of tools which aid in the rapid identification of an appropriate design. The STRIP design development procedures are further described in Secs. 3, 4, and 5.

In Step 3 of Fig. 2-1, the Composite Mathematical Model (CMM) predicts the complete array performance based on the anticipated characteristics of the driver amplifiers, transducer elements, array baffles, and the acoustic medium (including array interactions). Of course, the expected characteristics of the individual transducer elements are determined by the TDGS. The CMM determines if the transducer element design developed in the TDGS of Step 2 yields the required array performance. Step 3 is the fundamental verification of the entire design procedure. Even a trial design produced with arbitrary justification would be a candidate for consideration if, when analyzed in an adequate CMM, the predicted array performance was satisfactory.

Typically, the results of Step 3 will indicate that further adjustment of the design of the transducer element, or relaxation or adjustment of the array performance criteria, is necessary to achieve convergence of the predicted array performance to the desired array performance characteristics. The arrow closing the loop from Step 3 to Step 1 in Fig. 2-1 serves as a reminder that the design procedure is iterative.

As an illustration of how the GDA is implemented, consider the design problem of what was known as the Conformal/Planar Array Program or, more concisely, the C/P Program. This program required an array design consisting of about 3000 individually driven transducer elements. The array was required to operate at all steerings from endfire to broadside. The purpose of a projector array is to produce a specified sound field. In the C/P Program, a transducer radiating face velocity distribution for the 3000 array elements was chosen which, according to the radiation theory, would produce the specified sound field. This distribution was named the "Desired Velocity Distribution" and was designated as one constraint in Step 1. This velocity distribution was then used in the calculations of the TDGS of Step 2. Then, in Step 3, the actual velocity distribution of the collective transducer radiation faces was predicted based on the CMM. In general, such a predicted distribution will be different from the original desired distribution. The process is repeated until the difference reaches an acceptable value or until it is impractical to consider further refinements. At that point, the predicted velocity distribution could be used as the final desired velocity distribution constraint in Step 1 requiring a subsequent iteration through the three steps to optimize the design relative to this new constraint.

In the next section, the application of the TDGS is further illustrated using this example of the C/P Program.

3.0 AN EXAMPLE OF A TRIAL DESIGN GENERATION SCHEME

A Trial Design Generation Scheme (TDGS) may vary widely depending on such things as the designer's focus, the specific problem, constraints imposed by the application, and resources available. To clarify the concept of a TDGS, this section presents one specific example of a TDGS which was found to be useful in the C/P Program and other applications.

For the conformal/planar array, consisting of a large number of individually driven transducer elements, some form of velocity control was a necessity. Velocity control is simply any provision to insure that the desired velocity distribution for the array of transducer radiating faces will be at least approximately achieved. The TDGS had to supply a means for accommodating the velocity control constraint imposed in Step 1 of the GDA.

"Current velocity control" was chosen in the C/P Program as the means to achieve velocity control. By current velocity control is meant: 1) the magnitude and phase of the input current to each transducer element is controlled; and 2) the transducer element is designed to make the velocity of its radiating face proportional to the input current nearly independently of the radiation impedance on the face. Note that control of the current implies design constraints for the electronic amplifiers to be used to individually drive transducer elements.

Current Velocity Control

It can be shown that the following equations hold (Note: Quantities such as E_i, I_i, Z_r, and V_H are discussed in more detail in Secs. 4 and 5). The input electrical voltage E_i and current I_i are related to the velocity of the radiating face V_H by the following equations:

$$E_i = a(Z_r + Z_{ec})V_H \tag{3.1}$$

and

$$I_i = b(Z_r + Z_{ic})V_H, \tag{3.2}$$

where Z_r is the radiation impedance as seen by the radiating face, Z_{ec} is the mechanical impedance of the transducer configured with a short circuit across the main terminals, and Z_{ic} is the mechanical impedance of the transducer configured with an open circuit. For a given frequency, the quantities a, b, Z_{ec}, and Z_{ic} are constants for a given element design including any electrical components which are part of the design. The equations hold for any element in the array. However, it is assumed that a one-dimensional model is adequate to describe the transducer elements of interest. In a given problem, one may find that a one-dimensional model is not sufficient, especially for the CMM required in Step 3 of the GDA.

The input electrical impedance Z_i is simply E_i divided by I_i yielding

$$Z_i \equiv \frac{E_i}{I_i} = \frac{a}{b}\frac{Z_r + Z_{ec}}{Z_r + Z_{ic}}. \tag{3.3}$$

For current velocity control, one considers only transducer element designs which satisfy the following conditions:

$$|Z_{ic}| >> |Z_r| . \tag{3.4}$$

When this condition is satisfied, Eq. (3.2) reduces to:

$$I_i \simeq (bZ_{ic})V_H , \tag{3.2a}$$

where it can be seen that the velocity is proportional to the input current and independent of the radiation impedance.

When tested in the CMM, a TDGS based only on the constraint in Eq. (3.4) was not sufficient. Such a TDGS produced designs with the undesirable characteristic that the range of variation in input impedance Z_i was much greater than the corresponding variations in the radiation impedance Z_r. In order to produce designs with variations in Z_i about the same as those of Z_r, the designer added the constraint:

$$|Z_{ec}| << |Z_r| . \tag{3.5}$$

In the resulting TDGS, both Eqs. (3.4) and (3.5) hold; therefore, Eq. (3.3) reduces to:

$$Z_i \simeq \left(\frac{a}{bZ_{ic}}\right) Z_r . \tag{3.3a}$$

Thus, Z_i was forced to be proportional to Z_r, and the variations in electrical input impedance are made approximately the same as the variations in radiation impedance.

The resulting improved TDGS was comprised of two parts: a single frequency TDGS, and a frequency band TDGS. The single frequency TDGS is obtained by utilizing the mathematical relations between the element parameters implied by applying conditions A, B, and C at some chosen frequency ω_o.

Condition A: Maximize $|Z_{ic}|$ relative to Z_r at ω_o.

Condition B: Minimize $|Z_{ec}|$ relative to Z_r at ω_o.

Condition C: Comply with all other chosen design constraints.

Equation (3.2a) follows from condition A and is used for current velocity control. Combining conditions A and B yields Eq. (3.3a), making Z_i proportional to Z_r. It also follows from condition B that:

$$E_i \simeq a(Z_r V_H) = af_r , \tag{3.6}$$

where the force on the radiating face, $f_r = Z_r \cdot V_H$. Therefore, a consequence of condition B is that the input voltage is proportional to the force on the radiating face.

A further consequence of conditions A and B is:

$$E_i \cdot I_i \simeq (abZ_{ic}) f_r V_H . \tag{3.7}$$

Thus, the volt-amp product E_iI_i is proportional to the force-velocity product f_rV_H. In fact, when compliance with all other design constraints (Condition C) happens to lead to a transducer design with small internal losses, the volt-amp product E_iI_i is approximately equal to the force velocity product f_rV_H. That is,

$$E_iI_i \simeq f_rV_H. \tag{3.7a}$$

For this single frequency TDGS, it can be shown that the minimum value of $|E_iI_i|$ should ordinarily occur at a frequency very near ω_o. Low $|E_iI_i|$ is a desirable feature with respect to amplifier constraints. It can also be shown that a minimum value of $|E_i|$ in Eq. (3.6) should occur near ω_o. In the typical design configuration which employs current velocity control, the input voltage E_i is also the voltage applied to the active ferroelectric ceramic material. A low $|E_i|$ is highly desirable since it is important not to exceed the electrical field limit of the ceramic driver.

Figure 3-1 shows the $|Z_{ic}|$ of four radically different transducer element designs which will be used to illustrate some of the features of this specific TDGS. These designs were produced by the single frequency TDGS for the C/P Program constraints. Transducer elements 1, 2, and 3 were constrained to have nearly the same $|Z_{ic}|$ and, thus, the same degree of current velocity control over the frequency band as shown in curves 1, 2, and 3. However, they are radically different from each other in that elements 1 through 3 weigh approximately 75, 50, and 40 lbs, respectively. Transducer design #4 represented by curve #4 weighs the same as #3 (40 lbs), but design #4 is radically different from the first three. Specifically, $|Z_{ic}|$ for designs 1, 2, and 3 equals 35 MΩ at ω_o, but element 4 has a $|Z_{ic}|$ of only 15 MΩ at ω_o.

Figure 3-2 illustrates some of the characteristics of the E_iI_i product for transducer designs produced by the single frequency TDGS. The same four radically different designs associated with Fig. 3-1 are used. Notice that at ω_o all transducer elements produce essentially the same $|E_iI_i|$ product. A computer program searched out the greatest $|f_rV_H|$ in the 3000-element array for 21 different beam steerings and used this extreme to plot these four curves. Notice, also, that the absolute minimum of $|E_iI_i|$ is near ω_o.

The frequency band part of this specific TDGS consisted largely of using simplified predictive models and/or the computer implemented CMM predictive model to find those designs from the single frequency TDGS which best preserved the desirable features over the whole frequency band of interest. For example, if the only goodness criteria were to keep $|E_iI_i|$ as small as possible, element #4 in Fig. 3-2 represented by curve #4 would be chosen. However, $|Z_{ic}|$ is low for design #4 and it might be too low for current velocity control in a given array problem. If that were the case, one would then consider elements like 1, 2, and 3 all of which have the same larger $|Z_{ic}|$. Of elements 1, 2, and 3, one would pick element #1, represented by curve #1, as the lowest $|E_iI_i|$ over the band. However, element #1 weighs 75 lbs and, if a further design constraint were that no element could weigh more than 50 lbs., one would then pick element #2, represented by curve #2, as having the lower $|E_iI_i|$ consistent with the weight and $|Z_{ic}|$ constraints.

The example of employing current velocity control in this specific TDGS was presented primarily to clarify the meaning of a TDGS in the context of the GDA. There are other options which could have been exercised in this scheme to achieve slightly different results. For instance, consider the following: Condition A (maximize $|Z_{ic}|$ at ω_o) is often achieved by choosing the proper value for an inductor placed in parallel with the Ceramic Stack Assembly (CSA). Condition B (minimize $|Z_{ec}|$ at ω_o) is for practical purposes equivalent to adjusting the transducer element design such that the motion (of the radiating face) per volt (across the CSA) in air is maximized at ω_o). If, after completing the single frequency TDGS, the designer did not like the resulting average input impedance phase angle occurring over the array, this

phase angle could be adjusted by a slight alteration of the single frequency TDGS. For example, condition B could be made to occur at a slightly different frequency than ω_o, or instead, condition A could be similarly modified.

In summary, all quantities and constraints must be considered in the overall array design procedure, not just $|E_iI_i|$, $|Z_{ic}|$, and element weight. This is made feasible using modern high-speed digital computers which make it possible to examine enough design variations to insure that a reasonably optimum array configuration has been identified relative to the chosen constraints and goodness criteria. However, the cost and time required to complete a comprehensive design and analysis effort can be significantly reduced by using improved simplified predictive models in the TDGS. Further examples of simplified predictive models and associated design and analysis aids are presented in Secs. 4 and 5.

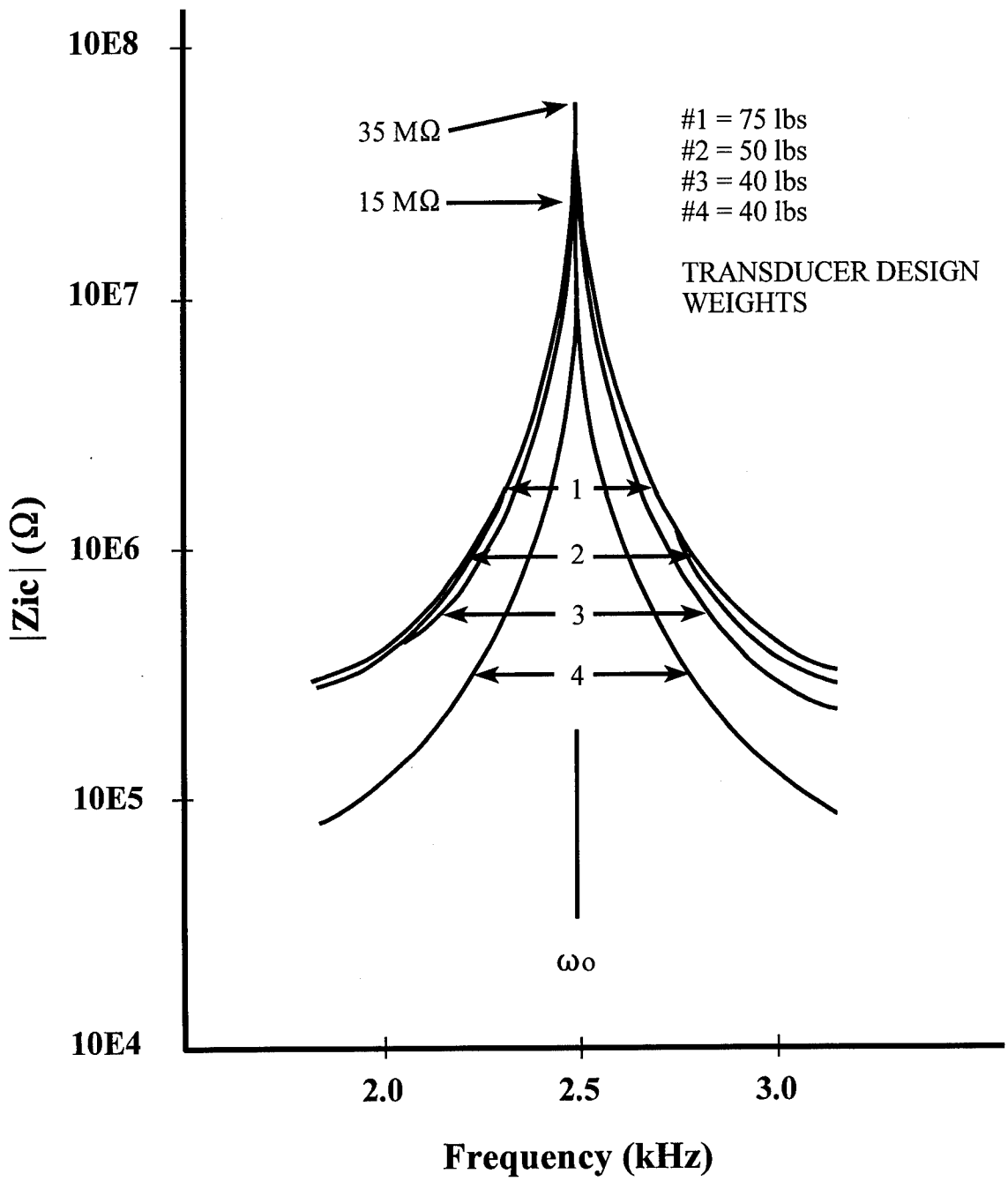

Fig. 3-1 — The magnitude of the mechanical input impedance Z_{ic} of four radically different transducer element designs

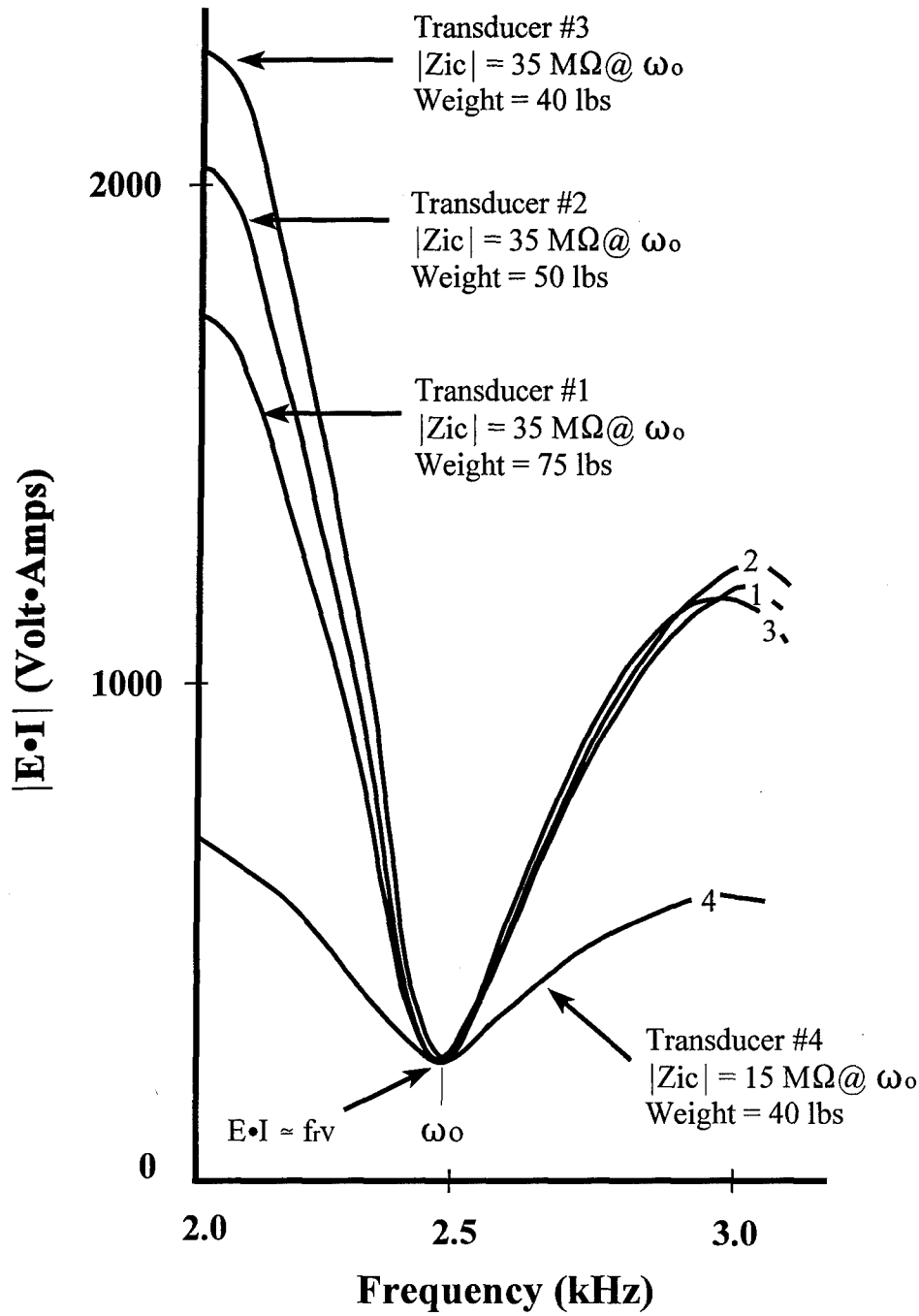

Fig. 3-2 — Characteristics of the E_iI_i product for four different transducer designs produced by the single frequency TDGS

4.0 CERAMIC STACK ASSEMBLY DESIGN AND ANALYSIS AIDS

4.1 Ceramic Stack Assembly/Fiberglass Tuning Ring Transfer Matrix

The performance of a transducer array and the transducer elements in that array is dependent upon the determination of the design of various design parameters. Limitations are placed on each component or subassembly in Step 1 of the General Design Approach (GDA). Listed below are some of the basic array and transducer element design parameters that must be considered.

Table 4.1 - Basic Array and Transducer Element Design Parameters

1.	Array geometry and construction.
2.	Transducer radiating face geometry and placement of these faces in the array.
3.	Desired array velocity and distribution for the radiating faces.
4.	Headmass assembly design.
5.	Tailmass assembly design.
6.	Electrical transformer and tuning inductor design.
7.	Watertight integrity design.
8.	Modular driver amplifier design. Note: It is assumed that each transducer element is driven by one of the driver amplifiers.
9.	Ceramic stack assembly (CSA) and fiberglass tuning ring (FTR) design [see Eqs. (4.1) and (4.1a)].

In Sec. 4 it is assumed that all of the transducer design parameters associated with items 1 through 8 are temporarily fixed. Section 4 considers only the effects of modifying the design parameters of the CSA and/or FTR (item 9).

The SGM [1] was specifically tailored to allow direct, economical, and efficient determination of the effects of adjustments in the piezoelectric CSA on 33-mode longitudinal vibrators. The original application of the SGM was to determine adjustments in the CSA (in combination with an FTR) which could be used to solve the piezoelectric ceramic reproducibility problem [2] for longitudinal vibrators. The design and analysis applications as they apply to the CSA are examined in this section.

The theory of the SGM will not be redeveloped here, since it has been presented in detail in Ref. 1. However, we will take from Ref. 1 a number of important relations which are then used to develop insight for generating trial designs for CSA and FTR components of the transducer element. A simple step-by-step method will be presented to help produce a near optimum design for the CSA and FTR relative to the constraints and goodness criteria of a given transducer design problem. Some of the other design parameters will be explicitly considered in Sec. 5.

One of the important relations which can be derived from the SGM is the transfer matrix equation [Eq. (4.1)]. The transfer matrix equation follows from the simplified equivalent circuit diagram of the CSA shown in Fig. 4-1, given the following assumptions:

1. The lengths of the individual ceramic rings (l_c) are short compared to a wavelength.

2. The ceramic stack length (L) is short compared to a wavelength.

3. The primary resonance frequency of the unloaded ceramic stack is much higher than the operating frequency band of the transducer.

4. The compliance of the stress rod is much greater than the compliance of the ceramic stack.

The transfer matrix equation relates the voltage (E) and current (I) applied to the CSA with a certain force (F) and a certain velocity of the radiating face (V) as indicated below:

$$\begin{pmatrix} E \\ I \end{pmatrix} = \begin{pmatrix} \frac{1}{Nd_{33}}[C_F + C) & \frac{1}{i\omega\, Nd_{33}} \\ i\omega \frac{A_c}{g_{33} l_c}(C_F + C') & \frac{A_c}{g_{33} l_c} \end{pmatrix} \begin{pmatrix} F \\ V \end{pmatrix}, \tag{4.1}$$

where: E is the voltage across the electrical terminals of the CSA,
I is the corresponding electric current flowing in the CSA,
d_{33} relates electric field to displacement,
g_{33} relates charge density to displacement,
N is the number of ceramic rings used to construct the CSA,
l_c is the length of any one of the N ceramic rings,
A_c is the electroded area of any one of the two ends of each of the N rings,
C_F is the compliance of the FTR,
C is the compliance of the CSA in the open-circuit configuration,
C′ is the compliance of the CSA in the short-circuited configuration,
F is a certain force (see discussion which follows), and
V is a certain velocity (see discussion which follows).

As is summarized in Sec. 4.2.1 and explained in detail in Ref. 1, when (as in all subsections of Sec. 4) the head and tail assemblies are assumed to be fixed, the force (F) and velocity (V) on the right side of Eq. (4.1) are proportional to the force F_H and velocity V_H interface of the fiberglass washer and the transducer radiating head assembly. In fact, given the assumptions of the SGM one finds that the constant of proportionality relating F to F_H is unity; that is, $F = F_H$.

The constant of proportionality relating V to V_H depends only on the frequency, the nature of the head and tail assembly, and the acoustic loading on the radiating face [see Eq. (4.13)].

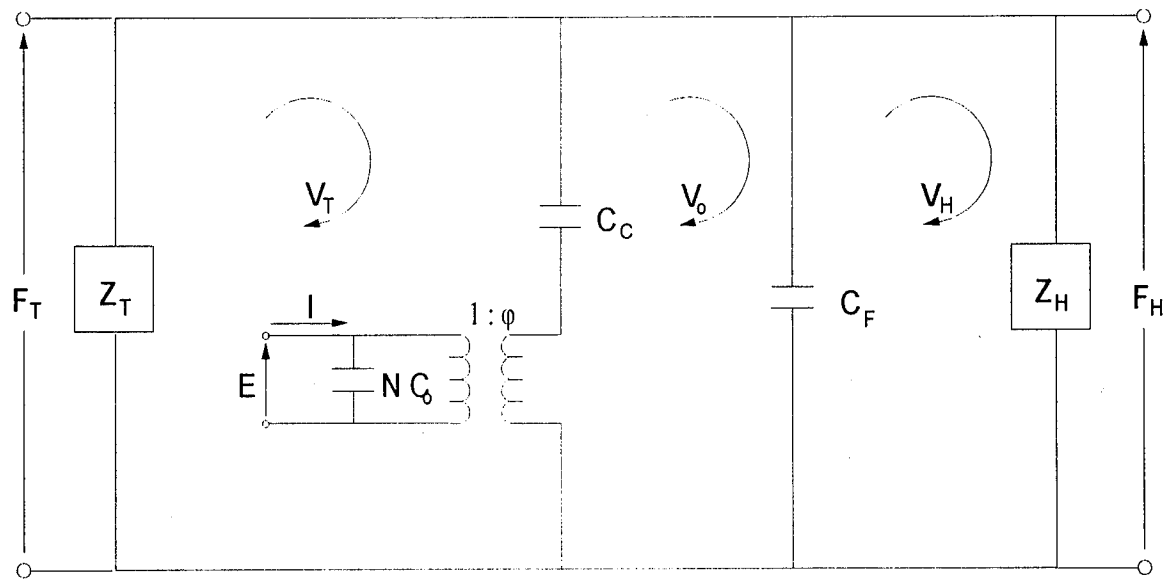

Fig. 4-1 — Simplified equivalent circuit of the CSA with combined head and tail impedances

Examination of Eq. (4.1) shows only two piezoelectric constants explicitly displayed; namely, d_{33} and g_{33}. Actually, a set of three independent piezoelectric constants is required to characterize the CSA. The third piezoelectric constant [for matrix Eq. (4.1)] is contained in CSA compliances, C (the CSA short-circuit compliance) and C′ (the CSA open-circuit compliance). These compliances are defined as follows:

$$C = S_{33}^{E} N \frac{1_c}{A_c} = S_{33}^{E} \frac{L}{A_c} \tag{4.2a}$$

and

$$C' = S_{33}^{D} N \frac{1_c}{A_c} = S_{33}^{D} \frac{L}{A_c}, \tag{4.2b}$$

where: S_{33}^{E} relates displacement to force when the CSA electrical terminals are short circuited,

S_{33}^{D} relates displacement to force when the CSA electrical terminals are open circuited, and

L is the total length of the CSA such that,

$$L = N\, 1_c. \tag{4.3}$$

However, S_{33}^{E} and S_{33}^{D} are not independent and only one of them need be used. They are related in the following way:

$$S_{33}^{D} = S_{33}^{E} - g_{33}d_{33}. \tag{4.4}$$

In light of the dependence expressed in Eq. (4.4), d_{33}, g_{33}, and S_{33}^{E} can be chosen as the set of three independent piezoelectric constants to fully characterize the CSA.

Using Eqs. (4.2) through (4.4), one can write

$$C' = C - \left(\frac{L}{A_c}\right)(g_{33}d_{33}). \tag{4.5}$$

Based on the above discussion, Eq. (4.1) can be re-expressed as follows to display the explicit dependence on the three chosen piezoelectric constants (d_{33}, g_{33}, S_{33}^{E}):

$$\begin{pmatrix} E \\ I \end{pmatrix} = \begin{pmatrix} \dfrac{1}{Nd_{33}}\left[C_F + \left(\dfrac{L}{A_c}S_{33}^{E}\right)\right] & \dfrac{1}{i\omega\, Nd_{33}} \\ \dfrac{i\omega\, N}{g_{33}\dfrac{L}{A_c}}\left[C_F + \dfrac{L}{A_c}\left(S_{33}^{E} - g_{33}d_{33}\right)\right] & \dfrac{N}{g_{33}\dfrac{L}{A_c}} \end{pmatrix} \begin{pmatrix} F \\ V \end{pmatrix}. \tag{4.1a}$$

Examination of Eqs. (4.1) and/or (4.1a) reveals the important fact that if any adjustments are made to the CSA and/or FTR (as reflected in the compliance C_F of the FTR) such that the coefficients of the 2 x 2 matrix remain the same, then the input/output performance of the adjusted transducer will be the same. The internal performance (such as electric field, mechanical strain, etc.) may be different, but all transducers with the same 2 x 2 matrix for Eq. (4.1) [or Eq. (4.1a)] will have the same externally measurable electro-acoustic performance. The electroacoustic performance characteristics of most general interest are

1. Source level per volt.
2. Source level per amp.
3. Input electrical impedance.
4. Open-circuit receive response.
5. Short-circuit receive response.

For the purposes of Sec. 4, any set of transducers which have the same coefficients in the transfer matrix will be said to have the same CSA/FTR transfer matrix. As noted above, these transducers will have identical characteristics with respect to the externally measurable quantities listed above.

4.2 Design Scenario 1 - Design Options Adjusting Only A_c and L (of CSA) but With L/A_c Ratio Fixed

This Section uses the SGM to develop some insight concerning design options and procedures available for the special case using only adjustments (changes) in the value of A_c and L (electrode area and total length of the CSA) subject to the additional constraint of a fixed value for the L/A_c ratio. For convenience, this special case will be referred to as Design Scenario 1.

As was emphasized in Sec. 3, any quantitative design calculations and predictions should be made using a good CMM. Therefore, in an actual application, the design engineer should have progressed far enough into a given iteration of the GDA to determine at least those Table 4.1 type parameters needed to perform corresponding Design Scenario 1 type calculations using the CMM. Please note, however, that during a given application of Design Scenario 1, all Table 4.1 type parameters are fixed except A_c and L.

For Design Scenario 1 perhaps the most important observations are the following: (1) In the CSA/FTR matrix [Eq. (4.1a)], the parameters A_c and L always occur together as the ratio L/A_c; (2) Even though we are changing the values of design parameters A_c and L, the fact that we are maintaining a fixed value for L/A_c means that all *Design Scenario 1 transducers have the same CSA/FTR transfer matrix and thus the same externally measurable electro-acoustic performance characteristics.* Yet it is also true that the transducers included in Design Scenario 1 can vary radically. With small values of L and A_c, only a relatively small volume of ceramic material would be contained in the CSA, while large values of L and A_c the CSA would contain a relatively large volume of ceramic material. The size of the transducer would of course vary accordingly.

In addition to physical size differences, there are several other variations accommodated by Design Scenario 1. The source level per volt applied to the ceramic is an externally measurable quantity and, therefore, is unaffected by changes permitted by Design Scenario 1. On the other hand, the source level per electric field would change as l_c (the length of the ceramic rings) is changed. Thus, the source level/electric field will be different and adjustable among transducers included in Design Scenario 1. Similarly, the mechanical stress and strain in the CSA is adjustable among Design Scenario 1 transducers. Specific insight concerning how to make such design adjustments (e.g., using an appropriate option of the CMM) is developed next with the aid of the SGM.

4.2.1 *Adjusting the CSA Electric Field (ε) by Adjusting L With Fixed L/A_c Ratio*

The theory of the SGM [1] shows that the force F and the velocity V are related as follows:

$$F = ZV, \tag{4.6}$$

where the impedance Z is the parallel combination of the impedance of the head assembly and tail assembly given by Eq. (4.7).

$$Z = \frac{Z_H Z_T}{Z_H + Z_T}. \tag{4.7}$$

In Eq. (4.7), Z_T is the impedance presented to the CSA by the tail assembly, and Z_H denotes the impedance presented at the FTR interface by the combined impedance of the head assembly and the acoustic loading.

Using F = ZV, it follows from Eqs. (4.1) or (4.1a) that

$$\frac{V}{E} = \frac{i\omega N d_{33}}{1+i\omega(C_F+C)Z}, \tag{4.8}$$

and if one defines the electric field as $\varepsilon = E/l_c$, then,

$$\frac{V}{\epsilon} = \frac{i\omega N l_c d_{33}}{1+i\omega(C_F+C)Z}, \tag{4.9}$$

or equivalently,

$$\frac{V}{\epsilon} = \frac{i\omega L d_{33}}{1+i\omega(C_F+C)Z}. \tag{4.9a}$$

Since the CSA consists of N ceramic rings wired in parallel, E is the voltage applied to a single ceramic ring as well as the entire CSA.

In a similar fashion, using F = ZV, it follows from Eqs. (4.1) or (4.1a) that

$$\frac{V}{I} = \frac{g_{33} l_c}{A_c} \frac{1}{1+i\omega(C_F+C')Z}. \tag{4.10}$$

Alternatively, using $L = l_c N$, this relationship can be expressed as

$$\frac{V}{I} = \frac{g_{33} L}{N A_c} \frac{1}{1+i\omega(C_F+C')Z}. \tag{4.10a}$$

In the development of the SGM, it is shown that the equivalent circuit for the longitudinal vibrator, Fig. 4.1, implies that

$$V_T = \frac{-Z_H V_H}{Z_T}, \tag{4.11}$$

and

$$V = V_H - V_T. \tag{4.12}$$

Combining Eqs. (4.11) and (4.12) gives

$$V = V_H - V_T = \left(1+\frac{Z_H}{Z_T}\right) V_H. \tag{4.13}$$

One important measure of performance is source level. Source level (not in decibels) is proportional to V_H at each frequency, and the constant of proportionality depends only on the frequency, the nature of the head mass assembly, and the acoustic loading. It, therefore, follows from Eq. (4.13) that V also

is proportional to source level, and the constant of proportionality does not depend on any of the quantities being allowed to change in the derivations presented (i.e., only CSA quantities and FTR quantities are allowed to vary here).

Thus, when all parameters except those for the CSA and FTR are fixed, the quantities V/E and V/I are equivalent to source level/volt on the ceramic (source level/E) and source level/amp (source level/I) into the ceramic as measures of performance. Thus, Eq. (4.8) shows explicitly why changing A_c and/or l_c does not affect the source level/E of a given transducer design; the source level/E is not a function of either l_c or A_c.

However, Eq. (4.9) shows that for fixed N (as in Design Scenario 1), the source level/electric field (source level/ε) is a function of l_c; as l_c is increased, the source level for a given field (ε) is also increased, In other words, the electric field required for a given source level can be reduced by increasing l_c. Notice, as shown explicitly by Eq. (4.9a), that the source level/ε is actually a function of the total length L of the CSA. In Design Scenario 1, since N is fixed and $L = Nl_c$ [Eq. (4.3)], the source level/ε is also a function of l_c. Later, in Design Scenario 3, where L is held fixed but both l_c and N may vary consistent with Eq. (4.3), the source level/ε does not change even though l_c is changed.

In a similar fashion, Eq. (4.10a) shows why only the source level/I is not affected by changes in L and A_c as long as the ratio L/A_c is held constant (which is true for Design Scenario 1 but not Design Scenario 2). Equation (4.10) could be altered to show that the source level/current density relation would be affected by changing A_c even if L/A_c is held fixed. However, current density is usually not an important factor in transducers of the type being considered.

4.2.2 *Adjusting CSA Stress by Adjusting A_c With Fixed L/A_c Ratio*

In a manner similar to the discussion of source level/E and source level/ε, the SGM may be used to "suggest" that mechanical stress in the CSA for a given source level can be reduced by increasing A_c and the mechanical strain in the CSA for a given source level can be reduced by increasing L. Thus, for Design Scenario 1, transducers, A_c and L can be increased so that L/A_c is fixed, but both stress and strain are reduced. This insight is explored further in the following paragraphs.

As is suggested by the SGM equivalent circuit diagrams of the longitudinal vibrator, given the approximations of the SGM, the forces at the various interfaces are equal; that is, $F_T = F_O = F_H$, where F_T is the force at the tail assembly to CSA interface, F_O is the force at the CSA to FTR interface, and F_H is the force at the FTR to head assembly interface. Since $F_H = Z_H V_H$ and since Z_H and the array velocity distribution are assumed fixed, one observes that in the SGM all these forces remain constant as one adjusts either A_c or L. Thus, since the average stress at each interface is the force divided by the area, one observes that as A_c is increased the average stress in the CSA (which is equal to $F_T/A_c = F_O/A_c = Z_H V_H/A_c$) is decreased. The statements about stress are true for any transducer for which the SGM holds and for fixed design parameters in the following:

1. Array geometry and construction.
2. Transducer radiating face geometry.
3. Array velocity distribution for the radiating faces.
4. Head mass assembly.

In Design Scenario 1, these conditions are met; therefore, this SGM-based discussion suggests that A_c may be varied to adjust the CSA stress levels. This SGM-based discussion spoke of average stress; but, in an actual design adjustment, an appropriate option of the CMM would consider the maximum stress in the CSA.

For later use, notice that the above discussion implies that a minimum value exists for A_c, say A_c^{min}, such that the stress limits associated with the CSA are not exceeded. Write this constraint as follows:

$$A_c \geq A_c^{min}. \tag{4.14}$$

A similar constraint on A_c might be developed relative to charge density, but this constraint is not considered here.

4.2.3 *Adjusting CSA Strain by Adjusting L With L/A_c Ratio Fixed*

Subject to the approximations of the SGM, the "average strain" in the CSA is proportional to $(V_O - V_T)/L$.

$$V_O = \left(Z_H + \frac{1}{i\omega C_F}\right) V_H. \tag{4.15}$$

Using Eqs. (4.11) and (4.15), $(V_O - V_T)/L$ may be expressed in terms of V_H as is shown in Eq. (4.16).

$$\frac{V_O - V_T}{L} = \left(Z_H + \frac{Z_H}{Z_T} + \frac{1}{i\omega C_F}\right)\frac{V_H}{L}. \tag{4.16}$$

For Design Scenario 1, all the quantities in the numerator of Eq. (4.16) are fixed; therefore, as L is increased, the average strain in the CSA decreases. This SGM-based discussion spoke of average strain; but, in an actual design adjustment, an appropriate option of the CMM would consider the maximum strain in the CSA.

The above discussion implies that a minimum value exists for L, say L^{minx}, such that the strain limits associated with the CSA are not exceeded. (These strain limits are also a function of the stress bias applied with the stress rod.) For subsequent use, it is convenient to express this constraint in the form

$$L \geq L^{minx}. \tag{4.17}$$

NOTE: In Sec. 4.3 another constraint is placed on the minimum value of L relative to the electric field limit and this minimum value is given the distinguishing symbol L^{minc}.

4.3 Design Scenario 2 - CSA L/A_c Ratio Optimization

In Sec. 4.2, the SGM was used to develop some insight concerning design options and procedures to determine (using the CMM) the "best choices" for the values for the CSA parameters A_c and L (with all

other design parameters held fixed) *subject to the additional constraint of a fixed value for the CSA L/A_c ratio*. In this section, the SGM is used to develop some insight concerning design options and procedures which may be used to determine (using the CMM) an optimum (or at least a practical optimum) value for the CSA L/A_c ratio; that is, how to determine $(L/A_c)^{opt}$. For convenience, this special case will be referred to as "Design Scenario 2."

The general approach used below to develop insight relative to Design Scenario 2 is:

1. The CSA/FTR compliance is "optimized" so as to result in a resonance frequency, f_e, for V/ε (or equivalently V/E) which minimizes the maximum value of the CSA electric field (ε) required to achieve the specified array source level (Sec. 4.3.1).

2. The "intrinsic frequency band width" of the transducer is adjusted to be as broad as practical so as to minimize the demands made on the power amplifier design (Sec. 4.3.2).

As previously emphasized, any quantitative design calculations and predictions should be made using a good CMM. Therefore, in an actual application the design engineer should have progressed far enough into a given iteration of the GDA to determine at least those Table 4.1 type parameters needed (using the CMM) to perform corresponding Design Scenario 2 type calculations. For example, the maximum CSA electric field needed to achieve the specified source level needs to be known; this means the CMM must be asked to calculate the electric field for all frequencies in the band of interest, all positions in the array, and all electrical steering angles. Since electric field limits are crucial in a piezoelectric ceramic type transducer, examination of this array performance data would show that there is a best location for the resonant frequency f_e, where f_e is defined as the frequency of maximum value for source level/ε (source level for a given electrical field on the ceramic).

As is explained below, during a given application of Design Scenario 2 all Table 4.1 type parameters are fixed except L/A_c and the compliance, C_f, of the FTR. Of course, during application of Design Scenario 2 one may temporarily take the point of view that L/A_c and the FTR are fixed and apply the Design Scenario 1 type adjustments to A_c and L.

For Design Scenario 2, the fact that we are <u>not</u> maintaining a fixed L/A_c ratio and/or FTR means that *Design Scenario 2 transducers do not have the same CSA/FTR transfer matrix and, thus, do not have the same externally measurable electro-acoustic performance.*

PREVIEW AND OVERVIEW OF GUIDELINES FOR OPTIMIZING THE L/A_c RATIO

The SGM-based insight development (presented directly below) for Design Scenario 2 is a little tedious, but the resulting guidelines may be simply and easily summarized as follows:

1. The L/A_c ratio is optimized by making it as large as practical.

2. To be consistent with 1 above (large L/A_c ratio), the compliance (C_f) of the FTR should be made as small as practical; in some cases this means that the FTR may be eliminated.

3. With the aid of the CMM the resonance frequency, f_e, for V/ε (or equivalently V/E) is adjusted to minimize the maximum value of the CSA electric field (ε) (or equivalently E), required to achieve a given specified array source level.

While reading the following explanation of Design Scenario 2, it is suggested that the reader keep in mind the above three-point summary of the resulting guidelines.

4.3.1 *Optimizing ε and E Over the Array by Adjusting the Resonance Frequency of V/ε*

Equation (4.9a) (repeated below for convenience) is used as a starting point for explaining how to shift f_e to optimize ε and E over the array for the transmit frequency band of interest.

$$\frac{V}{\epsilon} = \frac{i\omega L d_{33}}{1+i\omega(C_F+C)Z}. \tag{4.9a}$$

In this discussion, all of the transducer design parameters except the CSA and/or FTR design parameters (see Sec. 4) remain fixed. Thus, in Eq. (4.9a), Z is fixed. One observes in Eq. (4.9a) that for any given value of L and d_{33}, the only way to change the frequency f_e where the maximum value of V/ε occurs is to adjust the value of the composite compliance $C_F + C$. Let C_e be this composite compliance as in Eq. (4.18):

$$C_e = C_F + C = C_F + S_{33}^E \frac{L}{A_c}. \tag{4.18}$$

In Eq. (4.8), it does not matter whether the composite compliance C_e is changed by changing C_F (changing the FTR) or changing C (changing the short circuit CSA compliance). Therefore, C_e may be iteratively changed in the array CMM and the predictions may be used to determine a best location for the resonant frequency f_e, say f_e^{opt}, for the array source level/E and source level/ε. Corresponding to f_e^{opt} will be the best choice for C_e, say C_e^{opt}. For convenience, rewrite Eq. (4.8) as follows for the special case where $C_e = C_e^{opt}$:

$$\frac{V}{E} = \frac{i\omega N d_{33}}{1+i\omega(C_e^{opt})Z}. \tag{4.8a}$$

Notice that for any given values for N and d_{33}, the shape of the curve of a plot of V/E vs frequency is the same as the shape for another set of values for N and d_{33}. However, the curve can be shifted up or down by increasing or decreasing N and/or d_{33}.

In a corresponding fashion, rewrite Eq. (4.9a) as

$$\frac{V}{\epsilon} = \frac{i\omega L d_{33}}{1+i\omega(C_e^{opt})Z}. \tag{4.9b}$$

Equation (4.9b) shows that there is some minimum value of L, say L^{mine} required to give a high enough value of V/ε to comply with the given field limit on ε. For future use write this condition as

$$L \geq L^{mine}. \tag{4.19}$$

Equation (4.19) insures that for the array source level requirements

$$\epsilon \leq \epsilon^{max}. \tag{4.20}$$

For later use, note the following: two lower bound conditions have now been placed on the minimum value of L, L^{minx} [Eq. (4.17)] and L^{mine} [Eq. (4.19)]. Let L^{min} be the larger of these two lower bounds and write the resulting constraint on L as follows:

$$L \geq L^{\min}. \tag{4.21}$$

The above results also imply another constraint involving L which can be seen as follows. Recall that C is given by Eq. (4.2a) (repeated here for convenience).

$$C = \left(\frac{L}{A_c}\right) S_{33}^{E}. \tag{4.2a}$$

Using Eqs. (4.18) and (4.2a), and the known desired value for C_e; namely, C_e^{opt}, write the following equations:

$$C_F + C = C_e^{opt}, \tag{4.18a}$$

$$C = C_e^{opt} - C_F, \tag{4.18b}$$

and

$$\frac{L}{A_c} = \frac{1}{S_{33}^{E}}\left(C_e^{opt} - C_F\right). \tag{4.22}$$

Equation (4.22) is one of the two equations which will be used to develop insight concerning determination of the optimum value for the L/A_c ratio, that is, $(L/A_c)^{opt}$. The second equation [Eq. (4.5a)] is determined in the next subsection as a result of optimizing the bandwidth for the sake of the power amplifier.

4.3.2 *Optimizing Bandwidth for Sake of the Amplifier*

Although voltage E and electric field ε are the important electrical limits for the transducer element, the modular amplifiers have both a voltage and a current limit (also an E I product limit). For simplicity, assume that any tuning inductor is placed in parallel with the transducer so that E_{in} and ε have already been adjusted and optimized for all array conditions as explained in Sec. 4.3.1. The problem remaining is to adjust the transducer design so that I_{in} for frequencies not near f_e remains as low in value as possible and, thus, assuring that the bandwidth over which the current limits of the amplifier are not exceeded will be as large as practical.

The determination of the best value of L/A_c [subject to the constraint of Eq. (4.20)] and C_F for keeping I_{in} low over as large a frequency band as practical involves the frequency dependence of the head assembly, tail assembly and the acoustic loading of the array. These other design variables will be included starting in Sec. 5, but for now these complications will be by-passed by making two temporary design aid postulates. Later, when the other design variables are explicitly considered, these temporary postulates will not be needed. The two temporary design aid postulates are:

Design Aid Postulate 1

The greater the separation (difference) between the resonance frequency f_e for the maximum array source level/E (related to V/E) and the resonance frequency f_i for the maximum array source level/I (related to V/I), the greater the bandwidth over which the current limit of the amplifier will not be exceeded.

Comparing the denominator of Eq. (4.8) for V/E with the denominator of Eq. (4.10) for V/I suggests the second postulate.

Design Aid Postulate 2

The difference between f_e and f_i can be made as large as possible (that is, postulate 1 can be satisfied) by making the difference between $(C_F + C)$ and $(C_F + C')$ as large as possible.

The degree of validity and usefulness of these two design aid postulates may be examined in later sections where the nature of the acoustic loading, head assembly, and tail assemblies are combined with that of the CSA and FTR. In any given case the designer can easily check the validity by applying the computerized composite mathematical model for the transducer trial design in the array environment. These postulates have sometimes worked well in practice and for now are accepted as valid trial design generation aids.

Postulate 2 (and, thus, postulate 1) can be applied using the following form of Eq. (4.5):

$$(C_F + C) - (C_F + C') = \frac{L}{A_c}(g_{33}d_{33}). \tag{4.5a}$$

In Eq. (4.5a), with all other ceramic stack assembly parameters (Table 4.1) fixed, the only adjustment allowed is in L/A_c. Equation (4.5a) shows (as required by postulate 2) $(C_F + C')$ can be made as different as possible from $(C_F + C)$ by making L/A_c as large as possible.

The other relevant equation involving L/A_c is Eq. (4.22) which is repeated for convenience.

$$\frac{L}{A_c} = \frac{1}{S_{33}^E} \cdot \left(C_e^{opt} - C_F\right). \tag{4.22}$$

Equation (4.22) shows that L/A_c can be made as large as possible by making $C_F = 0$ (no FTR).

Therefore, the optimum value [however, also see Eqs. (4.22b) and (4.23c)] of L/A_c is given by

$$\left(\frac{L}{A_c}\right)^{opt} = \frac{C_e^{opt}}{S_{33}^E}. \tag{4.22a}$$

Recall that C_e^{opt} is the composite compliance needed to optimally locate f_e, the V/E resonance frequency.

These last observations can be made more directly by using Eq. (4.22) in Eq. (4.5a) to yield:

$$(C_F + C) - (C_F + C') = \frac{g_{33}d_{33}}{S_{33}^E}\left(C_e^{opt} - C_F\right), \tag{4.23}$$

or more simply,

$$(C - C') = \frac{g_{33}d_{33}}{S_{33}^E}\left(C_e^{opt} - C_F\right). \tag{4.23a}$$

Equation (4.23) shows directly that for a given choice for g_{33}, d_{33}, and S_{33}^E (which are temporarily assumed to be fixed), that the difference in the composite compliance $(C_F + C')$ and $(C_F + C)$ can be made as great as possible (to satisfy postulate 2) by making $C_F = 0$.

Equation (4.23a) is shown simply to emphasize the fact that making C′ as different as possible from C is equivalent to making $(C_F + C')$ as different as possible from $(C_F + C)$. This is really what is being accomplished by applying postulate 2.

4.3.2.1 Retention of a Minimum FTR Compliance

In practice, for many cases it is recommend that a minimum compliance FTR be retained in order to make the transducer reproducible on a production basis [2]. If for practical purposes a minimum FTR compliance C_F^{min} is retained, then the equation for $(L/A_c)^{opt}$ becomes

$$\left(\frac{L}{A_c}\right)^{opt} = \left(C_e^{opt} - C_F^{min}\right)\frac{1}{S_{33}^E}. \tag{4.22b}$$

For this condition, the difference in the two composite compliances is given by

$$(C_F + C) - (C_F + C') = \frac{g_{33}\,d_{33}}{S_{33}^E}\left(C_e^{opt} - C_F^{min}\right). \tag{4.23b}$$

4.3.2.2 Introduction of Coupling Coefficient K_{33}

For later use note, relative to Eqs. (4.23) and (4.23a), that an often tabulated piezoelectric ceramic quantity called coupling coefficient K_{33} may be defined as

$$K_{33}^2 = \frac{g_{33}d_{33}}{S_{33}^E}. \tag{4.24}$$

Using this expression for K_{33}^2, Eq. (4.23) may be written as

$$(C_F + C) - (C_F + C') = K_{33}^2\left(C_e^{opt} - C_F\right). \qquad \textbf{(4.23c)}$$

A large value for ceramic coupling coefficient, K_{33} is, in general, considered "good." In this regard, please note from Eq. (4.23c) that the larger K_{33} the greater (according to design aid postulates 1 and 2) the bandwidth over which the current limit of the modular amplifiers will not be exceeded.

4.3.3 *Sub-optimum L/A_c*

Thus far, Sec. 4.3 has provided insight concerning determination of $(L/A_c)^{opt}$, and Sec. 4.2 provided insight concerning determination of specific values for L and A_c. Consider now the case where, for practical reasons, one cannot use $(L/A_c)^{opt}$ in the design (e.g., a transducer length constraint), but must use a sub-optimal ratio $L/A_c < (L/A_c)^{opt}$. In conjunction with Eq. (4.21) it was pointed out that some minimum, L^{min}, ceramic stack length exists to satisfy both the electric field and strain limits. Suppose L^{min} is achievable, but the corresponding minimum allowable area A_c^{min} [Eq. (4.14)] is such that $L^{min}/A_c^{min} < (L/A_c)^{opt}$. A solution would be to make $L \geq L^{min}$. However, suppose the transducer length constraint is such that a maximum length of the CSA, say L^{max}, exists and $L^{max} \geq L^{min}$, but even using this maximum length the subject ratio is sub-optimal; that is, $L^{max}/A_c^{min} < (L/A_c)^{opt}$.

For this sub-optimal case one may proceed as follows. One wishes to retain C_e^{opt} as the value of the composite compliance in order to retain the optimization relative to ε and E discussed in Sec. 4.3.1 [Eqs. (4.8a) and (4.9b)]. From Eq. (4.22) one notes that in order to retain C_e^{opt} if the ratio L/A_c is reduced below its maximum (i.e., below its optimum) value, then the FTR compliance, C_f, must be increased in value. Applying this procedure to this sub-optimal case, the performance relative to the velocity/ε and velocity/E on the CSA using the L^{max}/A_c^{min} is the same as for a CSA using $(L/A_c)^{opt}$. For the case being considered, since $L \geq L^{min}$, Eq. (4.19) applied to Eq. (4.9b) ensures that the electric field ε is less than or equal to the maximum field ε^{max} [Eq. (4.20)]. However, the demands on the amplifier current and volt amp product requirements are greater. One can say that with $L/A_c < (L/A_c)^{opt}$, the bandwidth has been reduced over which a given amplifier design could drive the array. To increase the bandwidth using $L/A_c < (L/A_c)^{opt}$, one would have to design a larger capacity power amplifier.

4.4 Design Scenario 3 - Design Options Adjusting N and l_c (fixed L)

This section uses the SGM to develop some insight concerning design options and procedures available for the special case where the only changes allowed are adjustments in the value of N and l_c (number of ceramic rings and length of a ceramic ring) subject to the additional constraint of Eq. (4.3) ($L = Nl_c$) with a fixed value for L. For convenience this special case will be referred to as "Design Scenario 3."

4.4.1 *Main Application for Design Scenario 3*

Reduction (to acceptable values) of the required voltage E on the electrical wiring of the CSA is the main application for Design Scenario 3. Equation (4.8) indicates that, as N is increased there is a decrease in the voltage E required to achieve a given velocity V and, thus, the corresponding desired source level.

4.4.1.1 Things that Change in Design Scenario 3

In addition to the change just described ("improvement" of V/E and the source level/volt), V/I changes [Eq. (4.10a)] and the CSA/FTR transfer matrix changes [Eq. (4.1a)]. In regard to these last two changes, please note the following:

1. As N is changed the ratio V/I changes in the opposite direction of V/E; if V/E is increased, then V/I is decreased and visa versa.

2. Since the CSA/FTR transfer matrix changes as N is changed in Design Scenario 3, the corresponding externally measurable performance will also change. However, all such Design Scenario 3 transducers can be made to have the same CSA/FTR transfer matrix by adding an electrical transformer across the CSA electrical terminals. The turns ratio of this transformer can be selected to compensate for the change in N (see, for example, page 14 of Ref. 1).

4.4.1.2 Things That Do Not Change in Design Scenario 3

In Design Scenario 3 all transducer performance characteristics are fixed except for the three items indicated in Sec. 4.4.1.1. However, for definiteness it is useful to list some of these items that do not change.

1. V/ε [Eq. (4.9a)] and source level/ε do not change.

2. The mechanical stress (Sec. 4.2.2) and strain (Sec. 4.2.3) do not change.

3. The L/A_c ratio does not change.

4.5 Design Scenario 4 - Design Options Adjusting only CSA Piezoelectric Ceramic Parameters

In this section, it is no longer assumed that the piezoelectric parameters of the CSA are being held fixed. Instead, this section uses the SGM to develop some insight concerning design options when changes are allowed in the chosen set of three independent piezoelectric ceramic parameters (e.g., d_{33}, g_{33}, and S_{33}^E) with all other transducer design parameters held fixed. For convenience, this special case will be referred to as Design Scenario 4.

Return first to Eq. (4.23) which shows that the bandwidth over which the amplifier can drive the array (see design aid postulates 1 and 2) can be increased by increasing the product $g_{33}d_{33}/S_{33}^E$. As noted in Sec. 4.3.2, Eqs. (4.24) and (4.23c) show that this last observation is equivalent to saying that increasing the CSA coupling coefficient K_{33} will increase this bandwidth.

Examination of Eq. (4.8a) shows that increasing d_{33} increases the source level/E. In other words, increasing d_{33} decreases the voltage E on the CSA needed to achieve a given source level. Similarly, examination of Eq. (4.9a) shows that increasing d_{33} improves the source level/ε; that is, increasing d_{33} decreases the electric field on the CSA required to achieve a given source level. Analogous statements can be made about g_{33} and the source level/I.

If one increases g_{33} and/or d_{33}, as observed above, then the relative location of the resonance frequencies for source level/E and source level/I will be changed consistent with the above observation

concerning an increase in bandwidth due to an increase in the coupling coefficient K_{33}. If the S_{33}^E CSA parameter is held fixed, the resonance frequency f_e remains fixed and the resonance frequency f_i will be changed as d_{33} and/or g_{33} is changed. This can be seen by examination of Eqs. (4.18a), (4.2a), (4.2b), and (4.23a) (C_F and L/A_c are not allowed to change in Design Scenario 3). Furthermore, note that the compliance, C, is fixed [Eq. (4.2a)] and compliance C′ changes [Eq. (4.23a)] as d_{33} and/or g_{33} is changed.

Although only the projector array problem is being considered, such an array is often used as the receiver array. It is useful to note (by reciprocity) that the open-circuit receive response is increased by increasing g_{33} and the short-circuit receive response is be increased by increasing d_{33}.

4.5.1 *Replacing g_{33} With ε_{33}^T (and C_T)*

For many purposes in projector-type transducer designs, it is useful to replace g_{33} with ε_{33}^T (see, for example, Refs. 1 and 2 concerning piezoelectric ceramic reproducibility), using d_{33}, ε_{33}^T, and S_{33}^E as the set of independent material parameters. One reason is that ε_{33}^T is easily measurable because

$$C_T = A_c \epsilon_{33}^T / l_c \tag{4.25}$$

and C_T (the low-frequency capacitance of one ceramic ring) is easily measurable.

The main discussion of this change from g_{33} to ε_{33}^T occurs in Sec. 5; however, as one illustration, K_{33} will now be rewritten in terms of ε_{33}^T using Eq. (4.26).

$$g_{33} = d_{33} / \epsilon_{33}^T . \tag{4.26}$$

Using Eq. (4.26) in Eq. (4.24) gives

$$K_{33} = (d_{33})^2 / \epsilon_{33}^T S_{33}^E . \tag{4.27}$$

Recall that a large value for K_{33} is desirable and note that the smaller ε_{33}^T the larger K_{33}. Notice also from Eq. (4.25) that the smaller ε_{33}^T the smaller the low frequency capacitance, C_T. Thus, one can say that the smaller the value of low-frequency capacitance the better from the point-of-view of desiring a large coupling coefficient, K_{33}.

4.5.2 *Summary for Design Scenario 4*

The above discussion indicates why, consistent with other considerations (such as high drive stability, etc.), the projector designer will choose a high value for d_{33}, and a low value for ε_{33}^T (or equivalently a high value for g_{33}) and for a high value of S_{33}^E.

5.0 COMPOSITE TRANSDUCER DESIGN AND ANALYSIS AIDS

An array of acoustically interacting and complicated transducer elements can only be designed adequately with the help of computer aided design analysis. In cases where these costly and time-consuming computer-aided design calculations have been performed, certain design trends and design techniques were suggested by examination of the volumes of computer-generated graphs. As was indicated in the introduction (Sec. 1), the SGM may be augmented with simple models in such a way that, using only paper and pencil, an engineer may derive much of the same knowledge, skill, and insight as was gained from the elaborate, expensive computer-aided calculations. In fact, in some cases, more insight is gained from such a paper and pencil exercise. As was promised, the augmented SGM is also applied to derive and illustrate some of the pertinent design and analysis aids. Appendix B presents computer program prediction results for three selected examples taken from Sec. 5. As will be pointed out below, the three selected examples presented in Appendix B are associated respectively with Eqs. (5.34), (5.79), and (5.10) (see Secs. 5.2.2.1.2, 5.2.2.5, and 5.2.2.6.2.1.2, respectively).

The augmented SGM provides qualitative insight which helps to understand the performance obtained or obtainable from specific designs. The augmented SGM can guide the design engineer quickly to an approximate solution to his design problem -- without having to perform extensive computer-aided analysis. No claim is made that the augmented SGM can replace computer aided analysis. However, it can provide knowledge, skill, and insight which will significantly reduce the time and cost of completing the final design and analysis calculations. As was emphasized in Sec. 3, any quantitative design calculations and predictions should be made using a good CMM.

In Sec. 4, it was shown that the SGM could be used to determine transducer design aids for the case where only the CSA and FTR design parameters were assumed to be explicitly displayed and available for manipulation. All the other transducer design parameters were held fixed and not explicitly available for consideration. In this section, simple models for the head assembly, tail assembly, and radiation loading are selected and used in conjunction with the SGM representations of the CSA and FTR models.

5.1 The Radiation Model: Simplification of the Head and Tail Assemblies

In this simplified representation, the head and tail assemblies are represented by mass-like devices. Thus, the impedance Z_T, looking into the tail assembly, is represented as

$$Z_T = i\omega m_T, \tag{5.1}$$

where m_T is the mass of the tail assembly. The impedance for the head assembly in the case where there is no applied radiation loading (e.g., the transducer operating in air), is given by

$$Z_H = i\omega m_H \quad (\text{no radiation loading}), \tag{5.2}$$

where m_H is the mass of the head assembly. The tail representation [Eq. (5.1)] is quite realistic for a large class of longitudinal vibrators. The head representation [Eq. (5.2)] is fairly representative except where the head is thin enough to have significant flexing. For most cases, except where flexing head is a concern, these two equations provide an estimation of the impedances that correlates well with actual observations.

When radiation loading is present, the impedance of the head assembly is given by

$$Z_H = i\omega m_H + Z_r \quad \text{(with radiation loading)}, \tag{5.3}$$

where Z_r is the radiation impedance. Z_r is a complex number as shown in Eq. (5.4), where R is the real part and iX is the imaginary part of Z_r. In an array design problem, the radiation impedance (both R and X) for a given transducer element in the array is, in general, a function of many things such as the element position in the array, the electrical steering angles for the array and the velocity distribution in the array.

$$Z_r = R + iX. \tag{5.4}$$

For the design aid simplification purposes, it is assumed that this function can be represented by the following simple, artificial frequency-dependent, radiation impedance, Z_r. In this representation, R and X are taken to have the following linear dependence on ω:

$$R = \omega r \quad \text{and} \quad X = \omega x, \tag{5.5}$$

where r and x are constants (not functions of ω). Since we are interested in designing transducer elements to operate in an acoustically interactive array, we assume that this representation is useful for our purposes not only for the radiation loading for a single element operating alone, but also for the average or typical radiation loading for a single element operating in an array. This simple, artificial representation of Z_r departs radically from any actual frequency dependence for radiation impedance. Therefore, there was great concern that use of this simplified Z_r representation might lead to erroneous design insights. However, the results reported below using this selected simple Z_r representation agree qualitatively with design insights obtained using very sophisticated radiation models and computer-aided calculations and graphs.

With this simple model for Z_r, the impedance looking into the head assembly with a radiation load applied is given by

$$Z_H = \omega r + i\omega(m_H + x) \quad \text{(with radiation loading)}. \tag{5.6}$$

Let m be defined as the effective mass of the head mass assembly with radiation loading present.

$$m = m_H + x. \tag{5.7}$$

Then the head assembly impedance Z_H can be expressed as

$$Z_H = \omega r + i\omega m = \omega (r + im) \quad \text{(with radiation loading)}. \tag{5.8}$$

Equations (5.1) and (5.8) constitute our simplified model for the tail and head assembly impedances in the presence of an applied radiation loading.

5.2 Analysis Without a Tuning Inductor

These simple forms for Z_T, Z_r, and Z_H were used in the SGM to derive numerous forms of the basic equations which in turn were analyzed to illustrate certain conclusions concerning design trend, design aids, and design and analysis techniques. This section presents the resulting model equations for the composite transducer without an added tuning inductor. The emphasis is on transducer designs which best

meet the electric field constraints of the piezoelectric ceramic rings. Later, in Sec. 5.3, a parallel tuning inductor is included in the analysis of the composite transducer.

Where possible, we attempt to show the derivations of these model equations. In some cases, the complete derivations were too lengthy to be included without interrupting the flow of the discussion. In those cases, a more complete derivation is presented in Appendix A.

5.2.1 *Basic Forms for E/V_H and I/V_H*

The initial form for the input voltage (E) to the CSA required to achieve a given velocity of the radiation loaded head device V_H is given by (see Sec. A.1):

$$\frac{E}{V_H} = \frac{1}{i\omega Nd_{33}}\left(1 + \frac{Z_H}{Z_T}\right)\left[1 + i\omega C_e\left(\frac{Z_H Z_T}{Z_H + Z_T}\right)\right]. \tag{5.9}$$

Using the simplified forms for the head and tail mass impedances presented in Sec. 5.1, Eq. (5.9) can be rearranged (see Sec. A.2) into the following simpler form:

$$\frac{E}{V_H} = \frac{1}{\omega Nd_{33}}[rE_o - i(1 - mE_o)]. \tag{5.10}$$

The quantity E_o is defined by

$$E_o = \left(\omega^2 C_e - \frac{1}{m_T}\right). \tag{5.11}$$

Recall that C_e was defined [Eq. (4.18)] as the sum of the compliances of the fiberglass spring and the ceramic stack where the CSA is in the short-circuited configuration.

For many purposes, it is the magnitude of a complex quantity which is important. The magnitude of E/V_H may be written as

$$\left|\frac{E}{V_H}\right| = \frac{1}{\omega Nd_{33}}\sqrt{r^2E_o^2 + (1 - mE_o)^2}. \tag{5.12}$$

For convenience, define B_1 as

$$B_1 = r^2 E_o^2 + (1 - mE_o)^2. \tag{5.13}$$

Then, rewrite Eq. (5.12) as

$$\left|\frac{E}{V_H}\right| = \frac{1}{\omega N d_{33}}\sqrt{B_1}. \tag{5.14}$$

A similar equation to the one above (derived in Sec. A.3) relates the input current to the CSA (I) and the velocity of the radiating face (V_H).

$$\frac{I}{V_H} = \frac{A_c}{g_{33}1_c}\left(1 + \frac{Z_H}{Z_T}\right)\left[1 + i\omega C_e'\left(\frac{Z_H Z_T}{Z_H + Z_T}\right)\right]. \tag{5.15}$$

It can be simplified in the following way:

$$\frac{I}{V_H} = \frac{A_c}{g_{33}1_c}\left[\left(1 - mI_o\right) + irI_o\right], \tag{5.16}$$

where the quantity I_o is defined as

$$I_o = \left(\omega^2 C_e' - \frac{1}{m_T}\right). \tag{5.17}$$

The sum of the compliances of the fiberglass spring and the CSA in the open-circuited configuration is denoted by C_e' [see also Eq. (4.2b) for C′].

$$C_e' = C_F + C' = C_F + S_{33}^D \frac{L}{A_c} \tag{5.18}$$

Then, the magnitude of the complex quantity I/V_H is given by

$$\left|\frac{I}{V_H}\right| = \frac{A_c}{g_{33}1_c}\sqrt{r^2 I_o^2 + (1 - mI_o)^2}. \tag{5.19}$$

For convenience, define B_2 as

$$B_2 = r^2 I_o^2 + (1 - mI_o)^2. \tag{5.20}$$

Then rewrite Eq. (5.18) as

$$\left|\frac{I}{V_H}\right| = \frac{A_c}{g_{33}1_c}\sqrt{B_2}. \tag{5.21}$$

It is interesting to compare Eq. (5.14) for $|E/V_H|$ to Eq. (5.21) for $|I/V_H|$. Notice that the quantities B_1 and B_2 have exactly the same form for the frequency dependence. The only difference is that B_1

involves the short-circuit compliance C_e [see Eq. (5.11)], whereas B_2 involves the open circuit compliance C_e' [Eq. (5.17)]. All the frequency dependence for $|I/V_H|$ is contained in B_2. On the other hand, note that $|E/V_H|$ has the multiplier $1/\omega$. Therefore, if one fully characterizes either B_1 or B_2 as functions of variables such as m_T, m_H, and ω, then one would know all about the frequency dependence of $|I/V_H|$ and a great deal about $|E/V_H|$ within the limitations set by use of the simplified models (Sec. 5.1).

5.2.2 *Special Frequencies and Characteristics for E/V_H, ε/V_H, and I/V_H*

There exist special frequencies where B_1 and B_2 become especially simple. Thus, the expressions for E/V_H, ε/V_H (ε is the electric field), and I/V_H become especially simple. These special frequencies are useful for the development of design aids. In this section, we will consider the characteristics of E/V_H, ε/V_H, and I/V_H at these special frequencies. Some of the observations made here are not limited to situations where the simple radiation model is applicable; these more generally applicable observations will be pointed out as they are encountered.

5.2.2.1 **In-air Resonance Frequencies - ω_m and ω_n**

In this section, we will consider the characteristics of E/V_H, ε/V_H, and I/V_H in air for some special frequencies. Since the radiation impedance is effectively zero in air, the following observations are not a function of the simple radiation model. Let ω_m be the frequency where the quantity $|E/V_H|$ is a minimum in air; that is, the in-air resonance frequency for $|E/V_H|$. By setting r and x equal to zero (the idealized in-air condition), one derives from Eq. (5.12) the following expression:

$$\left|\frac{E}{V_H}\right|_{\text{in-air}} = \frac{1}{\omega N d_{33}} \sqrt{(1 - m_H E_o)^2}. \tag{5.22}$$

The minimum value of $|E/V_H|$ in air occurs when the quantity $1 - m_H E_o$ goes to zero. Let E_{om} be the value of function E_o which satisfies that condition. Then,

$$E_{om} = \frac{1}{m_H}. \tag{5.23}$$

Using Eq. (5.23) in Eq. (5.11) gives an expression for the angular frequency ω_m where the magnitude of E/V_H is minimized.

$$\omega_m^2 = \frac{1}{C_e}\left(\frac{1}{m_H} + \frac{1}{m_T}\right). \tag{5.24}$$

The corresponding equation to Eq. (5.22) for the in-air magnitude of I/V_H is

$$\left|\frac{I}{V_H}\right|_{\text{in-air}} = \frac{A_c}{g_{33} l_c} \sqrt{(1 - m_H I_o)^2}. \tag{5.25}$$

The magnitude of I/V_H is minimized when the quantity $1 - m_H I_o$ goes to zero. Let I_{om} be the value of function I_o which satisfies that condition. Then,

$$I_{om} = \frac{1}{m_H}. \tag{5.26}$$

The in-air angular resonance frequency ω_n for the quantity $|I/V_H|$ is given by

$$\omega_n^2 = \frac{1}{C_e'}\left(\frac{1}{m_H} + \frac{1}{m_T}\right). \tag{5.27}$$

This resonant frequency with respect to current is also sometimes called the antiresonant frequency.

Note that these results predict infinite in-air velocities at ω_m and ω_n. This unrealistic prediction occurs because in the SGM the losses in the CSA are assumed to be zero, and in the above assumed head and tail devices there are also no losses. In actual devices, there will be losses so that, although the velocities may be large, they are never infinite.

5.2.2.1.1 *Relation of the In-air Resonant Frequencies ω_m, ω_n to the Coupling Coefficient K_{33}* - As was discussed in Sec. 4, transducer engineers are sometimes interested in a commonly tabulated quantity called the coupling coefficient, K_{33}. It was defined in Sec. 4 as

$$K_{33}^2 = \frac{g_{33}d_{33}}{S_{33}^E}. \tag{4.24}$$

Recall that large values of K_{33} are associated with various goodness criteria.

K_{33} can be related to ω_m and ω_n as follows (see Sec. A.4 for more detailed derivation). The ratio of Eqs. (5.24) and (5.27) forms an expression for ω_n^2/ω_m^2. Since this quantity is squared, it must necessarily be greater than zero.

$$\frac{\omega_n^2}{\omega_m^2} = \frac{C_e}{C_e'} > 0. \tag{5.28}$$

This expression, plus the following three equations from other parts of this report:

$$C_e = S_{33}^E \frac{L}{A_c} + C_F, \tag{4.18}$$

$$C_e' = S_{33}^D \frac{L}{A_c} + C_F, \tag{5.18}$$

and

$$S_{33}^D = S_{33}^E - g_{33}d_{33}, \tag{4.4}$$

can be used to rewrite Eq. (5.28). (See Sec. A.4.)

$$\frac{\omega_n^2}{\omega_m^2} = \frac{S_{33}^E \frac{L}{A_c} + C_F}{S_{33}^D \frac{L}{A_c} + C_F} > 0 \tag{5.29}$$

then

$$\frac{\omega_n^2}{\omega_m^2} = \frac{1}{1 - \frac{g_{33}d_{33}}{S_{33}^E}\left(\frac{1}{1 + \frac{C_F A_c}{S_{33}^E L}}\right)} > 0. \tag{5.30}$$

Thus, substitution of the definition of K_{33} will yield the desired relationship between the in-air resonant frequencies and the coupling coefficient.

$$\frac{\omega_n}{\omega_m} = \frac{1}{\sqrt{1 - K_{33}^2\left(\frac{1}{1 + \frac{C_F A_c}{S_{33}^E L}}\right)}} > 0. \tag{5.31}$$

Limits can be placed on the value of the quantity under the radical sign by noticing that by definition C_F, A_c, S_{33}^E, and L are positive numbers. K_{33} is squared and, therefore, positive. In order for the inequality to be preserved in Eq. (5.31), it is necessary that

$$0 < 1 - K_{33}^2\left(\frac{1}{1 + \frac{C_F A_c}{S_{33}^E L}}\right) < 1. \tag{5.32}$$

From examination of Eqs (5.31) and (5.32), it is clear that

$$\omega_m < \omega_n. \tag{5.33}$$

Recalling the definition of C, the CSA short-circuit compliance,

$$C = \frac{S_{33}^E L}{A_c}. \tag{4.2a}$$

Equation (5.31) could be expressed as

$$\frac{\omega_n}{\omega_m} = \frac{1}{\sqrt{1 - K_{33}^2 \left(\frac{1}{1 + \frac{C_F}{C}} \right)}} . \qquad \textbf{(5.31a)}$$

In conclusion, we can make the following observations about the relationship between K_{33} and the resonant frequencies. If K_{33} is increased, ω_n/ω_m increases. This last observation suggests that increasing ω_n/ω_m should be accepted as a goodness criteria (ω_n/ω_m is often used in discussions of the "effective coupling coefficient"). Note that decreasing C_F also increases ω_n/ω_m. If increasing K_{33} is accepted as a goodness criteria, then decreasing C_F should also be accepted as a goodness criteria. This suggests that eliminating the fiberglass washer is good from the point of view of increasing the "effective coupling coefficient." Said another way, increasing C_F decreases the effective coupling coefficient. Recall (Sec. 4.3.2.1), however, that retention of a minimum FTR compliance was recommended to make the transducer reproducible on a production basis.

5.2.2.1.2 *In-Water Performance at ω_n and ω_m* - If one examines the in-water performance at the in-air resonance frequency ω_m, it is found that $|E/V_H|$ is proportional to the magnitude of the radiation impedance $|Z_r|$ and that the magnitude of the voltage $|E|$ is proportional to the magnitude of the radiation force $|F_r|$. These observations are independent of the form assumed for Z_r.

A derivation is presented in Sec. A.5 which shows that

$$\left| \frac{E}{V_H} \right|_{\omega = \omega_m} = \frac{1}{\omega_m^2 N d_{33} m_H} |Z_{rm}| \qquad \textbf{(5.34)}$$

In Eq. (5.34), Z_{rm} is the value of the radiation impedance at $\omega = \omega_m$. The above relationship between the magnitude of E/V_H and the magnitude of Z_{rm} was derived without making any assumptions about the form of the radiation impedance Z_r.

According to Eq. (5.34), if ω_m is held fixed [e.g., by adjusting C_e and/or m_T in Eq. (5.24)] then the bigger the head mass, m_H, the better: that is, the bigger the head mass, the less voltage E required for a given velocity V_H. Said another way, the bigger the head mass, the greater the source level for a given voltage E on the CSA. This result was at first suprising in that it seemed to violate experience gained using the sophisticated computerized models; namely, the idea that smaller head masses are always better. This point will be cleared up in Secs. 5.2.2.6 and 5.2.2.6.2.1 where it is shown that although a larger head mass improves the voltage to radiation velocity ratio, it also decreases a certain bandwidth flatness criteria. Thus, in this example, the simple model is not in disagreement with experience, but is, in fact, helping to provide further insight concerning observed trends.

Partly because of this, at first "strange" example in which "bigger head masses were better," this example was chosen as the first candidate applications of the computer program SGM-A1 to be used to "test" and "explore" the paper and pencil derived design aids and insights of Sec. 5. The SGM-A1 predictions are presented in Appendix B. Another reason for choosing this example as the first candidate application of the computer program SGM-A1 was because there was essentially no doubt that the above pencil and paper derivaton was correct and, thus, this example served to check the "new" computer

program, SGM-A1. The SGM-A1 predictions agreed with the above indicated pencil and paper derivation. In addition, the SGM-A1 predictions indicated that the pencil and paper example in which "bigger head masses were better" was not confined to some extremely narrow frequency band near ω_m (more details are presented in Appendix B).

For future purposes, it is useful to examine further the requirements of Eq. (5.24) in order to hold ω_m fixed as m_H is increased. Examination of Eq. (5.24) shows that one way to hold ω_m fixed is to decrease m_T as m_H is increased; another way is to decrease C_e as m_H is increased. According to Eq. (4.18), $C_e = C_F + C$, so one way to decrease C_e is to decrease the compliance of the FTR, C_F. Once C_F is reduced to zero (no FTR), then C_e could only be reduced by reducing C. According to Eq. (4.2a), $C = S_{33}^E L/A_c$; therefore, C could be reduced either by increasing the ceramic ring area A_c or reducing the length, L, of the CSA. Since reducing L would increase the electric field on the ceramic rings, one would prefer to increase A_c. Note that holding L fixed and increasing A_c would increase the volume of the ceramic material. Note also that none of the quantities m_T, L, or A_c are contained in Eq. (5.34) so changing these quantities does not change $|E/V_H|$ at $\omega = \omega_m$.

Equation (5.34) can be re-arranged to display the relationship of the drive voltage to the magnitude of the radiation force.

$$|E|_{\omega=\omega_m\ (in\text{-}water)} = \frac{|Z_{rm}|\,|V_H|}{\omega_m^2 N d_{33} m_H}. \tag{5.35}$$

Since the radiation force is given by $F_r = V_H Z_r$,

$$|F_r| = |V_H|\,|Z_r|, \tag{5.36}$$

we can see that

$$|E|_{\omega=\omega_m\ (in\text{-}water)} = \frac{|F_{rm}|}{\omega_m^2 N d_{33} m_H}. \tag{5.37}$$

In Eq. (5.37), F_{rm} is the value of F_r at $\omega = \omega_m$. Equation (5.37) shows that at $\omega = \omega_m$ when the transducer is operating in water, the magnitude of the drive voltage $|E|$ is proportional to the magnitude of the radiation force $|F_r|$. (A similar derivation can be conducted with E and F_r showing that E is proportional by a complex constant to F_r.)

Analogous relationships can be derived for the in-water performance for operation at the in-air resonance frequency ($\omega = \omega_n$). These are derived in Sec. A.5. The resulting relationships are summarized below.

$$\left|\frac{I}{V_H}\right| = \frac{A_c}{g_{33} l_c \omega_n m_H}\,|Z_{rn}|. \tag{5.38}$$

$$|I| = \frac{A_c |F_{rn}|}{g_{33}\, 1_c\, \omega_n\, m_H}. \tag{5.38a}$$

5.2.2.2 In-Water Phase Zero Crossing Frequency - ω_{eO} (also ω_{i9O})

Another special case of interest is the frequency, ω_{eO}, such that the phase angle between E and V_H is zero. When the phase angle between E and V_H is zero, the imaginary component of Eq. (5.10) goes to zero. Let E_{oa} be the value of E_o when the phase angle is zero. Then,

$$E_{oa} = \frac{1}{m}. \tag{5.39}$$

From the definition of E_o, [Eq. (5.11)], it can be seen that at the in-water phase zero crossing the angular frequency must be given by

$$\omega_{eO}^2 = \frac{1}{C_e}\left(\frac{1}{m} + \frac{1}{m_T}\right). \tag{5.40}$$

At $\omega = \omega_{eO}$, one obtains

$$\left|\frac{E}{V_H}\right|_{\omega=\omega_{eO}} = \frac{1}{\omega_{eO} N d_{33}} \frac{r}{m}. \tag{5.41}$$

Since in water $m = m_H + x$ and if $x \geq 0$ (see below), one finds, as in the case of ω_m, that for $\omega = \omega_{eO}$ bigger m_H is better in the sense that less voltage E is required to achieve a given velocity V_H. One reason for interest in ω_{eO} is that if r is small enough, then the phase zero crossing frequency is not much different than the in-water resonance frequency, ω_m, for the quantity $|E/V_H|$. An expression will be derived for ω_m, and it will be found that ω_m is a much more complicated function of C_e, m_H and m_T than that for ω_{eO} given by Eq. (5.40). For later purposes, also note that Eq. (5.40) may be written as

$$\omega_{eO}^2 = \frac{1}{C_e}\sqrt{\frac{1}{m^2} + \frac{1}{m_T^2} + \frac{2}{m m_T}}. \tag{5.42}$$

In general, the effective mass contributed by the radiation loading is greater than zero (although for a given frequency within an array there may be positions of some elements where $x \leq 0$). For $x > 0$, note that

$$\omega_{eO} < \omega_m , \tag{5.43}$$

as shown by comparison of Eqs. (5.24) and (5.40).

$$\omega_m^2 = \frac{1}{C_e}\left(\frac{1}{m_H} + \frac{1}{m_T}\right) > \frac{1}{C_e}\left(\frac{1}{m_H + x} + \frac{1}{m_T}\right) = \omega_{eO}^2 . \tag{5.44}$$

Similar results hold for I/V_H. In this case, there is a frequency, ω_{i90}, such that the phase angle between I and V_H is 90^O (not 0^o as in the case of E/V_H). Note that for this case the real part of I/V_H must be zero. The corresponding equations for this case are shown as Eqs. (5.45), (5.46), (5.47), and (5.48).

Referring back to Eq. (5.16),

$$\left|\frac{I}{V_H}\right|_{\omega=\omega_{i90}} = \frac{A_c}{g_{33} l_c}\,\frac{r}{m} . \tag{5.45}$$

and

$$I_{oa} = \frac{1}{m} . \tag{5.46}$$

From the definition of I_o [Eq. (5.17)], it can be seen that

$$\omega_{i90}^2 = \frac{1}{C_e'}\left(\frac{1}{m} + \frac{1}{m_T}\right). \tag{5.47}$$

After comparing Eq. (5.47) to Eq. (5.27), one finds that

$$\omega_{i90} < \omega_n . \tag{5.48}$$

With some slight reinterpretation, the above results concerning ω_{e0} and ω_{i90} hold for a more general frequency dependence for Z_r.

For the simple frequency dependence assumed for Z_r, one notes that

$$\frac{\omega_{i90}^2}{\omega_{eO}^2} = \frac{C_e}{C_e'} = \frac{\omega_n^2}{\omega_m^2} . \tag{5.49}$$

Thus, the relation between ω_{i90}/ω_{eO} and coupling coefficient, K_{33}, is the same as for $\omega_n\ \omega_m$. However, for a more general frequency dependence, this may not be true.

5.2.2.3 Velocity Control Frequencies - ω_{ev} and ω_{iv}

Another pair of special frequencies of interest are called the "velocity control" frequencies. These frequencies are of interest because the applied voltage and the input current are proportional to the velocity of the radiating face and independent of the radiation impedance. Furthermore, it will later be shown (Sec. 5.3) that an inductor may be chosen to adjust one or the other of these velocity control frequencies to any selected value.

The velocity control frequency for E/V_H occurs where E_o in Eq. (5.12) is zero.

$$E_{ov} = 0. \tag{5.50}$$

The corresponding frequency is obtained by substituting the condition above into Eq. (5.11) and solving for the velocity control frequency ω_{ev}.

$$\omega_{ev}^2 = \frac{1}{C_e m_T}. \tag{5.51}$$

When the magnitude of E/V_H is evaluated at ω_{ev}, we obtain

$$\left|\frac{E}{V_H}\right|_{\omega=\omega_{ev}} = \frac{1}{\omega_{ev} N d_{33}}. \tag{5.52}$$

From the above equation, it is apparent that not only is the velocity V_H proportional to E and independent of the radiation loading (i.e., independent of r and x), but for this special case of a mass-like head device, the velocity is independent of m_H.

A similar situation holds for $|I/V_H|$, the current velocity control frequency. The equations corresponding to Eqs. (5.50), (5.51), and (5.52) are shown here without derivation.

$$I_{iv} = 0, \tag{5.53}$$

$$\omega_{iv}^2 = \frac{1}{C_e' m_T}, \tag{5.54}$$

and

$$\left|\frac{I}{V_H}\right|_{\omega=\omega_{iv}} = \frac{A_c}{g_{33} l_c}. \tag{5.55}$$

Thus, the relationship between ω_{iv}/ω_{ev} and coupling coefficient K_{33} is the same as for ω_n/ω_m [Eq. (5.31)]. This can be seen by taking the ratio of Eqs. (5.51) and (5.54).

$$\frac{\omega_{iv}^2}{\omega_{ev}^2} = \frac{C_e}{C_e'} = \frac{\omega_n^2}{\omega_m^2}. \tag{5.56}$$

With some slight reinterpretation, the above results concerning ω_{ev} and ω_{iv} hold for a more general frequency dependence for Z_r.

5.2.2.4 Characterization of B_1 and B_2

At the end of Sec. 5.2.1, it was noted that if one characterizes either B_1 or B_2 [see Eqs. (5.13) and (5.20)], then one would know all about the frequency dependence of the quantity $|I/V_H|$ and a great deal about the frequency dependence of the quantities $|E/V_H|$ and $|\varepsilon/V_H|$ (where ε is the electric field on the CSA). In fact, it turns out that for many practical values of m_H and m_T, the frequency dependence of $|E/V_H|$ and/or $|\varepsilon/V_H|$ is qualitatively very similar to that of B_1. Full characterization of the frequency dependence of $|E/V_H|$; i.e., B_1, is a more difficult problem, so characterization of $|I/V_H|$; i.e., B_2, was considered first.

5.2.2.4.1 *Bandwidth Characterization of $|I/V_H|$ using Frequency ω_i (Resonance Frequency for $|I/V_H|$) to Minimize B_2* - The quantity B_2 can be characterized (see Sec. A.6) by finding the equation for the frequency ω_i which minimizes $(B_2)^{1/2}$. Since all the frequency dependence of $|I/V_H|$ is contained in B_2, ω_i is also the resonance frequency of $|I/V_H|$. One forms the partial derivative $\delta(B_2)^{1/2}/\delta\omega$ and sets this partial derivative equal to zero. The solution of that equation yields

$$\omega_i^2 = \frac{1}{C_e'}\left[\frac{m}{r^2 + m^2} + \frac{1}{m_T}\right]. \tag{5.57}$$

In the case of $|I/V_H|$ (as opposed to $|E/V_H|$, $|\varepsilon/V_H|$ and B_1), the frequency which minimizes $(B_2)^{1/2}$, ω_i, is actually the resonance frequency for $|I/V_H|$. This is true because, unlike $|E/V_H|$, all the frequency dependence for $|I/V_H|$ is contained in B_2. In terms of the resonance frequency, ω_i, one may write (see Sec. A.7) $|I/V_H|$ as shown below.

$$\left|\frac{I}{V_H}\right| = \frac{A_c}{g_{33}1_c}\sqrt{(r^2 + m^2)(\omega^2 - \omega_i^2)^2 (C_e')^2 + \frac{r^2}{r^2 + m^2}}. \tag{5.58}$$

At $\omega = \omega_i$, one obtains

$$\left|\frac{I}{V_H}\right|_{\omega=\omega_i} = \frac{A_c}{g_{33}1_c}\sqrt{\frac{r^2}{r^2 + m^2}}. \tag{5.59}$$

As with certain other special cases noted above, Eq. (5.59) leads to what may at first seem like a strange conclusion; namely, at least for some frequency region around the frequency $\omega_{i,}$, if $A_c/1_c$ is held fixed, then bigger head masses lead to a lower current for a given velocity V_H and, thus, for a given source level

per ampere. Of course, as m is changed, either C_e' or m_T or both (r is assumed fixed) must be changed to satisfy the requirements of Eq. (5.57) to maintain ω_i constant. For m > r, then as m increases, m_T or C_e' must be decreased. The compliance C_e could be decreased without changing L/A_c by reducing the thickness of the FTR (that is, by reducing C_F). However, once $C_F = 0$ (i.e., no FTR), then one must consider the reduction in the value of L/A_c necessary to further reduce C_e'; even when this is done, one finds that the limiting value of $|I/V_H|$, at $\omega = \omega_i$ with ω_i fixed, is zero.

The bandwidth characteristics of $|I/V_H|$ were investigated further by fixing ω_i and considering a bandwidth defined at two frequency band end-points, a lower frequency $\omega_L < \omega_i$ and an upper frequency $\omega_U > \omega_i$. At ω_L, the quantity $|I/V_H|$ was forced to be some fixed multiple, G_L', of the value at resonance.

$$\left|\frac{I}{V_H}\right|_{\omega=\omega_L} = G_L' \left|\frac{I}{V_H}\right|_{\omega=\omega_i}, \tag{5.60}$$

where

$$G_L' > 1. \tag{5.61}$$

Similarly, at ω_U the quantity $|I/V_H|$ was constrained as shown below.

$$\left|\frac{I}{V_H}\right|_{\omega=\omega_U} = G_U' \left|\frac{I}{V_H}\right|_{\omega=\omega_i}, \tag{5.62}$$

where

$$G_U' > 1. \tag{5.63}$$

It can be shown (Sec. A.8) that the bandwidth, defined as $\omega_U - \omega_L$ for a fixed value of ω_i, increases as the head mass m_H decreases. That is, as far as this bandwidth criteria is concerned, smaller head masses are better. This agrees with previous experience using more sophisticated models.

5.2.2.4.2 *Frequency ω_{ei} to Minimize B_1* - The quantity B_1 as it relates to $|E/V_H|$ is characterized by finding the equation for the frequency ω_{ei} which minimizes $(B_1)^{1/2}$. After the obvious change of variables, the steps in deriving ω_{ei} are the same as those for deriving ω_i (Sec. A.6). One forms the partial derivative $\delta(B_1)^{1/2}/(\delta\omega)$, and sets this partial derivative equal to zero. The solution of this equation for ω_{ei} yields

$$\omega_{ei}^2 = \frac{1}{C_e}\left(\frac{m}{r^2 + m^2} + \frac{1}{m_T}\right). \tag{5.64}$$

It is important to keep in mind that ω_{ei} is not the resonance frequency for $|E/V_H|$ or $|\varepsilon/V_H|$ (see ω_e discussion in Sec. 5.2.2.5). Even though ω_{ei} is not the resonance frequency for $|E/V_H|$, it is shown in Secs. 5.2.2.6.1 and A.12 that the quantity ω_{ei} can be used to provide some insight concerning the frequency characterization of $|E/V_H|$ and some insight into corresponding design trends as such things as m, m_T, and C_e are varied.

For convenience, it is useful to gather terms together and define a quantity M_1 as

$$M_1 = \frac{m}{r^2 + m^2} + \frac{1}{m_T}, \tag{5.65}$$

so that Eq. (5.64) can be written in the shorter form

$$\omega_{ei}^2 = \frac{1}{C_e} M_1 . \tag{5.66}$$

The magnitude of E/V_H can be expressed (Sec. A. 9) in the following form:

$$\left|\frac{E}{V_H}\right| = \frac{1}{\omega N d_{33}} \sqrt{(r^2 + m^2)(\omega^2 - \omega_{ei}^2)^2 C_e^2 + \frac{r^2}{r^2 + m^2}} . \tag{5.67}$$

At the frequency $\omega = \omega_{ei}$, the magnitude of $|E/V_H|$ reduced to

$$\left|\frac{E}{V_H}\right|_{\omega = \omega_{ei}} = \frac{1}{\omega_{ei} N d_{33}} \sqrt{\frac{r^2}{r^2 + m^2}} . \tag{5.68}$$

Equation (5.67) is most useful when both ω_{ei} and C_e are fixed. However, if C_e is allowed to vary, it is convenient to remove the apparent dependence upon C_e through the substitution of Eq. (5.66) in Eq. (5.67) to yield

$$\left|\frac{E}{V_H}\right| = \frac{1}{\omega N d_{33}} \sqrt{(r^2 + m^2)(\omega^2 - \omega_{ei}^2)^2 \frac{1}{\omega_{ei}^4} M_1^2 + \frac{r^2}{r^2 + m^2}} . \tag{5.69}$$

The electric field ε on the ceramic is given by

$$\epsilon = \frac{E}{1_c}, \tag{5.70}$$

where the quantity 1_c is the length of a ceramic ring. The various equations for ε/V_H are almost the same as those for E/V_H. The only difference is that in the multiplier $(1/\omega N d_{33})$, N is replaced by L where the quantity $L = N1_c$ is the total length of the CSA. For instance, the equations for ε/V_H corresponding to Eqs. (5.10) and (5.14) for E/V_H are as follows:

$$\frac{\epsilon}{V_H} = \frac{1}{\omega L d_{33}} [r E_o - i(1 - m E_o)], \tag{5.71}$$

and

$$\left|\frac{\epsilon}{V_H}\right| = \frac{1}{\omega L d_{33}} \sqrt{B_1} . \tag{5.72}$$

Similarly, Eqs. (5.74), (5.68), and (5.69) are related to Eqs. (5.73), (5.74), and (5.73a) presented below.

$$\left|\frac{\epsilon}{V_H}\right| = \frac{1}{\omega L d_{33}} \sqrt{(r^2 + m^2)(\omega^2 - \omega_{ei}^2)^2 C_e^2 + \frac{r^2}{r^2 + m^2}}, \tag{5.73}$$

$$\left|\frac{\epsilon}{V_H}\right| = \frac{1}{\omega L d_{33}} \sqrt{(r^2 + m^2)(\omega - \omega_{ei}^2)^2 \frac{1}{\omega_{ei}^4} M_1^2 + \frac{r^2}{r^2 + m^2}}, \tag{5.73a}$$

and

$$\left|\frac{\epsilon}{V_H}\right|_{\omega=\omega_{ei}} = \frac{1}{\omega_{ei} L d_{33}} \sqrt{\frac{r^2}{r^2 + m^2}}. \tag{5.74}$$

Since L (the length of the CSA) is a more fundamental design constraint than N (the number of rings in the CSA), the characterization of the frequency dependence implications of B_1 is more instructive in terms of ε/V_H instead of E/V_H. This characterization of B_1 is indicated below and, for more detailed elements of the derivation, see Sec. A.11.

Once again, we notice that somewhat contrary to general experience, Eq. (5.74) suggests that the larger head mass is an advantage. That is, for some frequency region around the frequency ω_{ei}, bigger head masses lead to a lower electric field for a given velocity V_H and, thus, for a given source level. On the other hand, as we shall see, when the bandwidth characteristics of $|\varepsilon/V_H|$ and $|E/V_H|$ are taken into consideration, it is clear that the larger head mass also decreases the bandwidth.

It is interesting to form the ratio ω_i/ω_{ei} from Eqs. (5.57) and (5.64). It can be seen that

$$\frac{\omega_i^2}{\omega_{ei}^2} + \frac{C_e}{C_e'} = \frac{\omega_n^2}{\omega_m^2}. \tag{5.75}$$

Thus, the relation between ω_i/ω_{ei} and coupling coefficient K_{33} is the same as that identified for ω_n/ω_m [Eq. (5.32)].

5.2.2.5 In-water Resonance Frequency for $|E/V_H|$ and $|\varepsilon/V_H|$ - ω_e

To derive an expression for the in-water resonance frequency (ω_e) for the quantities $|E/V_H|$ and $|\varepsilon/V_H|$, one forms the partial derivative $(\delta|E/V_H|)/\delta\omega)$, sets this partial derivative equal to zero, and solves for ω_e. (See Sec. A.10).

$$\omega_e^2 = \frac{1}{C_e} \sqrt{\frac{r^2 + (m + m_T)^2}{m_T^2 (r^2 + m^2)}}. \tag{5.76}$$

As previously stated, ω_e, the in-water resonant frequency for the quantities $|E/V_H|$ or $|\varepsilon/V_H|$ is different from ω_{ei}. However, it turns out that for many practical values of the design parameters such as r, x, m_H, and m_T, there is close correspondence between $|E/V_H|$ expressed as a function of the in-water

resonant frequency ω_e and $|E/V_H|$ expressed as a function of the frequency ω_{ei} which minimizes B_1. To help reveal this relation, Eq. (5.76) may be put in the form

$$\omega_e^2 = \omega_{ei}^2 \sqrt{1 + M_2^2}, \tag{5.77}$$

with M_2 given by

$$M_2 \equiv \frac{rm_T}{r^2 + m^2 + mm_T}. \tag{5.78}$$

Using Eqs. (5.24) and (5.77), it turns out that $|E/V_H|$ may be rewritten (see Sec. A.10) in terms of ω_e as

$$\left|\frac{E}{V_H}\right| = \frac{1}{\omega N d_{33}} \sqrt{(r^2 + m^2)\left(\omega^2\sqrt{1 + M_2^2} - \omega_e^2\right)^2 \frac{M_1^2}{\omega_e^4} + \frac{r^2}{r^2 + m^2}}. \tag{5.79}$$

Suppose the design variables are such that the condition

$$M_2 << 1 \tag{5.80}$$

is satisfied; then ω_e and ω_{ei} are approximately the same frequency [see Eq. (5.77)], and Eqs. (5.69) and (5.79) are essentially the same equation. As is explained in Secs. 5.2.2.6.1 and A.12, such conditions for which ω_{ei} is "sufficiently close" to ω_e form the basis for a useful approximation to study the bandwidth characteristics of $|E/V_H|$ and $|\varepsilon/V_H|$.

There are certainly values of design variables for which Eq. (5.80) is not true and, thus, ω_{ei} would not be "close to" ω_e. For example, suppose that m could be made as close to zero as desired. Then the conditions of Eq. (5.80) would not be met (for large enough values of m_T), and the design trends associated with fixed ω_{ei} would not then be expected to hold for fixed ω_e. Numerical tests were consistent with this assertion. For example, for very small m and fixed ω_e, it was found that larger m_T required longer CSA's in order to meet a given electric field requirement at ω_e.

Based on some of the other special cases considered above (e.g., $|E/V_H|$ at $\omega = \omega_{eO}$ or $\omega = \omega_{ei}$), one would expect that as m_H is made larger and larger with $\omega = \omega_e$, then $|E/V_H|$ as given by Eq. (5.79) would approach zero; that is, the voltage required for a given velocity or source level would decrease as m_H increases. With the help of one application of l'Hospital's rule (Sec. A.11), one can indeed show for a given tail mass that at $\omega = \omega_e$ then $|E/V_H|$ approaches zero as m_H approaches infinity. Also, an alternate direct proof is discussed in Sec. 5.2.2.6.2.1.2.

As just indicated, for this example of in-water performance at $\omega=\omega_e$ and with a fixed value of ω_e, the pencil and paper derivation of the proof that "bigger head masses are better" is more complicated than for previously considered examples. Because of this greater complexity and because of the importance of the in-water resonance frequency ω_e this $\omega=\omega_e$ example was chosen as the second candidate applications of the computer program SGM-A1 to be used to "test" and "explore" the paper and pencil derived design aids and insights. In addition, the SGM-A1 predictions again indicated that pencil and

paper example in which bigger head masses were better was not confined to some extremely narrow frequency band (see Appendix B, for more details).

The ratio ω_i/ω_e is obtained from Eqs. (5.75) and (5.77).

$$\frac{\omega_i^2}{\omega_e^2} = \frac{\omega_i^2}{\omega_{ei}^2}(1 + M_2^2)^{-1/2} + \frac{C_e}{C_e'}(1 + M_2^2)^{-1/2} = \frac{\omega_n^2}{\omega_m^2}(1 + M_2^2)^{-1/2} \tag{5.81}$$

In this case, we note that if Eq. (5.80) is satisfied; i.e., if $M_2 \ll 1$, then the relation between ω_i/ω_e and coupling coefficients K_{33} is nearly the same as for ω_n/ω_m [Eq. (5.30)]. If this condition on M_2 does not hold, then the effective coupling coefficient as represented by ω_i/ω_e will be less than that represented by ω_n/ω_m.

If $m > 0$ (that is, $x > 0$) and $r \neq 0$, then $\omega_e < \omega_{eo}$. To see this, start with a form equivalent to Eq. (5.76).

$$\omega_e^2 = \frac{1}{C_e}\sqrt{\frac{1}{r^2 + m^2} + \frac{1}{m_T^2} + \frac{2m}{m_T(r^2 + m^2)}}, \tag{5.82}$$

but

$$\frac{2m}{m_T(r^2 + m^2)} < \frac{2m}{m_T m^2} = \frac{2}{m m_T}, \tag{5.83}$$

and

$$\frac{1}{r^2 + m^2} < \frac{1}{m^2}. \tag{5.84}$$

Thus, using Eq. (5.42) for ω_{eo},

$$\omega_e^2 < \frac{1}{C_e}\sqrt{\frac{1}{m^2} + \frac{1}{m_T^2} + \frac{2}{m m_T}} = \omega_{eo}^2. \tag{5.85}$$

Examination of Eqs. (5.77) and (5.78) (for $r \neq 0$) shows that $\omega_{ei} < \omega_e$ [Eq. (5.86)].

$$\omega_{ei} < \omega_e. \tag{5.86}$$

For the case where $r \neq 0$, one may summarize the relative magnitudes for ω_{ei}, ω_e, and ω_{eo} as

$$\omega_{ei} < \omega_e < \omega_{eo}. \tag{5.87}$$

By comparing Eqs. (5.40), (5.61), and (5.76), one observes that as r approaches zero (that is, for small enough values of r), then ω_{ei}, ω_e, and ω_{eo} are nearly the same frequency. This point is summarized as: if $r \to 0$, then $\omega_{ei} \to \omega_e \to \omega_{eo}$, and as $r \to 0$.

$$\omega_{ei} \simeq \omega_e \simeq \omega_{eo} . \tag{5.88}$$

5.2.2.6 Bandwidth Characterization of $|E/V_H|$ and $|\varepsilon/V_H|$

It turns out that bandwidth characterization of $|E/V_H|$ and $|\varepsilon/V_H|$ is more difficult than that of $|I/V_H|$ (Sec. 5.2.2.4.1) because of the additional factor $1/\omega$ presents in the frequency dependency of $|E/V_H|$ and $|\varepsilon/V_H|$ (the last paragraph of Sec. 5.2.1). For this reason, it was found expedient and useful to consider certain approximations and/or special cases. The first consideration (Sec. 5.2.2.6.1) was based on an approximation involving ω_{ei}. The second consideration (Sec. 5.2.2.6.2) was based on two special cases of a more exact approach (involving ω_e) which we call the Fixed End-Points Analysis (FEPA). The FEPA is not only more exact but it also strongly suggests a very useful TDGS - see also Secs. 2, 3 and 5.2.2.6.2).

5.2.2.6.1 *Approximate Characterization of $|E/V_H|$ and $|\varepsilon/V_H|$ Using ω_{ei}* - One useful approximation was suggested by the discussion associated with Eqs. (5.77), (5.79), and (5.80) for conditions such that ω_{ei} is sufficiently "close" to the resonance frequency, ω_e, for $|E/V_H|$ and $|\varepsilon/V_H|$; then, a bandwidth analysis in which ω_{ei} is fixed and similar to that presented in Secs. 5.2.2.4.1 and A.8 for $|I/V_H|$, is instructive and useful.

As a first step, we must be more precise about the conditions to be considered under which ω_{ei} is sufficiently close to ω_e. Rearrange Eq. (5.78) as follows:

$$M_2 = \frac{r}{\dfrac{r^2 + m^2}{m_T} + m} . \tag{5.78a}$$

Suppose relatively large tail masses, m_T, are being considered such that

$$\frac{r^2 + m^2}{m_T} << m ; \tag{5.80a}$$

that is,

$$m_T >> \frac{r^2 + m^2}{m} , \tag{5.80b}$$

then

$$M_2 \simeq \frac{r}{m} . \tag{5.78b}$$

If

$$\frac{r}{m} << 1; \tag{5.78c}$$

i.e., if

$$r << m, \tag{5.78d}$$

then Eq. (5.80) holds (i.e., $M_2 << 1$).

Note also that Eq. (5.80b) may be written as

$$m_T >> \frac{r^2}{m} + m \tag{5.80c}$$

which implies

$$m_T >> m. \tag{5.80d}$$

Thus, the conditions under which ω_{ei} is sufficiently close to ω_e shall be taken to mean

Condition A:

$$m_T >> \frac{r^2 + m^2}{m} > m. \tag{5.80e}$$

Condition B:

$$r << m. \tag{5.78d}$$

In other words, we are considering large tail mass, m_T, compared to the quantity m. Recall $m = m_H + x$ [Eq. (5.7)] and that typically $x > 0$. Thus, Condition A [Eq. (5.80e)] typically is equivalent to considering large tail masses, m_T, compared to the head mass m_H. Practical experience indicates that the usual values of r attainable versus the limits on making m_H small; for example, due to flexing, radiating head masses mean that Condition B [Eq. (5.78d)] is a practical reality. Condition A [Eq. (5.80e)] is also achievable and is known to often be the outcome of a practical transducer design exercise.

When ω_{ei} is sufficiently close to the actual resonance frequency ω_e for $|E/V_H|$ and $|\epsilon/V_H|$, then it makes some sense to consider conditions analogous those in Eqs. (5.60), (5.61), (5.62), and (5.63). Consider ω_{ei} to be fixed and a lower frequency $\omega_L < \omega_{ei}$ and an upper frequency $\omega_U > \omega_{ei}$. At these two frequency band end-points, assume that the magnitude of the $|\epsilon/V_H|$ is forced to satisfy the following:

$$\left|\frac{\epsilon}{V_H}\right|_{\omega=\omega_L} = G_L \left|\frac{\epsilon}{V_H}\right|_{\omega=\omega_{ei}}, \tag{5.89}$$

and

$$\left|\frac{\epsilon}{V_H}\right|_{\omega=\omega_U} = G_U \left|\frac{\epsilon}{V_H}\right|_{\omega=\omega_{ei}} . \tag{5.90}$$

where G_L and G_U are constants. Since ω_{ei} is close to ω_e (by assumption), it makes some sense to consider the special values of ω_L and ω_U for which G_L and G_U also satisfy the following:

$$G_L > 1 . \tag{5.91}$$

$$G_U > 1 . \tag{5.92}$$

[Equations (5.91) and (5.92) would always be true if we were considering the resonance angular frequency, ω_e, instead of ω_{ei}.] For those limited conditions under which ω_{ei} is sufficiently close to ω_e and Eqs. (5.91) and (5.92) hold, one can characterize a bandwidth as $\omega_U - \omega_L$ for fixed ω_{ei} much as was done for $|I/V_H|$ in Secs. 5.2.2.4.1 and A.8.

The details of this bandwidth characterization of $|\varepsilon/V_H|$ and $|E/V_H|$ are derived in Sec. A.12. Some of the main results [at least for the limited conditions under which Eqs. (5.91) and (5.92) are valid] are as follows:

Larger tail masses, m_T, increase the bandwidth, $\omega_U - \omega_L$, and there is no penalty on the electric field if the mass of the head, m_H, is held fixed. However, with m_H held fixed and as m_T is increased, one must decrease the compliance, C_e, to hold ω_{ei} fixed. This can be done up to a point by decreasing C_F (using a thinner FTR). If further compliance reduction is needed, it should be accomplished using a larger ceramic ring area, A_c.

Smaller head masses, m_H, increase the bandwidth as long as the condition $m > r$ is met. However, there is an electric field penalty as the value of m_H is reduced. One way to avoid this electric field penalty is to increase the length, L, of the CSA and at the same time, increase the area A_c so as to hold the ratio L/A_c constant. With this adjustment, the real penalty is the increase in L which in many designs problems tends to quickly violate the practical constraints upon the length of the transducer design.

5.2.2.6.2 *Fixed End Point Analysis* - In each of the above mentioned bandwidth analyses, a certain chosen frequency was held fixed. In the following analysis, the frequencies ω_L and ω_U at the end points of the frequency band are held fixed and the required values of $|\varepsilon/V_H|$ at ω_L and ω_U are also held fixed. For convenience, this analysis will be referred to as a FEPA. Within the limits of the augmented SGM, the FEPA is exact; that is, no additional approximations are made. Also, full consideration of the fixed end-points analysis shows that all the necessary steps for a new and very useful TDGS - see also Secs. 2 and 3) are suggested by the FEPA. The new TDGS could and would be completely independent of the SGM. The new TDGS could and should be executed using the appropriate parts (transducer element model, array acoustic radiation interaction model, etc.) of the CMM (Composite Math Model - see Sec. 2) applicable to a given array design task. The essential idea of this independence from the SGM is illustrated in Sec. B.4)

In the FEPA, the resonance frequency, ω_e, was constrained to be between ω_L and ω_U as follows:

$$\omega_L < \omega_e < \omega_U. \tag{5.93}$$

In certain circumstances, one allowed

$$\omega_L \leq \omega_e, \tag{5.93a}$$

or

$$\omega_e \leq \omega_U. \tag{5.93b}$$

Because the resonance frequency was so constrained [Eq. (5.93)], it was assumed that achieving a given source level/ε at the edges of the band (that is, at ω_L and ω_U) was a limiting design constraint.

This FEPA not only automatically found a best location for ω_e, but provided insight into a method to arrive at the best choices for m_T and m_H. To help ensure that ω_e was, in fact, between ω_L and ω_U, the slope constraints shown as Eqs. (5.94) and (5.95) were applied.

$$\left.\frac{\delta\left|\frac{\epsilon}{V_H}\right|}{\delta\omega}\right|_{\omega=\omega_L} < 0 \tag{5.94}$$

and

$$\left.\frac{\delta\left|\frac{\epsilon}{V_H}\right|}{\delta\omega}\right|_{\omega=\omega_U} < 0. \tag{5.95}$$

For a given transducer design problem, the designer would determine the maximum piezoelectric ceramic electric field, say, ε_{max}, which the designer wished to allow. The designer would also determine the velocity magnitude of the radiating face needed at $\omega = \omega_L$, say $|V_H|_{\omega=\omega_L}$, and at $\omega = \omega_U$, say $|V_H|_{\omega=\omega_U}$, to achieve the desired sound level in the water. This would determine fixed values for $|\varepsilon/V_H|_{\omega=\omega_L}$ and $|V_H|_{\omega=\omega_U}$ as follows:

$$\left|\frac{\epsilon}{V_H}\right|_{\omega=\omega_L} = \frac{\epsilon_{max}}{|V_H|_{\omega=\omega_L}}, \tag{5.96}$$

and

$$\left|\frac{\epsilon}{V_H}\right|_{\omega=\omega_U} = \frac{\epsilon_{max}}{|V_H|_{\omega=\omega_U}}. \tag{5.97}$$

Recall Eq. (5.72).

$$\left|\frac{\epsilon}{V_H}\right| = \frac{1}{\omega d_{33} L}\sqrt{B_1}.$$

Use Eq. (5.72) to write

$$\left|\frac{\epsilon}{V_H}\right|_{\omega=\omega_L} = \frac{1}{\omega_L d_{33} L}\sqrt{B_{1L}}, \tag{5.98}$$

where B_{1L} is B_1 [see Eq. (5.13)] with $\omega = \omega_L$.

$$L\omega_L d_{33}\left|\frac{\epsilon}{V_H}\right|_{\omega=\omega_L} = \sqrt{B_{1L}}. \tag{5.99}$$

Let k_L be a constant defined as

$$k_L = \omega_L d_{33}\left|\frac{\epsilon}{V_H}\right|_{\omega=\omega_L}. \tag{5.100}$$

Use Eq. (5.100) to rewrite Eq. (5.99) as

$$L^2 k_L^2 = B_{1L}. \tag{5.101}$$

Similarly, define a constant k_U as

$$k_U = \omega_U d_{33}\left|\frac{\epsilon}{V_H}\right|_{\omega=\omega_U}, \tag{5.102}$$

and thus,

$$L^2 k_U^2 = B_{1U}. \tag{5.103}$$

5.2.2.6.2.1 *Use of An Equation for C_e for Fixed End Points Constraints to Study Bandwidth Characteristics* - In terms of the above described fixed end-points constraints, one may derive the following equation for the composite compliance C_e (see Sec. A.13):

$$C_e = -\frac{b_t}{2a_t} \pm \sqrt{\left(\frac{b_t}{2a_t}\right)^2 - \frac{c_t}{a_t}}, \tag{5.104}$$

where

$$a_t = (r^2 + m^2)(\omega_L^4 - \alpha^2\omega_U^4), \tag{5.105}$$

$$b_t = -2(\omega_L^2 - \alpha^2\omega_U^2)\left(\frac{r^2 + m^2}{m_T} + m\right), \tag{5.106}$$

$$c_t = \left(\frac{r^2 + m^2}{m_T^2} + \frac{2m}{m_T} + 1\right)(1 - \alpha^2), \tag{5.107}$$

and α is defined as

$$\alpha = \frac{k_L}{k_U}. \tag{5.108}$$

In principle, Eq. (5.104) for C_e could be used to study the bandwidth characteristics of $|\epsilon/V_H|$ (and also $|E/V_H|$) in general. However, only two special cases were analyzed. These two special cases are discussed next.

5.2.2.6.2.1.1 *Special Case 1 ($\alpha = 1$)* - Special Case 1 uses the value of C_e from Eq. (5.104) for the case where $\alpha = 1$ in Eq. (5.108). For $\alpha = 1$, note the following: Use Eqs. (5.100), (5.102), and (5.108) to write

$$\alpha = \frac{k_L}{k_U} = \frac{\omega_L d_{33}\left|\frac{\epsilon}{V_H}\right|_{\omega=\omega_L}}{\omega_U d_{33}\left|\frac{\epsilon}{V_H}\right|_{\omega=\omega_U}}. \tag{5.109}$$

But, with $\alpha = 1$, we obtain

$$\left|\frac{\epsilon}{V_H}\right|_{\omega=\omega_U} = \frac{\omega_L}{\omega_U}\left|\frac{\epsilon}{V_H}\right|_{\omega=\omega_L}. \tag{5.110}$$

Recall that at these end points (i.e., at ω_L and ω_U), we have set $\epsilon = \epsilon_{max}$. Therefore, we conclude that

$$|V_H|_{\omega=\omega_L} = \frac{\omega_L}{\omega_U}|V_H|_{\omega=\omega_U}. \tag{5.111}$$

Since $\omega_L < \omega_U$, we note that for $\alpha = 1$ (that is, Special Case 1), we have

$$|V_H|_{\omega=\omega_L} < |V_H|_{\omega=\omega_U}. \tag{5.111a}$$

and

$$\left.\frac{\delta\left|\frac{\epsilon}{V_H}\right|}{\delta\omega}\right|_{\omega=\omega_U} < 0, \tag{5.95}$$

then the above discussion for $\alpha = 1$ may be illustrated as shown in Fig. 5-1.

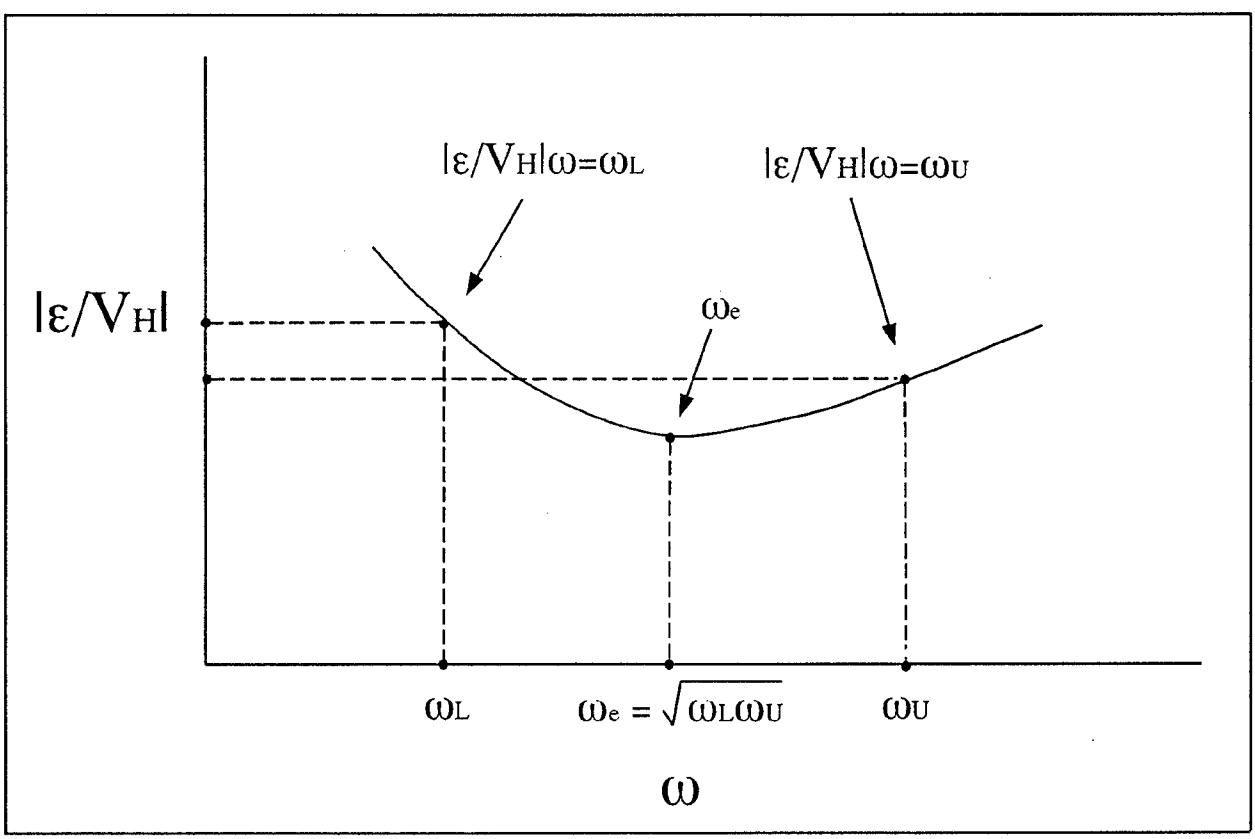

Fig. 5-1 — General shape of $|\varepsilon/V_H|$ versus ω for Case 1 ($\alpha = 1$) of the FEPA

For $\alpha = 1$, one obtains the following equation for C_e (see Sec. A.14):

$$C_e = \frac{2}{(\omega_L^2 + \omega_U^2)}\left(\frac{m}{r^2 + m^2} + \frac{1}{m_T}\right). \tag{5.104a}$$

Using M_1 from Eq. (5.65),

$$M_1 = \frac{m}{r^2 + m^2} + \frac{1}{m_T}, \tag{5.65}$$

one may write

$$C_e = \frac{2}{\omega_L^2 + \omega_U^2} M_1. \tag{5.104b}$$

Recall Eq. (5.66).

$$\omega_{ei}^2 = \frac{1}{C_e} M_1 \tag{5.66}$$

Comparing Eqs. (5.104a) and (5.66), one concludes that for Special Case 1 (i.e., $\alpha = 1$), the ω_{ei} is constrained as follows:

$$\omega_{ei}^2 = \frac{\omega_L^2 + \omega_U^2}{2}. \tag{5.112}$$

For the fixed end points constraints with $\alpha = 1$, we see that ω_{ei} is a fixed value given by Eq. (5.112).

Next, we determine for $\alpha = 1$ the conditions which are required to satisfy Eq. (5.93); that is,

$$\omega_L < \omega_e < \omega_U. \tag{5.93}$$

From Eq. (5.112) above, we find (see Sec. A.15) that

$$\omega_L < \omega_{ei} < \omega_U. \tag{5.113}$$

Recall Eq. (5.77).

$$\omega_e^2 = \omega_{ei}^2\sqrt{1 + M_2^2} \tag{5.77}$$

Thus, we note that $\omega_e > \omega_{ei}$ and write

$$\omega_L < \omega_{ei} < \omega_e. \tag{5.114}$$

Thus, the left half of Eq. (5.93) is automatically satisfied for $\alpha = 1$; that is,

$$\omega_L < \omega_e . \tag{5.93a}$$

From the definition of ω_e as the resonance frequency for $|\varepsilon/V_H|$ (and also $|E/V_H|$), we know that $\omega_e < \omega_U$ if and only if Eq. (5.95) holds; that is, if and only if

$$\left.\frac{\delta\left|\frac{\epsilon}{V_H}\right|}{\delta\omega}\right|_{\omega=\omega_U} > 0 . \tag{5.95}$$

We also know that $\omega_e = \omega_U$ if and only if

$$\left.\frac{\delta\left|\frac{\epsilon}{V_H}\right|}{\delta\omega}\right|_{\omega=\omega_U} = 0. \tag{5.95a}$$

This new information may be illustrated by adding to Fig. 5-1 to produce Fig. 5-2.

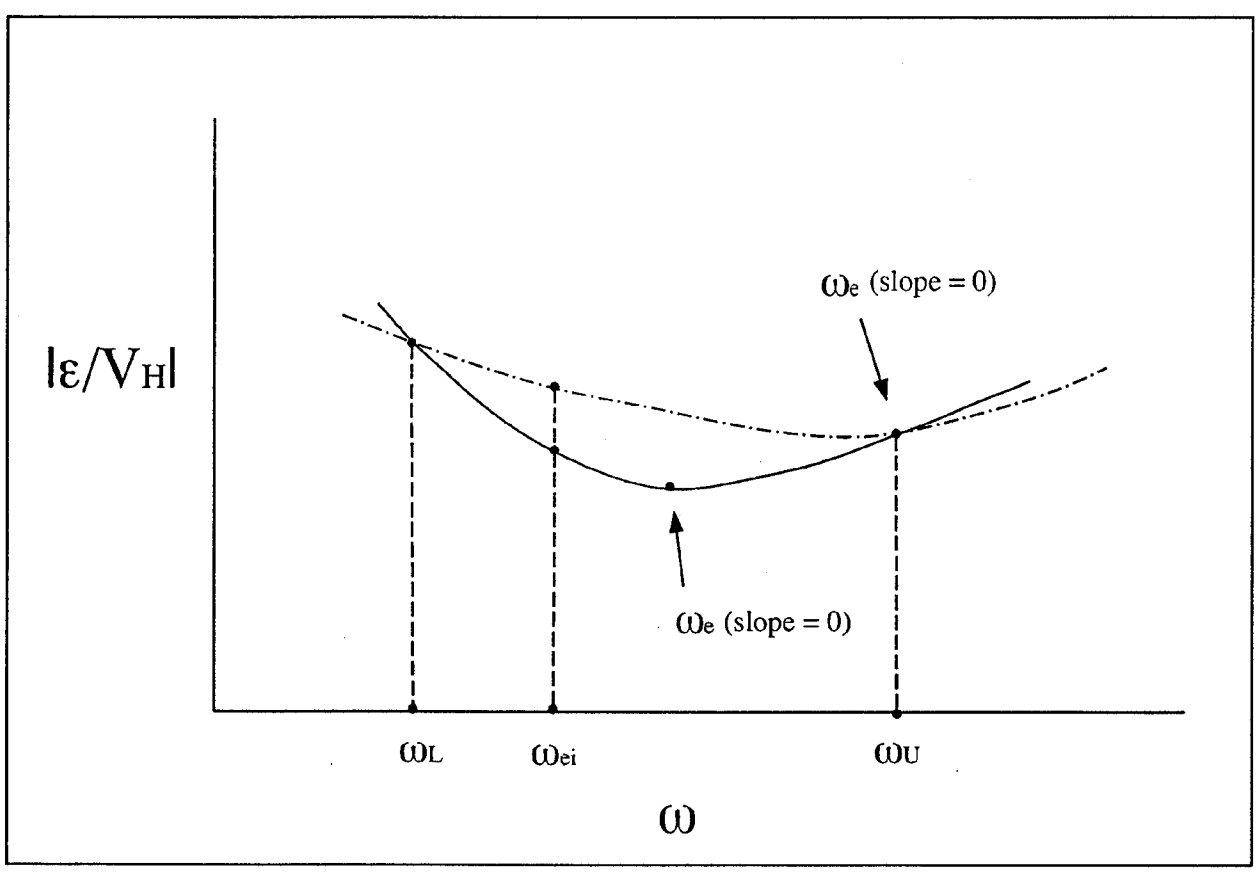

Fig. 5-2 — Relation of slope, ω_e, and "flatness" for Case 1 (α = 1) of the FEPA

From this information, we see that the best one could do to flatten the frequency response of $|\varepsilon/V_H|$ in this fixed end points approach with $\alpha = 1$, is to determine how to change m_T and/or m to try to make

$$\omega_e = \omega_U. \tag{5.115}$$

Reviewing at this point, we have the following situation. We have found that ω_{ei} is fixed for Special Case 1 and given by

$$\omega_{ei} = \frac{\omega_L^2 + \omega_U^2}{2}. \tag{5.112}$$

We know that the best thing we can do to flatten the frequency response is to try to move ω_e up and, if possible, move it up so much that

$$\omega_e = \omega_U. \tag{5.115}$$

We also know that

$$\omega_e = \omega_{ei}\sqrt{1+M_2^2}, \tag{5.77}$$

where [this appears as Eq. (A.10.5) in Sec. A.10]

$$M_2^2 = \frac{r^2}{\left[m + \left(\frac{r^2 + m^2}{m_T}\right)\right]^2}.$$

Thus, in general, we observe that increasing M_2^2 will move ω_e up relative to the fixed ω_{ei}. From Eq. (A.10.5) we observe, in general, that we can increase M_2^2 by increasing m_T and/or decreasing m. Thus, a general conclusion for the $\alpha = 1$ case is that to flatten the frequency response, one should increase m_T and decrease m (i.e., decrease m_H) until $\omega_e = \omega_U$ or, failing that, until some practical limits are reached in increasing m_T and decreasing m_H.

One can be more specific concerning practical limits for m and m_T by proceeding as follows. Using Eqs. (5.115) and (5.112) in Eq. (5.77) we write

$$\frac{2\omega_U^2}{\omega_L^2 + \omega_U^2} = \sqrt{1 + M_2^2}, \tag{5.116}$$

or

$$\left(\frac{2}{\frac{\omega_L^2}{\omega_U^2} + 1}\right)^2 = 1 + M_2^2, \tag{5.116a}$$

or

$$M_2 = \sqrt{\left(\frac{2}{\frac{\omega_L^2}{\omega_U^2} + 1}\right)^2 - 1}. \tag{5.116b}$$

For convenience, let

$$b_{tl} = \sqrt{\left(\frac{2}{\frac{\omega_L^2}{\omega_U^2} + 1}\right)^2 - 1}. \tag{5.117}$$

Note that $b_{tl} > 0$ since $\omega_L/\omega_U < 1$ and, therefore, since $M_2 > 0$, Eq. (5.116b) has real number solutions.

Write

$$M_2 = b_{tl}. \tag{5.116c}$$

Equation (A.10.5) for M_2^2:

$$M_2^2 = \frac{r^2}{\left[m + \left(\frac{r^2 + m^2}{m_T}\right)\right]^2},$$

so

$$\frac{r}{m + \frac{r^2 + m^2}{m_T}} = b_{tl}, \tag{5.116d}$$

or

$$r = b_{tl}\left(m + \frac{r^2 + m^2}{m_T}\right), \tag{5.116e}$$

thus,

$$\frac{1}{m_T} = \frac{(r - mb_{tl})}{b_{tl}(r^2 + m^2)}. \tag{5.116f}$$

Since $1/m_T \geq 0$, we require

$$r - mb_{tl} \geq 0, \tag{5.118}$$

or

$$\frac{r}{m} \geq b_{tl}, \tag{5.118a}$$

or using the definition of b_{tl} [Eq. (5.117)],

$$\frac{r}{m} \geq \sqrt{\left(\frac{2}{\frac{\omega_L^2}{\omega_U^2} + 1}\right)^2 - 1}. \tag{5.118b}$$

For a very narrow band design, ω_U would be only slightly larger than ω_L and in the limit of $\omega_U \rightarrow \omega_L$, one finds

$$\frac{r}{m} \geq 0. \tag{5.118c}$$

In the usual case, this is always true. Thus, in general, for a narrow band design, there might be many combinations of $1/m_T$ and m which would satisfy Eq. (5.116f) and, thus, many ways to flatten the frequency response by making $\omega_e = \omega_U$.

For a very wide band design where ω_U is much larger than ω_L, the limiting case from Eq. (5.118b) is

$$\frac{r}{m} \geq \sqrt{3} = 1.73. \tag{5.118d}$$

In practical problems, r cannot be made large enough and m cannot be made small enough to satisfy Eq. (5.121d). Thus, for large bandwidths, one concludes (for Special Case 1, $\alpha = 1$) that the best one could do is make m_T as large as possible and m_H as small as possible, and even then $\omega_e < \omega_U$ and we would not have achieved the flattest band where $\omega_e = \omega_U$.

One more special bandwidth will be considered between these last two limiting cases of a very narrow and a very large bandwidth. Traditionally, there has been an interest in the half power points in the bandwidth. Since for $\alpha = 1$ we now know the best we can do is make $\omega_e = \omega_U$, let us assume that this has been done and reinterpret ω_L as the lower half power frequency relative to the resonance frequency $\omega_e = \omega_U$. In general, the acoustic power P is given by

$$P = |V_H|^2 R. \tag{5.119}$$

Recall for our special simplifying radiation assumptions

$$R = \omega r. \tag{5.5}$$

Thus,

$$P = |V_H|^2 \omega r. \tag{5.119a}$$

Let P_L be P for $\omega = \omega_L$ and P_e be P for $\omega = \omega_e = \omega_U$.

We want

$$P_L = \frac{1}{2} P_e. \tag{5.120}$$

Using Eq. (5.119a) gives

$$|V_H|^2_{\omega=\omega_L} \omega_L r = \frac{1}{2} |V_H|^2_{\omega=\omega_e} \omega_e r. \tag{5.120a}$$

However, for $\alpha = 1$ (Special Case 1),

$$|V_H|_{\omega=\omega_L} = \frac{\omega_L}{\omega_U} |V_H|_{\omega=\omega_U}. \tag{5.111}$$

Since now we have $\omega_e = \omega_U$, Eq. (5.120a) may be written as

$$\left(\frac{\omega_L}{\omega_e}\right)^2 |V_H|^2_{\omega=\omega_e} \omega_L = \frac{1}{2} |V_H|^2_{\omega=\omega_e} \omega_e, \tag{5.120b}$$

or

$$\left(\frac{\omega_L}{\omega_e}\right)^3 = \frac{1}{2}, \tag{5.120c}$$

or

$$\left(\frac{\omega_L}{\omega_e}\right) = \left(\frac{1}{2}\right)^{1/3} = 0.793. \tag{5.120d}$$

Use of Eq. (5.120d) in Eq. (5.118b) gives

$$\frac{r}{m} \geq \sqrt{\left[\frac{2}{\left(\frac{1}{2}\right)^{2/3} + 1}\right]^2 - 1}, \tag{5.118e}$$

$$\frac{r}{m} \geq 0.711. \tag{5.118f}$$

It turns out that, in practice, even this seemingly modest ratio of r/m is usually not achievable. To carry the example a little farther, suppose Eq. (5.118f) were just barely achievable; that is, suppose

$$\frac{r}{m} = 0.711. \tag{5.118g}$$

Then, according to Eqs. (5.118) and (5.116f), one required $m_T = \infty$; that is,

$$\frac{1}{m_T} = 0, \tag{5.116g}$$

and, of course, from Eq. (5.118g),

$$m = \frac{r}{.711} = 1.406r. \tag{5.118h}$$

In summary, for Special Case 1 ($\alpha = 1$), we have illustrated the following design trend:

> For flatter frequency response of $|\varepsilon/V_H|$ and $|E/V_H|$ for the usual situation of desiring the largest possible bandwidth, one ends up choosing the largest practical tail mass, m_T, and the smallest practical head mass, m_H. This happens because of the physical limits of increasing the radiation resistance $R = \omega r$ and decreasing the quantity $m = m_H + x$.

However, we also have an example where for narrow band designs, equal flatness could be achieved with a family of m_T and m_H pairs.

Next (for Special Case 1), we examine the requirements on the length of the CSA, L, in order to always operate at the chosen field limit of $\varepsilon = \varepsilon_{max}$ at the end points of the frequency band. For $\alpha = 1$, we found that

$$\left|\frac{\epsilon}{V_H}\right|_{\omega=\omega_U} = \frac{\omega_L}{\omega_U}\left|\frac{\epsilon}{V_H}\right|_{\omega=\omega_L}. \tag{5.110}$$

Therefore, one may use the equation for $|\varepsilon/V_H|$ at either end of the frequency band to determine the required value of L to satisfy both end point conditions. If we choose the ω_L end point, then one suitable equation is (see Sec. A.16)

$$k_L^2 L^2 = (r^2 + m^2)\left(\frac{m}{r^2 + m^2} + \frac{1}{m_T}\right)^2 b_{t2}^2 + \frac{r^2}{r^2 + m^2}, \tag{5.121}$$

where b_{t2}^2 is defined as

$$b_{t2}^2 = \left(\frac{\omega_U^2 - \omega_L^2}{\omega_U^2 + \omega_L^2}\right)^2. \tag{5.122}$$

Note that since $\omega_L < \omega_U$,

$$0 < b_{t2}^2 < 1. \tag{5.122a}$$

The situation versus the mass of the tail, m_T, is very straightforward; namely, the larger the m_T, the shorter the length of CSA, L, needed to meet the field constraint of $\varepsilon = \varepsilon_{max}$. Since large m_T also was found to flatten the frequency response, we see that large tail masses have no length penalty and, in fact, have an advantage. There seems to be no exception to the rule that the larger m_T, the better.

The situation is not as simple concerning m. One may observe from Eq. (5.124) that for $1/m_T \neq 0$, then for large enough m, L increases as m increases. So, we know that for large enough m and $m_T \neq \infty$, the slope of $k_L^2 L^2$ must be positive. One may show (see Sec. A.16) that

$$\frac{1}{2}\frac{\delta k_L^2 L^2}{\delta m} = \frac{mr^2}{r^2 + m^2}\left(b_{t2}^2 - 1\right) + \frac{1}{m_T}\left(1 + \frac{m}{m_T}\right)b_{t2}^2, \tag{5.123}$$

where

$$b_{t2}^2 - 1 < 0. \tag{5.124}$$

For $m \simeq 0$, the slope starts out positive. We also note, as before, that for large enough m, the slope must be positive. What happens in between these extremes? Note that for $1/m_T = 0$ ($m_T = \infty$), that since $b_{t1}^2 - 1 < 0$, the slope is negative. Thus, for the special case of $m_T = \infty$, larger m means smaller L. This is a somewhat unexpected result and is similar to other findings where large head masses seem to require a lower field. Suppose next that

$$\frac{m}{m_T} << 1, \tag{5.125}$$

$$(\text{but } \frac{1}{m_T} \neq 0).$$

Then, as long as Eq. (5.125) holds, we have the approximation

$$\frac{1}{2}\frac{\delta k_L^2 L^2}{\delta \omega} \simeq \frac{mr^2}{r^2 + m^2}\left(b_{tl}^2 - 1\right) + \frac{b_{tl}^2}{m_T}. \qquad \textbf{(5.123a)}$$

For small enough m, the slope is positive and then as m increases [if we don't violate Eq. (5.125)], the slope would become zero and then become negative. In other words, we would find a relative maximum for L. However, as m continues to increase, we would eventually have to violate Eq. (5.125), at which point we know that for sufficiently large m, the slope must again become positive. It, therefore, appears that under certain conditions, one might have the situation illustrated in Fig. 5-3.

Equation (5.123a) also shows directly that for $m_T = \infty$, the slope would always be negative because $b_{tl}^2 - 1 < 0$.

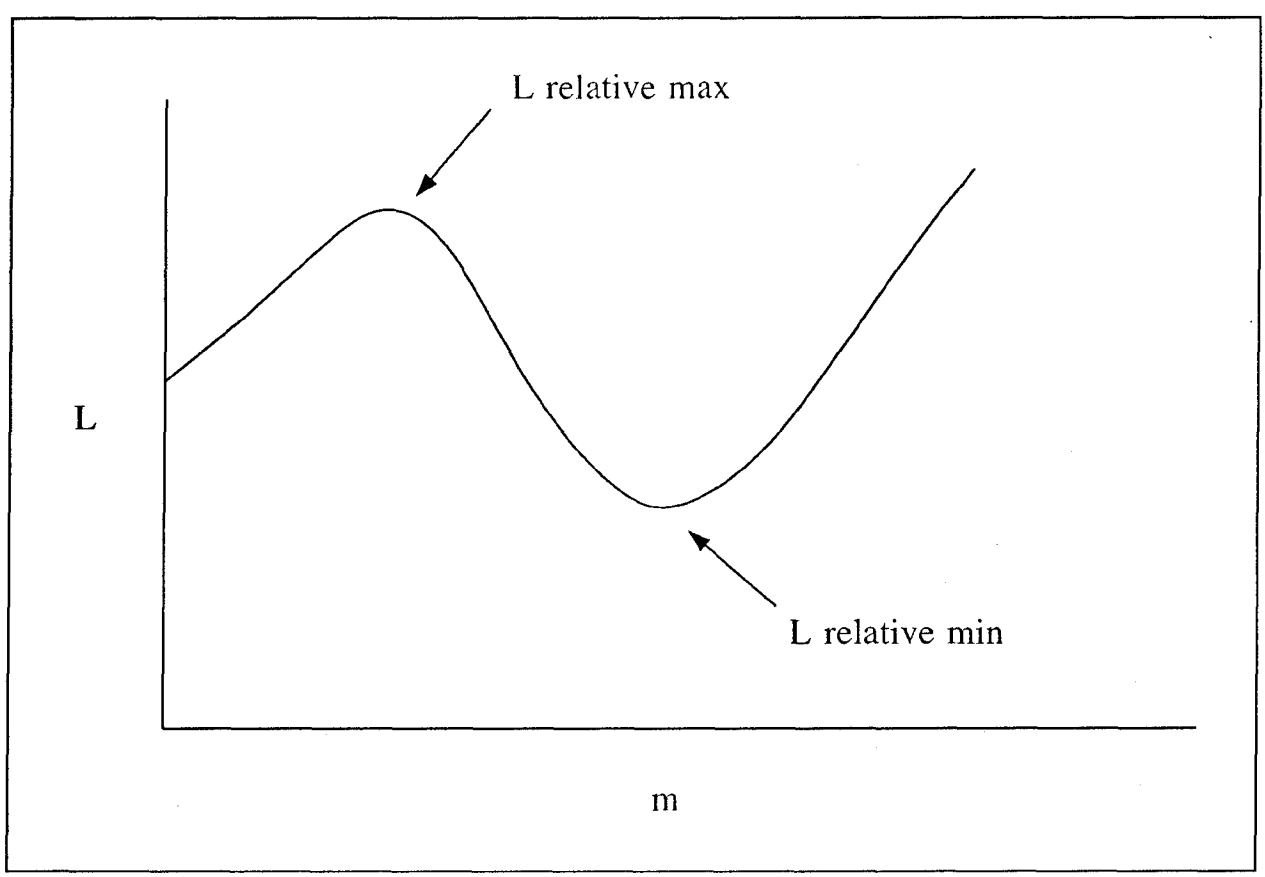

Fig. 5-3 — One possible relation of L (total length of the CSA) as a function of m for Case 1 ($\alpha = 1$) of the FEPA

For Special Case 1 (i.e., for $\alpha = 1$), the equation for C_e is the same as that found in Sec. 5.2.2.6.1 for ω_{ei} fixed; thus, the conclusions concerning C_e are the same.

5.2.2.6.2.1.2 *Special Case 2* [see Eq. (5.126) below] - Before beginning the discussion of Special Case 2, it is noted that Special Case 2 was chosen as the third candidate application of the computer program SGM-A1 to be used to "test" and "explore" the pencil and paper derived design aids and insights of Sec. 5. The SGM-A1 predictions and associated observations are presented in Appendix B. The reader may find it useful to consult this Appendix B third candidate application in conjunction with studying Special Case 2.

Special Case 2 was chosen as the third candidate application of the computer program SGM-A1 for the following three reasons:

1. The special importance of the FEPA approach (also see Sec. 5.2.2.6.2.2),
2. The relative complexity of the paper and pencil derived design aids and insights for the FEPA,
3. The relation of this third candidate application (Special Case 2 of the FEPA approach) to the second candidate application (bigger head masses are better performance at $\omega=\omega_e$ with a fixed value of ω_e).

The general results of this third candidate application of the computer program SGM-A1 were the same as for the first two applications; namely,

1. The corresponding derivations and design insights of Sec. 5 were fully consistent with subject computer predictions; this provided a strong indication that there were no significant errors in the associated pencil and paper derivations of Sec. 5.
2. The predictions provided additional clarity and understanding concerning the "design aid insights" as originally developed from the pencil and paper derivations of Sec. 5.

The defining condition for Special Case 2 is the following:

$$\left|\frac{\epsilon}{V_H}\right|_{\omega=\omega_L} = \left|\frac{\epsilon}{V_H}\right|_{\omega=\omega_U} . \qquad \textbf{(5.126)}$$

In other words, the motion per electric field (or per volt) is the same at the end points (ω_L and ω_U) of the frequency band. Using Eq. (5.108) for α, Eq. (5.100) for k_L and Eq. (5.102) for k_U, one obtains

$$\alpha = \frac{k_L}{k_U} = \frac{\omega_L}{\omega_U}\frac{d_{33}}{d_{33}}\frac{\left|\frac{\epsilon}{V_H}\right|_{\omega=\omega_L}}{\left|\frac{\epsilon}{V_H}\right|_{\omega=\omega_U}} . \qquad \textbf{(5.109)}$$

Because of Eq. (5.126), one obtains for Special Case 2

$$\alpha = \frac{\omega_L}{\omega_U}. \tag{5.127}$$

For $\alpha = \omega_L/\omega_U$, one obtains the following equation for C_e (see Sec. A.17):

$$C_e = \frac{1}{\omega_L \omega_U}\sqrt{\left(\frac{r^2 + m^2}{m_T^2} + \frac{2m}{m_T} + 1\right)\frac{1}{r^2 + m^2}}. \tag{5.104c}$$

See Eq. (A.10.43) (printed here for your convenience).

$$M_e^2 = \frac{1}{m_T^2} + \frac{2m}{m_T(r^2 + m^2)} + \frac{1}{r^2 + m^2}.$$

Note that C_e may be written

$$C_e = \frac{1}{\omega_L \omega_U} M_e. \tag{5.104d}$$

From Eq. (A.10.40) we have:

$$\omega_e^2 = \frac{1}{C_e} M_e.$$

Comparing Eqs. (5.104d) and (A.10.40), we conclude that for Special Case 2, we may identify ω_e as

$$\omega_e^2 = \omega_L \omega_U. \tag{5.128}$$

Thus, for Special Case 2 (or equivalently for $\alpha = \omega_L/\omega_U$) in this FEPA, the resonance frequency ω_e is a fixed value given by Eq. (5.128).

Notice that since $\omega_L < \omega_U$, then $\omega_L^2 < \omega_L \omega_U < \omega_U^2$, and, thus, for $\alpha = \omega_L/\omega_U$, we automatically satisfy the requirements of Eq. (5.93).

$$\omega_L < \omega_e < \omega_U. \tag{5.93}$$

The above information for Special Case 2 may be illustrated as shown in Fig. 5-4.

The best that can be done to flatten the frequency response is to adjust m and m_T so as to maximize the value of $|\epsilon/V_H|_{\omega=\omega_e}$. From Eq. (5.72), one may write

$$\left|\frac{\epsilon}{V_H}\right|_{\omega=\omega_e} = \frac{1}{\omega_e L d_{33}}\sqrt{B_{1e}}, \tag{5.129}$$

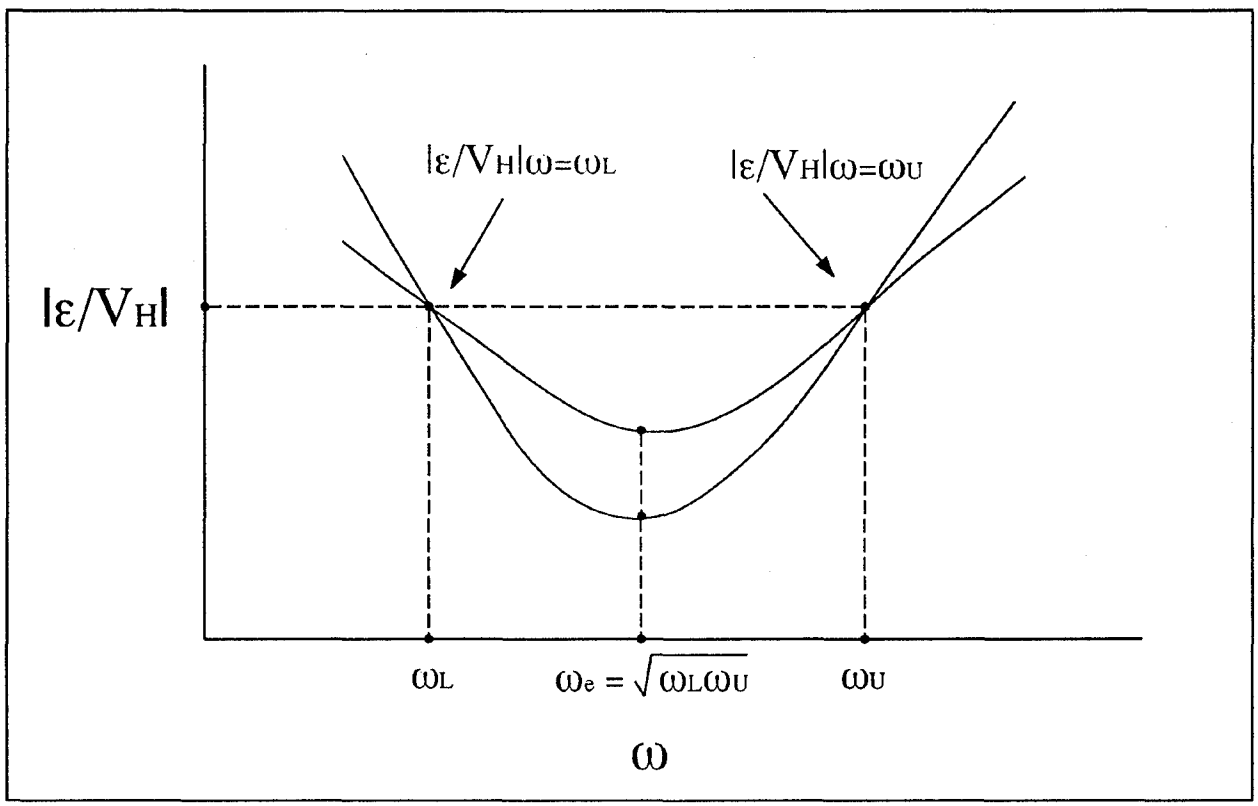

Fig. 5-4 — General shape of $|\epsilon/V_H|$ versus ω for Case 2 ($\alpha = \omega_L/\omega_U$) of the FEPA

where B_{1e} is the value of B_1 for $\omega = \omega_e$. Consider first the partial derivative of $|\epsilon/V_H|_{\omega=\omega_e}$ with respect to m_T. This is equivalent to considering $\delta B_{1e}/\delta m_T$. One finds (see Sec. A.18)

$$\frac{\delta B_{1e}}{\delta m_T} = 2F_{e1}F_{e2}, \tag{5.130}$$

where

$$F_{e1} = \sqrt{\left(\frac{r^2 + m^2}{m_T} + m\right)^2 + r^2} - \left(\frac{r^2 + m^2}{m_T} + m\right), \tag{5.131}$$

and

$$F_{e2} = \frac{1}{m_T^2}\left[1 - \frac{\left(\frac{1}{m_T} + \frac{m}{r^2 + m^2}\right)}{\sqrt{\left(\frac{1}{m_T} + \frac{m}{r^2 + m^2}\right)^2 + \frac{r^2}{(r^2 + m^2)^2}}}\right]. \qquad \textbf{(5.132)}$$

Examination of Eqs. (5.131) and (5.132) shows that for all values of m and mT

$$F_{e1} > 0, \qquad \textbf{(5.131a)}$$

and

$$F_{e2} > 0. \qquad \textbf{(5.132a)}$$

Thus,

$$\frac{\delta B_{1e}}{\delta m_T} > 0. \qquad \textbf{(5.130a)}$$

Therefore, we conclude that as m_T increases, $|\varepsilon/V_H|_{\omega=\omega_e}$ increases which means that, once again, increasing m_T flattens the frequency response of $|\varepsilon/V_H|$ (and $|E/V_H|$). The best possible value would be $m_T = \infty$.

Next, the partial derivative of $|\varepsilon/V_H|_{\omega=\omega_e}$ with respect to m was considered. Although a general expression was derived (see Sec. A.19), it did not lend itself to easy general interpretation. Therefore, only the special case where $m_T \to \infty$ was considered. Then (see Sec. A.19),

$$\frac{\delta B_{1e}}{\delta m} = -\frac{2r^2}{(r^2 + m^2)^{3/2}}, \qquad \textbf{(5.133)}$$

for

$$m_T \to \infty.$$

Thus, for $m_T \to \infty$, the slope is always negative and, thus, the smaller m, the larger $|\varepsilon/V_H|_{\omega=\omega_e}$. Once again, we find that the smaller m, the flatter the frequency response.

When Eq. 5.133a holds, one has an alternate proof to that presented in Sec. 5.2.2.5 which shows that for fixed ω_e, then as m increases, $|\varepsilon/V_H|_{\omega=\omega_e}$ decreases. Thus, the bigger m, the better as far as the required electric field ε for a given source level at $\omega = \omega_e$. However, as we just noticed, this is the opposite of what is needed for a flat frequency response.

Next (for Special Case 2), we examine the requirements on the length of the CSA, L, in order to always operate at the chosen field point limit of $\varepsilon = \varepsilon_{max}$ at the end points of the frequency band. For Special Case 2, the defining constraints were

$$\left|\frac{\epsilon}{V_H}\right|_{\omega=\omega_L} = \left|\frac{\epsilon}{V_H}\right|_{\omega=\omega_U}. \tag{5.126}$$

Therefore, one may use the equation for $|\varepsilon/V_H|$ at either end of the frequency band to determine the required value of L to satisfy both end point conditions. If we choose the ω_L end point, then one suitable equation is (see Sec. A.20)

$$k_L^2 L^2 = r^2\left(\frac{\omega_L}{\omega_U}M_e - \frac{1}{m_T}\right)^2 + \left[1 - m\left(\frac{\omega_L}{\omega_U}M_e - \frac{1}{m_T}\right)\right]^2. \tag{5.134}$$

One form given for M_e in Sec. A.10 is [Eq. (A.10.46) is printed here for your convenience]

$$M_e = \sqrt{\left(\frac{1}{m_T} + \frac{m}{r^2 + m^2}\right)^2 + \frac{r^2}{r^2 + m^2}}.$$

Using Eq. (A.10.46) in Eq. (5.134), one may calculate the required L for any choices of m and m_T.

Next, the $\delta L^2/\delta m_T$ for Eq. (5.134) was derived (see Sec. A.20) for use in further characterizing the behavior of L versus changes in m_T. This partial derivative is useful because for those conditions where we find that this partial derivative is negative then we know that the slope of Eq. (5.134) is negative and, thus, as m_T is increased, L decreases. Similarly, for those conditions where we find that this partial derivative is poistive, we know that as m_T is increased, L increases. We will, in fact, find that for most transducer designs the subject partial derivative is negative.

The resulting equation for this partial derivative is

$$k_L^2\frac{\delta L^2}{\delta m_T} = \frac{2}{m_T^2}\frac{\omega_L}{\omega_U}\left(\frac{r^2 + m^2}{m_T} + m^2\right)(F_{1L})\left(F_{2L} - \frac{\omega_U}{\omega_L}\right), \tag{5.135}$$

where

$$F_{1L} = 1 - \frac{\frac{\omega_L}{\omega_U}\left(\frac{1}{m_T} + \frac{m}{r^2 + m^2}\right)}{\sqrt{\left(\frac{1}{m_T} + \frac{m}{r^2 + m^2}\right)^2 + \frac{r^2}{(r^2 + m^2)^2}}}, \tag{5.136}$$

and

$$F_{2L} = \sqrt{1 + \frac{r^2}{\left(\frac{r^2 + m^2}{m_T} + m\right)^2}}. \tag{5.137}$$

Since $\omega_L/\omega_U < 1$ and it can be seen that the rest of the right-hand side of Eq. (5.137) is less than "1" (divide the numerator into the denominator), we conclude from Eq. 5.136 that

$$F_{1L} > 0. \tag{5.136a}$$

Thus, from Eq. (5.135), we conclude that the sign of $\delta L^2/\delta m_T$ is determined by the sign of quantity $(F_{2L} - \omega_U/\omega_L)$.

First, notice that Eq. (5.137) shows that at least for small enough values of m_T then F_{2L} can be made arbitrarily close to a value of 1 and, thus, less than the fixed number $\omega_U/\omega_L > 1$. Therefore,

$$F_{2L} - \frac{\omega_U}{\omega_L} < 0. \tag{5.137a}$$

We can conclude that for small enough values of m_T the sign of the subject partial derivative is negative. Thus, for small enough values of mT , as mT is increased, L decreases.

Second, notice that as m_T increases, the F_{2L} increases. Then, one may ask what are the conditions such that

$$F_{2L} - \frac{\omega_U}{\omega_L} \geq 0 \quad \text{(for what conditions)}. \tag{5.138}$$

This is the same as asking the following question: As we increase m_T starting from small enough values of m_T, what are the conditions such that the sign of the subject partial derivative will change from negative to positive? This, in turn, is the same as asking, as we increase m_T starting from small enough value of m_T, what are the conditions such that as we increase m_T will we reach a minimum value of L after which as m_T is further increased, L will also increase.

One finds (see Sec. A.20) that Eq. (5.138) is equivalent to the following:

$$\frac{1}{m_T} \leq \frac{m}{r^2 + m^2}\left(\frac{r}{m}\frac{1}{\sqrt{\frac{\omega_U^2}{\omega_L^2} - 1}} - 1\right). \tag{5.138a}$$

Since $1/m_T > 0$ (except for $m_T = \infty$), then Eq. (5.138a) leads to the following requirement:

$$r > m\sqrt{\frac{\omega_U^2}{\omega_L^2} - 1}. \qquad \textbf{(5.138b)}$$

Notice that if the

$$\sqrt{\omega_U^2/\omega_L^2 - 1} > 1, \quad (\text{thus, } \omega_U \geq \sqrt{2}\omega_L),$$

then Eq. (5.138a) [and similarly Eq. (5.138)] requires r > m and that the larger the bandwidth (i.e., larger ω_U/ω_L), the larger r must be in relation to m in order for Eq. (5.138) to hold.

As has already been explained, in most practical cases r < m. Thus, in most practical cases where one is seeking as broad a bandwidth as possible, the usual situation will be for Eq. (5.137) [not Eq. (5.138)] to hold, even for the largest practical values of m_T. If Eq. (5.137) holds (i.e., $F_{2L} - \omega_U/\omega_L < 0$), then we have $\delta L^2/\delta m_T < 0$. Therefore, we have just found for the usual broad band design that as m_T is increased, the length of the CSA, L, required to meet the electric field constraints at the ends of the band, decreases. (See also the third candidate application of the SGM presented in Appendix B.)

Not only does the frequency response flatten, but the length L may be shortened as m_T increases. Thus, we can see why for broad band designs, the design trend is to require the largest practical value for m_T.

However, for narrow band designs, one notes that r < m is acceptable according to Eq. (5.138b). In these narrow band cases one could have, for practical head masses m_H, the condition of Eq. (5.138) and, thus, have $\delta L^2/\delta m_T > 0$. Then, increasing m_T would increase the length of L required to meet the end point electric field constraints.

The only characterization of L versus changes in m was for the special case of $m_T = \infty$. For that case, Eq. (A.10.46) (printed below for your convenience) shows that

$$M_e \underset{(\text{for } m_T=\infty)}{=} \frac{1}{\sqrt{r^2 + m^2}},$$

and Eq. (5.134) becomes

$$k^2L^2 \underset{(\text{for } m_T=\infty)}{=} \frac{\omega_L^2}{\omega_U^2}\frac{r^2}{r^2 + m^2} + \left(1 - \frac{\omega_L}{\omega_U}\frac{m}{\sqrt{r^2 + m^2}}\right)^2. \qquad \textbf{(5.134a)}$$

We observe from Eq. (5.134a) that as m is decreased (for example, to flatten the frequency response), the length L needed to meet the end point field constraints would increase. Thus, at least for the special case of $m_T = \infty$, the penalty paid for decreasing m to flatten the frequency response is the requirement to lengthen L to meet field constraints.

Consider next Eq. (5.104c) for the composite C_e.

$$C_e = \frac{1}{\omega_U \omega_L} \sqrt{\left(\frac{r^2 + m^2}{m_T^2} + \frac{2m}{m_T} + 1 \right) \frac{1}{r^2 + m^2}} \qquad \textbf{(5.104c)}$$

With m held fixed, then as m_T is increased (which we know is the desirable trend), then Eq. (5.104c) shows that C_e must be decreased; that is, the CSA and FTR combination needs to be made stiffer. This is the same trend as for Special Case 1.

For large values of m_T one has

$$C_e \simeq \frac{1}{\omega_U \omega_L} \frac{1}{\sqrt{r^2 + m^2}} . \qquad \textbf{(5.104e)}$$

Then, as m is decreased to flatten the frequency response, C_e must be increased (m_T held fixed). This is the same trend as found in Special Case 1.

5.2.2.6.2.2 *Summary of FEPA* - The above described FEPA, showed why in the usual practical longitudinal design problem, large tail masses, m_T, and small head masses are desirable to flatten the frequency response of the transducer. If it were possible to produce larger radiation resistances, R, than the usual physical constraints dictate, then there would be exceptions to this design trend of always using large m_T and small m_H.

The analysis also showed that in most but not all usual circumstances, the larger the tail mass, m_T, the shorter the length of the CSA, L, needed to meet the electric field constraint, ε_{max}, for the CSA. However, the larger m_T, the smaller the composite compliance C_e (i.e., the stiffer the CSA/FTR assembly), needed. This means that one should use the thinnest practical FTR and one must increase the area A_c of the piezoelectric ceramic rings. The fact that L may be shortened with larger m_T helps in the process of decreasing C_e.

Decreasing the head mass, m_H, to flatten the frequency response was shown under usual circumstances to increase the CSA length, L, required to meet the field constraint, ε_{max}, and required an increase in compliance C_e.

The FEPA explicitly illustrated that the best location for the resonance frequency, ω_e, is a function of the acoustic field constraints of the design problem. This, in turn, suggested that design approaches that start out by fixing ω_e (or some other interesting special frequency) are not an efficient way to arrive at a near optimum design. A better approach would be to choose ω_L and ω_U and fix the corresponding values of $|\varepsilon/V_H|$ at these end points as indicated above.

The FEPA suggests all the necessary steps for a new and very useful TDGS which would be completely independent of the SGM. It could and should be executed using the appropriate parts of the CMM (Composite Math Model - see Sec. 2). The essential idea of this independence from the SGM is illustrated in Sec. B.4. The development of such a fixed end-point TDGS for the general frequency dependence case would involve a computer aided iterative approach in the CMM.

5.3 **Analysis with Tuning Inductor**

The analysis presented in Sec. 5.2 did not consider inclusion of an electrical tuning inductor as part of the transducer element. However, the basic equations already presented are all that is needed to proceed with an analysis which includes a tuning inductor. Although not presented in this paper, one could use these basic equations already presented to provide insight into the use of an electrical tuning inductor to help minimize the demands on the power amplifier used to drive the transducer element.

In the remainder of this book, three examples are presented to illustrate how one might proceed to use the basic equations to characterize the effects of including a tuning inductor. Only a parallel tuning inductor (see Fig. 5-5) is considered.

Figure 5-5 indicates the main quantities to be used to begin consideration of adding a parallel tuning inductor with inductance Γ to the previously considered transducer element without a tuning inductor.

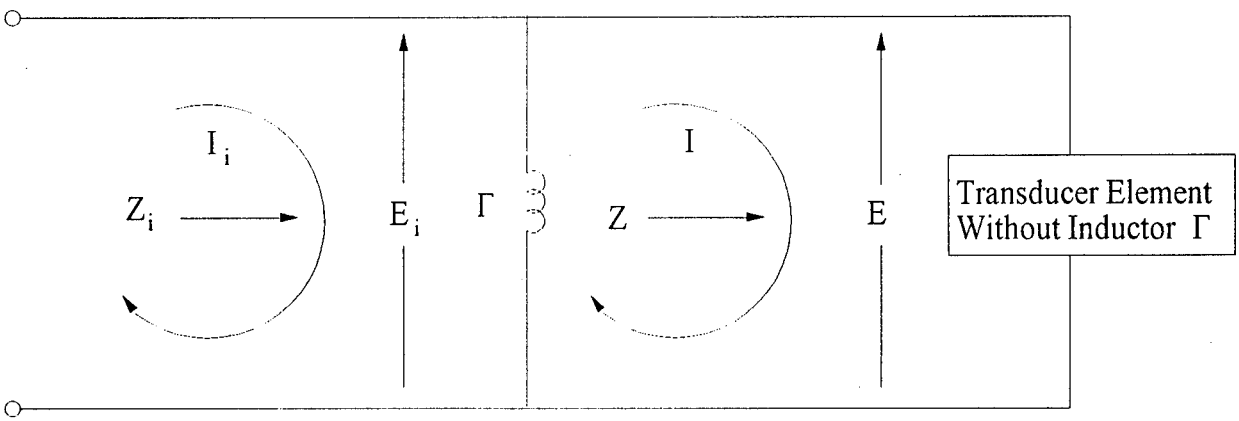

Fig. 5-5 — Inclusion of an inductor Γ in the equivalent circuit of the transducer

With a parallel tuning inductor, note that the input voltage E_i to the composite transducer is the same as the voltage E on the CSA; that is,

$$E_i = E. \tag{5.139}$$

The input current I_i is given by

$$I_i = I + \frac{1}{i\omega\Gamma} E. \tag{5.140}$$

Thus, the motion relative to I_i is given by

$$\frac{I_i}{V_H} = \frac{I}{V_H} + \frac{1}{i\omega\Gamma}\frac{E}{V_H}. \tag{5.141}$$

Recall the following equations:

$$\frac{E}{V_H} = \frac{1}{\omega N d_{33}}[rE_o - i(1 - mE_o)], \tag{5.10}$$

$$\frac{I}{V_H} = \frac{A_c}{g_{33}1_c}[(1-mI_o) + irI_o], \tag{5.16}$$

and rewrite Eq. (5.141) as

$$\frac{I_i}{V_H} = \frac{A_c}{g_{33}1_c}[(1-mI_o)+irI_o] + \frac{1}{i\omega\Gamma}\frac{1}{\omega N d_{33}}[rE_o - i(1-mE_o)]. \tag{5.142}$$

Equation (5.142) could be manipulated, similar to the examples in Sec. 5.2 for I/V_H, to study the various affects of the inductor in I_i/V_H. For example, for I/V_H, one interesting quantity was the in-air resonance frequency ω_n. For I_i/V_H, let the in-air resonance frequency be $\omega_{n'}$. Since in-air r = 0 and m = m_H, one has

$$\left.\frac{I_i}{V_H}\right|_{in-air} = \frac{A_c}{g_{33}1_c}[(1 - m_H I_o)] - \frac{1}{i\omega^2\Gamma}\frac{i}{Nd_{33}}(1 - mE_o), \tag{5.143}$$

or

$$\left.\frac{I_i}{V_H}\right|_{in-air} = \left[\frac{A_c}{g_{33}1_c}(1 - m_H I_o) - \frac{1}{\omega^2\Gamma N d_{33}}(1 - mE_o)\right], \tag{5.144}$$

where E_o and I_o are evaluated at $\omega = \omega_{n'}$.

In this idealized case of no losses in air, one could derive an expression for $\omega_{n'}$ by setting the right side of Eq. (5.144) equal to zero and solving for ω. An easier characterization is to solve for Γ as follows:

$$\frac{A_c}{g_{33}1_c}(1 - m_H I_o) - \frac{1}{\omega_{n'}^2\Gamma N d_{33}}(1 - mE_o) = 0 \tag{5.145}$$

and

$$\frac{1}{\Gamma} = \omega_{n'}^2 \frac{NA_c d_{33}}{g_{33} l_c} \frac{(1 - m_H I_o)}{(1 - mE_o)}. \tag{5.146}$$

In Eqs. (5.145) and (5.146), I_o and E_o must be evaluated at $\omega=\omega_{n'}$. One can show (see Sec. A.21) that the low-frequency capacitance C_T is given by

$$C_T = \frac{NA_c d_{33}}{g_{33} l_c}. \tag{5.147}$$

Thus,

$$\Gamma = \frac{1}{\omega_{n'}^2 C_T} \frac{(1 - m_H E_o)}{(1 - m_H I_o)}. \tag{5.148}$$

One can also show (see Sec. A.21)

$$E_o = I_o + \frac{(\omega N d_{33})^2}{C_T}. \tag{5.149}$$

Thus,

$$\Gamma = \frac{1}{\omega_{n'}^2 C_T} \frac{\left[1 - m_H I_o - \dfrac{m_H (\omega_{n'} N d_{33})^2}{C_T}\right]}{(1 - m_H I_o)}, \tag{5.150}$$

$$\Gamma = \frac{1}{\omega_{n'}^2 C_T}\left[1 - \frac{(\omega_{n'} N d_{33})^2}{C_T} \frac{m_H}{(1 - m_H I_o)}\right], \tag{5.151}$$

with I_o evaluated at $\omega = \omega_{n'}$. In Sec. A.22, it is shown that Eq. (5.151) may be rewritten as follows (for $\omega = \omega_{n'}$):

$$\Gamma = \frac{1}{\omega_{n'}^2 C_T}\left[\frac{\omega_n^2}{\omega_m^2} \frac{(\omega_{n'}^2 - \omega_m^2)}{(\omega_{n'}^2 - \omega_n^2)}\right]. \tag{5.152}$$

Recall that $\omega_m < \omega_n$. Thus, if $\omega_m < \omega_n < \omega_{n'}$, that is, if $\omega_{n'} > \omega_n$, then the right-hand side of Eq. (5.152) is positive, and since $\Gamma > 0$, there are values of Γ that satisfy Eq. (5.152).

Note that if $\omega_{n'} > \omega_n$, then as $\omega_{n'}$ approaches ω_n (from the right), Γ increases without limit because $\omega_{n'}^2 - \omega_n^2$ approaches zero. This checks with the fact that $\Gamma = \infty$ is the same as no parallel inductor, in which case $\omega_{n'} = \omega_n$.

If $\omega_m < \omega_{n'} < \omega_n$, then $\omega_{n'}^2 - \omega_n^2 < 0$ and $\omega_{n'}^2 - \omega_m^2 > 0$, so Eq. (5.152) would call for negative inductances which, of course, do not exist.

If $\omega_{n'} = \omega_m$, then $\Gamma = 0$, which would be the same as a parallel short circuit for the transducer element.

If $\omega_{n'} < \omega_m < \omega_n$, then both $\omega_{n'}^2 - \omega_n^2$ and $\omega_{n'}^2 - \omega_m^2$ are negative and thus, Eq. (5.152) again calls for $\Gamma > 0$.

Thus, it appears that for any inductance other than $\Gamma = 0$ or $\Gamma = \infty$, there are two in-air resonances for I_i/V_H, one above ω_n and one below ω_m.

Graphically, these conclusions are illustrated in Fig. 5-6.

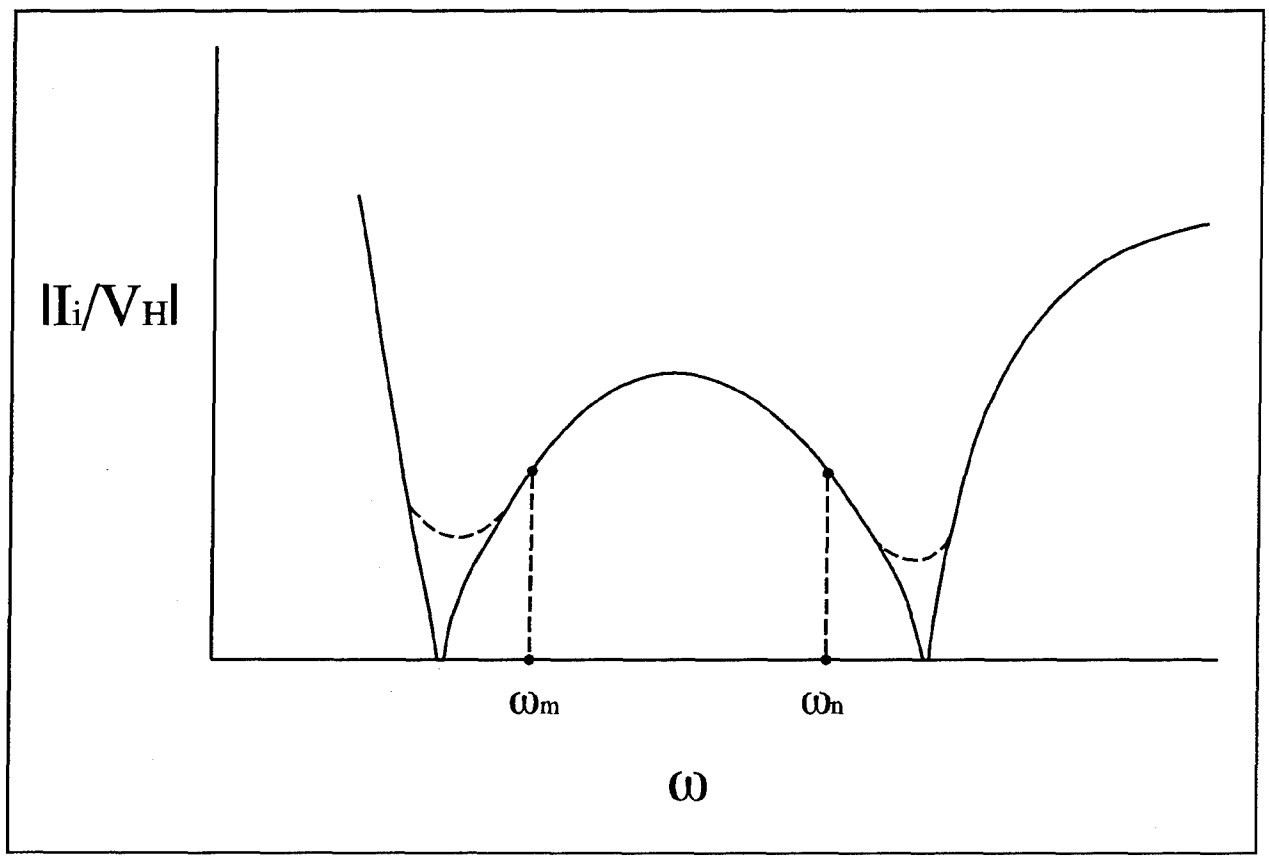

Fig. 5-6 — Qualitative character of $|I_i/V_H|$ (includes parallel inductor); solid line: no losses, dotted line: with small losses

Although not analyzed above, we know (for example, from the law of conservation of energy) that $|I_i/V_H|$ would not reach a value of zero, but would behave as illustrated with the dashed portions of the curve.

As a second example of use of the previously derived equations to characterize the affects of including a parallel inductor, consider the following. Equation (5.142) for I_i/V_H (which includes the inductor) may be shown (see Sec. A.23) to be analogous to Eq. (5.16) for I_i/V_H (which does not include the inductor).

$$\frac{I_i}{V_H} = \frac{A_c}{g_{33}l_c}\left\{\left[\left(1 - \frac{1}{\omega^2\Gamma C_T}\right) - mI_{o'}\right] + irI_{o'}\right\}, \tag{5.153}$$

where

$$I_{o'} = I_o - \frac{E_o}{\omega^2\Gamma C_T}. \tag{5.154}$$

Note that, as previously observed, if $\Gamma = \infty$, then the equation for I_i/V_H reduces Eq. (5.16) for I_i/V_H (no inductor).

Recall that with no inductor, we noted that for $I_o = 0$, the I/V_H was independent of the radiation loading (independent of r and x). This was considered a "current velocity control condition." For no inductor, the current velocity control angular frequency ω_{iv} was given by

$$\omega_{iv}^2 = \frac{1}{C_e' m_T}, \tag{5.54}$$

and at this frequency,

$$\left|\frac{I}{V_H}\right|_{\omega=\omega_{iv}} = \frac{A_c}{g_{33}l_c}. \tag{5.55}$$

Similarly, from Eq. (5.153), we note that if

$$I_{o'} = 0, \tag{5.155}$$

then

$$\frac{I_i}{V_H} = \frac{A_c}{g_{33}l_c}\left(1 - \frac{1}{\omega_{iv'}^2\Gamma C_T}\right), \tag{5.156}$$

where $\omega_{iv'}$ is the angular frequency such that Eq. (5.155) holds, that is, the current velocity control angular frequency with a parallel inductor.

When Eq. (5.155) holds, we see from Eq. (5.154) that the following also holds:

$$I_o - \frac{E_o}{\omega_{iv'}^2 \Gamma C_T} = 0, \tag{5.157}$$

or (providing $E_o \neq 0$)

$$\frac{1}{\omega_{iv'}^2 \Gamma C_T} = \frac{I_o}{E_o}. \tag{5.158}$$

Thus, Eq. (5.156) may be rewritten as (for $\omega = \omega_{iv'}$)

$$\frac{I_i}{V_H} = \frac{A_c}{g_{33} l_c}\left(1 - \frac{I_o}{E_o}\right). \tag{5.159}$$

Note that if $I_o = 0$ (which we have noted requires $\Gamma = \infty$, i.e., no parallel inductor), then Eq. (5.159) reduces to the no-inductor case of Eq. (5.55).

Equation (5.158) may be solved for the Γ needed for a selected current velocity control frequency $\omega_{iv'}$.

$$\Gamma = \frac{1}{\omega_{iv'}^2 C_T} \frac{E_o}{I_o} \tag{5.160}$$

with E_o and I_o evaluated at $\omega = \omega_{iv}'$.

Equation (5.149) above may be used to rewrite Eq. (5.160) as

$$\Gamma = \frac{1}{\omega_{iv'}^2 C_T}\left(1 + \frac{1}{I_o} \frac{(\omega N d_{33})^2}{C_T}\right). \tag{5.161}$$

Note that if $I_o > 0$, then since $\Gamma > 0$, there would exist a value of Γ corresponding to such choices of $\omega_{iv'}$. It turns out that $I_o > 0$ covers all usual practical cases. To see this, observe the following. Recall

$$I_o = \omega^2 C_e' - \frac{1}{m_T}, \tag{5.17}$$

for no parallel inductor ($\Gamma = \infty$) $I_o \simeq 0$ for $\omega = \omega_{iv}$. Thus, if

$$\omega_{iv'} > \omega_{iv}, \tag{5.162}$$

then

$$I_o > 0. \tag{5.163}$$

Thus, we see that for $\omega_{iv'}$ "close" to ω_{iv}, one would require a large inductance value for Γ, and as $\omega_{iv'}$ is increased in value above that of ω_{iv}, then I_o increases, and, thus, by Eq. 5. (170), the required value of Γ decreases. Next, we need an equation to compare ω_{iv} with ω_n. Since $\omega_{iv}^2 = 1/C_e' m_T$ [see Eq. (5.54)] and $\omega_n^2 = 1/C_e' (1/m_H + 1/m_T)$ [see Eq. (5.27)], the desired equation is

$$\omega_{iv}^2 = \frac{1}{\left(\frac{m_T}{m_H} + 1\right)} \omega_n^2. \tag{5.164}$$

As we have already observed, "good transducer designs" have very large values of m_T/m_H and, ideally, $m_T/m_H \to \infty$. Thus, from Eq. (5.164), we see that normally ω_{iv} has a very small value and in the limiting case approaches zero. Thus, in turn, from Eq. (5.162) we see that in these "good designs" that for all practical values of $\omega_{iv'}$, we have $I_o > 0$ [Eq. (5.163)] and, thus, a parallel inductor will exist [Eq. (5.161)] for such values of $\omega_{iv'}$.

As a third and last example of use of previously derived equations to characterize the affects of including a parallel inductor, we give some consideration to the input impedance Z_i with a parallel inductor included.

Referring to Fig. 5-5, the input impedance Z_i is given by

$$Z_i = \frac{E_i}{I_i} \tag{5.165}$$

but,

$$E_i = E \tag{5.139}$$

so

$$Z_i = \frac{E}{I_i}. \tag{5.166}$$

One may also note from Eq. (5.166) that

$$Z_i = \frac{\left(\frac{E}{V_H}\right)}{\left(\frac{I_i}{V_H}\right)}. \tag{5.167}$$

From the characteristics already presented for E/V_H and I_i/V_H, we may note that in air at ω_m, E/V_H goes to zero and, referring to Fig. 5-6, we note that at two frequencies I_i/V_H goes to zero. Thus, qualitatively, we expect Z_i in-air to be shown in Fig. 5-7.

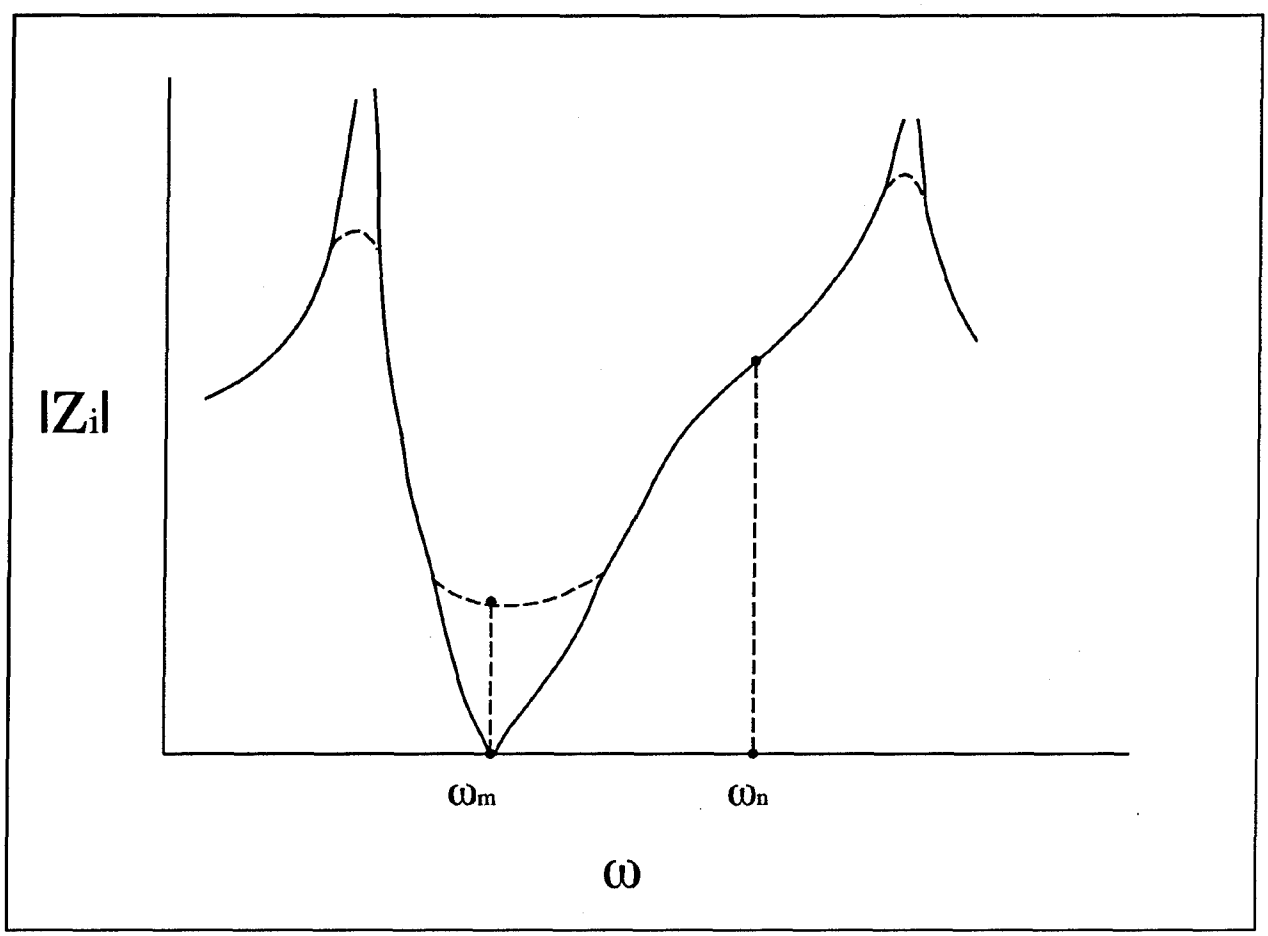

Fig. 5-7 — Qualitative character of $|Z_i|$ (with parallel inductor); solid line: no losses, dotted line: with small losses

As previously discussed, with small losses included, these zero conditions would not occur and one would expect the qualitative behavior indicated by the dashed lines.

As $\Gamma \rightarrow \infty$, we have found that we approach the previously studied case with no parallel inductor, then the highest frequency peak in Fig. 5-7 moves down to the angular frequency ω_n and the lowest frequency peak moves down to $\omega = 0$.

The behavior of Z_i in air vs the in air directly measurable quantities C_T, ω_m and ω_n was of some special interest in the STRIP (the program where the simplified guidance model, used in this document, was developed) effort and so this characterization is pursued further as follows.

Rewrite Eq. (5.166) as follows:

$$\frac{1}{Z_i} = \frac{I_i}{E}. \tag{5.166a}$$

Use Eq. (5.140) to rewrite Eq. (5.167) as follows:

$$\frac{1}{Z_i} = \frac{I}{E} + \frac{1}{i\omega\Gamma}. \tag{5.168}$$

But,

$$\frac{1}{Z} = \frac{I}{E}. \tag{5.169}$$

where Z is the input impedance (see Fig. 5-5) to the transducer element without the parallel tuning inductor. Use Eq. (5.169) to rewrite Eq. (5.168) as follows:

$$\frac{1}{Z_i} = \frac{1}{Z} + \frac{1}{i\omega\Gamma}. \tag{5.170}$$

In Sec. A.24, it is shown that

$$\left.\frac{1}{Z}\right|_{\text{in-air}} = i\omega C_T \left(\frac{\omega_m}{\omega_n}\right)^2 \frac{\left(\omega_n^2 - \omega^2\right)}{\left(\omega_m^2 - \omega^2\right)}. \tag{5.171}$$

Notice that at $\omega = \omega_m$, $1/Z\big|_{\text{in-air}} = \infty$; that is, $Z\big|_{\text{in-air}} = 0$ and at $\omega = \omega_n$, then $1/Z\big|_{\text{in-air}} = 0$. These facts agree with previous derivations concerning $E/V_H\big|_{\text{in-air}}$ and $I/V_H\big|_{\text{in-air}}$.

Use of Eq. (5.171) in Eq. (5.170) gives

$$\left.\frac{1}{Z_i}\right|_{\text{in-air}} = i\left[\omega C_T \left(\frac{\omega_m}{\omega_n}\right)^2 \frac{\left(\omega_n^2 - \omega^2\right)}{\left(\omega_m^2 - \omega^2\right)} - \frac{1}{\omega\Gamma}\right]. \tag{5.172}$$

Note the following:

1. For $\omega << \omega_m < \omega_n$, then

$$\left.\frac{1}{Z_i}\right|_{\text{in-air}} \simeq i\left(\omega C_T - \frac{1}{\omega\Gamma}\right). \tag{5.172a}$$

2. For $\omega < \omega_m < \omega_n$, then $(\omega_n^2 - \omega^2) > 0$ and $(\omega_m^2 - \omega^2) > 0$, so an Γ exists which makes

$$\left.\frac{1}{Z_i}\right|_{\text{in-air}} = 0. \tag{5.172b}$$

3. For $\omega = \omega_m$, the $1/Z_i = 1/Z = \infty$ independent of the value of Γ. In the actual case of some internal losses, it is found that this tendency is still present in that changes in Γ at $\omega = \omega_m$ do not have a big effect.

4. For $\omega_m < \omega < \omega_n$, then $(\omega_m^2 - \omega^2) < 0$ and $(\omega_n^2 - \omega^2) > 0$ so the factor $\omega C_T(\omega_m/\omega_n)^2/(\omega_n^2 - \omega^2)/\omega_m^2 - \omega^2) < 0$, and since $\Gamma > 0$, there is no Γ which cause $1/Z_i\big|_{\text{in-air}} = 0$ for $\omega_m < \omega < \omega_n$.

5. For $\omega_m < \omega_n < \omega$, then $(\omega_m^2 - \omega^2) < 0$ and $(\omega_n^2 - \omega^2) < 0$ so that the factor $\omega C_T(\omega_m/\omega_n)^2/ (\omega_n^2 - \omega^2)/\omega_m^2 - \omega^2) > 0$, and Γ exists so that $1/Z_i\big|_{\text{in-air}} = 0$.

These five observations agree with the quantitative information shown in Fig. 5-7.

Suppose that in an actual transducer the values of C_T, or ω_m/ω_n (or equivalently ω_n/ω_m), or ω_m or ω_n vary from some desired baseline value. How could one adjust Γ to compensate and, thus, cause the maximum and minimums of $1/Z_i\big|_{\text{in-air}}$ to still occur at about the same baseline frequency values? Equation (5.172) yields the following guidance:

1. ω_m (the frequency of the maximum $1/Z_i\big|_{\text{in-air}}$) is independent (or with small losses nearly independent) of Γ (see item 3 above). Therefore, Γ is not effective in controlling ω_m and, thus, the FTR should be used to try to adjust ω_m to the baseline value.

2. Increases in C_T or ω_m/ω_n (or decreases in ω_n/ω_m) or ω_n require decreases in Γ in order to adjust one or the other of the minimum values of $1/Z_i\big|_{\text{in-air}}$ to occur at the baseline frequency.

Similar decreases in C_T or ω_m/ω_n or ω_n require increases in Γ to compensate.

6.0 REFERENCES

1. G.W. Benthien and D.L. Carson, "A Simplified Guidance Model for Longitudinal Vibrators," NOSC Tech Rpt 1209, Naval Ocean Systems Center, San Diego, Mar 1988.

2. D.L. Carson and A.C. Tims, "Piezoelectric Ceramic Reproducibility (for K_{33} - Mode Transducer Applications)," NRL Report. 9223, Mar 1990.

Appendix A

DETAILED DERIVATIONS

A.0 DETAILED DERIVATIONS

In order to avoid interrupting the flow of thought in Secs. 4 and 5, the details of the derivations of some relationships were omitted from Secs. 4 and 5. These derivations have been gathered together in this Appendix. In some cases, the details are presented only for the convenience of the interested reader. In other cases, the reader may find that the details and accompanying observations and analysis are essential for a complete understanding.

A.1 DERIVATION OF THE INITIAL FORM FOR E/V_H [EQ. (5.9)]

The starting point for the derivation of Eq. (5.9) is Eq. (4.8) from Sec. 4 which follows.

$$\frac{V}{E} = \frac{i\omega N d_{33}}{1 + i\omega(C_F + C)Z}.$$

Equation (4.8) must be reformulated in terms of V_H, Z_H and Z_T which is done using Eqs. (4.7) and (4.13), respectively, repeated below from Sec. 4.

$$Z = \frac{Z_H Z_T}{Z_H + Z_T},$$

and

$$V = \left(1 + \frac{Z_H}{Z_T}\right) V_H.$$

These last two equations used in Eq. (4.8) yield the following:

$$\frac{V_H\left(1 + \dfrac{Z_H}{Z_T}\right)}{E} = \frac{i\omega N d_{33}}{1 + i\omega(C_F + C)Z_H Z_T/(Z_H + Z_T)}. \qquad \textbf{(A.1.1)}$$

Thus,

$$\frac{E}{V_H} = \left(1 + \frac{Z_H}{Z_T}\right)\frac{1}{i\omega N d_{33}}\left[1 + i\omega(C_F + C)\frac{Z_H Z_T}{Z_H + Z_T}\right]. \qquad \textbf{(A.1.2)}$$

A slight rearrangement of Eq. (A.2) and use of Eq. (4.18) ($C_e = C_F + C$) yield the desired result; namely, Eq. (5.9) which is reprinted here for convenience.

$$\frac{E}{V_H} = \frac{1}{i\omega N d_{33}}\left(1 + \frac{Z_H}{Z_T}\right)\left[1 + i\omega\, C_e\left(\frac{Z_1 Z_T}{Z_H + Z_T}\right)\right].$$

A.2 DERIVATION OF A SIMPLER FORM FOR E/V_H [EQ. (5.10)]

The starting point for the derivation of Eq. (5.10) is Eq. (5.9) (derived above in Sec. A.1). First multiply through the left-hand side of Eq. (5.9) by the 1/i factor.

$$\frac{E}{V_H} = \frac{1}{\omega N d_{33}}\left(1 + \frac{Z_H}{Z_T}\right)\left[\omega\, C_e\left(\frac{Z_H Z_T}{Z_H + Z_T}\right) - i\right]. \qquad \textbf{(A.2.1)}$$

Then perform a series of algebraic manipulations as follows.

$$\frac{E}{V_H} = \frac{1}{\omega N d_{33}}\left(\frac{Z_H + Z_T}{Z_T}\right)\left[\omega\, C_e\left(\frac{Z_H Z_T}{Z_H + Z_T}\right) - i\right], \qquad \textbf{(A.2.2)}$$

$$\frac{E}{V_H} = \frac{1}{\omega N d_{33}}\left[\omega\, C_e Z_H - i\left(\frac{Z_H + Z_T}{Z_T}\right)\right], \qquad \textbf{(A.2.3)}$$

and

$$\frac{E}{V_H} = \frac{1}{\omega N d_{33}}\left[\omega\, C_e Z_H - i\left(\frac{Z_H}{Z_T} + 1\right)\right]. \qquad \textbf{(A.2.4)}$$

Substitute the simplified forms for Z_T and Z_H from Sec. 5.1 which are; $Z_T = i\omega m_T$ [Eq. (5.1)] and $Z_H = \omega(r + im)$ [Eq. (5.8)].

$$\frac{E}{V_H} = \frac{1}{\omega N d_{33}}\left[\omega^2 C_e (r + im) - i\left(\frac{\omega(r + im)}{i\omega m_T} + 1\right)\right], \qquad \textbf{(A.2.5)}$$

$$\frac{E}{V_H} = \frac{1}{\omega N d_{33}}\left[\omega^2 C_e (r + im) - \left(\frac{(r + im)}{m_T} + i\right)\right], \tag{A.2.6}$$

$$\frac{E}{V_H} = \frac{1}{\omega N d_{33}}\left[\left(\omega^2 C_e r - \frac{r}{m_T}\right) + i\left(\omega^2 C_e m - \frac{m}{m_T} - 1\right)\right], \tag{A.2.7}$$

and

$$\frac{E}{V_H} = \frac{1}{\omega N d_{33}}\left[r\left(\omega^2 C_e - \frac{1}{m_T}\right) + i\left(m\left\{\omega^2 C_e - \frac{1}{m_T}\right\} - 1\right)\right]. \tag{A.2.8}$$

At this point, use the symbol E_o from Eq. (5.11) in Sec. 5.2.1 which is

$$E_o = \left(\omega^2 C_e - \frac{1}{m_T}\right),$$

to obtain

$$\frac{E}{V_H} = \frac{1}{\omega N d_{33}}\left[rE_o + i(mE_o - 1)\right]. \tag{A.2.9}$$

This last equation is equivalent to Eq. (5.10).

A.3 DERIVATION OF A SIMPLER FORM FOR I/V_H [EQS. (5.15) AND (5.16)]

This section presents the derivations of the various expressions for I/V_H. These derivations are almost identical to those for E/V_H presented above, but are documented below for the convenience of the reader.

First, we present a derivation of the expression for I/V_H as it appears in Eq. (5.15). The starting point for the derivation is Eq. (4.10) shown below.

$$\frac{V}{I} = \frac{g_{33} l_c}{A_c} \frac{1}{1 + i\omega (C_F + C')Z}.$$

Equation (4.10) must be reformulated in terms of V_H, Z_H and Z_T using Eqs. (4.7) and (4.13) which were also repeated above in Sec. A.2.

$$\frac{I}{V_H\left(1 + \frac{Z_H}{Z_T}\right)} = \frac{A_c}{g_{33}1_c}\left[1 + i\omega(C_F + C')\frac{Z_H Z_T}{Z_H + Z_T}\right], \qquad \textbf{(A.3.1)}$$

and

$$\frac{I}{V_H} = \frac{A_c}{g_{33}1_c}\left(1 + \frac{Z_H}{Z_T}\right)\left[1 + i\omega(C_F + C')\frac{Z_H Z_T}{Z_H + Z_T}\right]. \qquad \textbf{(A.3.2)}$$

Use of Eq. (5.18) ($C'_e = C_F + C'$) yields the desired results; namely, Eq. (5.15) below

$$\frac{I}{V_H} = \frac{A_c}{g_{33}1_c}\left(1 + \frac{Z_H}{Z_T}\right)\left[1 + i\omega C'_e\left(\frac{Z_H Z_T}{Z_H + Z_T}\right)\right].$$

Next, we present the derivation of an alternate expression for I/V_H given in Eq. (5.16). To do this, Eq. (5.15) is rearranged to appear as follows:

$$\frac{I}{V_H} = \frac{A_c}{g_{33}1_c}\left[\left(1 + \frac{Z_H}{Z_T}\right) + i\omega C'_e Z_H\right]. \qquad \textbf{(A.3.3)}$$

At this point, use the radiation model approximations for Z_T and Z_H which are $Z_T = i\omega m_T$ [Eq. (5.1)] and $Z_H = \omega(r + im)$ [Eq. (5.8)].

$$\frac{I}{V_H} = \frac{A_c}{g_{33}1_c}\left[1 + \frac{\omega(r + im)}{i\omega m_T} + i\omega^2 C'_e(r + im)\right], \qquad \textbf{(A.3.4)}$$

$$\frac{I}{V_H} = \frac{A_c}{g_{33}1_c}\left[1 - i\frac{r}{m_T} + \frac{m}{m_T} + i\omega^2 C'_e r - \omega^2 C'_e m\right], \qquad \textbf{(A.3.5)}$$

$$\frac{I}{V_H} = \frac{A_c}{g_{33}1_c}\left[\left(1 - \omega^2 C'_e m + \frac{m}{m_T}\right) + i\left(\omega^2 C'_e r - \frac{r}{m_T}\right)\right], \qquad \textbf{(A.3.6)}$$

and

$$\frac{I}{V_H} = \frac{A_c}{g_{33}1_c}\left[1 - m\left(\omega^2 C'_e - \frac{1}{m_T}\right) + ir\left(\omega^2 C'_e - \frac{1}{m_T}\right)\right]. \qquad \textbf{(A.3.7)}$$

At this point substitution of the symbol I_o from Sec. 5.2.1, where $I_o \equiv \omega^2 C'_e - 1/m_T$ [Eq. (5.17)], yields the desired results, Eq. (5.16) below

$$\frac{I}{V_H} = \frac{A_c}{g_{33} l_c}[(1 - mI_o) + irI_o].$$

A.4 DERIVATION OF AN EXPRESSION FOR ω_n/ω_m [EQ. (5.31)]

The starting point for the derivation of Eq. (5.31) is the pair of equations for the idealized in-air resonance frequency [Eqs. (5.24) and (5.27) from Sec. 5.2.2.1]:

$$\omega_m^2 = \frac{1}{C_e}\left(\frac{1}{m_H} + \frac{1}{m_T}\right),$$

and

$$\omega_n^2 = \frac{1}{C_e'}\left(\frac{1}{m_H} + \frac{1}{m_T}\right).$$

Taking the ratio of these two relations one obtains Eq. (5.28) the following:

$$\frac{\omega_n^2}{\omega_m^2} = \frac{C_e}{C_e'} > 0.$$

Next one assembles Eqs. (4.2a), (4.2b), (4.4), (4.18), and (5.18), respectively.

$$C = S_{33}^E \frac{L}{A_c},$$

$$C' = S_{33}^D \frac{L}{A_c},$$

$$S_{33}^D = S_{33}^E - g_{33} d_{33},$$

$$C_e = C_F + C,$$

and

$$C_e' = C_F + C'.$$

Using these equations in Eq. (5.28) yields the following steps.

$$\frac{\omega_n^2}{\omega_m^2} = \frac{C + C_F}{C' + C_F}, \tag{A.4.1}$$

$$\frac{\omega_n^2}{\omega_m^2} = \frac{S_{33}^E \frac{L}{A_c} + C_F}{S_{33}^D \frac{L}{A_c} + C_F}, \tag{A.4.2}$$

$$\frac{\omega_n^2}{\omega_m^2} = \frac{S_{33}^E \frac{L}{A_c} + C_F}{\left(S_{33}^E - g_{33}d_{33}\right)\frac{L}{A_c} + C_F}, \tag{A.4.3}$$

$$\frac{\omega_n^2}{\omega_m^2} = \frac{S_{33}^E \frac{L}{A_c} + C_F}{S_{33}^E \frac{L}{A_c} + C_F - \frac{g_{33}d_{33}L}{A_c}}, \tag{A.4.4}$$

$$\frac{\omega_n^2}{\omega_m^2} = \frac{1}{1 - \frac{g_{33}d_{33}L}{A_c}\left(\frac{1}{S_{33}^E \frac{L}{A_c} + C_F}\right)}, \tag{A.4.5}$$

and

$$\frac{\omega_n^2}{\omega_m^2} = \frac{1}{1 - \frac{g_{33}d_{33}}{S_{33}^E}\left(\frac{1}{1 + \frac{C_F A_c}{S_{33}^E L}}\right)}. \tag{A.4.6}$$

Recall the following definition of K_{33} found in Eq. (4.24).

$$K_{33}^2 = \frac{g_{33}d_{33}}{S_{33}^E}.$$

Substitution of this definition into Eq. (A.4.6) yields the desired result [Eq. (5.31)].

$$\frac{\omega_n}{\omega_m} = \frac{1}{\sqrt{1 - K_{33}^2\left(\frac{1}{1 + \frac{C_F A_c}{S_{33}^E L}}\right)}}. \tag{5.31}$$

A.5 DERIVATION OF EXPRESSIONS FOR THE IN-WATER VALUE OF $|E/V_H|$ AND $|I/V_H|$ AT THE IN-AIR RESONANT FREQUENCIES, ω_m AND ω_n [EQS. (5.34) AND (5.38)]

Equations (5.34) and (5.38) are expressions for $|E/V_H|$ at ω_m and $|I/V_H|$ at ω_n respectively and both assume the assumptions of the simplified radiation model [Eqs. (5.1), (5.2), and (5.3)]. However, the relations are shown here to be special cases of two more general relations, derived here without use of the radiation model.

The starting point for the derivation of Eq. (5.34) is the basic expression for E/V_H found in Eq. (5.9).

$$\frac{E}{V_H} = \frac{1}{i\omega N d_{33}}\left(1 + \frac{Z_H}{Z_T}\right)\left[1 + i\omega C_e\left(\frac{Z_H Z_T}{Z_H + Z_T}\right)\right].$$

In-air impedance of the head assembly experiences no radiation loading.

$$Z_{H_{\text{in-air}}} = Z_H$$

and

$$Z_{H_{\text{in-water}}} = Z_H + Z_r.$$

At the resonant frequency ω_m in air, E/V_H is minimized. Thus,

$$\omega_m = \frac{i}{C_e}\left(\frac{Z_H + Z_T}{Z_H Z_T}\right). \tag{A.5.1}$$

In water, when E/V_H is evaluated at the in-air resonant frequency ω_m we get

$$\frac{E}{V_H} = \frac{1}{\omega_m i N d_{33}}\left(\frac{Z_T + Z_{H_{\text{in-water}}}}{Z_T}\right)\left[1 - \left(\frac{Z_{H_{\text{in-air}}} + Z_T}{Z_{H_{\text{in-air}}} Z_T}\right)\left(\frac{Z_{H_{\text{in-water}}} Z_T}{Z_{H_{\text{in-water}}} + Z_T}\right)\right], \tag{A.5.2}$$

and

$$\frac{E}{V_H} = \frac{1}{i N d_{33}\omega_m}\left(\frac{Z_T + Z_H + Z_{rm}}{Z_T}\right)\left[1 - \frac{(Z_H + Z_T)(Z_H + Z_{rm}) Z_T}{Z_H Z_T (Z_H + Z_{rm} + Z_T)}\right], \tag{A.5.3}$$

where Z_{rm} is the radiation impedance at ω_m.

$$\frac{E}{V_H} = \frac{1}{iNd_{33}\omega_m}\frac{1}{Z_T}\left[\frac{(Z_H + Z_{rm} + Z_T)(Z_H Z_T) - (Z_H + Z_T)(Z_H + Z_m)Z_T}{(Z_H Z_T)}\right], \tag{A.5.4}$$

$$\frac{E}{V_H} = \frac{1}{iNd_{33}\omega_m}\frac{1}{Z_T}\left[(Z_H + Z_{rm} + Z_T) - \frac{(Z_H + Z_T)(Z_H + Z_{rm})}{Z_H}\right], \tag{A.5.5}$$

$$\frac{E}{V_H} = \frac{1}{iNd_{33}\omega_m}\frac{1}{Z_T}\left(Z_H + Z_{rm} + Z_T - Z_H - Z_{rm} - Z_T - \frac{Z_T Z_{rm}}{Z_H}\right), \tag{A.5.6}$$

$$\frac{E}{V_H} = \frac{-1}{iNd_{33}\omega_m}\frac{1}{Z_T}\left(-\frac{Z_T Z_{rm}}{Z_H}\right), \tag{A.5.7}$$

and

$$\frac{E}{V_H} = \frac{1}{iNd_{33}\omega_m}\frac{Z_{rm}}{Z_H}. \tag{A.5.8}$$

When we substitute the simplified model for the head assembly operating in air [Eq. (5.2)] into the expression above, we obtain Eqs. (A.5.9) and (5.34), respectively.

$$\frac{E}{V_H} = \frac{-Z_{rm}}{iNd_{33}\omega_m(i\omega_m m_H)}, \tag{A.5.9}$$

and

$$\left|\frac{E}{V_H}\right| = \frac{1}{Nd_{33}\omega_m^2 m_H}|Z_{rm}|.$$

In a similar fashion a derivation of Eq. (5.38) can be obtained. The starting point is Eq. (5.15),

$$\frac{I}{V_H} = \frac{A_c}{g_{33}l_c}\left(1 + \frac{Z_H}{Z_T}\right)\left[1 + i\omega C_e'\left(\frac{Z_H Z_T}{Z_H + Z_T}\right)\right].$$

Notice that the form of this expression for I/V_H differs from the corresponding equation for E/V_H by only a constant. Thus all of the steps of the derivation of Eq. (5.34) are equivalent to that for the derivation of Eq. (5.38) provided the constant $1/i\omega Nd_{33}$ is replaced by $A_c/g_{33}l_c$.

Making this change relative to Eq. (A.5.9) yields the corresponding general relation for I/V_H [Eqs. (A.5.10) and (5.38), respectively].

$$\frac{I}{V_H} = \frac{A_c}{ig_{33}1_c\,\omega_n m_H} Z_{rn}, \tag{A.5.10}$$

and, therefore,

$$\left|\frac{I}{V_H}\right| = \frac{A_c}{g_{33}1_c\,\omega_n m_H}|Z_m|.$$

A.6 DERIVATION OF AN EXPRESSION FOR ω_1, THE FREQUENCY WHICH MINIMIZES B_2 [EQ. (5.57)]

In Eq. (5.20) of Sec. 5.2.1 the function B_2 was defined as

$$B_2 = r^2 I_o^2 + (1 - mI_o)^2,$$

where I_o is given by Eq. (5.17) as

$$I_o = \left(\omega^2 C_e' - \frac{1}{m_T}\right).$$

The minimum of B_2 with respect to variation of frequency is obtained by taking the derivative of B_2 with respect to ω and setting the result equal to zero.

$$\frac{\delta B_2}{\delta \omega} = 2r^2 I_o \frac{\delta I_o}{\delta \omega} + 2(1 - mI_o)(-m)\frac{\delta I_o}{\delta \omega}, \tag{A.6.1}$$

and

$$\frac{\delta B_2}{\delta \omega} = \left[r^2 I_o - m(1 - mI_o)\right] 2\frac{\delta I_o}{\delta \omega}. \tag{A.6.2}$$

But from Eq. (5.17)

$$\frac{\delta I_o}{\delta \omega} = 2\omega C_e'. \tag{A.6.3}$$

Thus, Eq. (A.6.2) may be written

$$\frac{\delta B_2}{\delta \omega} = [(r^2 + m^2) I_o - m]4\omega C_e'. \tag{A.6.4}$$

Since we are not interested in the solution $\omega_i = 0$, we make $\delta B_2/\delta\omega = 0$ by setting the other factor of Eq. (A.6.4) equal to zero as follows:

$$(r^2 + m^2) I_o - m = 0 \qquad \textbf{(A.6.5)}$$

and

$$I_o = \frac{m}{r^2 + m^2}. \qquad \textbf{(A.6.6)}$$

Using Eq. (5.17) for I_o and identifying ω_i as the angular frequency which solves Eq. (A.6.6) gives the desired equation {Eq. (5.57)].

$$\omega_i^2 = \left[\frac{1}{C_e'}\left(\frac{m}{r^2 + m^2} + \frac{1}{m_T}\right)\right].$$

We must still show that ω_i is the value of ω which minimizes the value of B_2. To do this, consider Eq. (A.6.4). Since $4\omega C_e' > 0$, then the other factor of this equation determines the sign of $\delta B_2/\delta\omega$. For convenience, let D_1 be the symbol for the other factor; that is,

$$D_1 = (r^2 + m^2) I_o - m. \qquad \textbf{(A.6.7)}$$

We know that at $\omega = \omega_i$ the value of I_o is such that $D_1 = 0$. Examination of Eq. (5.17) shows that as ω is increased from a value of $\omega = 0$, I_o starts out as a negative number and increases, eventually becoming a positive number. Thus, according to Eq. (A.6.7), D_1 and thus, the slope $\delta B_2/\delta\omega$ starts out as a negative number, goes to zero at $\omega = \omega_i$, and then the slope becomes positive for $\omega > \omega_i$. Thus, ω_i is indeed the angular frequency which minimizes B_2.

Notice that since $|I/V_H|$ is proportional to B_2 [i.e., Eq. (5.21)] the frequency ω_i which minimizes B_2 is also a resonant frequency for $|I/V_H|$.

A.7 DERIVATION OF AN EXPRESSION FOR $|I/V_H|$ AT ω_i [EQ. (5.58)]

The starting point for the derivation of Eq. (5.58) is Eq. (5.16), the basic equation for I/V_H assuming the simplified radiation model.

$$\frac{I}{V_H} = \frac{A_c}{g_{33} l_c}\left[\left(1 - mI_o\right) + irI_o\right],$$

where I_o is given by Eq. (5.17) to be

$$I_o = \left(\omega^2 C_e' - \frac{1}{m_T}\right).$$

Alternately, from Eq. (5.19) we have

$$\left|\frac{I}{V_H}\right| = \frac{A_c}{g_{33}l_c}\sqrt{r^2I_o^2 + (1 - mI_o)^2}.$$

Recall Eq. (5.59) from the previous section. It can be solved for m_T in terms of the resonant frequency ω_i.

$$\frac{1}{m_T} = C_e'\omega_i^2 - \frac{m}{r^2 + m^2}. \tag{A.7.1}$$

Then for this value of $1/m_T$,

$$I_o = \left(\omega^2 C_e' - C_e'\omega_i^2 + \frac{m}{r^2 + m^2}\right). \tag{A.7.2}$$

From Eq. (5.19) above we can see that

$$\left|\frac{I}{V_H}\right| = \frac{A_c}{g_{33}l_c}\left[(1 - mI_o)^2 + r^2I_o^2\right]^{1/2}, \tag{A.7.3}$$

$$\left|\frac{I}{V_H}\right| = \frac{A_c}{g_{33}l_c}\left[1 - 2mI_o + (m^2 + r^2)I_o^2\right]^{1/2}, \tag{A.7.4}$$

$$\left|\frac{I}{V_H}\right| = \frac{A_c}{g_{33}l_c}\left\{1 - 2m(\omega^2 - \omega_i^2)C_e' - \frac{2m^2}{r^2 + m^2} + (m^2 + r^2)\left[(\omega^2 - \omega_i^2)C_e' + \frac{m}{r^2 + m^2}\right]^2\right\}^{1/2}, \tag{A.7.5}$$

$$\left|\frac{I}{V_H}\right| = \frac{A_c}{g_{33}l_c}\left\{1 - 2m(\omega^2 - \omega_i^2)C_e' - \frac{2m^2}{r^2 + m^2} + (m^2 + r^2)\left[(\omega^2 - \omega_i^2)^2C_e'^2 + \frac{2m}{r^2 + m^2}(\omega^2 - \omega_i^2)C_e' + \frac{m^2}{(r^2 + m^2)^2}\right]\right\}^{1/2}, \tag{A.7.6}$$

$$\left|\frac{I}{V_H}\right| = \frac{A_c}{g_{33}1_c}\left\{1 - \frac{2m^2}{r^2+m^2} + \frac{m^2}{r^2+m^2} + (m^2+r^2)\left(\omega^2-\omega_i^2\right)^2 C_e'^2\right\}^{1/2}, \qquad \textbf{(A.7.7)}$$

and finally we have Eq. (5.58),

$$\left|\frac{I}{V_H}\right| = \frac{A_c}{g_{33}1_c}\left\{\frac{r^2}{r^2+m^2} + (m^2+r^2)\left(\omega^2-\omega_i^2\right)^2 C_e'^2\right\}^{1/2}.$$

Before we leave this section, it is useful for later derivations to point out that by comparison of Eq. (5.58) with Eq. (5.21), we can identify the function B_2 as

$$B_2 = \frac{r^2}{r^2+m^2} + (m^2+r^2)(\omega^2-\omega_i^2)^2\, C_e'^2. \qquad \textbf{(A.7.8)}$$

A.8 DEMONSTRATION THAT THE $|I/V_H|$ BANDWIDTH INCREASES WHEN THE HEAD MASS DECREASES AND/OR THE TAIL MASS INCREASES

For this discussion, ω_i is held fixed (see Sec. 5.2.2.4.1) and the bandwidth of $|I/V_H|$ is defined as the difference between two frequencies, ω_U the upper frequency and ω_L the lower frequency, which bracket the fixed resonant frequency ω_i

$$\omega_L < \omega_i < \omega_U. \qquad \textbf{(A.8.1)}$$

The lower frequency is that frequency at which the magnitude of $|I/V_H|_{\omega=\omega_L}$ is some multiple (G_L') of the $|I/V_H|_{\omega=\omega_i}$ at resonance. Thus, from Eq. (5.60) we have the following relationship

$$\left|\frac{I}{V_H}\right|_{\omega=\omega_L} = G_L'\left|\frac{I}{V_H}\right|_{\omega=\omega_i}.$$

Similarly, the upper frequency is selected by satisfying Eq. (5.62)

$$\left|\frac{I}{V_H}\right|_{\omega=\omega_U} = G_U'\left|\frac{I}{V_H}\right|_{\omega=\omega_i}.$$

In this section we show that, in general, for predetermined values of G_L' and G_U', the subject bandwidth $\omega_U - \omega_L$ (ω_i fixed) increases when the mass of the head assembly, m_H, decreases and/or the mass of the tail assembly, m_T, increases.

Notice that since $|I/V_H|$ is minimized at the resonance frequency, ω_i, then $|I/V_H|$ at both the upper and lower frequency is greater in magnitude. Thus,

$$G_L' > 1 \tag{A.8.2}$$

and

$$G_U' > 1\,. \tag{A.8.3}$$

As indicated in Sec. 5.2.2.4, the frequency dependence of I/V_H is contained in the function B_2. Thus, Eqs. (5.60) and (5.62) can be re-expressed using, by substituting the definition of B_2, Eq. 5.19 to yield:

$$\underset{\text{at } \omega_U}{\frac{A_c}{g_{33}l_c}\sqrt{B_2}} = G_L' \underset{\text{at } \omega_i}{\frac{A_c}{g_{33}l_c}\sqrt{B_2}} \tag{A.8.4}$$

and

$$\underset{\text{at } \omega_U}{\frac{A_c}{g_{33}l_c}\sqrt{B_2}} = G_U' \underset{\text{at } \omega_i}{\frac{A_c}{g_{33}l_c}\sqrt{B_2}} \tag{A.8.5}$$

These two equations are more simply stated as

$$B_{2L} = G_L'^2 B_{2i} \tag{A.8.6}$$

and

$$B_{2U} = G_U'^2 B_{2i}\,. \tag{A.8.7}$$

where $B_{2L} = B_2$ at ω_L, $B_{2U} = B_2$ at ω_U, and $B_{2i} = B_2$ at ω_i.

Using Eq. (A.7.8) to express B_2 at ω_L, ω_U, and ω_i, we now get

$$(r^2 + m^2)(\omega_L^2 - \omega_i^2)^2 C_e'^2 + \frac{r^2}{r^2 + m^2} = G_L'^2 \frac{r^2}{r^2 + m^2} \tag{A.8.8}$$

and

$$(r^2 + m^2)(\omega_U^2 - \omega_i^2)^2 C_e'^2 + \frac{r^2}{r^2 + m^2} = G_U'^2 \frac{r^2}{r^2 + m^2}\,. \tag{A.8.9}$$

$$(\omega_L^2 - \omega_i^2)^2 = \frac{(G_L'^2 - 1)r^2}{(r^2 + m^2)^2 C_e'^2} \tag{A.8.10}$$

and

$$(\omega_U^2 - \omega_i^2)^2 = \frac{(G_U'^2 - 1)r^2}{(r^2 + m^2)^2 C_e'^2}. \tag{A.8.11}$$

By definition, ω_L is the frequency lower than ω_i which yields the chosen magnitude of $|I/V_H|$. Thus,

$$(\omega_L^2 - \omega_i^2) = -\sqrt{\frac{(G_L'^2 - 1)r^2}{(r^2 + m^2)^2 C_e'^2}} \tag{A.8.12}$$

and

$$(\omega_U^2 - \omega_i^2) = +\sqrt{\frac{(G_U'^2 - 1)r^2}{(r^2 + m^2)^2 C_e'^2}}. \tag{A.8.13}$$

For convenience, define M ' as follows:

$$M' = \frac{r^2}{(r^2 + m^2)^2 C_e'^2}. \tag{A.8.14}$$

Using M'^2 from Eq. (A.8.14), rewrite Eqs. (A.8.12) and (A.8.13) as follows:

$$\omega_L^2 - \omega_i^2 = -\sqrt{M'^2(G_L'^2 - 1)} \tag{A.8.12a}$$

and

$$\omega_U^2 - \omega_i^2 = +\sqrt{M'^2(G_U'^2 - 1)}. \tag{A.8.13a}$$

From these last two equations one may make the following observations. As M ' increases, ω_L decreases (moving farther "below" the fixed ω_i) and ω_U increases (moving farther "above" the fixed ω_i). Thus, a bandwidth defined as $\omega_U - \omega_L$ (for a fixed value of ω_i increases as M increases.

M ' can be increased various ways but in this analysis all such changes are subject to the constraint of holding ω_i fixed; the constraining equation [Eq. (5.57)] is repeated for convenience

$$\omega_i^2 = \frac{1}{C_e'}\left(\frac{m}{r^2 + m^2} + \frac{1}{m_T}\right).$$

From the definition of M ' [Eq. (A.8.14)], one may write

$$M' = \frac{1}{C_E'} \frac{r}{r^2 + m^2}. \qquad \text{(A.8.15)}$$

The last two equations will be used to discuss three cases or ways to increase M ' and thus increase the subject bandwidth or flatness of $|I/V_H|$. In all cases ω_i is held fixed.

Case 1 Fix C_e' (vary m and m_T)

With both ω_i and C_e' held fixed, Eq. (A.8.15) shows that M ' can be increased by decreasing m. Since $m = m_H + x$ and for $m_H + x > 0$, one observes that m can be decreased by decreasing the mass of the head, m_H. Thus, for Case 1, decreasing the mass of the head increases the bandwidth and "flattens" the frequency response for $|I/V_H|$. For Case 1, Eq. (5.57) shows that as m is changed m_T must also be changed to hold ω_i fixed with C_e' also fixed. It turns out (as will be shown) that if $m > r$ then as m is decreased m_T must be increased to comply with Eq. (5.57) and if $m < r$ then m_T must be decreased as m_H is decreased. For $m = r$ one requires the largest value for m_T to comply with a fixed value of ω_i and C_e' in Eq. 5.62. Since the usual situation is for $m > r$, then for Case 1 it is concluded that the usual design trend calls for a smaller head mass and a larger tail mass in order to flatten the frequency response and increase the subject bandwidth $\omega_U - \omega_L$ for $|I/V_H|$.

The behavior of the quantity $m/(r^2 + m^2)$ versus changes in m determines what changes in m_T are needed in the above discussion. The graph of this function has the general shape shown in Fig. A-1.

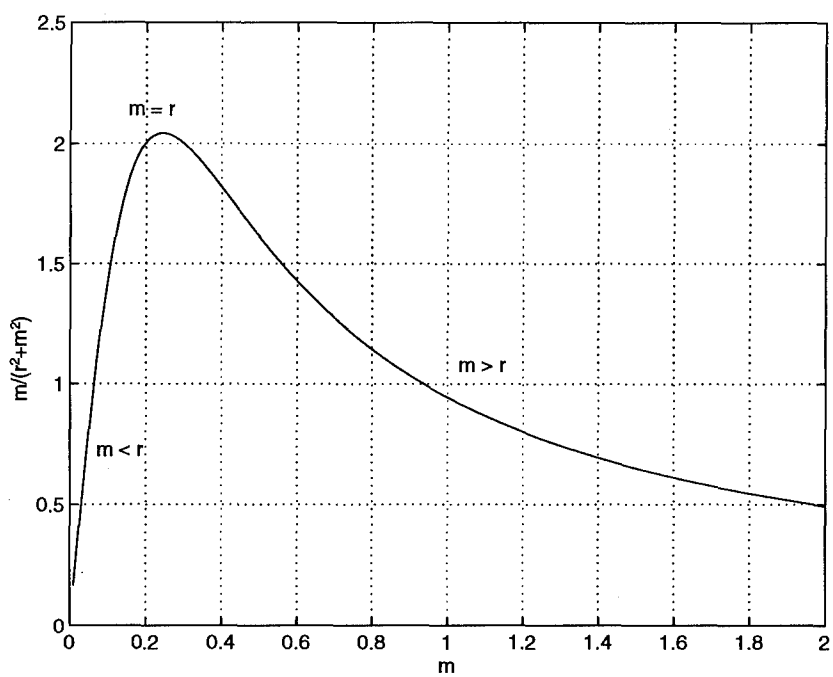

Fig. A-1 — Behavior of the quantity $m/(r^2 + m^2)$ versus changes in m

To see this, proceed as follows.

$$\frac{\delta \dfrac{m}{r^2 + m^2}}{\delta m} = \frac{1}{r^2 + m^2} - \frac{m}{(r^2 + m^2)^2}(2m), \tag{A.8.16}$$

$$\frac{\delta \dfrac{m}{r^2 + m^2}}{\delta m} = \frac{1}{(r^2 + m^2)^2}(r^2 + m^2 - 2m^2), \tag{A.8.17}$$

and

$$\frac{\delta \dfrac{m}{r^2 + m^2}}{\delta m} = \frac{1}{(r^2 + m^2)^2}(r^2 - m^2). \tag{A.8.18}$$

Thus, as shown in the figure, for m < r the slope is positive, for m > r the slope is negative, and for m = r the function has a maximum and the value of the function at m = r is 1/2r.

Case 2 Fix m_T (vary m and C_e')

With both ω_i and m_T held fixed, it is convenient to solve Eq. (5.57) for C_e' obtaining the following.

$$C_e' = \frac{1}{\omega_i^2}\left(\frac{m}{r^2 + m^2} + \frac{1}{m_T}\right). \tag{A.8.19}$$

Also, use C_e' from this last equation to rewrite Eq. (A.8.15) as follows.

$$M' = \frac{r}{(r^2 + m^2)} \frac{\omega_i^2}{\left(\dfrac{m}{r^2 + m^2} + \dfrac{1}{m_T}\right)}, \tag{A.8.20}$$

and

$$M' = \frac{\omega_i^2 r}{\left(m + \dfrac{r^2 + m^2}{m_T}\right)}. \tag{A.8.21}$$

Again, in Case 2 as in Case 1, one observes [from Eq. (A.8.21)] that M' is increased as m is decreased. Thus, once again, the bandwidth and flatness of $|I/V_H|$ is improved by decreasing the head mass. In Case 2, m_T is held fixed so according to Eq. (A.8.19), C_e' must be changed as M is changed.

As before, using the behavior of $m/(r^2 + m^2)$ one concludes that if $m > r$ then as m decreases C_e' must be increased, and if $m < r$ then as m decreases C_e' must be decreased and for $m = r$ one requires the maximum value for C_e'. Since the usual practical situation is for $m > r$ then one obtains the conclusion that as m_H is decreased, the compliance C_e' must be increased to maintain a fixed frequency (in this case ω_i).

How would the compliance C_e' be adjusted? Recall Eq. (5.18).

$$C_e' = S_{33}^D \frac{L}{A_c} + C_F$$

In the case where C_e' needs increasing, one could increase the compliance C_F of the FTR. Better yet, one could increase the length L of the CSA if geometric constraints permitted, and this would have the added benefit of decreasing the electric field ε. One could also decrease the area A_c down to some lower limit corresponding to mechanical stress and strain limits. The case where C_e' needs decreasing is discussed below in Case 3.

Case 3 Fix m_H (vary m_T and C_e')

With both ω_i and m_H (and, thus, m) fixed one can consider varying m_T and C_e'. Equation (A.8.21) shows that M ' can be increased by increasing m_T. Thus, it is concluded that the larger the tail mass (with m_H held fixed and C_e' adjusted to hold ω_i fixed), then the better the bandwidth and flatness of the quantities $|I/V_H|$. Equation (A.8.10) shows that as m_T is increased then the compliance C_e' must be decreased to maintain the fixed frequency ω_i.

How should C_e' be decreased as m_T is increased? From Eq. (5.18) above, one could decrease C_e' by decreasing L, but this would increase the electric field. One could decrease C_e' by decreasing the compliance C_F of the FTR up to the limit of removing the FTR entirely. One could further decrease C_e' by increasing the area A_c, which would, in turn, reduce the mechanical stress and strain.

Summary

In summary, one may state that for the usual practical case of $m > r$ then the smaller the head mass and the larger the tail mass the better the bandwidth, $\omega_U - \omega_L$ for a fixed ω_i and, correspondingly, the flatter the frequency response of $|I/V_H|$ and $|E/V_H|$.

In the above analysis, the value of $|I/V_H|$ at the ends of the frequency band were constrained to be proportional to the value at the frequency $\omega = \omega_i$ [see Eqs. (5.60) and (5.62)]. At $\omega = \omega_i$, $|I/V_H|$ is given by Eq. (5.59) to be

$$\left|\frac{I}{V_H}\right|_{\omega=\omega_i} = \frac{A_c}{g_{33} l_c} \sqrt{\frac{r^2}{r^2 + m^2}}.$$

Equation (5.59) shows that as m is decreased the value of $|I/V_H|$ at $\omega = \omega_i$ is increased; that is, it requires a higher electric field to achieve a given velocity, V_H, and, thus, to achieve a given source level.

Thus, as m is decreased to obtain a flatter frequency response, the required current is increased, not only at ω_i, but at the end points [Eqs. (5.85) and (5.86)]. The current could be held constant by increasing L, the length of the CSA, as m is decreased to flatten the frequency response of $|I/V_H|$. However, according to Eq. (5.18), one would also have to increase A_c and/or decrease C_F in order to maintain the desired value of C_e'. Thus, any time m is decreased (Cases 1 and 2 above) there is a penalty; namely, L and perhaps A_c must be increased in order to not exceed a given current limit. Increasing the length L of the CSA usually leads to an encounter with a length constraint for the transducer design. Among other things, it is this length constraint that often leads the designer to operate at the highest practical value of electric field.

In Case 3, m (and, thus, m_H) was fixed but the tail mass m_T was increased in order to flatten the frequency response (and C_e' was decreased to keep ω_i constant). Thus in Case 3, one observes that there is no current level penalty for increasing the tail mass, m_T, if m is being held fixed. One might ask, however, how is C_e' to be decreased as required. According to Eq. (5.18), one could shorten L but this would increase the field requirement. Instead, L could be held fixed and the area, Ac, of the ceramic could be increased to stiffen the CSA (decrease C_e'). Thus, in a sense, there is also a penalty for increasing m_T, but increasing the area A_c may be possible whereas increasing the length L (when m is decreased) is usually a more severe space constraint penalty.

A.9 DERIVATION OF AN EXPRESSION FOR $|E/V_H|$ IN TERMS OF ω_{ei}, THE FREQUENCY WHICH MINIMIZES B_1 [EQ. (5.67)]

The starting point for the derivation of Eq. (5.67) is Eq. (5.64). Equation (5.64) can be used to define $1/m_T$ in terms of the special frequency ω_{ei}.

$$\frac{1}{m_T} = C_e\omega_{ei}^2 - \frac{m}{r^2 + m^2} \tag{A.9.1}$$

Substituting this into Eq. (5.11) gives

$$E_o = \left[(\omega^2 - \omega_{ei}^2)C_e + \frac{m}{r^2 + m^2}\right] \tag{A.9.2}$$

This in turn can be substituted into Eq. (5.13).

$$B_1 = (r^2 + m^2)\left[(\omega^2 - \omega_{ei}^2)C_e + \frac{m}{(r^2 + m^2)}\right]^2 + 1 - 2m\left\{(\omega^2 - \omega_{ei}^2)C_e + \frac{m}{(r^2 + m^2)}\right\}, \tag{A.9.3}$$

$$B_1 = (r^2 + m^2)(\omega^2 - \omega_{ei}^2)^2 C_e^2 + 2m\,C_e(\omega^2 - \omega_{ei}^2) + \frac{m^2}{(r^2 + m^2)} + \frac{r^2 + m^2}{r^2 + m^2} - \frac{2m^2}{(r^2 + m^2)} - 2m\,(\omega^2 - \omega_{ei}^2)\,C_e, \tag{A.9.4}$$

and

$$B_1 = (r^2 + m^2)(\omega^2 - \omega_{ei}^2)^2 C_e^2 + \frac{r^2}{r^2 + m^2}. \qquad \textbf{(A.9.5)}$$

When this expression for B_1 is substituted into Eq. (5.14), we obtain the expected expression for $|E/V_H|$; namely, Eq. (5.67).

$$\left|\frac{E}{V_H}\right| = \frac{1}{\omega N d_{33}}\left[(r^2 + m^2)(\omega^2 - \omega_{ei}^2)^2 C_e^2 + \frac{r}{r^2 + m^2}\right]^{1/2}.$$

A.10 DERIVATION OF THE IN-WATER RESONANCE FREQUENCY, ω_e [(EQ. (5.76)], FOR $|\varepsilon/V_H|$ AND $|E/V_H|$

This subsection derives the expression for the in-water resonance frequency, ω_e, [Eq. (5.76)], of the quantities $|E/V_H|$ and $|\varepsilon/V_H|$. Also included is the derivation of an equation for ω_e in terms of ω_{ei} [Eq. (5.77)] and derivation of an equation for $|E/V_H|$ in terms of ω_e [Eq. (5.79)]. As pointed out in Sec. 5.2.2.4.2, the equations for $|\varepsilon/V_H|$ are the same as for $|E/V_H|$ except for the factor $1/\omega N d_{33}$ which changes to $1/\omega L d_{33}$ for the equations involving $|\varepsilon/V_H|$.

Equation (5.76) is repeated for convenience.

$$\omega_e^2 = \frac{1}{C_e}\sqrt{\frac{r^2 + (m + m_T)^2}{m_T^2(r^2 + m^2)}}.$$

The starting point for the derivation is Eq. (5.14) which is repeated next.

$$\left|\frac{E}{V_H}\right| = \frac{1}{\omega N d_{33}}\sqrt{B_1}.$$

Proceed as follows.

$$\left|\frac{E}{V_H}\right| = \frac{1}{N d_{33}}\sqrt{\frac{B_1}{\omega^2}}, \qquad \textbf{(A.10.1)}$$

$$\frac{\delta\left|\frac{E}{V_H}\right|}{\delta\omega} = \frac{1}{N d_{33}}\frac{\delta\sqrt{\frac{B_1}{\omega^2}}}{\delta\omega}, \qquad \textbf{(A.10.2)}$$

and

$$\frac{\delta\left|\frac{E}{V_H}\right|}{\delta\omega} = \frac{1}{2}\frac{1}{Nd_{33}}\frac{1}{\sqrt{\frac{B_1}{\omega^2}}}\frac{\delta\left(\frac{B_1}{\omega^2}\right)}{\delta\omega}. \tag{A.10.3}$$

But from Eq. (5.13) one writes

$$\frac{B_1}{\omega^2} = r^2\left(\frac{E_o}{\omega}\right)^2 + \left(\frac{1}{\omega} - m\frac{E_o}{\omega}\right)^2. \tag{A.10.4}$$

Thus,

$$\frac{\delta\left|\frac{B_1}{\omega^2}\right|}{\delta\omega} = 2r^2\left(\frac{E_o}{\omega}\right)\frac{\delta\left(\frac{E_o}{\omega}\right)}{\delta\omega} + 2\left(\frac{1}{\omega} - m\frac{E_o}{\omega}\right)\frac{\delta\left(\frac{1}{\omega} - m\frac{E_o}{\omega}\right)}{\delta\omega}, \tag{A.10.5}$$

or

$$\frac{\delta\left|\frac{B_1}{\omega^2}\right|}{\delta\omega} = \frac{2}{\omega}\left[r^2 E_o\frac{\delta\left(\frac{E_o}{\omega}\right)}{\delta\omega} + (1 - mE_o)\frac{\delta\left(\frac{1}{\omega} - m\frac{E_o}{\omega}\right)}{\delta\omega}\right]. \tag{A.10.6}$$

Let

$$B_3 = r^2E_o\frac{\delta\left(\frac{E_o}{\omega}\right)}{\delta\omega} + (1 - mE_o)\frac{\delta\left(\frac{1}{\omega} - m\frac{E_o}{\omega}\right)}{\delta\omega}. \tag{A.10.7}$$

So

$$\frac{\delta\frac{B_1}{\omega}}{\delta\omega} = \frac{2}{\omega}B_3 \tag{A.10.8}$$

From Eq. (5.11) one may write

$$\frac{E_o}{\omega} = \omega C_e - \frac{1}{\omega m_T}. \tag{A.10.9}$$

Thus,

$$\frac{\delta\left(\frac{E_o}{\omega}\right)}{\delta\omega} = \left(C_e + \frac{1}{\omega^2 m_T}\right). \tag{A.10.10}$$

Also,

$$\frac{\delta\left(\frac{1}{\omega} - m\frac{E_o}{\omega}\right)}{\delta\omega} = -\left(\frac{1}{\omega^2} + m\frac{\delta\frac{E_o}{\omega}}{\delta\omega}\right). \tag{A.10.11}$$

Using Eq. (A.10.10) in Eq. (A.10.11) yields:

$$\frac{\delta\left(\frac{1}{\omega} - m\frac{E_o}{\omega}\right)}{\delta\omega} = -\left(\frac{1}{\omega^2} + m\left[C_e + \frac{1}{\omega^2 m_T}\right]\right). \tag{A.10.12}$$

Using Eqs. (A.10.10) and (A.10.11) in Eq. (A.10.7) gives the following:

$$B_3 = r^2 E_o\left(C_e + \frac{1}{\omega^2 m_T}\right) - (1 - mE_o)\left[\frac{1}{\omega^2} + m\left(C_e + \frac{1}{\omega^2 m_T}\right)\right] \tag{A.10.13}$$

and

$$B_3 = (r^2 + m^2)\left(C_e + \frac{1}{\omega^2 m_T}\right)E_o - m\left(C_e + \frac{1}{\omega^2 m_T}\right) - \frac{(1 - mE_o)}{\omega^2}. \tag{A.10.14}$$

Form the following definitions.

$$B_4 = \frac{(1 - mE_o)}{\omega^2}, \tag{A.10.15}$$

$$B_5 = m\left(C_e + \frac{1}{\omega^2 m_T}\right), \tag{A.10.16}$$

and

$$B_6 = \left(C_e + \frac{1}{\omega^2 m_T}\right)E_o. \tag{A.10.17}$$

Using these definitions, rewrite Eq. (A.10.14) as follows.

$$B_3 = (r^2 + m^2) B_6 - (B_4 + B_5). \tag{A.10.18}$$

Use Eq. (5.11) in Eq. (A.10.15) to write

$$B_4 = \frac{1}{\omega^2} - \frac{m}{\omega^2}\left(\omega^2 C_e - \frac{1}{m_T}\right) \tag{A.10.19}$$

and

$$B_4 = \frac{1}{\omega^2} - mC_e + \frac{m}{\omega^2 m_T}. \tag{A.10.20}$$

Also, Eq. (A.10.16) may be rewritten as follows:

$$B_5 = 0 + mC_e + \frac{m}{\omega^2 m_t}. \tag{A.10.21}$$

Combining Eqs. (A.10.20) and (A.10.21) gives

$$B_4 + B_5 = \frac{1}{\omega^2} + \frac{2m}{\omega^2 m_T} \tag{A.10.22}$$

and

$$B_4 + B_5 = \frac{1}{\omega^2}\left(1 + \frac{2m}{m_T}\right). \tag{A.10.23}$$

Also, using Eq. (5.11) in Eq. (A.10.17) gives

$$B_6 = \left(C_e + \frac{1}{\omega^2 m_T}\right)\left(\omega^2 C_e - \frac{1}{m_T}\right), \tag{A.10.24}$$

$$B_6 = \omega^2 C_e^2 + \frac{C_e}{m_T} - \frac{C_e}{m_T} - \frac{1}{\omega^2 m_T^2}, \tag{A.10.25}$$

and

$$B_6 = \omega^2 C_e^2 - \frac{1}{\omega^2 m_T^2}. \tag{A.10.26}$$

Using Eqs. (A.10.23) and (A. 10.26) in Eq. (A.10.18) gives

$$B_3 = (r^2 + m^2)\left(\omega^2 C_e^2 - \frac{1}{\omega^2 m_T^2}\right) - \frac{1}{\omega^2}\left(1 + \frac{2m}{m_T}\right) \qquad \textbf{(A.10.27)}$$

and

$$B_3 = \frac{(r^2 + m^2)}{\omega^2}\left[\omega^4 C_e^2 - \frac{1}{m_T^2} - \frac{1}{(r^2 + m^2)}\left(1 + \frac{2m}{m_T}\right)\right]. \qquad \textbf{(A.10.28)}$$

Define B_7 as follows:

$$B_7 = \left(\omega^4 C_e^2 - \frac{1}{m_T^2}\right) - \frac{1}{r^2 + m^2}\left(1 + \frac{2m}{m_T}\right), \qquad \textbf{(A.10.29)}$$

so

$$B_3 = \frac{r^2 + m^2}{\omega^2} B_7. \qquad \textbf{(A.10.30)}$$

Combining equations

$$\frac{\delta\left|\frac{E}{V_H}\right|}{\delta\omega} = \frac{1}{2}\frac{1}{Nd_{33}}\frac{1}{\sqrt{\frac{B_1}{\omega^2}}}\left(\frac{2}{\omega}\right)\left(\frac{r^2 + m^2}{\omega^2}\right)B_7. \qquad \textbf{(A.10.31)}$$

All the quantities on the right end of Eq. (A.10.31) are greater than zero for all $\omega > 0$ except B_7. Therefore, the sign of $\delta|E/V_H|/\delta\omega$ is determined by B_7 and this partial derivative equals zero if and only if $B_7 = 0$.

Examination of Eq. (A.10.29) for B_7 shows that as ω increases from some small value near to but greater than zero the sign of B_7 starts out as negative, remains negative until for some value of $\omega = \omega_e$, B_7 goes through a value of zero after which the sign of B_7 changes and remains positive. Thus, at ω_e

$$\frac{\delta\left|\frac{E}{V_H}\right|}{\delta\omega} = 0 \qquad \textbf{(A.10.32)}$$

and one has shown that $|E/V_H|$ has its one and only minimum value at ω_e. The expression for ω_e is determined by considering $B_7 = 0$ as follows.

$$\left(\omega_e^4 C_e^2 - \frac{1}{m_T^2}\right) = \frac{1}{r^2 + m^2}\left(1 + \frac{2m}{m_T}\right), \tag{A.10.33}$$

$$\omega_e^4 C_e^2 = \left(\frac{1}{r^2 + m^2}\right)\left(1 + \frac{2m}{m_T}\right) + \frac{1}{m_T^2}, \tag{A.10.34}$$

$$\omega_e^4 C_e^2 = \frac{m_T^2\left(1 + \frac{2m}{m_T}\right) + (r^2 + m^2)}{m_T^2(r^2 + m^2)}, \tag{A.10.35}$$

$$\omega_e^4 C_e^2 = \frac{r^2 + m^2 + 2mm_T + m_T^2}{m_T^2(r^2 + m^2)}, \tag{A.10.36}$$

$$\omega_e^4 C_e^2 = \frac{r^2 + (m + m_T)^2}{m_T^2(r^2 + m^2)}, \tag{A.10.37}$$

and

$$\omega_e^4 = \frac{1}{C_e^2}\left[\frac{r^2 + (m + m_T)^2}{m_T^2(r^2 + m^2)}\right]. \tag{A.10.38}$$

The desired equation for ω_e^2 [Eq. (5.76)] is obtained by taking the square root of both sides of Eq. (A.10.38).

The next goal is to derive Eq. (5.77) which is repeated for convenience.

$$\omega_e^2 = \omega_{ei}^2\sqrt{1 + M_2^2}.$$

The following previously derived equations [Eqs. (5.66) and (5.65), respectively] are used in the derivation.

$$\omega_{ei}^2 = \frac{1}{C_e} M_1,$$

where

$$M_1 = \frac{m}{r^2 + m^2} + \frac{1}{m_T}.$$

For convenience, define M_e as follows.

$$M_e^2 = \frac{r^2 + (m + m_T)^2}{m_T^2(r^2 + m^2)}. \qquad \textbf{(A.10.39)}$$

Comparison with Eq. (5.76) shows that one can write the following.

$$\omega_e^2 = \frac{1}{C_e}\sqrt{M_e^2}. \qquad \textbf{(A.10.40)}$$

It will be shown next that

$$M_e^2 = M_1^2 + \frac{r^2}{(r^2 + m^2)^2}. \qquad \textbf{(A.10.41)}$$

Manipulate M_e^2 as follows.

$$M_e^2 = \frac{r^2 + m^2 + 2mm_T + m_T^2}{m_T^2(r^2 + m^2)}, \qquad \textbf{(A.10.42)}$$

$$M_e^2 = \frac{1}{m_T^2} + \frac{2m}{m_T(r^2 + m^2)} + \frac{1}{r^2 + m^2}, \qquad \textbf{(A.10.43)}$$

$$M_e^2 = \frac{1}{m_T^2} + \frac{2m}{m_T(r^2 + m^2)} + \frac{m^2}{(r^2 + m^2)^2} + \frac{1}{r^2 + m^2} - \frac{m^2}{(r^2 + m^2)^2}, \qquad \textbf{(A.10.44)}$$

$$M_e^2 = \left(\frac{1}{m_T} + \frac{m}{r^2 + m^2}\right)^2 + \frac{1}{(r^2 + m^2)^2}(r^2 + m^2 - m^2), \qquad \textbf{(A.10.45)}$$

and

$$M_e^2 = \left(\frac{1}{m_T} + \frac{m}{r^2 + m^2}\right)^2 + \frac{r^2}{(r^2 + m^2)^2}. \qquad \textbf{(A.10.46)}$$

Using the definition of M_1, one obtains Eq. (A.10.41) as desired. Next use Eq. (A.10.41) in Eq. (A.10.40) and proceed as follows.

$$\omega_e^2 = \frac{1}{C_e}\sqrt{M_1^2 + \frac{r^2}{(r^2 + m^2)^2}} \tag{A.10.47}$$

and

$$\omega_e^2 = \frac{M_1}{C_e}\sqrt{1 + \frac{r^2}{(r^2 + m^2)^2}\frac{1}{M_1^2}}. \tag{A.10.48}$$

Use Eq. (5.66) and write

$$\omega_e^2 = \omega_{ei}^2\sqrt{1 + \frac{r^2}{(r^2 + m^2)^2}\frac{1}{M_1^2}}. \tag{A.10.49}$$

Define M_2^2 as follows.

$$M_2^2 = \frac{r^2}{(r^2 + m^2)^2}\frac{1}{M_1^2}. \tag{A.10.50}$$

Use Eq. (5.65) in Eq. (A.10.50) and continue as follows.

$$M_2^2 = \frac{r^2}{(r^2 + m^2)^2\left(\dfrac{m}{r^2 + m^2} + \dfrac{1}{m_T}\right)^2}. \tag{A.10.51}$$

$$M_2^2 = \frac{r^2}{\left(m + \dfrac{r^2 + m^2}{m_T}\right)^2}. \tag{A.10.52}$$

$$M_2^2 = \frac{r^2 m_T^2}{\left(r^2 + m^2 + mm_T\right)^2}. \tag{A.10.53}$$

Taking the square root yields Eq. (5.78) which is repeated for convenience.

$$M_2 = \frac{rm_T}{r^2 + m^2 + mm_T}.$$

Use of M_2 in Eq. (A.10.49) yields one of the desired equations; namely, Eq. (5.77).

The next goal is to derive Eq. (5.79) which is repeated for convenience.

$$\left|\frac{E}{V_H}\right| = \frac{1}{\omega N d_{33}} \sqrt{(r^2 + m^2)\left(\omega^2\sqrt{1 + M_2^2} - \omega_e^2\right)^2 \frac{M_1^2}{\omega_e^4} + \frac{r^2}{r^2 + m^2}}.$$

The starting point for the derivation is Eq. (5.69) which is also repeated.

$$\left|\frac{E}{V_H}\right| = \frac{1}{\omega N d_{33}} \sqrt{(r^2 + m^2)\left(\omega^2 - \omega_{ei}^2\right)^2 \frac{1}{\omega_{ei}^4} M_1^2 + \frac{r^2}{r^2 + m^2}}.$$

One solves Eq. (5.77) for ω_{ei}^2 as follows.

$$\omega_{ei}^2 = \omega_e^2 \frac{1}{\sqrt{1 + M_2^2}}. \qquad \textbf{(A.10.54)}$$

Use Eq. (A.10.54) in Eq. (5.69) to write

$$\left|\frac{E}{V_H}\right| = \frac{1}{\omega N d_{33}} \sqrt{(r^2 + m^2)\left(\omega^2 - \frac{\omega_e^2}{\sqrt{1 + M_2^2}}\right)^2 \frac{M_1^2}{\omega_e^4}(1 + M_2^2) + \frac{r^2}{r^2 + m^2}}. \qquad \textbf{(A.10.55)}$$

Multiplying through by the factor $1 + M_2^2$ yields Eq. (5.79) as desired.

A.11 BEHAVIOR OF $|E/V_H|$ AT $\omega = \omega_e$

The goal in this section is to show that with m_T held fixed, as m_H is increased sufficiently ($m_H > 0$) then the value of $|E/V_H|$ at $\omega = \omega_e$ can be made as small as desired. The starting point will be Eq. (5.79) which is repeated for convenience.

$$\left|\frac{E}{V_H}\right| = \frac{1}{\omega N d_{33}} \sqrt{(r^2 + m^2)\left(\omega^2\sqrt{1 + M_2^2} - \omega_e^2\right)^2 \frac{M_1^2}{\omega_e^4} + \frac{r^2}{r^2 + m^2}}.$$

At $\omega = \omega_e$ one obtains

$$\left|\frac{E}{V_H}\right|_{\omega = \omega_e} = \frac{1}{\omega_e N d_{33}} \sqrt{(r^2 + m^2)\left(\sqrt{1 + M_2^2} - 1\right)^2 M_1^2 + \frac{r^2}{r^2 + m^2}}. \qquad \textbf{(A.11.1)}$$

The quantity under the radical, which shall be called B_{1e} [see Eq. (A.11.2) which follows], determines the behavior of $|E/V_H|$ $\omega = \omega_e$ as m is increased.

$$B_{1e} = (r^2 + m^2)\left(\sqrt{1 + M_2^2} - 1\right)^2 M_1^2 + \frac{r^2}{r^2 + m^2}. \tag{A.11.2}$$

Rewrite as follows.

$$B_{1e} = (r^2)\left(\sqrt{1 + M_2^2} - 1\right)^2 M_1^2 + \frac{r^2}{r^2 + m^2} + m^2\left(\sqrt{1 + M_2^2} - 1\right)M_1^2. \tag{A.11.3}$$

Let

$$T_1 = r^2\left(\sqrt{1 + M_2^2} - 1\right)^2 M_1^2, \tag{A.11.4}$$

$$T_2 = \frac{r^2}{r^2 + m^2}, \tag{A.11.5}$$

and

$$T_3^{2\backslash} = m^2\left(\sqrt{1 + M_2^2} - 1\right)^2 M_1^2. \tag{A.11.6}$$

Recall Eqs. (5.64) and (5.78) shown below.

$$M_1 = \frac{m}{r^2 + m^2} + \frac{1}{m_T}$$

and

$$M_2 = \frac{rm_T}{r^2 + m^2 + mm_T}.$$

Using this information, one notes the following.

$$\lim M_{1_{m \to \infty}} = \frac{1}{m_T}, \tag{A.11.7}$$

$$\lim M_{2_{m \to \infty}} = 0, \tag{A.11.8}$$

$$\lim T_{1_{m \to \infty}} = 0, \tag{A.11.9}$$

and

$$\lim T_{2_{m \to \infty}} = 0, \tag{A.11.10}$$

but

$$\lim T_{3_{m\to\infty}} = \frac{1}{m_T}(\infty \text{ times } 0). \tag{A.11.11}$$

If by an application of L'Hospital's rule one could show that lim T_3 as $m \to \infty$ was, in fact, zero, then the desired goal would have been reached; namely, one would have shown that lim $B_{1e} = 0$ and, therefore, $|E/V_H|$ at $\omega = \omega_e$ can be made as small as desired by making m large enough (m is made large by making the head mass, m_H, large since $m = m_H + x$).

The last step then is to apply L'Hospital's rule as indicated.

Let T_4 be defined as

$$T_4 = m\left(\sqrt{1 + M_2^2} - 1\right). \tag{A.11.12}$$

Note that

$$T_3 = T_4 M_1, \tag{A.11.13}$$

$$\lim T_{3_{m\to\infty}} = \lim M_{1_{m\to\infty}} \lim T_{4_{m\to\infty}}, \tag{A.11.14}$$

and

$$\lim T_{3_{m\to\infty}} = \frac{1}{m_T} \lim T_{4_{m\to\infty}}. \tag{A.11.15}$$

Thus, it will be sufficient to apply L'Hospital's rule to the factor T_4 as follows. Let

$$T_4 = \frac{T_5}{T_6}, \tag{A.11.16}$$

where

$$T_5 = \sqrt{1 + M_2^2} - 1 \tag{A.11.17}$$

and

$$T_6 = \frac{1}{m}. \tag{A.11.18}$$

Applying L'Hospital's rule,

$$\frac{\delta T_5}{\delta m} = \frac{1}{2} \frac{2M_2}{\sqrt{1 + M_2^2}} \frac{\delta M_2}{\delta m}, \tag{A.11.19}$$

$$\frac{\delta M_2}{\delta m} = - \frac{rm_T(2m + m_T)}{(r^2 + m^2 + mm_T)^2}, \tag{A.11.20}$$

$$\frac{\delta M_2}{\delta m} = \frac{-1}{rm_T} \left(\frac{rm_T}{r^2 + m^2 + mm_T} \right)^2 (2m + m_T), \tag{A.11.21}$$

and

$$\frac{\delta M_2}{\delta m} = - \frac{1}{rm_T} M_2^2 (2m + m_T). \tag{A.11.22}$$

Thus,

$$\frac{\delta T_5}{\delta m} = - \frac{M_2^3}{rm_T \sqrt{1 + M_2^2}} (2m + m_T) \tag{A.11.23}$$

and

$$\frac{\delta T_6}{\delta m} = - \frac{1}{m^2}. \tag{A.11.24}$$

Combining this information gives

$$\lim T_{4_{m \to \infty}} = \lim \frac{T_5}{T_{6_{m \to \infty}}}, \tag{A.11.25}$$

$$\lim T_{4_{m \to \infty}} = \lim \frac{m^2 M_2^3 (2m + m_T)}{rm_T \sqrt{1 + M_2^2}} \Big|_{m \to \infty}, \tag{A.11.26}$$

$$\lim T_{4_{m \to \infty}} = \frac{1}{rm_T} \left(\lim \frac{1}{\sqrt{1 + M_2^2}} \right)_{m \to \infty} \left[\left(\lim 2m^3 M_2^3 \right)_{m \to \infty} + \left(m_T \lim m^2 M_2^3 \right)_{m \to \infty} \right], \tag{A.11.27}$$

$$\lim T_{4_{m\to\infty}} = \frac{1}{rm_T}\left[2\lim\left(\frac{rm_T}{\frac{r^2}{m}+m+m_T}\right)^3\right]_{m\to\infty} + \left[m_T\lim\frac{1}{m}\left(\frac{rm_T}{\frac{r^2}{m}+m+m_T}\right)^3\right]_{m\to\infty}, \qquad \textbf{(A.11.28)}$$

$$\lim T_4 = \frac{1}{rm_{T_{m\to\infty}}}2(0) + (m_T)(0), \qquad \textbf{(A.11.29)}$$

and

$$\lim T_{4_{m\to\infty}} = 0. \qquad \textbf{(A.11.30)}$$

As indicated above, this is the last step in the proof that

$$\lim\left|\frac{E}{V_H}\right|_{\omega=\omega_{e_{m\to\infty}}} = 0.$$

A.12 A BANDWIDTH CHARACTERIZATION OF $|E/V_H|$ AND $|\varepsilon/V_H|$ IN TERMS OF ω_{el}

Even though ω_{ei} is not the resonance frequency of $|E/V_H|$ (or, equivalently, $|\varepsilon/V_H|$) it has proven useful, as is indicated in Sec. 5.2.2.6, to approximately characterize the frequency dependence characteristics of $|E/V_H|$ in terms of ω_{ei}. Although the general conclusions are similar to those for $|I/V_H|$, the analysis steps are somewhat different because of the fact $1/\omega$ found in the equation for $|E/V_H|$ [Eq. (5.67)] and $|\varepsilon/V_H|$ [Eq. (5.73a)] but not found in the equation for $|I/V_H|$ [Eq. (5.58)]. There are also some differences due to the fact that $|E/V_H|$ and $|\varepsilon/V_H|$ are not a function of the area A_c.

The starting point for a bandwidth characterization of $|E/V_H|$ uses the constraints explained in Sec. 5.2.2.6 and embodied in the following equations [Eqs. (5.89), (5.91), (5.90), (5.92), respectively] repeated for convenience.

$$\left|\frac{\epsilon}{V_H}\right|_{\omega=\omega_L} = G_L\left|\frac{\epsilon}{V_H}\right|_{\omega=\omega_{el}},$$

$$G_L > 1,$$

$$\left|\frac{\epsilon}{V_H}\right|_{\omega=\omega_U} = G_U\left|\frac{\epsilon}{V_H}\right|_{\omega=\omega_{el}},$$

and

$$k_U > 1 .$$

Next, use Eq. (5.73a) to write out the following.

$$\left|\frac{\epsilon}{V_H}\right|_{\omega=\omega_L} = \frac{1}{\omega_L L d_{33}} \sqrt{(r^2 + m^2)\left(\omega_L^2 - \omega_{ei}^2\right)^2 C_e^2 + \frac{r^2}{r^2 + m^2}} . \qquad \textbf{(A.12.1)}$$

Also use Eq. (5.74) repeated here for convenience.

$$\left|\frac{\epsilon}{V_H}\right|_{\omega=\omega_{ei}} = \frac{1}{\omega_{ei} L d_{33}} \sqrt{\frac{r^2}{r^2 + m^2}} .$$

Use Eqs. (A.12.1), (5.74), and (5.85) to write

$$\frac{1}{\omega_L L d_{33}} \sqrt{(r^2 + m^2)\left(\omega_L^2 - \omega_{ei}^2\right)^2 C_e^2 + \frac{r^2}{r^2 + m^2}} = \frac{G_L}{\omega_{ei} L d_{33}} \sqrt{\frac{r^2}{r^2 + m^2}} , \qquad \textbf{(A.12.2)}$$

$$(r^2 + m^2)\left(\omega_L^2 - \omega_{ei}^2\right)^2 C_e^2 + \frac{r^2}{r^2 + m^2} = G_L^2 \frac{\omega_L^2}{\omega_{ei}^2} \frac{r^2}{r^2 + m^2} , \qquad \textbf{(A.12.3)}$$

and

$$\omega_{ei}^4 \left(\frac{\omega_L^2}{\omega_{ei}^2} - 1\right)^2 C_e^2 + \frac{r^2}{(r^2 + m^2)^2} = G_L^2 \frac{\omega_L^2}{\omega_{ei}^2} \frac{r^2}{(r^2 + m^2)^2 \omega_{ei}^4 C_e^2} . \qquad \textbf{(A.12.4)}$$

Let

$$M^2 = \frac{r^2}{(r^2 + m^2)^2 \omega_{ei}^4 C_e} . \qquad \textbf{(A.12.5)}$$

So,

$$M = \frac{r}{(r^2 + m^2)\omega_{ei}^2 C_e} > 0 . \qquad \textbf{(A.12.6)}$$

So in terms of M^2 write

$$\left(\frac{\omega_L^2}{\omega_{ei}^2} - 1\right)^2 + M^2 = G_L^2 \frac{\omega_L^2}{\omega_{ei}^2} M^2, \tag{A.12.7}$$

$$\left(\frac{\omega_L}{\omega_{ei}}\right)^4 - 2\left(\frac{\omega_L}{\omega_{ei}}\right)^2 - G_L^2\left(\frac{\omega_L}{\omega_{ei}}\right)^2 M^2 + (M^2 + 1) = 0, \tag{A.12.8}$$

and

$$\left(\frac{\omega_L}{\omega_{ei}}\right)^4 - 2\left(1 + \frac{G_L^2 M^2}{2}\right)\left(\frac{\omega_L}{\omega_{ei}}\right) + (M^2 + 1) = 0. \tag{A.12.9}$$

Use the quadratic formula with

$$a = 1,$$

$$b = -2\left(1 + \frac{G_L^2 M^2}{2}\right),$$

and

$$c = M^2 + 1$$

to write

$$\left(\frac{\omega_L}{\omega_{ei}}\right)^2 = \frac{2\left(1 + \frac{G_L^2 M^2}{2}\right) \pm \sqrt{4\left(1 + \frac{G_L^2}{2} M^2\right)^2 - 4(M^2 + 1)}}{2}, \tag{A.12.10}$$

$$\left(\frac{\omega_L}{\omega_{ei}}\right)^2 = \left(1 + \frac{G_L^2 M^2}{2}\right) \pm \sqrt{\left(1 + \frac{G_L^2}{2} M^2\right)^2 - (M^2 + 1)}, \tag{A.12.11}$$

$$\left(\frac{\omega_L}{\omega_{ei}}\right)^2 = \left(1 + \frac{G_L^2 M^2}{2}\right) \pm \sqrt{1 + G_L^2 M^2 + \frac{G_L^4 M^4}{4} - M^2 - 1}, \tag{A.12.12}$$

and

$$\left(\frac{\omega_L}{\omega_{ei}}\right)^2 = \left(1 + \frac{G_L^2 M^2}{2}\right) \pm \sqrt{1 + \frac{G_L^4}{4} M^4 + M^2(G_L^2 - 1)}. \qquad \textbf{(A.12.13)}$$

Since $G_L > 1$, then $G_L^2 > 1$ and $G_L^2 - 1 > 0$ and, thus, the discriminate is positive so there is a real number solution for Eq. (A.12.13). Rewrite the last equation as follows.

$$\left(\frac{\omega_L}{\omega_{ei}}\right)^2 - 1 = \frac{K_L^2}{2} M^2 \pm \sqrt{\frac{K_L^4}{4} M^4 + M^2(K_L^2 - 1)}. \qquad \textbf{(A.12.14)}$$

Note that $\omega_L < \omega_{ei}$ (by definition), so $\omega_L/\omega_{ei} < 1$, $(\omega_L/\omega_{ei})^2 < 1$, and $(\omega_L/\omega_{ei}) - 1 < 0$. Therefore, one must choose the negative sign and write the following.

$$\left(\frac{\omega_L}{\omega_{ei}}\right)^2 - 1 = \frac{G_L^2}{2} M^2 - \sqrt{\frac{G_L^4}{4} M^4 + M^2(G_L^2 - 1)}. \qquad \textbf{(A.12.15)}$$

By similar steps one concludes also the following.

$$\left(\frac{\omega_U}{\omega_{ei}}\right)^2 - 1 = \frac{G_U^2}{2} M^2 + \sqrt{\frac{G_U^4}{4} M^4 + M^2(G_L^2 - 1)}. \qquad \textbf{(A.12.16)}$$

From these last two equations one may make the following observations. As M increases, ω_L decreases (moving farther "below" the fixed ω_{ei}) and ω_U increases (moving farther "above" the fixed ω_{ei}). Thus, a bandwidth defined as $\omega_U - \omega_L$ (for a fixed value of ω_{ei}) increases as M increases.

M can be increased various ways but in this analysis all such changes are subject to the constraint of holding ω_{ei} fixed; the constraining equation [Eq. (5.64)] is repeated for convenience.

$$\omega_{ei}^2 = \frac{1}{C_e}\left(\frac{m}{r^2 + m^2} + \frac{1}{m_T}\right).$$

From the definition of M one obtained Eq. (A.12.6) repeated below.

$$M = \frac{r}{(r^2 + m^2)\omega_{ei}^2 C_e}. \qquad \textbf{(A.12.6)}$$

The last two equations will be used to discuss three cases or ways to increase M and thus increase the bandwidth or flatness of $|\varepsilon/V_H|$ and $|E/V_H|$. In all cases ω_{ei} is held fixed.

Case 1 Fix C_e (vary m and m_T)

With both ω_{ei} and C_e held fixed, Eq. (A.12.6) shows that M can be increased by decreasing m. Since $m = m_H + x$ and for $m_H + x > 0$, one observes that m can be decreased by decreasing the mass of the head, m_H. Thus, for Case 1, decreasing the mass of the head increases the bandwidth and "flattens" the frequency response for $|\varepsilon/V_H|$ and $|E/V_H|$. For Case 1, Eq. (5.64) shows that as m is changed m_T must also be changed to hold ω_{ei} fixed with C_e also fixed. It turns out (as will be shown) that if $m > r$ then as m is decreased m_T must be increased to comply with Eq. (5.57) and if $m < r$ then m_T must be decreased as m_H is decreased. For $m = r$ one requires the largest value for m_T to comply with a fixed value of ω_{ei} and C_e in Eq. (5.64). Since the usual situation is for $m > r$, then for Case 1 it is concluded that the usual design trend calls for a smaller head mass and a larger tail mass in order to flatten the frequency response and increase the subject bandwidth $\omega_U - \omega_L$ for $|\varepsilon/V_H|$ and $|E/V_H|$.

The behavior of the quantity $m/(r^2 + m^2)$ vs. changes in m determines what changes in m_T are needed in the above discussion. The graph of this function was discussed in Sec. A.8 in conjunction with Fig. A-1 and Eqs. (A.8.16) through (A.8.18).

Thus, as shown in Fig. A-1, for $m < r$ the slope is positive, for $m > r$ the slope is negative, and for $m = r$ the function has a maximum and the value of the function at $m = r$ is $1/2r$.

Case 2 Fix m_T (vary m and C_e)

With both ω_{ei} and m_T held fixed, it is convenient to solve Eq. (5.69) for C_e obtaining the following.

$$C_e = \frac{1}{\omega_{ei}^2}\left(\frac{m}{r^2 + m^2} + \frac{1}{m_T}\right). \qquad \textbf{(A.12.17)}$$

Also, use C_e from this last equation to rewrite Eq. (A.12.6) as

$$M = \frac{r}{(r^2 + m^2)} \frac{\omega_{ei}^2}{\omega_{ei}^2\left(\frac{m}{r^2 + m^2} + \frac{1}{m_T}\right)} \qquad \textbf{(A.12.18)}$$

and

$$M = \frac{r}{\left(m + \frac{r^2 + m^2}{m_T}\right)}. \qquad \textbf{(A.12.19)}$$

Again in Case 2 as in Case 1, one observes [from Eq. (A.12.19)] that M is increased as m is decreased. Thus, once again, the bandwidth and flatness of $|\varepsilon/V_H|$ and $|E/V_H|$ are improved by decreasing the head mass. In Case 2, m_T is held fixed so according to Eq. (A.12.17), C_e must be changed as M is changed.

As before, using the behavior of $m/(r^2 + m^2)$ one concludes that if $m > r$ then as m decreases C_e must be increased, and if $m < r$ then as m decreases C_e must be decreased and for $m = r$ one requires the maximum value for C_e. Since the usual practical situation is for $m > r$ then one obtains the conclusion that as m_H is decreased, the compliance C_e must be increased to maintain a fixed frequency (in this case ω_{ei}).

How would the compliance C_e be adjusted? Recall Eq. (4.18).

$$C_e = C_F + S_{33}^E \frac{L}{A_c}.$$

In the case where C_e needs increasing, one could increase the compliance C_F of the FTR. Better yet, one could increase the length L of the CSA if geometric constraints permitted, and this would have the added benefit of decreasing the electric field ε. One could also decrease the area A_c down to some lower limit corresponding to mechanical stress and strain limits.

Case 3 Fix m_H (vary m_T and C_e)

With both ω_{ei} and m_H (and, thus, m) fixed one can consider varying m_T and C_e. Equation (A.12.19) shows that M can be increased by increasing m_T. Thus, once again, it is concluded that the larger the tail mass (with m_H held fixed and C_e adjusted to hold ω_{ei} fixed), then the better the subject bandwidth and flatness of the quantities $|E/V_H|$ and $|\varepsilon/V_H|$. Equation (A.12.17) shows that as m_T is increased then the compliance C_e must be decreased to maintain the fixed frequency ω_{ei}.

How should C_e be decreased as m_T is increased? From Eq. (4.18), one could decrease C_e by decreasing L, but this would increase the electric field. One could decrease C_e by decreasing the compliance C_F of the FTR up to the limit of removing the FTR entirely. One could further decrease C_e by increasing the area A_c, which would in turn reduce the mechanical stress and strain.

SUMMARY

In summary, one may state that for the usual practical case of $m > r$ then the smaller the head mass and the larger the tail mass the better the bandwidth, $\omega_U - \omega_L$ for a fixed ω_{ei} and correspondingly the flatter the frequency response of $|\varepsilon/V_H|$ and $|E/V_H|$.

In the above analysis, the value of $|\varepsilon/V_H|$ at the ends of the frequency band were constrained to be proportional to the value at the frequency $\omega = \omega_{ei}$ [see Eqs. (5.89) and (5.90)]. At $\omega = \omega_{ei}$, $|\varepsilon/V_H|$ was given by Eq. (5.74)

$$\left|\frac{\epsilon}{V_H}\right|_{\omega=\omega_{ei}} = \frac{1}{\omega_{ei} L d_{33}} \sqrt{\frac{r^2}{r^2 + m^2}}.$$

Equation (5.74) shows that as m is decreased the value of $|\varepsilon/V_H|$ at $\omega = \omega_{ei}$ is increased; that is, it requires a higher electric field to achieve a given velocity, V_H, and, thus, to achieve a given source level. Therefore, as m is decreased to obtain a flatter frequency response, the required electric field is increased, not only at ω_{ei}, but at the end points [Eqs. (5.89) and (5.90)]. The electric field could be held constant

by increasing L, the length of the CSA, as m is decreased to flatten the frequency response of $|\varepsilon/V_H|$ and $|E/V_H|$. However, according to Eq. (4.18), one would also have to increase A_c and/or decrease C_F in order to maintain the desired value of C_e. Thus, any time m is decreased (Case 1 and Case 2 above) there is a penalty; namely, L and perhaps A_c must be increased in order to not exceed a given field limit. Increasing the length L of the CSA usually leads to an encounter with a length constraint for the transducer design. Among other things, it is this length constraint that often leads the designer to operate at the highest practical value of electric field.

In Case 3, m_H (and, thus, m) was fixed but the tail mass m_T was increased in order to flatten the frequency response (and C_e was decreased to keep ω_{ei} constant). In Case 3, one observes that there is no electric field penalty for increasing the tail mass, m_T, if m_H is being held fixed. One might ask, however, how is C_e to be decreased as required. According to Eq. (4.18), one could shorten L, but this would increase the field requirement. Alternately, L could be held fixed and the area, Ac, of the ceramic could be increased to stiffen the CSA (decrease C_e). In a sense, there is also a penalty for increasing m_T, but increasing the area A_c may be possible whereas increasing the length L (when m is decreased) is usually a more severe space constraint penalty.

A.13 DERIVATION OF C_e FOR FIXED END POINTS CONSTRAINTS

A derivation of Eq. (5.104) for C_e as used in Sec. 5.2.2.6.2.1 is presented. Equations (5.105), (5.106), and (5.107), respectively, are repeated for convenience.

$$C_e = \frac{-b_t}{2a_t} \pm \sqrt{\left(\frac{b_t}{2a_t}\right)^2 - \left(\frac{c_t}{a_t}\right)},$$

where

$$a_t = (r^2 + m^2)(\omega_L^4 - \alpha^2\omega_U^4),$$

$$b_t = -2(\omega_L^2 - \alpha^2\omega_U^2)\left(\frac{r^2 + m^2}{m_T} + m\right),$$

$$c_t = \left(\frac{r^2 + m^2}{m_T^2} + \frac{2m}{m_T} + 1\right)(1 - \alpha^2),$$

and α was defined by Eq. (5.108)

$$\alpha = \frac{k_L}{k_U}.$$

The starting point is to use Eqs. (5.101) and (5.103) to form the following ratio

$$\frac{k_L^2 L^2}{k_U^2 L^2} = \frac{B_{1L}}{B_{1U}}. \tag{A.13.1}$$

Where B_1 was given by Eq. (5.13)

$$B_1 = r^2 E_o^2 + (1 - mE_o)^2,$$

and E_o by Eq. (5.11)

$$E_o = \left(\omega^2 C_e - \frac{1}{m_T}\right)$$

and B_{1L} is B_1 with $\omega = \omega_L$ and B_{1U} is B_1 with $\omega = \omega_U$. Similarly, E_{oL} is E_o for $\omega = \omega_L$ and E_{oU} is E_o for $\omega = \omega_U$.

Using α from Eq. (5.108), write

$$\alpha^2 = \frac{k_L^2}{k_U^2} = \frac{B_{1L}}{B_{1U}}. \tag{A.13.2}$$

Use Eqs. (5.13) and (A.13.2) to write

$$\alpha^2\left[r^2 E_{oU}^2 + (1 - mE_{ou})^2\right] = r^2 E_{oL}^2 + (1 - mE_{oL})^2, \tag{A.13.3}$$

$$\alpha^2\left[(r^2 + m^2)E_{oU}^2 - 2mE_{oU} + 1\right] = (r^2 + m^2)E_{oL}^2 - 2mE_{oL} + 1, \tag{A.13.4}$$

and

$$(r^2 + m^2)(E_{oL}^2 - \alpha^2 E_{oU}^2) - 2m(E_{oL} - \alpha^2 E_{oU}) + (1 - \alpha^2) = 0. \tag{A.13.5}$$

Next use E_o from Eq. (5.11) to form E_{oL} and E_{oU} and continue as follows to form the desired quadratic equation for C_e.

$$E_{oL} = \left(\omega_L^2 C_e - \frac{1}{m_T}\right), \tag{A.13.6}$$

$$E_{oU} = \left(\omega_U^2 C_e - \frac{1}{m_T}\right), \tag{A.13.7}$$

$$\left(E_{oL} - \alpha^2 E_{oU}\right) = \omega_L^2 C_e - \frac{1}{m_T} - \alpha^2\left(\omega_U^2 C_e - \frac{1}{m_T}\right), \tag{A.13.8}$$

$$\left(E_{oL} - \alpha^2 E_{oU}\right) = \left(\omega_L^2 - \alpha^2\omega_U^2\right)C_e - (1 - \alpha^2)\frac{1}{m_T}, \tag{A.13.9}$$

also

$$\left(E_{oL}^2 - \alpha^2 E_{oU}^2\right) = \left(\omega_L^2 C_e - \frac{1}{m_T}\right)^2 - \alpha^2\left(\omega_U^2 C_e - \frac{1}{m_T}\right)^2, \tag{A.13.10}$$

$$\left(E_{oL}^2 - \alpha^2 E_{oU}^2\right) = \omega_L^4 C_e^2 - \frac{2\omega_L^2 C_e}{m_T} + \frac{1}{m_T^2} - \alpha^2\left(\omega_U^4 C_e^2 - \frac{2\omega_U^2 C_e}{m_T} - \frac{1}{m_T^2}\right), \tag{A.13.11}$$

and

$$\left(E_{oL}^2 - \alpha^2 E_{oU}^2\right) = \left(\omega_L^4 - \alpha^2\omega_U^4\right)C_e^2 - \frac{2}{m_T}\left(\omega_L^2 - \alpha^2\omega_U^2\right)C_e + (1 - \alpha^2)\frac{1}{m_T^2}. \tag{A.13.12}$$

Equations (A.13.9) and (A.13.12) may be used in Eq. (A.13.5) to form a standard quadratic equation for C_e as follows.

$$a_t C_e^2 + b_t C_e + c_t = 0. \tag{A.13.13}$$

The "temporary symbols" a_t, b_t and c_t are defined by Eqs. (5.105), (5.106), and (5.107) above. Provided $a_t \neq 0$, then use of the standard quadratic formula yields Eq. (5.104) as desired. If $a_t = 0$, then one has

$$C_e = \frac{-c_t}{b_t} \tag{A.13.13a}$$

A.14 EQUATION FOR C_e FOR SPECIAL CASE 1 ($\alpha = 1$)

To derive an equation C_e for $\alpha = 1$, one may proceed as follows. Recall Eq. (5.105)

$$a_t = (r^2 + m^2)(\omega_L^4 - \alpha^2\omega_U^4).$$

For $\alpha = 1$, obtain

$$a_t = (r^2 + m^2)(\omega_L^4 - \omega_U^4. \tag{A.14.1}$$

Recall Eq. (5.106)

$$b_t = -2(\omega_L^2 - \alpha^2\omega_U^2)\left(\frac{r^2 + m^2}{m_T} + m\right).$$

For $\alpha = 1$, obtain

$$b_t = -2(\omega_L^2 - \omega_U^2)\left(\frac{r^2 + m^2}{m_T} + m\right). \tag{A.14.2}$$

Recall Eq. (5.107)

$$c_t = \left(\frac{r^2 + m^2}{m_T^2} + \frac{2m}{m_T} + 1\right)(1 - \alpha^2).$$

For $\alpha = 1$,

$$c_t = 0. \tag{A.14.3}$$

These values used in Eq. (5.104) give

$$C_e = \frac{-b_t}{2a_t} \pm \frac{b_t}{2a_t} \tag{A.14.4}$$

Note from Eqs. (A.14.1) and (A.14.2) that $b_t/2a_t < 0$ and, thus, we must choose the minus sign, giving

$$C_e = \frac{-2b_t}{2a_t} = \frac{-b_t}{a_t}. \tag{A.14.4a}$$

Therefore, for $\alpha = 1$, one finds

$$C_e = \frac{2(\omega_L^2 - \omega_U^2)\left(\frac{r^2 + m^2}{m_T} + m\right)}{(r^2 + m^2)(\omega_L^4 - \omega_U^4)} \tag{A.14.4b}$$

or

$$C_e = \frac{2(\omega_L^2 - \omega_U^2)}{(\omega_L^2 + \omega_U^2)(\omega_L^2 - \omega_U^2)}\left(\frac{m}{r^2 + m^2} + \frac{1}{m_T}\right) \tag{A.14.4c}$$

which gives Eq. (5.104a) as desired.

$$C_e = \left(\frac{2}{\omega_L^2 + \omega_U^2}\right)\left(\frac{m}{r^2 + m^2} + \frac{1}{m_T}\right).$$

A.15 DEMONSTRATION THAT $\omega_L < \omega_{ei} < \omega_U$ FOR $\alpha = 1$

For Special Case 1 (i.e., for $\alpha = 1$), we wish to prove Eq. (5.113)

$$\omega_L < \omega_{ei} < \omega_U.$$

By assumption $\omega_L < \omega_U$, so

$$\omega_L^2 < \omega_U^2, \tag{A.15.1}$$

$$2\omega_L^2 < \omega_L^2 + \omega_U^2, \tag{A.15.2}$$

$$\omega_L^2 < \frac{\omega_L^2 + \omega_U^2}{2}, \tag{A.15.3}$$

but Eq. (5.112) showed

$$\omega_{ei}^2 = \frac{\omega_L^2 + \omega_U^2}{2}.$$

Thus,

$$\omega_L^2 < \omega_{ei}^2 \tag{A.15.4}$$

and

$$\omega_L < \omega_{ei}. \tag{A.15.5}$$

Similarly,

$$\frac{\omega_U^2 + \omega_U^2}{2} > \frac{\omega_U^2 + \omega_L^2}{2}, \tag{A.15.6}$$

so,

$$\omega_U^2 > \frac{\omega_U^2 + \omega_L^2}{2}, \tag{A.15.7}$$

$$\omega_U^2 > \omega_{ei}^2, \tag{A.15.8}$$

and

$$\omega_{ei} < \omega_U. \tag{A.15.9}$$

Combining Eqs. (A.15.5) and (A.15.9) gives Eq. (5.113) as desired.

A.16 DERIVATION OF EQS. (5.121), (5.123), AND (5.124)

Recall Eq. (5.101)

$$L^2 k_L^2 = B_{1L}.$$

Recall Eq. (A.9.5) for B_1

$$B_1 = (r^2 + m^2)(\omega^2 - \omega_{ei}^2)^2 C_e^2 + \frac{r^2}{r^2 + m^2} \tag{A.9.5}$$

for $\omega = \omega_L$, this gives

$$B_{1L} = (r^2 + m^2)(\omega_L^2 - \omega_{ei}^2)^2 C_e^2 + \frac{r^2}{r^2 + m^2}. \tag{A.16.1}$$

However, for Special Case 1 (i.e., $\alpha = 1$), recall Eqs. (5.112) and (5.104a)

$$\omega_{ei}^2 = \frac{\omega_L^2 + \omega_U^2}{2}$$

and

$$C_e = \left(\frac{2}{\omega_L^2 + \omega_U^2}\right)\left(\frac{m}{r^2 + m^2} + \frac{1}{m_T}\right).$$

Use these last two equations to rewrite Eq. (A.16.1) as follows:

$$B_{1L} = (r^2 + m^2)\left(\frac{m}{r^2 + m^2} + \frac{1}{m_T}\right)^2 \left(\omega_L^2 - \frac{\omega_L^2 + \omega_U^2}{2}\right)^2 \left(\frac{2}{\omega_L^2 + \omega_U^2}\right)^2 + \frac{r^2}{r^2 + m^2} \tag{A.16.2}$$

and

$$B_{1L} = (r^2 + m^2)\left(\frac{m}{r^2 + m^2} + \frac{1}{m_T}\right)^2 \left(\frac{\omega_U^2 - \omega_L^2}{\omega_L^2 + \omega_U^2}\right)^2 + \frac{r^2}{r^2 + m^2}. \tag{A.16.3}$$

Define [Eq. (5.122)]

$$b_{t2}^2 = \left(\frac{\omega_U^2 - \omega_L^2}{\omega_L^2 + \omega_U^2}\right)^2.$$

Use Eq. (5.122) in Eq. (A.16.3) to write

$$B_{1L} = (r^2 + m^2)\left(\frac{m}{r^2 + m^2} + \frac{1}{m_T}\right)^2 b_{t2}^2 + \frac{r^2}{r^2 + m^2}. \tag{A.16.4}$$

Use Eq. (A.16.4) in Eq. (5.101) to write Eq. (5.121)

$$k_L^2 L^2 = (r^2 + m^2)\left(\frac{m}{r^2 + m^2} + \frac{1}{m_T}\right)^2 b_{t2}^2 + \frac{r^2}{r^2 + m^2}.$$

Now continue as follows to produce Eq. (5.123).

Rewrite Eq. (5.121) as

$$k_L^2 L^2 = \left(\frac{m^2}{r^2 + m^2} + \frac{2m}{m_T} + \frac{r^2 + m^2}{m_T^2}\right) b_{t2}^2 + \frac{r^2}{r^2 + m^2}, \tag{A.16.5}$$

$$k_L^2 L^2 = \frac{r^2 + b_{t2}^2 m^2}{(r^2 + m^2)} + \left(\frac{2m}{m_T} + \frac{r^2 + m^2}{m_T^2}\right) b_{t2}^2, \tag{A.16.6}$$

$$\frac{\delta k_L^2 L^2}{\delta m} = \frac{2m(b_{t2}^2)}{r^2 + m^2} - 2m\frac{\left(r^2 + b_{t2}^2 m^2\right)}{(r^2 + m^2)^2} + \left(\frac{2}{m_T} + \frac{2m}{m_T^2}\right) b_{t2}^2, \tag{A.16.7}$$

and

$$\frac{1}{2} k_L^2 \frac{\delta L^2}{\delta m} = \frac{m}{(r^2 + m^2)^2}\left[b_{t2}^2(r^2 + m^2) - (r^2 + b_{t2}^2 m^2)\right] + \frac{1}{m_T}\left(1 + \frac{m}{m_T^2}\right) b_{t2}^2, \tag{A.16.8}$$

which yields Eq. (5.123) as desired.

$$\frac{1}{2}k_L^2\frac{\delta L^2}{\delta m} = \frac{m}{(r^2+m^2)^2}\left[r^2(b_{t2}^2 - 1)\right] + \frac{1}{m_T}\left(1 + \frac{m}{m_T^2}\right)b_{t2}^2.$$

Now consider b_{t2}^2 - 1 using Eq. (5.122)

$$b_{t2}^2 = \left(\frac{\omega_U^2 - \omega_L^2}{\omega_L^2 + \omega_U^2}\right)^2,$$

where

$$\omega_U^2 - \omega_L^2 < \omega_U < \omega_L^2 + \omega_U^2, \tag{A.16.9}$$

$$\omega_U^2 - \omega_L^2 < \omega_U^2 + \omega_L^2, \tag{A.16.10}$$

and

$$\frac{\omega_U^2 - \omega_L^2}{\omega_L^2 + \omega_U^2} < 1. \tag{A.16.11}$$

Thus,

$$b_{t2}^2 < 1 \tag{A.16.12}$$

so as desired

$$b_{t2}^2 - 1 < 0.$$

A.17 EQUATION FOR C_e FOR SPECIAL CASE 2 ($\alpha = \omega_L/\omega_U$)

To derive an equation for C_e for Special Case 2, one may proceed as follows. Special Case 2 is equivalent to Eq. (5.127)

$$\alpha = \frac{\omega_L}{\omega_U}.$$

Recall Eq. (5.105)

$$a_t = (r^2 + m^2)(\omega_L^4 - \alpha^2\omega_U^4).$$

For $\alpha = \omega_L/\omega_U$, obtain

$$a_t = (r^2 + m^2)\left(\omega_L^4 - \frac{\omega_L^2}{\omega_U^2}\omega_U^4\right), \tag{A.17.1}$$

or

$$a_t = (r^2 + m^2)\left(\omega_L^4 - \omega_L^2\omega_U^2\right). \tag{A.17.2}$$

Thus,

$$a_t = (r^2 + m^2)\omega_L^2\left(\omega_L^2 - \omega_U^2\right). \tag{A.17.3}$$

Note that since $\omega_L < \omega_U$, then $-a_t > 0$.

Recall Eq. (5.106)

$$b_t = -2\left(\omega_L^2 - \alpha^2\omega_U^2\right)\left(\frac{r^2 + m^2}{m_T} + m\right).$$

For $\alpha = \omega_L/\omega_U$, obtain

$$b_t = -2\left(\omega_L^2 - \frac{\omega_L^2}{\omega_U^2}\omega_U^2\right)\left(\frac{r^2 + m^2}{m_T} + m\right). \tag{A.17.4}$$

Thus,

$$b_t = 0. \tag{A.17.5}$$

Recall Eq. (5.107)

$$c_t = \left(\frac{r^2 + m^2}{m_T^2} + \frac{2m}{m_T} + 1\right)(1 - \alpha^2).$$

For $\alpha = \omega_L/\omega_U$, obtain Eq. (A.17.6)

$$c_t = \left(\frac{r^2 + m^2}{m_T^2} + \frac{2m}{m_T} - 1\right)\left(1 - \frac{\omega_L^2}{\omega_U^2}\right). \tag{A.17.6}$$

These values [Eqs. (A.17.3), (A.17.5), and (A.17.6)] used in Eq. (5.104) gives

$$C_e = \pm\sqrt{\frac{c_t}{-a_t}}. \tag{A.17.7}$$

Since $C_t > 0$ and $-a_t > 0$ and $C_e > 0$, one chooses the positive sign; therefore,

$$C_e = +\sqrt{\frac{c_t}{-a_t}}. \tag{A.17.8}$$

Using Eq. (A.17.3) for a_t and Eq. (A.17.5) for c_t gives

$$C_e = \sqrt{\frac{\left(\frac{r^2 + m^2}{m_T^2} + \frac{2m}{m_T} + 1\right)\left(1 - \frac{\omega_L^2}{\omega_U^2}\right)}{(r^2 + m^2)(\omega_U^2 - \omega_L^2)\omega_L^2}} \tag{A.17.9}$$

or

$$C_e = \sqrt{\left(\frac{r^2 + m^2}{m_T^2} + \frac{2m}{m_T} + 1\right)\frac{1}{r^2 + m^2}\left(\frac{\omega_U^2 - \omega_L^2}{\omega_U^2 - \omega_L^2}\right)\frac{1}{\omega_L^2\omega_U^2}}, \tag{A.17.10}$$

which gives Eq. (5.104c) as desired

$$C_e = \frac{1}{\omega_L\omega_U}\sqrt{\left(\frac{r^2 + m^2}{m_T^2} + \frac{2m}{m_T} + 1\right)\frac{1}{r^2 + m^2}}.$$

A.18 DERIVATION OF $\delta B_{1e}/\delta m_T$ FOR SPECIAL CASE 2

The starting point for the derivation of an equation for $\delta B_{1e}/\delta m_T$ was Eq. (5.13) for B_1.

$$B_1 = r^2E_o^2 + (1 - mE_o)^2 \quad .$$

Recall that B_{1e} [see Eq. (A.11.2)] is B_1 for $\omega = \omega_e$. Thus,

$$B_{1e} = r^2E_{oe}^2 + (1 - mE_{oe})^2 \quad , \tag{A.18.1}$$

where E_{oe} is E_o for $\omega = \omega_{eo}$

$$\frac{\delta B_{1e}}{\delta m_T} = 2r^2E_{oe}\frac{\delta E_{oe}}{\delta m_T} - 2m(1 - mE_{oe})\frac{\delta E_{oe}}{\delta m_T} \tag{A.18.2}$$

and

$$\frac{\delta B_{1e}}{\delta m_T} = 2\left[(r^2 + m^2)E_{oe} - m\right]\frac{\delta E_{oe}}{\delta m_T} \quad . \tag{A.18.3}$$

Define F_{el} as

$$F_{el} = (r^2 + m^2)E_{oe} - m. \tag{A.18.4}$$

Recall Eq. (5.11) for E_o

$$E_o = \omega^2 C_e - \frac{1}{m_T},$$

so,

$$E_{oe} = \omega_e^2 C_e - \frac{1}{m_T}. \tag{A.18.5}$$

Recall Eq. (A.10.40)

$$\omega_e^2 = \frac{1}{c_e}\sqrt{M_e^2}. \tag{A.10.40}$$

Thus,

$$\omega_e^2 C_e = M_e \tag{A.18.6}$$

Use Eq. (A.18.6) in Eq. (A.18.5) to write

$$E_{oe} = M_e - \frac{1}{m_T}. \tag{A.18.7}$$

Use Eq. (A.18.7) in Eq. (A.18.4) to write

$$F_{el} = (r^2 + m^2)\left(M_e - \frac{1}{m_T}\right) - m. \tag{A.18.8}$$

Next, recall Eq. (A.10.46)

$$M_e^2 = \left(\frac{1}{m_T} + \frac{m}{r^2 + m^2}\right)^2 + \frac{r^2}{(r^2 + m^2)^2}.$$

Thus,

$$(r^2 + m^2)^2 M_e^2 = \left(\frac{r^2 + m^2}{m_T} + m\right)^2 + r^2 \tag{A.18.9}$$

and

$$(r^2 + m^2)M_e = \sqrt{\left(\frac{r^2 + m^2}{m_T} + m\right)^2 + r^2}. \tag{A.18.10}$$

Use Eq. (A.18.10) in Eq. (A.18.8) to write Eq. (5.131) (reprinted below) as desired

$$F_{el} = \sqrt{\left(\frac{r^2 + m^2}{m_T} + m\right)^2 + r^2} - \left(\frac{r^2 + m^2}{m_T} + m\right).$$

It should be noted that $F_{el} > 0$ for all values of m_T and m.

At this point, we now have [from Eqs. (A.18.4) and (A.18.3)]

$$\frac{\delta B_{1e}}{\delta m_T} = 2F_{1e}\frac{\delta E_{oe}}{\delta m_T}. \tag{A.18.3a}$$

We need an expression for $\delta E_{oe}/\delta m_T$. Using Eq. (A.18.7) above, write

$$\frac{\delta E_{oe}}{\delta m_T} = \frac{\delta M_e}{\delta m_T} + \frac{1}{m_T^2}. \tag{A.18.11}$$

Use Eq. (A.10.46) to form $\delta M_e/\delta m_T$ as follows

$$\frac{\delta M_e}{\delta m_T} = \frac{\delta\sqrt{\left(\frac{1}{m_T} + \frac{m}{r^2 + m^2}\right)^2 + \frac{r^2}{(r^2 + m^2)^2}}}{\delta m_T}, \tag{A.18.12}$$

$$\frac{\delta M_e}{\delta m_T} = \frac{1}{2M_e}2\left(\frac{1}{m_T} + \frac{m}{r^2 + m^2}\right)\left(-\frac{1}{m_T^2}\right), \tag{A.18.13}$$

and

$$\frac{\delta M_e}{\delta m_T} = \frac{-1}{M_e}\left(\frac{1}{m_T} + \frac{m}{r^2 + m^2}\right)\frac{1}{m_T^2}. \tag{A.18.14}$$

Use Eq. (A.18.14) in Eq. (A.18.11) to write

$$\frac{\delta E_{oe}}{\delta m_T} = \frac{1}{m_T^2}\left[1 - \frac{1}{M_e}\left(\frac{1}{m_T} + \frac{m}{r^2 + m^2}\right)\right] \tag{A.18.15}$$

or using Eq. (A.10.46) for M_e

$$\frac{\delta E_{oe}}{\delta m_T} = \frac{1}{m_T^2}\left[1 - \frac{\left(\frac{1}{m_T} + \frac{m}{r^2 + m^2}\right)}{\sqrt{\left(\frac{1}{m_T} + \frac{m}{r^2 + m^2}\right)^2 + \frac{r^2}{(r^2 + m^2)^2}}}\right]. \tag{A.18.16}$$

If one identifies F_{e2} as

$$F_{e2} = \frac{\delta E_{oe}}{\delta m_T}, \tag{A.18.17}$$

one obtains Eq. (5.132) as desired. It should be noted that $F_{e2} > 0$ for all values of m and m_T.

A.19 DERIVATION OF $\delta B_{1e}/\delta m$ FOR SPECIAL CASE 2

The starting point for the derivation of an equation for $\delta B_{1e}/\delta m$ was Eq. (A.18.1) (see Sec. A.18). Thus,

$$\frac{\delta B_{1e}}{\delta m} = \frac{\delta\left[r^2 E_{oe}^2 + (1 - mE_o)^2\right]}{\delta m}, \tag{A.19.1}$$

$$\frac{\delta B_{1e}}{\delta m} = 2r^2 E_{oe}\frac{\delta E_{oe}}{\delta m} - 2(1 - mE_o)\frac{\delta mE_o}{\delta m}, \tag{A.19.2}$$

but

$$\frac{\delta mE_o}{\delta m} = \left(E_o + m\frac{\delta E_o}{\delta m}\right), \tag{A.19.3}$$

so

$$\frac{1}{2}\frac{\delta B_{1e}}{\delta m} = r^2 E_{oe}\frac{\delta E_{oe}}{\delta m} - (1 - mE_o)\left(E_{oe} + m\frac{\delta E_{oe}}{\delta m}\right) \tag{A.19.4}$$

and

$$\frac{1}{2}\frac{\delta B_{1e}}{\delta m} = \left[(r^2 + m^2)E_{oe} - m\right]\frac{\delta E_{oe}}{\delta m} - E_{oe}(1 - mE_{oe}). \tag{A.19.5}$$

Recall Eq. (A.18.7)

$$E_{oe} = M_e - \frac{1}{m_T}$$

thus,

$$\frac{\delta E_{oe}}{\delta m} = \frac{\delta M_e}{\delta m}. \tag{A.19.6}$$

Recall Eq. (A.10.43)

$$M_e^2 = \frac{1}{m_T^2} + \frac{2m}{m_T(r^2 + m^2)} + \frac{1}{r^2 + m^2}$$

or

$$M_e = \sqrt{\frac{1}{m_T^2} + \left(\frac{2m}{m_T} + 1\right)\frac{1}{r^2 + m^2}}, \tag{A.19.7}$$

so

$$\frac{\delta M_e}{\delta m} = \frac{1}{2M_e}\left[\frac{2}{m_T}\frac{1}{r^2 + m^2} - \left(\frac{2m}{m_T} + 1\right)\frac{2m}{(r^2 + m^2)^2}\right], \tag{A.19.8}$$

$$\frac{\delta M_e}{\delta m} = \frac{1}{M_e(r^2 + m^2)^2 m_T}\left[r^2 + m^2 - \left(\frac{2m}{m_T} + 1\right)mm_T\right], \tag{A.19.9}$$

$$\frac{\delta M_e}{\delta m} = \frac{1}{m_T M_e(r^2 + m^2)^2}(r^2 + m^2 - 2m^2 - mm_T), \tag{A.19.10}$$

$$\frac{\delta M_e}{\delta m} = \frac{1}{m_T M_e(r^2 + m^2)^2}(r^2 - m^2 - mm_T), \tag{A.19.11}$$

and

$$\frac{\delta M_e}{\delta m} = \frac{r^2 - m(m + m_T)}{m_T M_e (r^2 + m^2)^2}. \qquad \textbf{(A.19.12)}$$

Use of Eqs. (A.18.7) and (A.19.12) in Eq. (A.19.50) yields a general expression for 1/2 $\delta B_{1e}/\delta m$. However, due to the apparent complexness of the general form, only the special case where $m_T \to \infty$ was given consideration.

If $2m/m_T << 1$, then Eq. (A.19.7) becomes

$$M_e \simeq \sqrt{\frac{1}{m_T^2} + \frac{1}{r^2 + m^2}}. \qquad \textbf{(A.19.7a)}$$

If $1/m_T^2 << 1/r^2 + m^2$, then

$$M_e \simeq \frac{1}{\sqrt{r^2 + m^2}}. \qquad \textbf{(A.19.7b)}$$

Under these same conditions,

$$E_{oe} \simeq M_e = \frac{1}{\sqrt{r^2 + m^2}} \qquad \textbf{(A.18.7a)}$$

and

$$\frac{\delta M_e}{\delta m} \simeq \frac{-m}{M_e (r^2 + m^2)} = \frac{-m}{(r^2 + m^2)^{3/2}}. \qquad \textbf{(A.19.12a)}$$

Using these approximate values in Eq. (A.19.5) yields

$$\frac{1}{2}\frac{\delta B_{1e}}{\delta m} = \left[\frac{(r^2 + m^2)}{\sqrt{r^2 + m^2}} - m\right]\left[\frac{-m}{(r^2 + m^2)^{3/2}}\right] - \frac{1}{\sqrt{r^2 + m^2}}\left(1 - \frac{m}{\sqrt{r^2 + m^2}}\right) \qquad \textbf{(A.19.5a)}$$

and

$$\frac{1}{2}\frac{\delta B_{1e}}{\delta m} = \frac{-1}{(r^2 + m^2)^{3/2}}\left[m\sqrt{r^2 + m^2} - m^2 + (r^2 + m^2)\left(1 - \frac{m}{\sqrt{r^2 + m^2}}\right)\right] \qquad \textbf{(A.19.5b)}$$

or Eq. (5.133) as desired.

$$\frac{\delta B_{1e}}{\delta m} = \frac{-2r^2}{(r^2 + m^2)^{3/2}}.$$

Eq. (5.133) may also be derived directly from B_{1e} with $m_T = \infty$.

A.20 DERIVATION OF EQS. (5.134), (5.135), AND (5.138a)

Recall Eq. (5.134)

$$k_L^2 L^2 = r^2\left(\frac{\omega_L}{\omega_U}M_e - \frac{l}{m_T}\right)^2 + \left[1 - m\left(\frac{\omega_L}{\omega_U}M_e - \frac{1}{m_T}\right)\right]^2.$$

The starting point for deriving Eq. (5.134) is Eq. (5.101) reprinted here.

$$k_L^2 L^2 = B_{1L}.$$

For B_{1L}, recall Eq. (5.133)

$$B_1 = r^2 E_o^2 + (1 - mE_o)^2.$$

Evaluate B_1 at $\omega = \omega_L$ to yield

$$B_{1L} = r^2 E_{oL}^2 + (1 - mE_{oL})^2, \tag{A.20.1}$$

where E_{oL} is E_o with $\omega = \omega_L$.

Recall Eq. (5.11)

$$E_o = \omega^2 C_e - \frac{1}{m_T}$$

so

$$E_{oL} = \omega_L^2 C_e - \frac{1}{m_T}. \tag{A.20.2}$$

However, for Special Case 2, recall Eq. (5.104d)

$$C_e = \frac{1}{\omega_L \omega_U} M_e.$$

Thus,

$$E_{oL} = \frac{\omega_L^2}{\omega_L \omega_U} M_e - \frac{1}{m_T} \tag{A.20.3}$$

and

$$E_{oL} = \frac{\omega_L}{\omega_U} M_e - \frac{1}{m_T} \tag{A.20.4}$$

Use of Eqs. (A.20.4) and (A.20.1) in Eq. (5.101) yields Eq. (5.134) as desired.

Next, we derive Eq. (5.135) repeated for convenience.

$$k_L^2 \frac{\delta L^2}{\delta m_T} = \frac{2}{m_T^2} \frac{\omega_L}{\omega_u} \left(\frac{r^2 + m^2}{m_T} + m^2 \right) (F_{1L}) \left(F_{2L} - \frac{\omega_U}{\omega_L} \right).$$

Start with Eq. (5.101) (repeated above) and write

$$k_L^2 \frac{\delta L^2}{\delta m_T} = \frac{\delta B_{1L}}{\delta m_T}. \tag{A.20.5}$$

Next, use Eq. (A.20.1) to write

$$\frac{\delta B_{1L}}{\delta m_T} = 2r^2 E_{oL} \frac{\delta E_{oL}}{\delta m_T} - 2m(1 - mE_{oL}) \frac{\delta E_{oL}}{\delta m_T} \tag{A.20.6}$$

or

$$\frac{\delta B_{1L}}{\delta m_T} = 2 \frac{\delta E_{oL}}{\delta m_T} \left[(r^2 + m^2) E_{oL} - m \right]. \tag{A.20.7}$$

Use Eq. (A.20.4) and write

$$\frac{\delta E_{oL}}{\delta m_T} = \frac{\omega_L}{\omega_U} \frac{\delta M_e}{\delta m_T} + \frac{1}{m_T^2}. \tag{A.20.8}$$

Recall Eq. (A.18.14) for $\delta M_e / \delta m_T$.

$$\frac{\delta M_e}{\delta m_T} = -\frac{1}{M_e} \left(\frac{1}{m_T} + \frac{m}{r^2 + m^2} \right) \frac{1}{m_T^2}.$$

Use Eq. (A.18.14) in Eq. (A.20.8)

$$\frac{\delta E_{oL}}{\delta m_T} = \frac{1}{m_T^2} \left[1 - \frac{\omega_L}{\omega_U} \frac{1}{M_e} \left(\frac{1}{m_T} + \frac{m}{r^2 + m^2} \right) \right]. \tag{A.20.9}$$

Define F_{1L} as

$$F_{1L} = \left[1 - \frac{\omega_L}{\omega_U} \frac{1}{M_e} \left(\frac{1}{m_T} + \frac{m}{r^2 + m^2} \right) \right]. \tag{A.20.10}$$

Use Eq. (A.10.46) for M_e in Eq. (A.20.10) and obtain Eq. (5.136) (reprinted here)

$$F_{1L} = 1 - \frac{\frac{\omega_L}{\omega_U}\left(\frac{1}{m_T} + \frac{m}{r^2 + m^2}\right)}{\sqrt{\left(\frac{1}{m_T} + \frac{m}{r^2 + m^2}\right)^2 + \frac{r^2}{(r^2 + m^2)^2}}}.$$

Note that since $\omega_L/\omega_U < 1$, then Eq. (5.136a) is obtained.

$$F_{1L} > 0.$$

Use Eq. (A.20.10) in Eq. (A.20.9) to write

$$\frac{\delta E_{oL}}{\delta m_T} = \frac{1}{m_T^2} F_{1L}. \tag{A.20.11}$$

Use Eq. (A.20.1)1 in Eq. (A.20.7) and write

$$\frac{\delta B_{1L}}{\delta m_T} = \frac{2}{m_T^2} F_{1L}\left[(r^2 + m^2)E_{oL} - m\right]. \tag{A.20.12}$$

For convenience, define F_{tL} as

$$F_{tL} = \left[(r^2 + m^2)E_{oL} - m\right] \tag{A.20.13}$$

and write

$$\frac{\delta B_{1L}}{\delta m_t} = \frac{2}{m_T^2} F_{1L} F_{tL}. \tag{A.20.14}$$

Note that since $F_{1L} > 0$ [see Eq. (5.136a)], the sign of $\delta B_{1L}/\delta m_T$ is determined by F_{tL}. Therefore, continue manipulating F_{tL} as follows. Use E_{oL} from Eq. (A.20.4) and write

$$F_{tL} = (r^2 + m^2)\frac{\omega_L}{\omega_U} M_e - \left(\frac{r^2 + m^2}{m_T} + m\right). \tag{A.20.15}$$

Recall Eq. (A.18.10)

$$(r^2 + m^2)M_e = \sqrt{\left(\frac{r^2 + m^2}{m_T} + m\right)^2 + r^2}.$$

Use this in Eq. (A.20.15)

$$F_{tL} = \frac{\omega_L}{\omega_U}\sqrt{\left(\frac{r^2 + m^2}{m_T} + m\right)^2 + r^2} - \left(\frac{r^2 + m^2}{m_T} + m\right) \qquad \textbf{(A.20.16)}$$

or

$$F_{tL} = \frac{\omega_L}{\omega_U}\left(\frac{r^2 + m^2}{m_T} + m\right)\left[\sqrt{1 + \frac{r^2}{\left(\frac{r^2 + m^2}{m_T} + m\right)^2}} - \frac{\omega_U}{\omega_L}\right]. \qquad \textbf{(A.20.17)}$$

Define F_{2L} as follows to obtain Eq. (5.137)

$$F_{2L} = \sqrt{1 + \frac{r^2}{\left(\frac{r^2 + m^2}{m_T} + m\right)^2}}.$$

Thus,

$$F_{tL} = \frac{\omega_L}{\omega_U}\left(\frac{r^2 + m^2}{m_T} + m\right)\left(F_{2L} - \frac{\omega_U}{\omega_L}\right) \qquad \textbf{(A.20.18)}$$

Use Eq. (A.20.18) in Eq. (A.20.14)

$$\frac{\delta B_{1L}}{\delta m_T} = \frac{2}{m_T}\frac{\omega_L}{\omega_U}\left(\frac{r^2 + m^2}{m_T} + m\right)(F_{1L})\left(F_{2L} - \frac{\omega_U}{\omega_L}\right). \qquad \textbf{(A.20.19)}$$

Eq. (A.20.19) used in Eq. (A.20.5) yields Eq. (5.135) as desired.

Next, we derive Eq. (5.138a). Start with Eq. (5.138).

$$F_{2L} - \frac{\omega_U}{\omega_L} \geq 0.$$

Use Eq. (5.137)

$$\sqrt{1 + \frac{r^2}{\left(\frac{r^2 + m^2}{m_T} + m\right)^2}} - \frac{\omega_U}{\omega_L} \geq 0. \qquad \textbf{(A.20.20)}$$

Continue manipulating as follows:

$$1 + \frac{r^2}{\left(\frac{r^2 + m^2}{m_T} + m\right)^2} \geq \frac{\omega_U^2}{\omega_L^2}, \tag{A.20.21}$$

$$\frac{r^2}{\left(\frac{r^2 + m^2}{m_T} + m\right)^2} > \left(\frac{\omega_U^2}{\omega_L^2} - 1\right), \tag{A.20.22}$$

$$\frac{r}{\left(\frac{r^2 + m^2}{m_T} + m\right)} \geq \sqrt{\frac{\omega_U^2}{\omega_L^2} - 1}, \tag{A.20.23}$$

$$\left(\frac{r^2 + m^2}{m_T} + m\right) \leq \frac{r}{\sqrt{\frac{\omega_U^2}{\omega_L^2} - 1}}, \tag{A.20.24}$$

$$\frac{1}{m_T} \leq \frac{1}{r^2 + m^2}\left(\frac{r}{\sqrt{\frac{\omega_U^2}{\omega_L^2} - 1}} - m\right), \tag{A.20.25}$$

which yields Eq. (5.138a) as desired.

$$\frac{1}{m_T} \leq \frac{m}{r^2 + m^2}\left(\frac{r}{m}\frac{1}{\sqrt{\frac{\omega_U^2}{\omega_L^2} - 1}} - 1\right).$$

A.21 DERIVATION OF EQS. (5.147) AND (5.149)

Recall Eq. (5.147).

$$C_T = \frac{NA_c d_{33}}{g_{33} l_c}.$$

The starting point for derivation of Eq. (5.147) is the definition of the low frequency capacitance C_T for the N ring CSA. Since the N rings are wired in parallel, C_T is N times the capacitance of one of the ceramic rings (all assumed to be identical). For one ring, the capacitance is $A_c\varepsilon_{33}^T/l_c$. Thus, for N rings,

$$C_T = \frac{NA_c \epsilon_{33}^T}{l_c}. \tag{A.21.1}$$

One important piezoelectric ceramic parameter relation is as follows:

$$g_{33} = \frac{d_{33}}{\epsilon_{33}^T}. \tag{A.21.2}$$

Thus,

$$\epsilon_{33}^T = \frac{d_{33}}{g_{33}}. \tag{A.21.3}$$

Use of Eq. (A.21.3) in Eq. (A.21.1) yields the desired result; namely, Eq. (5.147) above.

Next, recall Eq. (5.149).

$$E_o = I_o + \frac{(\omega N d_{33})^2}{C_T}.$$

The starting point to derive Eq. (5.149) is to compare the defining equations for E_o and I_o [Eqs. (5.11) and (5.17), respectively].

$$E_o = \omega^2 C_e - \frac{1}{m_T}$$

and

$$I_o = \omega^2 C_e' - \frac{1}{m_T}.$$

We need an equation relating C_e to C_e'. Recall Eqs. (4.18), (5.18), and (4.4) reprinted below

$$C_e = S_{33}^E \frac{L}{A_c} + C_F,$$

$$C_e' = S_{33}^D \frac{L}{A_c} + C_F,$$

and

$$S_{33}^D = S_{33}^E - g_{33} d_{33}.$$

Use Eq. (4.4) in Eq. (4.18) and write

$$C_e = \left(S_{33}^D + g_{33} d_{33}\right)\frac{L}{A_c} + C_F \qquad \textbf{(A.21.4)}$$

and

$$C_e = \left(S_{33}^D \frac{L}{A_c} + C_F\right) + g_{33} d_{33} \frac{L}{A_c}. \qquad \textbf{(A.21.5)}$$

Note from Eq. (5.18a), we may rewrite Eq. (A.21.5) as

$$C_e = C_e' + g_{33} d_{33} \frac{L}{A_c}. \qquad \textbf{(A.21.6)}$$

Note: Eq. (A.21.6) is equivalent to Eq. (4.5a).

Use g_{33} from Eq.(A.21.2) in Eq. (A.21.6) to write

$$C_e = C_e' + d_{33}^2 \frac{L}{A_c \epsilon_{33}^T}. \qquad \textbf{(A.21.7)}$$

Rewrite as follows:

$$C_e = C_e' + \frac{N d_{33}^2 L}{N A_c \epsilon_{33}^T}. \qquad \textbf{(A.21.7a)}$$

Recall Eq. (4.3)

$$L = N l_c.$$

Rewrite Eq. (A.21.7a) as

$$C_e = C_e' + N^2 d_{33}^2 \frac{1_c}{NA_c \epsilon_{33}^T} . \qquad \textbf{(A.21.8)}$$

Use Eq. (A.21.1) for C_T in Eq. (A.21.8).

$$C_e = C_e' + \frac{(Nd_{33})^2}{C_T} \qquad \textbf{(A.21.8a)}$$

Use C_e from Eq. (A.21.8a) in Eq. (5.11) to write

$$E_o = \left(\omega^2 C_e' - \frac{1}{m_T}\right) + \frac{(\omega N d_{33})^2}{C_T} . \qquad \textbf{(A.21.9)}$$

Using the definition of I_o from Eq. (5.17) in Eq. (A.21.9) yields the desired results; namely, Eq. (5.149).

A.22 DERIVATION OF EQ. (5.152)

Recall Eq. (5.152)

$$\Gamma = \frac{1}{\omega_{n'}^2 C_T}\left[\frac{\omega_n^2}{\omega_m^2}\frac{(\omega_{n'}^2 - \omega_m^2)}{(\omega_{n'}^2 - \omega_n^2)}\right].$$

The starting point for the derivation of Eq. (5.152) was Eq. (5.151).

$$\Gamma = \frac{1}{\omega_{n'}^2 C_T}\left[1 - \frac{(\omega_{n'} N d_{33})^2}{C_T}\frac{m_H}{(1 - m_H I_o)}\right],$$

with I_o evaluated at $\omega = \omega_n'$. In Eq. (5.151), recall that $\omega = \omega_{n'}$. First, we show that

$$\frac{m_H}{(1 - m_H I_o)} = -\omega_n^2 \frac{m_H m_T}{m_H + m_T}\frac{1}{(\omega_{n'}^2 - \omega_n^2)} . \qquad \textbf{(A.22.1)}$$

To do this, recall ω_n (the in-air resonance frequency from I/V_H) was given by Eq. (5.27)

$$\omega_n^2 = \frac{1}{C_e'}\left(\frac{1}{m_H} + \frac{1}{m_T}\right);$$

thus,

$$C_e' = \frac{1}{\omega_n^2}\left(\frac{1}{m_H} + \frac{1}{m_T}\right). \tag{A.22.2}$$

Use C_e' from Eq. (A.22.2) in Eq. (5.17) (reprinted here for convenience)

$$I_o = \omega^2 C_e' - \frac{1}{m_T}$$

to yield

$$I_o|_{\omega=\omega_{n'}} = \frac{\omega_{n'}^2}{\omega_n^2}\left(\frac{1}{m_H} + \frac{1}{m_T}\right) - \frac{1}{m_T}. \tag{A.22.3}$$

Use Eq. (A.22.3) to write the following:

$$\left.\frac{m_H}{1 - m_H I_o}\right|_{\omega=\omega_{n'}} = \frac{m_H}{1 - m_H \dfrac{\omega_{n'}^2}{\omega_n^2}\left(\dfrac{1}{m_H} + \dfrac{1}{m_T}\right) + \dfrac{m_H}{m_T}}, \tag{A.22.4}$$

$$\left.\frac{m_H}{1 - m_H I_o}\right|_{\omega=\omega_{n'}} = \frac{m_H}{1 - \dfrac{\omega_{n'}^2}{\omega_n^2} - \dfrac{\omega_{n'}^2}{\omega_n^2}\dfrac{m_H}{m_T} + \dfrac{m_H}{m_T}}, \tag{A.22.5}$$

$$\left.\frac{m_H}{1 - m_H I_o}\right|_{\omega=\omega_{n'}} = \frac{m_H}{\left(1 - \dfrac{\omega_{n'}^2}{\omega_n^2}\right) + \dfrac{m_H}{m_T}\left(1 - \dfrac{\omega_{n'}^2}{\omega_n^2}\right)}, \tag{A.22.6}$$

$$\left.\frac{m_H}{1 - m_H I_o}\right|_{\omega=\omega_{n'}} = \frac{m_H}{\left(1 - \dfrac{\omega_{n'}^2}{\omega_n^2}\right)\left(1 + \dfrac{m_H}{m_T}\right)}, \tag{A.22.7}$$

and

$$\left.\frac{m_H}{1 - m_H I_o}\right|_{\omega=\omega_{n'}} = \omega_n^2 \frac{m_H m_T}{(m_H + m_T)} \frac{1}{\left(\omega_n^2 - \omega_{n'}^2\right)}. \qquad \textbf{(A.22.8)}$$

Multiplying the right side by -1/-1 and rearranging yields Eq. (A.22.1) above.

Second, show that

$$\frac{(\omega_n N d_{33})^2}{C_T} = \frac{1}{\omega_n^2} \frac{\omega_{n'}^2}{\omega_m^2} \frac{(m_H + m_T)}{m_H m_T} \left(\omega_n^2 - \omega_m^2\right). \qquad \textbf{(A.22.9)}$$

To do this, recall Eq. (5.28)

$$\frac{\omega_n^2}{\omega_m^2} = \frac{C_e}{C_e'}$$

and Eq. (A.21.8)

$$C_e = C_e' + \frac{(N d_{33})^2}{C_T}.$$

Use C_e from Eq. (A.21.8) in Eq. (5.28) to write

$$\frac{\omega_n^2}{\omega_m^2} = 1 + \frac{1}{C_e'} \frac{(N d_{33})^2}{C_T}. \qquad \textbf{(A.22.10)}$$

Rewrite Eq. (5.27) as

$$\frac{1}{C_e'} = \omega_n^2 \frac{m_H m_T}{(m_H + m_T)}. \qquad \textbf{(A.22.11)}$$

Use $1/C_e'$ from Eq. (A.22.11) in Eq. (A.22.10).

$$\frac{\omega_n^2}{\omega_m^2} = 1 + \omega_n^2 \frac{m_H m_T}{(m_H + m_T)} \frac{(N d_{33})^2}{C_T} \qquad \textbf{(A.22.12)}$$

or

$$\frac{(Nd_{33})^2}{C_T} = \frac{1}{\omega_n^2}\frac{(m_H + m_T)}{(m_H m_T)}\left(\frac{\omega_n^2}{\omega_m^2} - 1\right) \qquad \textbf{(A.22.13)}$$

or

$$\frac{(Nd_{33})^2}{C_T} = \frac{1}{\omega_n^2\omega_m^2}\frac{(m_H + m_T)}{(m_H m_T)}\left(\omega_n^2 - \omega_m^2\right). \qquad \textbf{(A.22.14)}$$

Multiplying both sides of Eq. (A.22.14) by $\omega_{n'}^2$ yields Eq. (A.22.9).

Third, use Eqs. (A.22.9) and (A.22.1) to write

$$\frac{(\omega_{n'}Nd_{33})^2}{C_T}\frac{m_H}{(1 - m_H I_o)} = -\frac{\omega_n^2\omega_{n'}^2}{\omega_n^2\omega_m^2}\frac{(m_H + m_T)}{(m_H m_T)}\left(\omega_n^2 - \omega_m^2\right)\frac{m_H m_T}{m_H + m_T}\frac{1}{\left(\omega_{n'}^2 - \omega_n^2\right)} \qquad \textbf{(A.22.15)}$$

or

$$\frac{(\omega_{n'}Nd_{33})^2}{C_T}\frac{m_H}{(1 - m_H I_o)} = \left[-\frac{\omega_{n'}^2}{\omega_m^2}\frac{\left(\omega_n^2 - \omega_m^2\right)}{\left(\omega_{n'}^2 - \omega_n^2\right)}\right], \qquad \textbf{(A.22.16)}$$

with I_o evaluated at $\omega = \omega_n'$.

Use the results of Eq. (2.16) to rewrite Eq. (5.151) as follows:

$$\Gamma = \frac{1}{\omega_{n'}^2 C_T}\left[\frac{\omega_m^2\omega_{n'}^2 - \omega_m^2\omega_n^2 + \omega_{n'}^2\omega_n^2 - \omega_m^2\omega_{n'}^2}{\omega_m^2(\omega_{n'}^2 - \omega_n^2)}\right] \qquad \textbf{(A.22.17)}$$

which yields the desired result; namely, Eq. (5.152).

A.23 DERIVATION OF EQ. (5.153)

Recall Eqs. (5.153), and (5.154), respectively.

$$\frac{I_i}{V_H} = \frac{A_c}{g_{33}1_c}\left\{\left[\left(1 - \frac{1}{\omega^2\Gamma C_T}\right) - mI_{o'}\right] + irI_{o'}\right\},$$

where

$$I_{o'} = I_o - \frac{E_o}{\omega^2 \Gamma C_T}.$$

The starting point for the derivation of Eq. (5.153) was Eq. (5.142) (reprinted here)

$$\frac{I_i}{V_H} = \frac{A_c}{g_{33} l_c}[(1 - mI_o) + irI_o] + \frac{1}{i\omega\Gamma} \frac{1}{\omega N d_{33}}[rE_o - i(1 - mE_o)].$$

First note that

$$\frac{1}{\omega N d_{33}} = \frac{A_c}{g_{33} l_c} \frac{g_{33} l_c}{N A_c d_{33}}. \tag{A.23.1}$$

Recall Eq. (5.147)

$$C_T = \frac{N A_C d_{33}}{g_{33} l_c}.$$

Thus,

$$\frac{1}{\omega N d_{33}} = \frac{A_c}{g_{33} l_c} \frac{1}{C_T}. \tag{A.23.1a}$$

Use Eq. (A.23.2) to rewrite Eq. (5.142) as

$$\frac{I_i}{V_H} = \frac{A_c}{g_{33} l_c}[(1 - mI_o) + irI_o] + \frac{1}{i\omega\Gamma C_T} \frac{A_c}{g_{33} l_c}[rE_o - i(1 - mE_o)] \tag{A.23.2}$$

or

$$\frac{I_i}{V_H} = \frac{A_c}{g_{33} l_c}\left\{[(1 - mI_o) + irI_o] + \frac{1}{i\omega\Gamma C_T}[rE_o - i(1 - mE_o)]\right\} \tag{A.23.3}$$

or

$$\frac{I_i}{V_H} = \frac{A_c}{g_{33} l_c}\left\{\left[1 - mI_o - \frac{(1 - mE_o)}{\omega\Gamma C_T}\right] + ir\left(I_o - \frac{E_o}{\omega\Gamma C_T}\right)\right\} \tag{A.23.4}$$

or

$$\frac{I_i}{V_H} = \frac{A_c}{g_{33} l_c}\left\{\left[\left(1 - \frac{1}{\omega\Gamma C_T}\right) - m\left(I_o - \frac{E_o}{\omega\Gamma C_T}\right)\right] + ir\left(I_o - \frac{E_o}{\omega\Gamma C_T}\right)\right\}. \tag{A.23.5}$$

Using I_o' as defined by Eq. (5.154) yields the desired results; namely, Eq. (5.153).

A.24 DERIVATION OF EQ. (5.171)

Recall Eq. (5.171)

$$\left.\frac{1}{Z}\right|_{\text{in-air}} = \omega C_T \left(\frac{\omega_m}{\omega_n}\right)^2 \frac{\left(\omega_n^2 - \omega^2\right)}{\left(\omega_m^2 - \omega^2\right)}.$$

The starting point for the derivation of Eq. (5.171) was Eq. (5.169)

$$\frac{1}{Z} = \frac{I}{E}$$

or

$$\frac{1}{Z} = \frac{\frac{I}{V_H}}{\frac{E}{V_H}}. \tag{A.24.1}$$

Recall Eqs. (5.10) and (5.16), respectively.

$$\frac{E}{V_H} = \frac{1}{\omega N d_{33}}[rE_o - i(1 - mE_o)]$$

and

$$\frac{I}{V_H} = \frac{A_c}{g_{33} 1_c}[(1 - mI_o) + irI_o].$$

So,

$$\frac{1}{Z} = \frac{\omega N A_c d_{33}}{g_{33} 1_c} \frac{[(1 - mI_o) + irI_o]}{[rE_o - i(1 - mE_o)]}. \tag{A.24.2}$$

In-air r = 0 and m = m_H, so

$$\left.\frac{1}{Z}\right|_{\text{in-air}} = \frac{\omega N A_c d_{33}(1 - m_H I_o)}{g_{33} 1_c(-i)(1 - m_H E_o)} \tag{A.24.3}$$

or

$$\left.\frac{1}{Z}\right|_{\text{in-air}} = i\omega \frac{N A_c d_{33}}{g_{33} 1_c} \frac{(1 - m_H I_o)}{(1 - m_H E_o)}. \tag{A.24.4}$$

Recall Eq. (5.147)

$$C_T = \frac{NA_c d_{33}}{g_{33}\, l_c}.$$

Thus,

$$\left.\frac{1}{Z}\right|_{\text{in-air}} = i\omega C_T \frac{(1 - m_H I_o)}{(1 - m_H E_o)}. \tag{A.24.5}$$

Next, recall Eq. (5.149)

$$E_o = I_o + \frac{(\omega N d_{33})^2}{C_T}.$$

Thus,

$$I_o = E_o - \frac{(\omega N d_{33})^2}{C_T}. \tag{A.24.6}$$

Equation (A.24.6) used in Eq. (A.24.5) yields

$$\left.\frac{1}{Z}\right|_{\text{in-air}} = i\omega C_T \frac{\left[1 - m_H E_o + m_H \dfrac{(\omega N d_{33})^2}{C_T}\right]}{(1 - m_H E_o)} \tag{A.24.7}$$

or

$$\left.\frac{1}{Z}\right|_{\text{in-air}} = i\omega C_T \left[1 + \frac{(\omega N d_{33})^2}{C_T} \frac{m_H}{(1 - m_H E_o)}\right]. \tag{A.24.8}$$

Recall Eqs. (5.11) and (5.24), respectively

$$E_o = \left(\omega^2 C_e - \frac{1}{m_T}\right)$$

and

$$\omega_m^2 = \frac{1}{C_e}\left(\frac{1}{m_H} + \frac{1}{m_T}\right).$$

So,

$$C_e = \frac{1}{\omega_m^2}\left(\frac{1}{m_H} + \frac{1}{m_T}\right). \tag{A.24.9}$$

Use of this C_e in Eq. (5.11) gives

$$E_o = \frac{\omega^2}{\omega_m^2}\left(\frac{1}{m_H} + \frac{1}{m_T}\right) - \frac{1}{m_T}. \tag{A.24.10}$$

Thus,

$$m_H E_o = \frac{\omega^2}{\omega_m^2}\left(1 + \frac{m_H}{m_T}\right) - \frac{m_H}{m_T}. \tag{A.24.11}$$

So,

$$1 - m_H E_o = \left(1 + \frac{m_H}{m_T}\right) - \frac{\omega^2}{\omega_m^2}\left(1 + \frac{m_H}{m_T}\right) \tag{A.24.12}$$

or

$$1 - m_H E_o = \left(1 + \frac{m_H}{m_T}\right)\left(1 - \frac{\omega^2}{\omega_m^2}\right) \tag{A.24.13}$$

or

$$\frac{m_H}{1 - m_H E_O} = \frac{m_H m_T}{(m_H + m_T)} \frac{1}{\left(1 - \dfrac{\omega}{\omega_m^2}\right)} \tag{A.24.14}$$

or

$$\frac{m_H}{(1 - m_H E_O)} = \omega_m^2 \frac{m_H m_T}{(m_H + m_T)} \frac{1}{\left(\omega_m^2 - \omega^2\right)}. \tag{A.24.15}$$

Recall Eq. (A.22.14)

$$\frac{(Nd_{33})^2}{C_T} = \frac{1}{\omega_n^2 \omega_m^2} \frac{(m_H + m_T)}{(m_H m_T)} \left(\omega_n^2 - \omega_m^2\right).$$

So,

$$\frac{(\omega N d_{33})^2}{C_T} = \frac{\omega^2}{\omega_n^2 \omega_m^2} \frac{(m_H + m_T)}{(m_H m_T)} \left(\omega_n^2 - \omega_m^2\right). \tag{A.24.16}$$

Use of Eqs. (A.24.16) and (A.24.15) in Eq. (A.24.8) gives

$$\left.\frac{1}{Z}\right|_{\text{in-air}} = i\omega C_T \left[1 + \frac{\omega^2 \omega_m^2}{\omega_n^2 \omega_m^2} \frac{(m_H + m_T)}{(m_H m_T)} \frac{m_H m_T}{(m_H + m_T)} \frac{\left(\omega_n^2 - \omega_m^2\right)}{\left(\omega_m^2 - \omega^2\right)}\right], \tag{A.24.17}$$

$$\left.\frac{1}{Z}\right|_{\text{in-air}} = i\omega C_T \left[1 + \frac{\omega^2}{\omega_n^2} \frac{\left(\omega_n^2 - \omega_m^2\right)}{\left(\omega_m^2 - \omega^2\right)}\right], \tag{A.24.18}$$

$$\left.\frac{1}{Z}\right|_{\text{in-air}} = i\omega C_T \left[\frac{\omega_n^2 \omega_m^2 - \omega_n^2 \omega^2 + \omega_n^2 \omega^2 - \omega^2 \omega_m^2}{\omega_n^2 \left(\omega_m^2 - \omega^2\right)}\right], \tag{A.24.19}$$

and

$$\left.\frac{1}{Z}\right|_{\text{in-air}} = i\omega C_T \frac{\omega_n^2 \omega_m^2 - \omega^2 \omega_m^2}{\omega_n^2 \left(\omega_m^2 - \omega^2\right)}. \tag{A.24.20}$$

Factoring out ω_m in the numerator yields the desired results; namely, Eq. (5.171).

Appendix B

PRACTICAL ILLUSTRATIONS OF THE SGM ANALYSIS

B.0 PRACTICAL ILLUSTRATIONS OF THE SGM ANALYSIS

In an effort to insure a clear understanding of several key expressions presented in Sec. 5, this appendix presents graphical illustrations of these analytical results using a simple SGM-based computer program (with various subroutines) written in Matlab®, a numeric computation and visualization software package. By design, these programs make use of the fundamental expressions of the augmented SGM [primarily Eqs. (5.10) and (5.16)] and do not make use of the other pencil and paper derived equations in Sec. 5. (In order to distinguish between the equations used in the SGM-based numerical model and the other pencil and paper derived expressions, this appendix refers to the latter category of expressions as "insight oriented" design aid equations.) If we find that the numerical computer predictions agree with the corresponding insight oriented predictions, then this fact can be taken as a strong indication that there were no significant errors in the Sec. 5 analysis.

In order to apply the subject SGM-based computer program, a specific transducer model had to be produced. For this purpose a simplified version of the TR-330A (a Navy fleet sonar transducer) was chosen as the transducer to model. The resulting model is referred to below as the "STR-330A" model as a reminder that the STR-330A model is vastly simplified compared to the complete TR-330A model used in previous performance predictions, which should be used in any future quantitative performance predictions for the TR-330A. Please remember, as has been emphasized throughout this report, the STR-330A Model predictions need only agree qualitatively (not quantitatively) with the design insight data derived from the complete TR-330A model and/or experiments. In those cases where there is also good quantitative agreement, this fact represents an unexpected extra confidence factor.

This choice of using a simplified version of the TR-330A as the transducer to model in the SGM-based computer model was made for two reasons:

1. A great deal of theoretical and experimental TR-330A data exists (for example, see the STRIP reports) for comparison with the data produced using the STR-330A model.

2. All TR-330A data is UNCLASSIFIED, making it much more useful for our purposes.

   [Note that because the graphical illustrations to be presented and discussed in this appendix are designed to facilitate a better intuitive understanding for the reader, the angular frequency symbol ω (rad/s) given in the text will represented in linear frequency units (Hz).]

The reader will find that results of the numerical predictions to be presented compare remarkably well with the results found using the insight oriented design aids derived in Sec. 5. They also have shown to enhance the clarity and understanding concerning the use of the SGM design aids.

B.1 THE IN-WATER SGM RESULTS OF THE STR-330A TONPILZ TRANSDUCER MODEL

We will begin testing the simplified model presented in Secs. 5.1 and 5.2 by graphing various quantities that are pertinent to the electrical and acoustical performance of the TR-330A transducer. This transducer consists primarily of an aluminum head mass, a steel tail mass, four PZT-4 (Navy Type I) piezoceramic rings, and two GE-11 fiberglass tuning rings, one located at the front of the ceramic stack and the other near the rear of the ceramic stack. Specific transducer properties employed in the performance calculations are given in the following list:

d_{33} = 302.2 × 10-12 m/V (piezoelectric charge coefficient of ceramic ring)

g_{33} = 24.9 × 10-3 Vm/N (piezoelectric voltage coefficient of ceramic ring)

S_{33}^{E} = 15.5 × 10-12 m^2/N (elastic constant for ceramic ring)

S_{33}^{D} = 8.216 × 10-12 m^2/N (elastic constant for ceramic ring)

A_c = 8.8674 × 10-4 m^2 (electroded area of ceramic ring)

l_c = 0.01090 m (length of ceramic ring)

N = 4 (number of ceramic rings in CSA)

S_{33f}^{E} = 114 × 10-12 m^2/N (elastic constant for fiberglass tuning ring)

A_f = 0.0019 m^2 (area of fiberglass tuning ring)

l_f = 0.0028 m (length of fiberglass tuning ring)

m_H = 0.568 kg (head mass)

m_T = 1.53 kg (tail mass)

In addition to these transducer quantities, the radiation loading effects of the medium were also required. Referring back to Eq. (5.4) in Sec. 5.2, we find that the radiation impedance, Z_r, is given by

$$Z_r = R + iX.$$

For the purposes of the design simplification, it is assumed that this function can be represented by quantities, R and X, that have a linear dependence with frequency [Eq. (5.5)].

$$R=r\omega \quad \textit{and} \quad X=x\omega .$$

First, realistic values for the radiation resistance constant, r, and the radiation reactance constant, x, need to be determined for the in-water loading condition. In order to accomplish this, the transducer is assumed to have the same radiation impedance as that of a baffled circular piston of radius, a, given by

$$Z_r=\rho c \pi a^2[R_1(2ka)- X_1(2ka)], \tag{B.1}$$

with

$$R_1(2ka)=1 - \frac{2J_1(2ka)}{(2ka)} \quad \textit{and} \quad X_1(2ka) = \frac{2H_1(2ka)}{(2ka)}, \tag{B.2}$$

where $J_1(2ka)$ and $H_1(2ka)$ are the Bessel function and the Struve function of the first order.

Upon calculating the transducer's impedance over the desired frequency bandwidth of 5,000 Hz (31,416 rad/s) to 15,000 Hz (94,248 rad/s), the mid-band impedance at 10,000 Hz (62,832 rad/s) is chosen to represent radiation impedance constants in the simplified transducer model. (However, if we wanted to use this numerical model in an actual transducer design, we could easily modify the model to use the exact impedance function over the frequency range. This was not done in the following analysis, since our purposes were to verify the Sec. 5 transducer design aids.) Specifically, the impedance constants at 10,000 Hz are determined to be:

$$r = 0.2447 \quad \textit{and} \quad x = 0.0953. \tag{B.3}$$

Now that all the needed baseline transducer parameters have been determined, we can make some pertinent transducer performance calculations, such as the input voltage per unit head velocity (E/V_H), the input current per unit head velocity (I/V_H), and the input electric field per unit head velocity (ε/V_H) as functions of frequency using Eqs. (5.10), (5.16), and (4.8.1), respectively. The frequency band considered covers from 5,000 to 15,000 Hz. Plots of the magnitudes and phases of these quantities over this band are given in Figs. B.1-1, B.1-2, B.1-3, B.1-4, and B.1-5. It can be easily seen from the $|E/V_H|$ versus frequency plot (Fig. B.1-1), that the in-water resonance frequency, ω_e, is located at approximately 7,500 Hz. From the phase data given in Fig. B.1-2, notice that the in-water phase zero crossing frequency, ω_{e0}, also occurs at 7,500 Hz. (This expected behavior is discussed in detail in Sec. 5.2.2.2.) Similar conclusions can be drawn when one examines the magnitude and phase plots of I/V_H versus frequency, as shown in Figs. B.1-3 and B.1-4, respectively. The anti-resonance frequency occurs at approximately 9,500 Hz, the point where $|I/V_H|$ is minimum and the phase angle between I and V_H is 90°; i.e., ω_{i90}. Using a very conservative value for the electric field of 2 V/mil applied to the transducer's ceramic stack assembly (much higher fields may be applied in practice), specific values for the resulting head velocity (V_H), radiated acoustic power (P), and the electrical power input (P_{in}) are calculated over the frequency range of interest. The graphs of the magnitudes of V_H and P versus frequency are shown in Figs. B.1.6 and B.1.7, respectively. The graphs showing P_{in} and the phase between E and I over the frequency band of interest are provided in Fig. B.1-8 and Fig. B.1-9.

Each of these results for the modeled TR-330A transducer compared very well qualitatively (which is all that is required for our purposes), and surprisingly well quantitatively with actual TR-330A data, thus providing a good measure of verification for the simplified guidance model developed in Sec. 5. It must be mentioned, however, that the results are limited due to the fact that the flexing head and mechanical losses in the molded rubber around the head, found in the actual TR-330A transducer, have not been accounted for in the model. Nevertheless, much design insight can still be acquired. In the following subsections, we will build upon this simplified model, and investigate the effects of changing certain parameters such as the head mass and tail mass on the transducer's performance.

B.2 THE IN-WATER SGM RESULTS OF THE STR-330A TONPILZ TRANSDUCER MODEL: VARIABLE m_H, FIXED m_T AND ω_m

The next illustration exhibits the in-water transducer performance as the head mass, m_H, is varied, but holding the tail mass, m_T, and the in-air resonance angular frequency, ω_m, fixed. In Sec. 5.2.2.1.2, it is

stated that the in-water $|E/V_H|$ at $\omega=\omega_m$ [Eq. (5.12)] can be expressed more concisely in Eq. (5.34) (shown below) as

$$\left|\frac{E}{V_H}\right|_{\omega=\omega_m} = \frac{1}{\omega_m^2 N d_{33} m_H} |Z_{rm}| .$$

This form of $|E/V_H|$ claims that if the in-air resonance frequency ω_m is held constant, then as m_H increases, the voltage E required to obtain a given head velocity V_H decreases around ω_m. Since at first this conclusion seemed to violate experience gained using sophisticated computer models, it was important to determine if the same conclusion would be drawn by directly evaluating the more general relationship for $|E/V_H|$ given by Eq. (5.12) under the same conditions. This was accomplished by solving for ω_m^2 in the following form [Eq. (5.24)]:

$$\omega_m^2 = \frac{1}{C_e}\left(\frac{1}{m_H} + \frac{1}{m_T}\right).$$

Using the baseline parameters for C_e, m_T and m_H, this calculation results in an in-air resonance frequency occurring at approximately 8,100 Hz. This frequency becomes the baseline in-air resonance frequency ω_m for the model. With this same relationship the effective compliance C_e may be changed such that for any variation of m_H, the in-air resonance frequency remains fixed. It can be readily seen from Eq. (5.24) that as m_H is increased, C_e must be decreased to maintain this condition. The $|E/V_H|$ in Eq. (5.12) may now be numerically evaluated for the baseline head mass (m_H), a 10% larger head mass (m_H+10%), and a 10% smaller head mass (m_H–10%).

Figure B.2-1 shows the computed values of $|E/V_H|$ as a function of frequency for each different m_H. It can be readily seen that the results implied by Eq. (5.34) are, in fact, confirmed; i.e., the larger m_H the lower the required E to produce a given V_H around ω_m. It may also be pointed out that the in-water resonance frequencies for the three cases of m_H vary slightly. Figure B.2.2 shows the phase of E/V_H over the same frequency band. Since the electric field $\epsilon = E/l_c$, the values of $|\epsilon/V_H|$ for each m_H versus frequency, shown in Fig. B.2-3, have the same shape as the curves found in Fig. B.2-1. Using each m_H and the corresponding C_e required to maintain a fixed value of ω_m, the amplitude and phase of I/V_H are also determined and illustrated in Figs. B.2-4 and B.2-5. For an applied electric field of 78,740 V/m (or equivalently 2 V/mil), the complex electrical quantities E, I, Z_e, and P_{in} are also calculated. Plots of $|I|$, $|E|\bullet|I|$ product, and P_{in} are given in Figs. B.2-6, B.2-7, and B.2-8, respectively. As seen in Fig. B.2-8, the increased m_H results in an increased input electrical power around resonance.

B.3 THE IN-WATER SGM RESULTS OF THE STR-330A TONPILZ TRANSDUCER MODEL: VARIABLE m_H, FIXED m_T AND ω_e

In an analysis similar to the one described in the previous section, this subsection attempts to further illustrate the effects of changing the transducer head mass m_H on the transducer performance. (See Sec. 5.2.2.5.) The only difference being that in this case the in-water resonance frequency ω_e shall be held fixed, instead of the in-air resonance frequency ω_m. Following the derivation presented in Sec. A.10, we find that the in-water resonance frequency ω_e for the quantities $|E/V_H|$ and $|\epsilon/V_H|$ is given by Eq. (5.76)

$$\omega_e^2 = \frac{1}{C_e}\sqrt{\frac{r^2 + (m + m_T)^2}{m_T^2(r^2 + m^2)}}.$$

Using the same procedure as described in the fixed ω_m case, along with Eq. (5.76), we determine that the effective compliance C_e must be decreased when m_H is increased in order to maintain the fixed ω_e condition. E/V_H was computed for each of the following three values for the head mass: m_H, m_H+10%, and m_H-10%. The magnitude and phase of E/V_H for these cases are graphically illustrated in Figs. B.3-1 and B.3-2, while $|\epsilon/V_H|$ is shown in Fig. B.3-3. Similar trends are seen as in the fixed ω_m case; namely, that as m_H is increased, E/V_H (or equivalently ϵ/V_H) decreases around the resonance frequency ω_e. For this fixed ω_e case it may be observed in Figs. B.3-1 and B.3-3 that away from resonance there is a slight reduction in the bandwidth as a result of increasing m_H. This trend should become more obvious as m_H continues to deviate from the baseline value. These graphs also illustrate that there are two particular frequencies, one below ω_e ($\approx$ 6,000 Hz) and the other above ω_e ($\approx$ 9,300 Hz), at which all three curves for m_H intersect. As we will see in more detail in the next subsection, this candidate application of the SGM added some additional insight into the insight oriented design aids presented in Sec. 5. It is interesting to note that if this phenomenon had been observed when the original insight-oriented analyses were done, it could have facilitated the development the Fixed End Point Analysis of Sec. 5.2.2.6.2 which is illustrated in the third candidate application of the SGM in Sec. B.5.

Other pertinent transducer performance quantities such as $|I/V_H|$, phase of I/V_H, $|I|$, $|Z_e|$, phase of Z_e, $|E|\bullet|I|$ product, and P_{in}, using the applied electric field of 2 V/mil are illustrated for each m_H as a function of frequency in Figs. B.3-4 through B.3-10, respectively. As in the case of fixed ω_m, the input electrical power P_{in} required by the transducer around resonance increased with m_H.

B.4 THE IN-WATER SGM RESULTS OF THE STR-330A TONPILZ TRANSDUCER MODEL: FIXED END POINT ANALYSIS, SPECIAL CASE 2

In this subsection we will attempt to illustrate one of the most important conclusions drawn by the augmented simplified guidance model analysis. Hopefully, it will result in more insight for the transducer designer. In the Fixed End Point Analysis (FEPA) (See Secs. 5.2.2.6.2 and A.13), the lower and upper end points of the frequency band of interest, ω_L and ω_U, are held fixed. Additionally, design constraints are placed on the values of ω_e and the $|\epsilon/V_H|$ at the end point frequencies. As given by Eq. (5.93), ω_e is constrained to be located between the lower and upper end point frequencies, ω_L and ω_U. The constraint on $|\epsilon/V_H|$ in the FEPA depends on the specific case of interest. In Sec. 5, two of these cases are discussed in detail: Special Case 1 and Special Case 2.

Special Case 1 uses the value of C_e from Eq. (5.104) for the case where $\alpha = 1$ in Eq. (5.108). Special Case 2 imposes the design constraint that the $|\epsilon/V_H|$ must be equal at the lower and upper end points, ω_L and ω_U. Both of these special cases provide useful insights to the designer, however, only Special Case 2 will be graphically illustrated here. For convenience, we repeat the design constraint given by Eq. (5.126),

$$\left|\frac{\epsilon}{V_H}\right|_{\omega=\omega_L} = \left|\frac{\epsilon}{V_H}\right|_{\omega=\omega_U}.$$

This relationship causes the α parameter defined in Eq. (5..108) to be Eq. (5.127) below

$$\alpha = \frac{\omega_L}{\omega_U}.$$

It is the intention of this candidate application of the SGM to verify the trends pointed out by the insight oriented derivations contained in the FEPA in Sec. 5 and Appendix A. The FEPA provides insight into a method to select best choices for m_H and m_T, while automatically finding a best location for ω_e. In this illustration, we will be using an iterative approach. The purpose of using this iterative approach as opposed to directly implementing a few of the insight oriented analytical expressions derived in Sec. 5.2.2.6.2.1.2 is to show that the SGM may provide satisfactory results with primarily the use of the transducer designer's insight. (In practice, however, the procedure can be automated with a computer program to do this much more efficiently.) The same procedure can be used as a TDGS in conjunction with a full-scale computer model. The transducer performance calculations employed in the following analysis will be the same general expressions utilized in previous subsections of this Appendix. The analysis encompases all the necessary design principles discussed in Secs. 4 and 5. In other words, it demonstrates how the designer should modify the necessary transducer parameters (components) to meet the overall transducer performance objectives.

In the first Case 2 example, we will look at the situation where m_H is varied, but m_T is held fixed. In addition to the Case 2 design constraint given by Eq. (5.126), we will insure that the $|\varepsilon/V_H|$ at the end points for each m_H is the same as the $|\varepsilon/V_H|$ at the end points using the baseline m_H. Five different values of the head mass are tested in the FEPA. They include m_H (the baseline value), m_H+10%, m_H-10%, m_H+20%, and m_H-20%. Initially, let's analyze the inherent effect of changing m_H; i.e., before application of the FEPA, on the numerical model's calculation of $|\varepsilon/V_H|$ [Eq. (5.16)]. This is shown in Fig. B.4.1. As expected, $|\varepsilon/V_H|$ varies considerably over the 5,000 to 11,100 Hz band. The resonance frequency also shifts as m_H is varied. These results demonstrate that considerable changes occur in the transducer's performance; thereby, demonstrating the need to implement a procedure to compensate for these differences in $|\varepsilon/V_H|$ at the frequency end points. Next we will apply the FEPA which serves as a systematic procedure for adjusting these parameters to meet the imposed design constraints. It can be summarized as follows:

1. Apply Eq. (5.16) to the baseline transducer model over the frequency band, and choose the fixed end point frequencies ω_L and ω_U such that $|\varepsilon/V_H|_b$ at $\omega = \omega_L$ is equal to $|\varepsilon/V_H|_b$ at $\omega = \omega_U$, where $|\varepsilon/V_H|_b$ is defined as the baseline electric field per unit head velocity.

2. Modify the value of m_H in the model, and recompute $|\varepsilon/V_H|$ as a function of frequency and compare $|\varepsilon/V_H|$ at ω_L and ω_U.

3. Make iterative modifications to the effective compliance C_e such that $|\varepsilon/V_H|$ at $\omega = \omega_L$ is equal to $|\varepsilon/V_H|$ at $\omega = \omega_U$ for the new m_H.

4. Adjust the length of each ceramic ring (l_c) in the CSA so that $|\varepsilon/V_H| = |\varepsilon/V_H|_b$ at the fixed end points ω_L and ω_U.

5. Modify the area of each ceramic ring A_c according to

$$A_c = \frac{S_{33}^E L}{(C_e - C_f)} \tag{B.4}$$

which is determined using a combination of Eqs. (4.2a) and (4.18).

6. Finally, implement the new value for A_c into the transducer model and recompute $|\varepsilon/V_H|$.

7. Repeat steps 2 through 6 for each new value of m_H.

The FEPA procedure was applied to the transducer using arbitrarily chosen lower and upper end points of 5,000 and 11,100 Hz, respectively. The $|\varepsilon/V_H|$ results from the application of the FEPA for each case of m_H are plotted over the frequency range in Fig. B.4-2. Note the dramatic improvement in the agreement of the curves for the various m_H cases when compared to the curves illustrated in the "uncorrected" cases found in Fig. B.4-1. Additionally, after performing the FEPA the resonance frequencies ω_e for all the cases of m_H now coincide. (This obtained identical results as the second candidate application shown in Sec. B.3 where ω_e was required to remain fixed.) In other words, if one completes the FEPA, then ω_e is automatically adjusted to the desired location. It is demonstrated once again that the larger m_H the lower the electric field required to produce a desired source level or head velocity around resonance. It also demonstrates that the smaller m_H the flatter the frequency response of the transducer. Consequently, the size of the head mass the designer chooses depends on the specific transducer performance requirements. If we choose flatness as a goodness criteria, then we would want to choose a smaller m_H in our transducer design. Table B.1 provides the tabulated values for C_e, L, A_c, and L/A_c required to complete the FEPA.

Table B.1 - Example of Fixed End Point Analysis: Case 2 Variation of m_H; m_T Held Fixed

Head Mass	$C_e x10^{-8}$ (m/N)	l_c (m)	L (m)	A_c (m^2)	L/A_c (1/m)
mH	0.093012	0.01090	0.04360	0.000886	49.2
mH + 10%	0.088733	0.01099	0.04396	0.000947	46.4
mH - 10%	0.097941	0.01060	0.04240	0.000809	52.3
mH + 20%	0.085357	0.01130	0.04520	0.001021	44.2
mH - 20%	0.104303	0.01055	0.04220	0.000747	56.5

We can see from this data that as the head mass increases the effective compliance must decrease, and the ceramic stack length must increase. Other pertinent transducer performance quantities of interest such as $|E/V_H|$, phase of E/V_H, $|I/V_H|$, phase of I/V_H, $|I|$, $|Z_e|$, phase of Z_e, $|E| \bullet |I|$ product, and P_{in}, using an applied electric field of 2 V/mil, are illustrated for each m_H in Figs. B.4-3 through B.4-11, respectively. Note that there is also close agreement in the antiresonance frequency for each case of m_H from the input current magnitude per unit head velocity ($|I/VH|$) found in Fig. B.4-5.

In the second Case 2 example, we will look at the situation where m_T is varied, but m_H is held fixed. Our goal is now to insure that the $|\varepsilon/V_H|$ at ω_L and ω_U for each m_T is the same as the $|\varepsilon/V_H|_b$ at ω_L

and ω_U using the baseline m_T. This application of the FEPA is analogous to the procedure in the first example discussed above. Before applying the FEPA, let's consider what ordinarily happens to $|\varepsilon/V_H|$ as m_T is changed. (See Fig. B.4-12.) As expected, $|\varepsilon/V_H|$ varies considerably over the 5,000 to 11,100 Hz band. The resonance frequency is also shifted. Next, we will illustrate in Fig. B.4-13 the results obtained after applying the FEPA to the transducer. Note the improved agreement in $|\varepsilon/V_H|$ at ω_L and ω_U, as well as the location of ω_e. This figure also demonstrates the trend that larger tail masses give larger $|\varepsilon/V_H|$ values at ω_e and flatten the frequency response. (Refer to Sec. 5.2.2.6.2.1.2 for a detailed analysis of why this behavior is expected.) However, the differences in $|\varepsilon/V_H|$ seen here are much less than those differences seen as m_H is varied. Table B.2 provides the tabulated values for C_e, L, A_c, and L/A_c required to complete the FEPA.

Table B.2 - Example of Fixed End Point Analysis: Case 2 Variation of m_T; m_H Held Fixed

Tail Mass	$C_e x10^{-8}$ (m/N)	l_c (m)	L (m)	A_c (m^2)	L/A_c (1/m)
mT	0.093012	0.01090	0.04360	0.886740	49.2
mT + 10%	0.090407	0.01062	0.04248	0.894526	47.5
mT - 10%	0.096267	0.01125	0.04500	0.877718	51.3
mT + 20%	0.088361	0.01042	0.04168	0.902777	46.2
mT - 20%	0.100452	0.01172	0.04688	0.868636	54.0

It is readily seen from the data that as m_T is increased, C_e and L must decrease to meet the electric field end point requirements. The trend for C_e to decrease with increasing m_T is predicted by Eq. (5.104c) in the main text. The decrease in L is expected assuming that the following condition [Eq. (5.137) below] holds:

$$F_{2L} = \sqrt{1 + \frac{r^2}{\left(\frac{r^2 + m^2}{m_T} + m\right)^2}}.$$

This is the condition for which the slope of L with respect to m_T is negative. If one performs a similar derivation to the one required to obtain Eq. (5.138b), it logically follows from Eq. (5.137) that

$$r < m\sqrt{\left(\frac{\omega_U}{\omega_L}\right)^2 - 1}. \qquad \textbf{(B.5)}$$

In order to meet this condition for our TR-330A transducer, where $m = m_H + x = 0.6633$ and the frequency end points are 5,000 and 11,100 Hz, then

$$r < 1.3147. \qquad \textbf{(B.6)}$$

Since in our case r = 0.2447 (found using the radiation impedance model of a baffled piston), this condition has indeed been met. Therefore, we conclude that our example fits into the broad-band design

and the trend suggested by the augmented SGM is in good agreement with the computational results. In fact, Eq. (B.3) suggests that the ceramic stack length L should continue the trend to decrease with increasing m_T until $\omega_U/\omega_L = 1.07$, the point at which L would start increasing with increasing m_T. That case would be considered a very narrow band transducer design. However, in practice the broad-band design is the most common type encountered.

In order to complete our characterization of the transducer upon application of the FEPA Special Case 2, other transducer performance calculations are included for the case where m_T is varied. Illustrated in Figs. B.4-14 through B.4-22 are $|E/V_H|$, phase of E/V_H, $|I/V_H|$, phase of I/V_H, $|I|$, $|Z_e|$, phase of Z_e, $|E| \bullet |I|$ product, and P_{in} using the typical applied electric field of 2 V/mil.

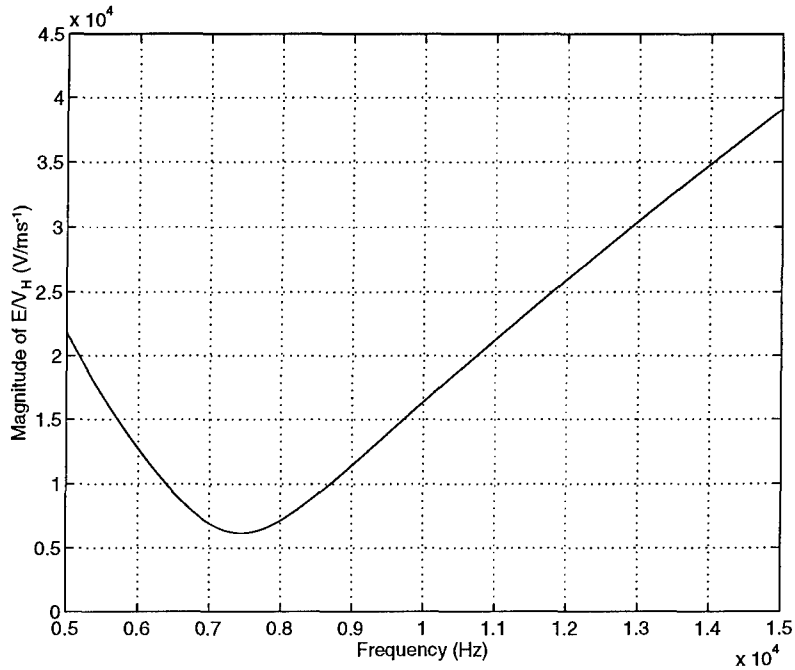

Fig. B.1-1 — STR-330A Model's in-water $|E/V_H|$ versus frequency

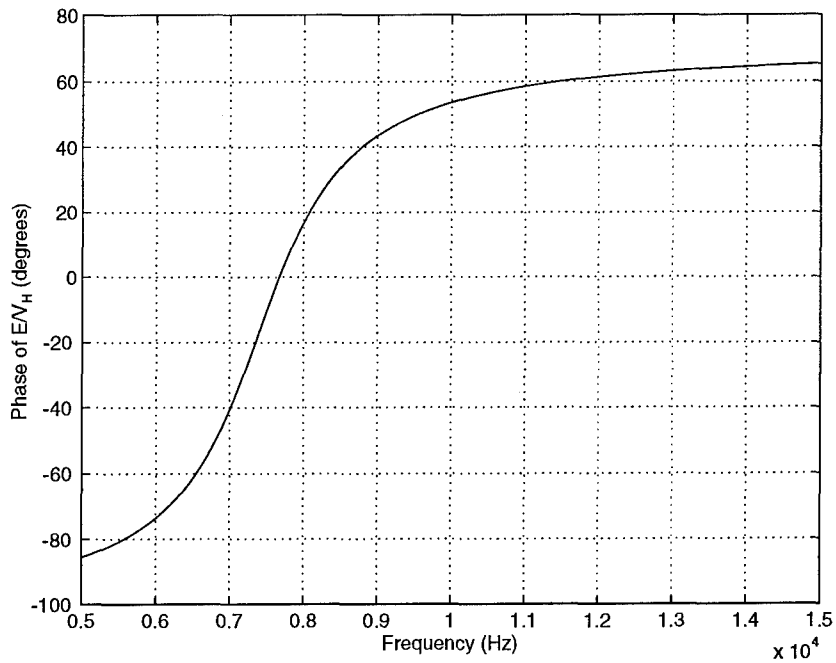

Fig. B.1-2 — STR-330A Model's in-water phase of E/V_H versus frequency

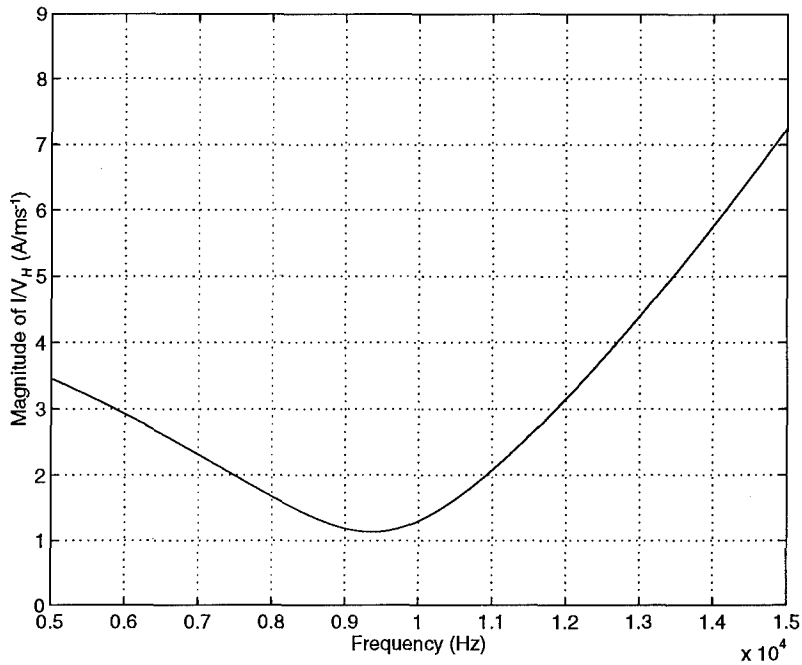

Fig. B.1-3 — STR-330A Model's in-water $|I/V_H|$ versus frequency

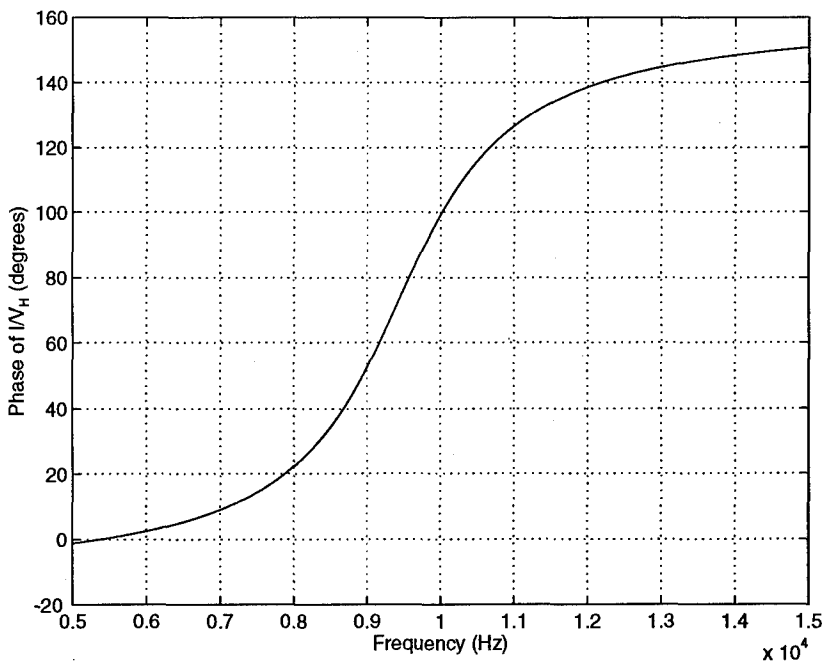

Fig. B.1-4 — STR-330A Model's in-water phase of I/V_H versus frequency

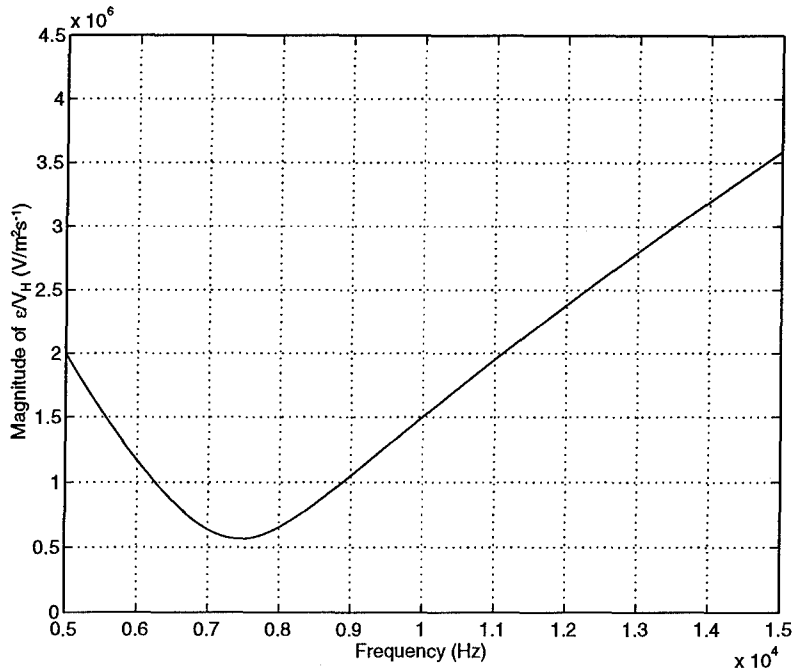

Fig. B.1-5 — STR-330A Model's in-water $|\epsilon/V_H|$ versus frequency

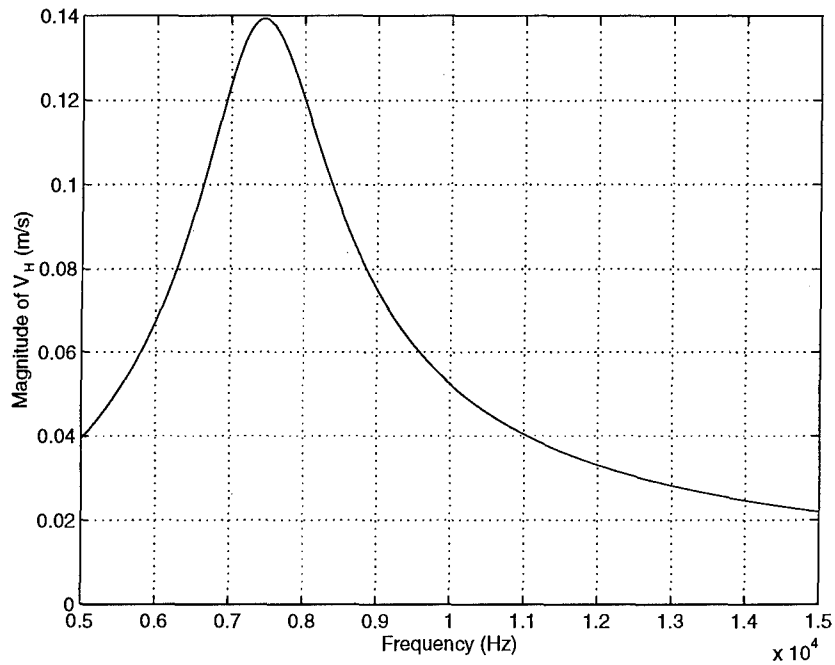

Fig. B.1-6 — STR-330A Model's in-water $|V_H|$ versus frequency; ϵ = 2V/mil

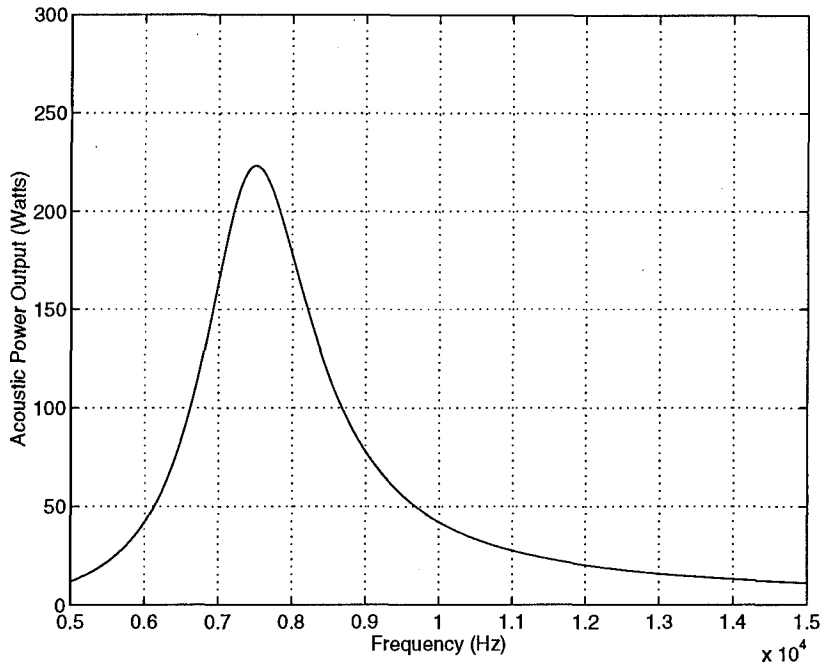

Fig. B.1-7 — STR-330A Model's in-water acoustic power output versus frequency; ϵ = 2V/mil

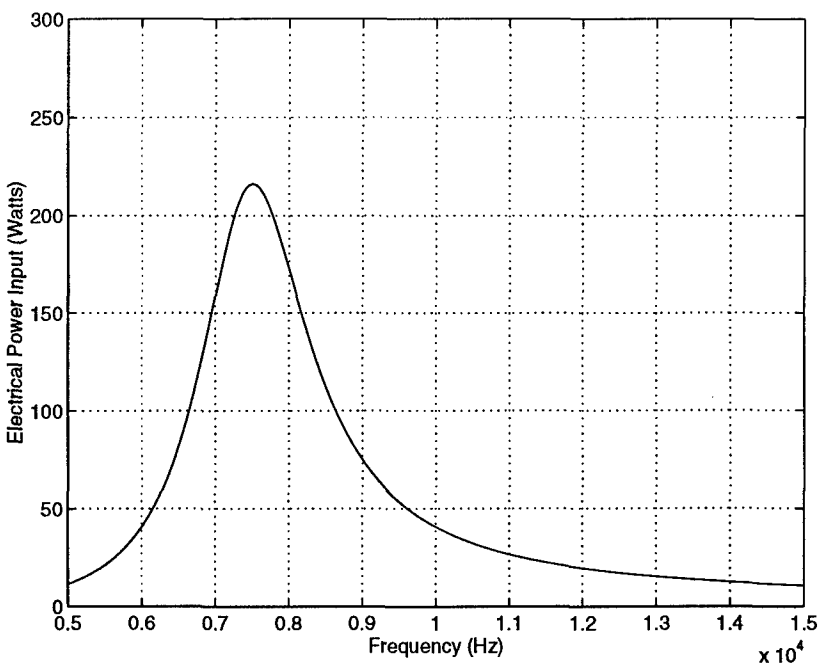

Fig. B.1-8 — STR-330A Model's in-water electrical power input versus frequency; ϵ = 2V/mil

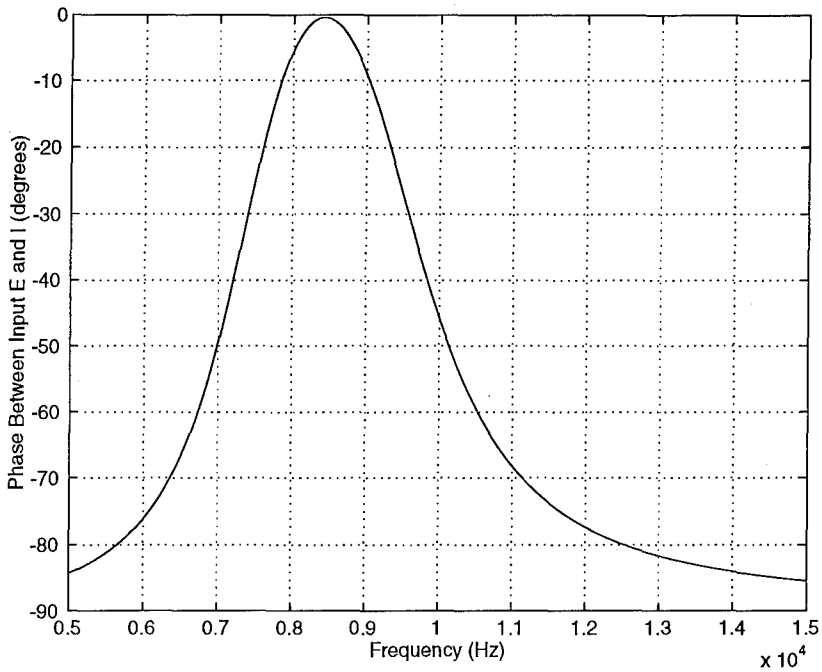

Fig. B.1-9 — STR-330A Model's in-water phase between input voltage and current versus frequency; ϵ = 2V/mil

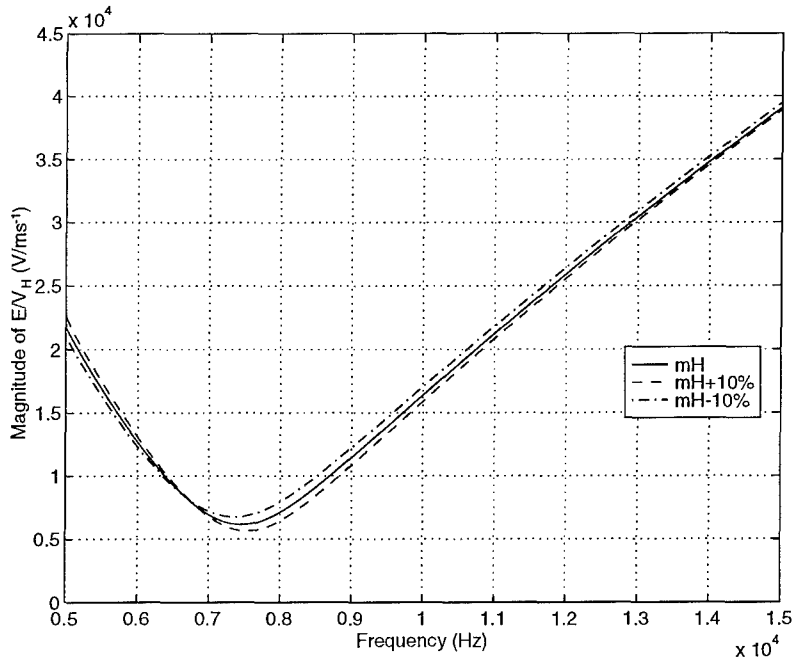

Fig. B.2-1 — STR-330A Model's in-water $|E/V_H|$ versus frequency for three different values of m_H; fixed ω_m, and m_r

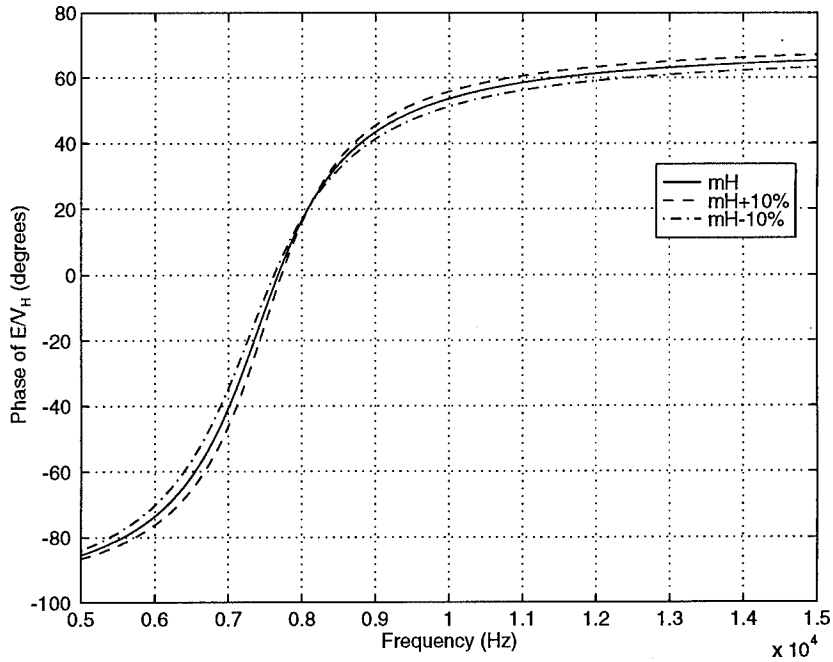

Fig. B.2-2 — STR-330A Model's in-water phase of E/V_H versus frequency for three different values of m_H; fixed ω_m, and m_T

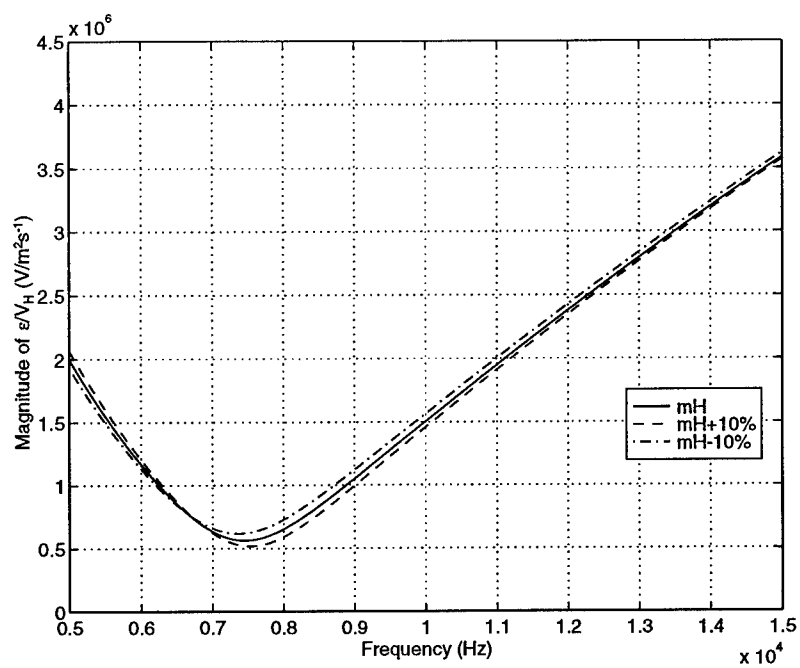

Fig. B.2-3 — STR-330A Model's in-water $|\epsilon/V_H|$ versus frequency for three different values of m_H; fixed ω_m, and m_T

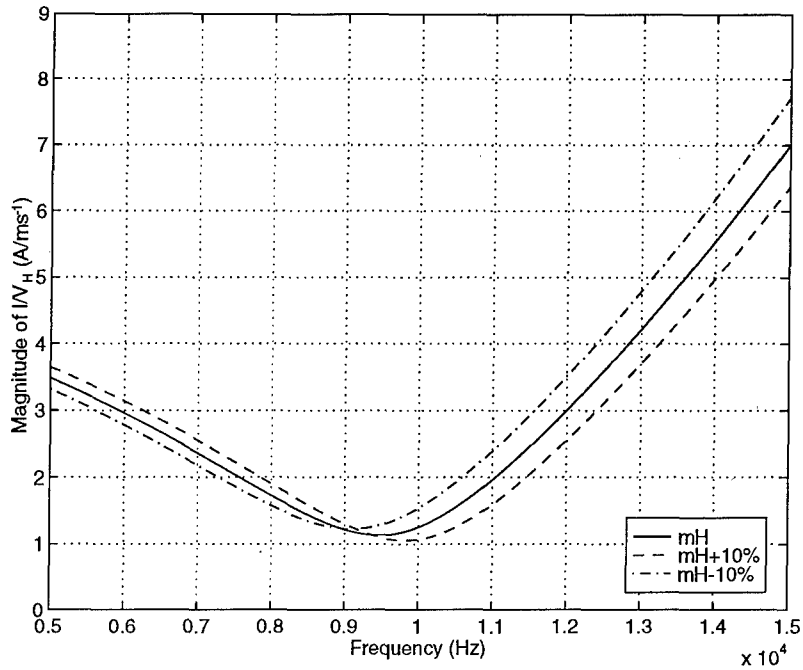

Fig. B.2-4 — STR-330A Model's in-water $|I/V_H|$ versus frequency for three different values of m_H; fixed ω_m, and m_T

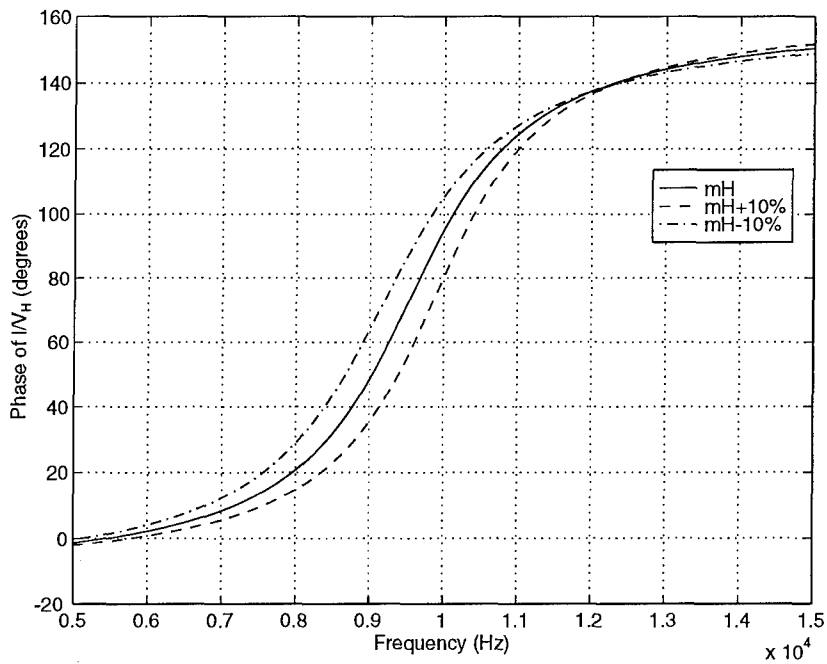

Fig. B.2-5 — STR-330A Model's in-water phase of I/V_H versus frequency for three different values of m_H; fixed ω_m, and m_T

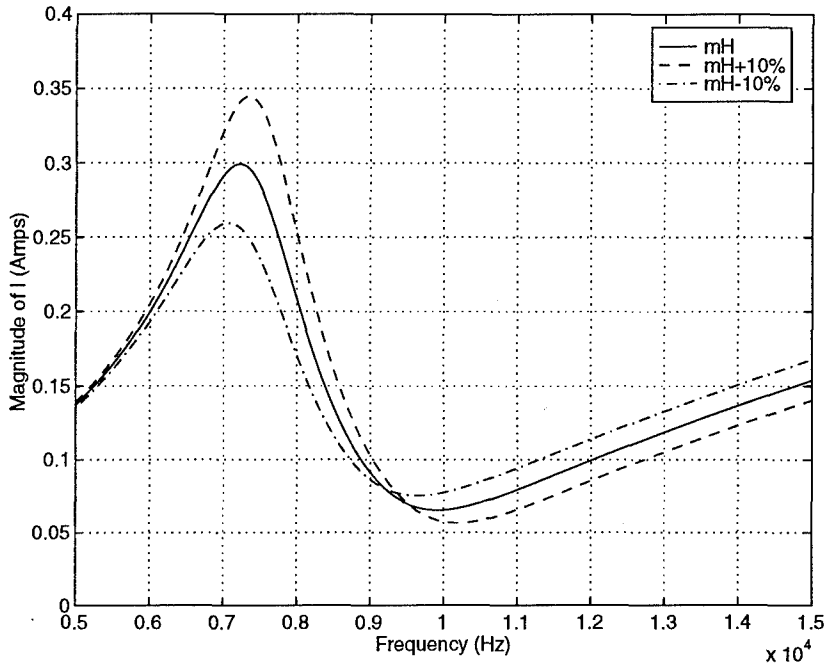

Fig. B.2-6 — STR-330A Model's in-water |I| versus frequency for three different values of m_H; fixed ω_m, and m_T

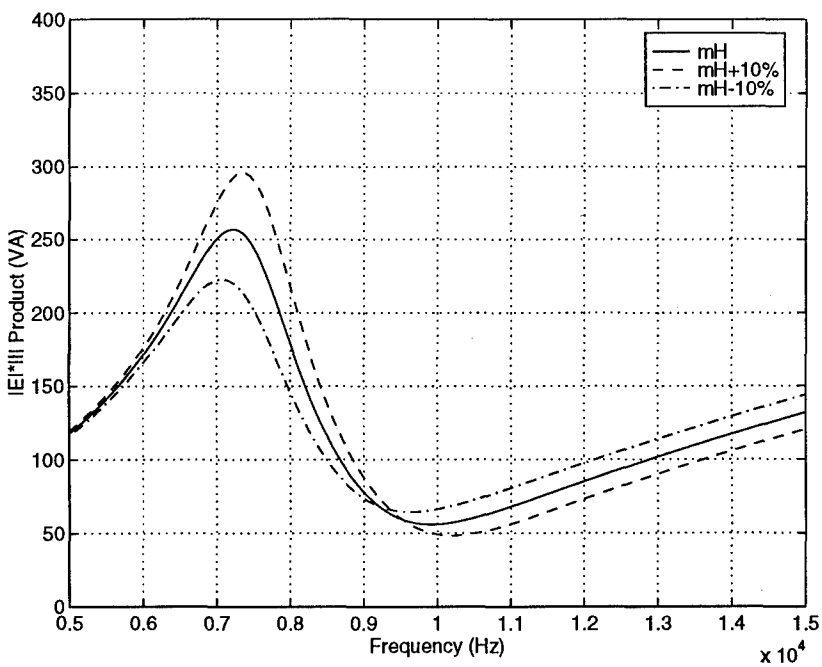

Fig. B.2-7 — STR-330A Model's in-water |E|• |I| product versus frequency for three different values of m_H; fixed ω_m, and m_T

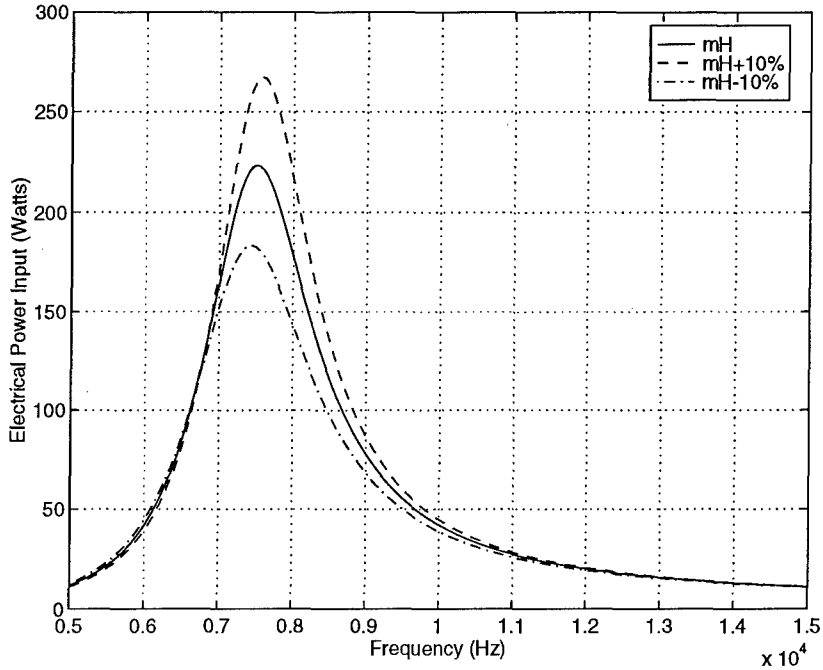

Fig. B.2-8 — STR-330A Model's in-water electrical power input versus frequency for three different values of m_H; fixed ω_m, and m_T

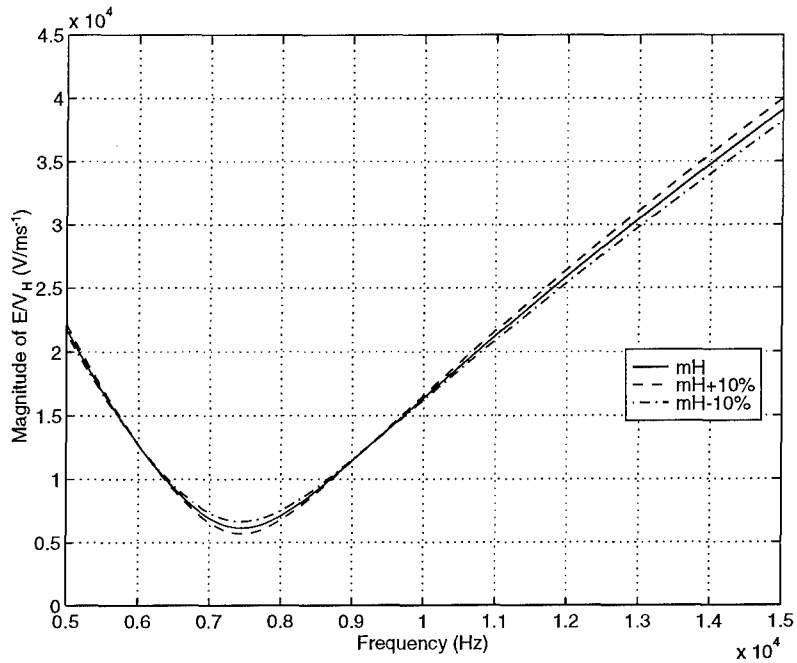

Fig. B.3-1 — STR-330A Model's in-water $|E/V_H|$ versus frequency for three different values of m_H; fixed ω_e, and m_T

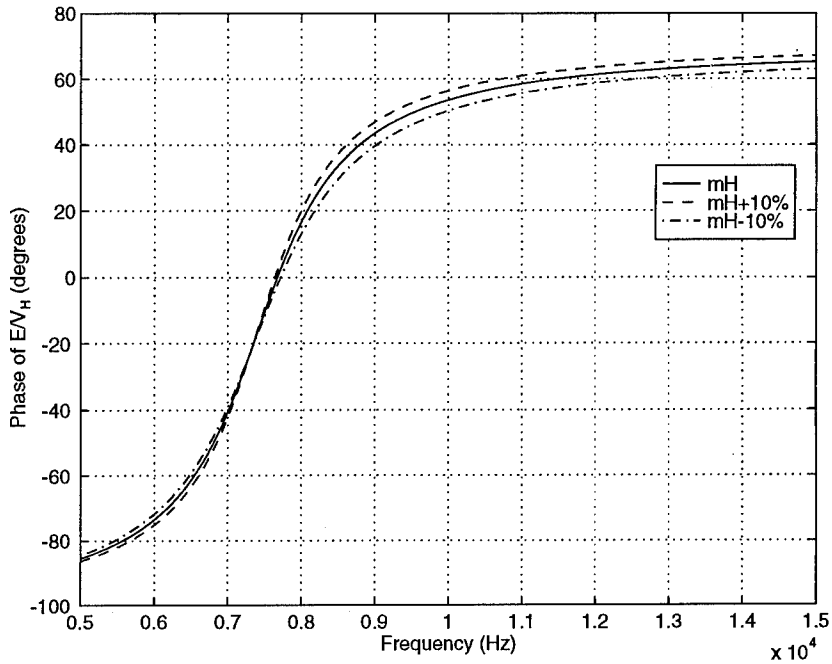

Fig. B.3-2 — STR-330A Model's in-water phase of E/V_H versus frequency for three different values of m_H; fixed ω_e, and m_T

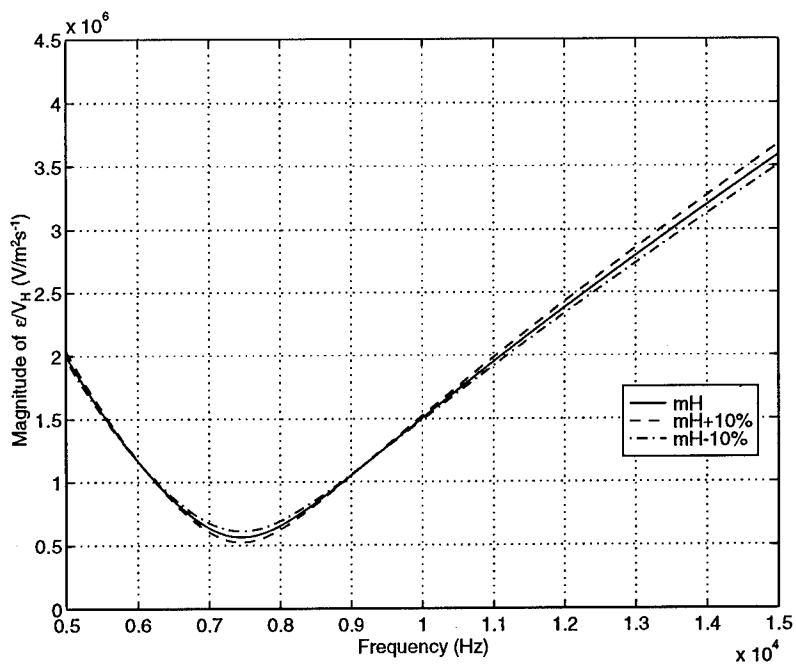

Fig. B.3-3 — STR-330A Model's in-water $|\epsilon/V_H|$ versus frequency for three different values of m_H; fixed ω_e, and m_T

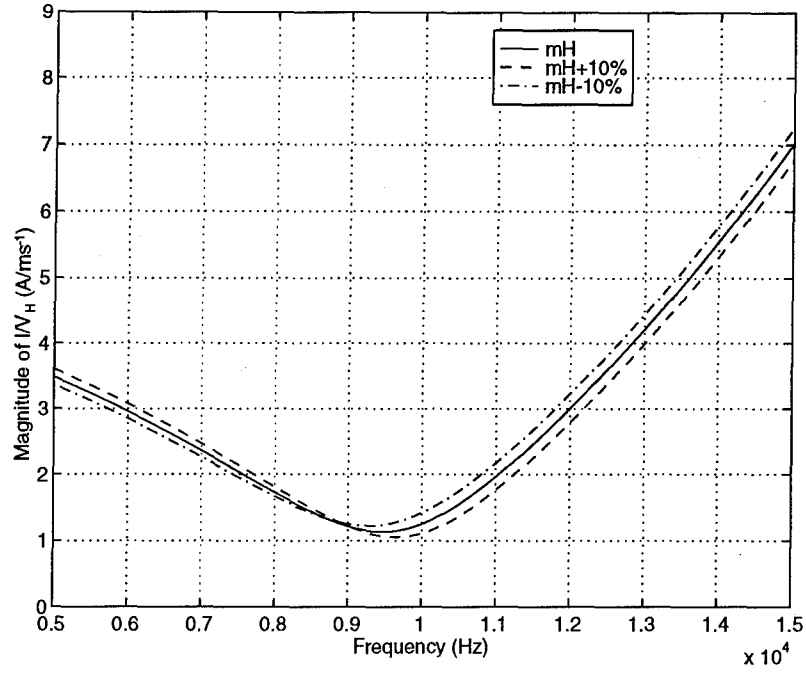

Fig. B.3-4 — STR-330A Model's in-water $|I/V_H|$ versus frequency for three different values of m_H; fixed ω_e, and m_T

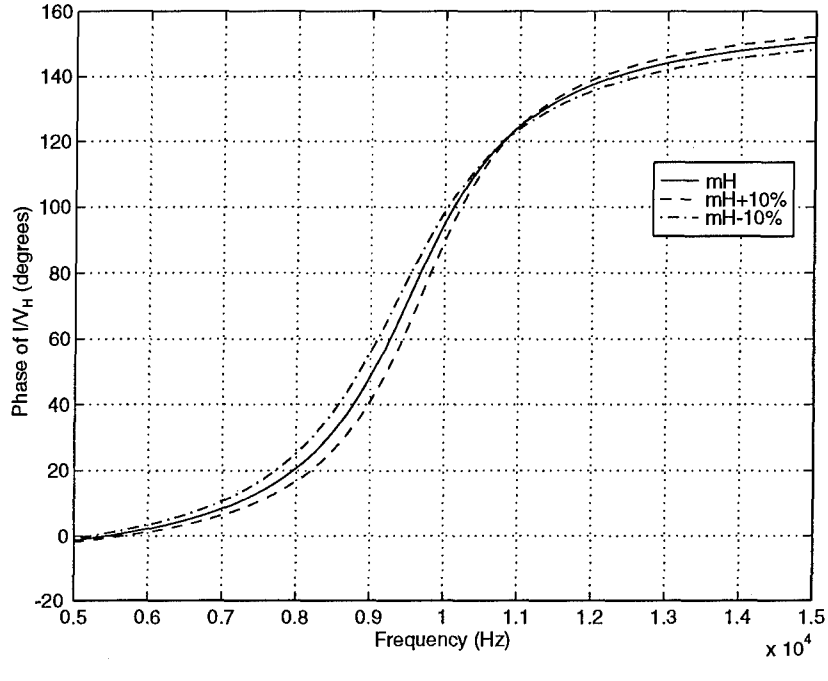

Fig. B.3-5 — STR-330A Model's in-water phase of I/V_H versus frequency for three different values of m_H; fixed ω_e, and m_T

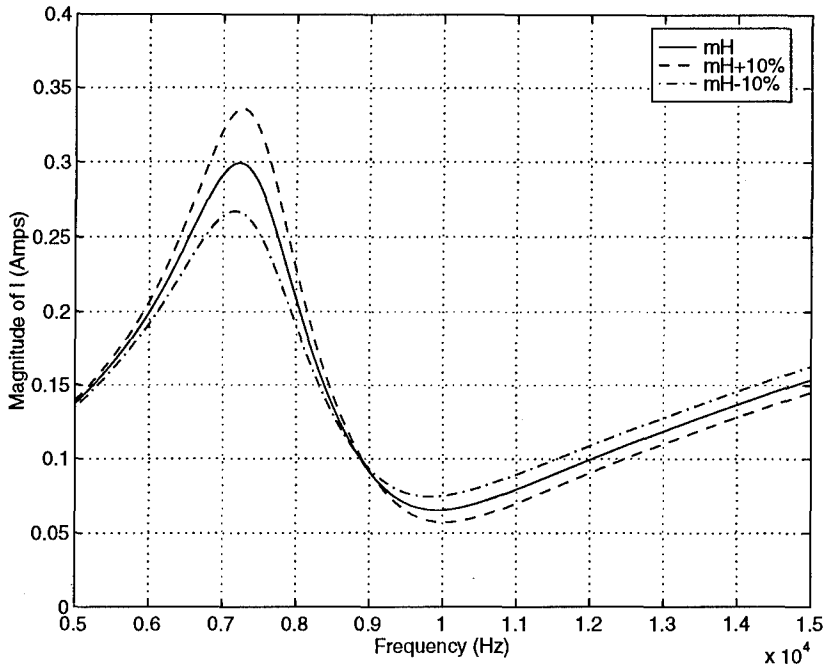

Fig. B.3-6 — STR-330A Model's in-water |I| versus frequency for three different values of m_H; fixed ω_e, and m_T

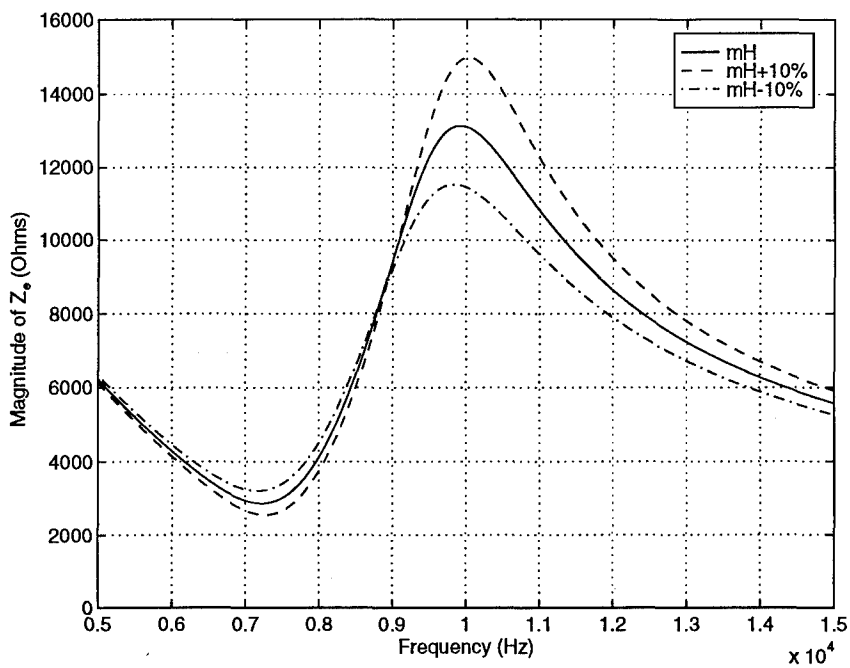

Fig. B.3-7 — STR-330A Model's in-water $|Z_e|$ versus frequency for three different values of m_H; fixed ω_e, and m_T

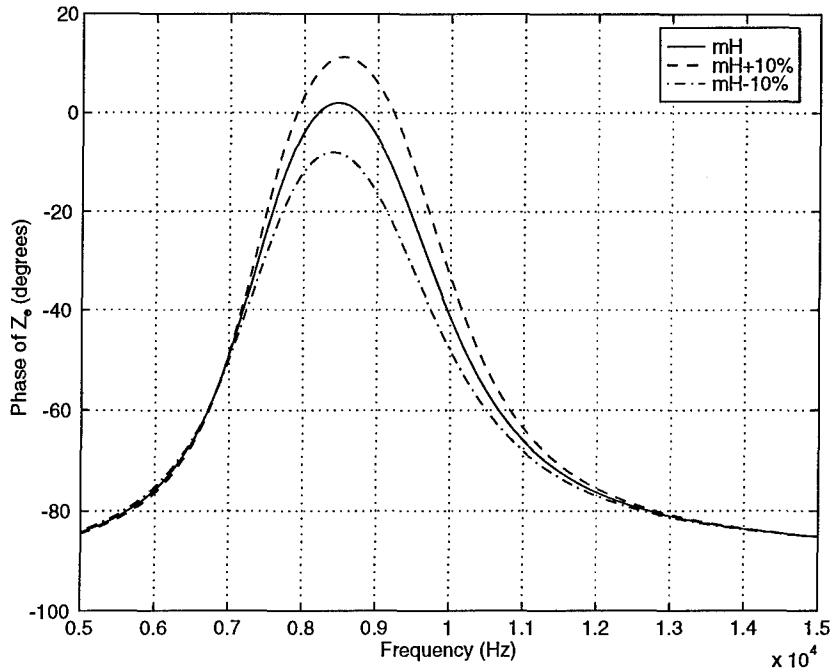

Fig. B.3-8 — STR-330A Model's in-water phase of Z_e versus frequency for three different values of m_H; fixed ω_e, and m_T

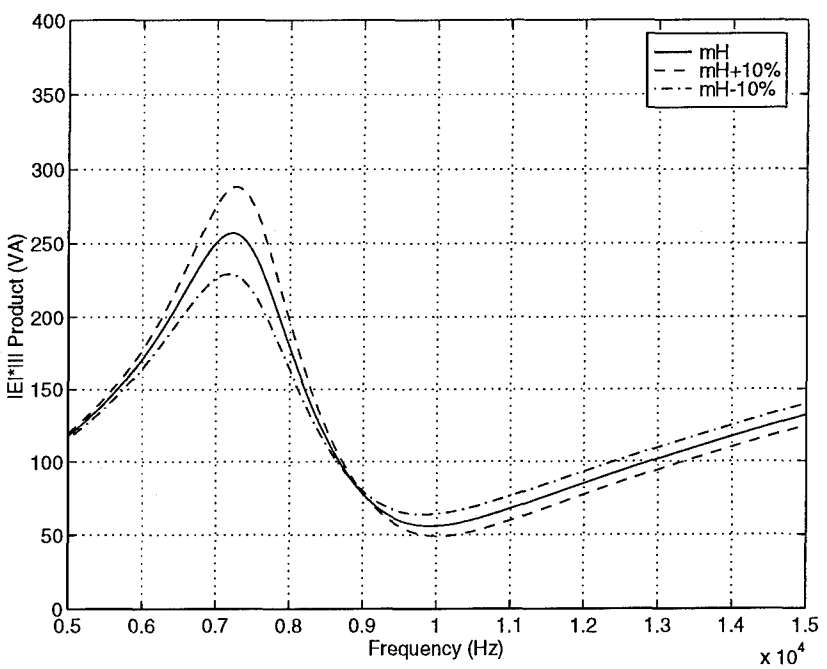

Fig. B.3-9 — STR-330A Model's in-water $|E| \bullet |I|$ product versus frequency for three different values of m_H; fixed ω_e, and m_T

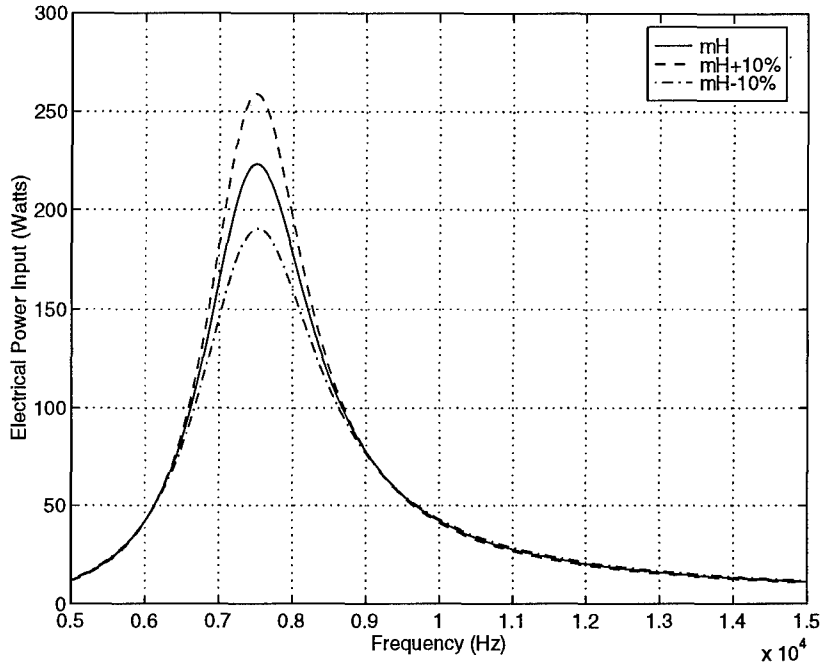

Fig. B.3-10 — STR-330A Model's in-water electrical power input versus frequency for three different values of m_H; fixed ω_e, and m_T

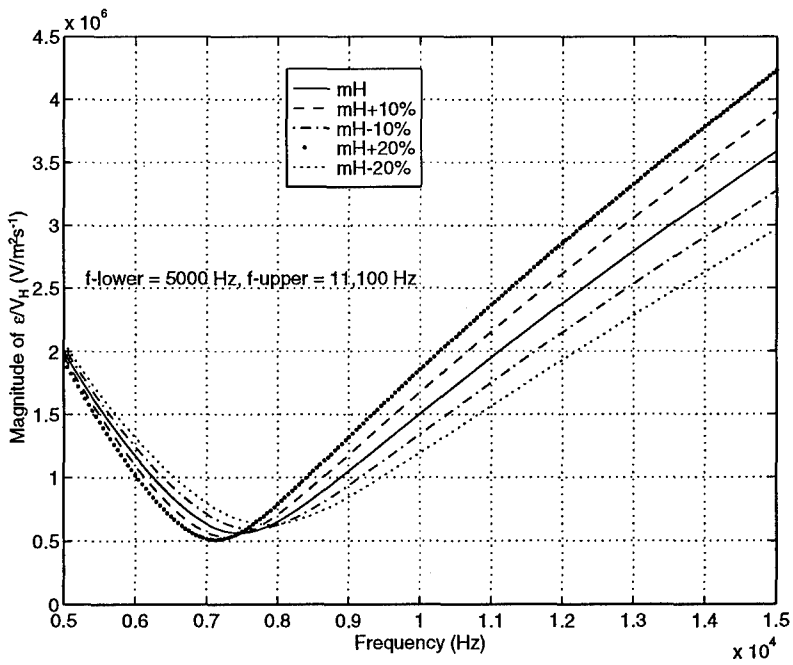

Fig. B.4-1 — STR-330A Model Results Before Application of FEPA Case 2: In-water $|\epsilon/V_H|$ versus frequency for various m_H; fixed ω_L, ω_U, and m_T

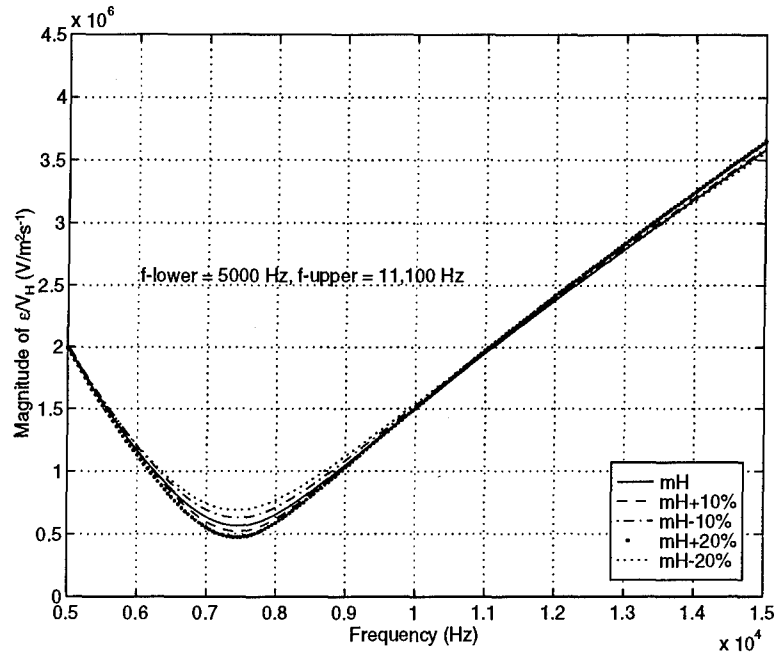

Fig. B.4-2 — STR-330A Model Results After Application of FEPA Case 2: In-water $|\epsilon/V_H|$ versus frequency for various m_H; fixed ω_L, ω_U, and m_T

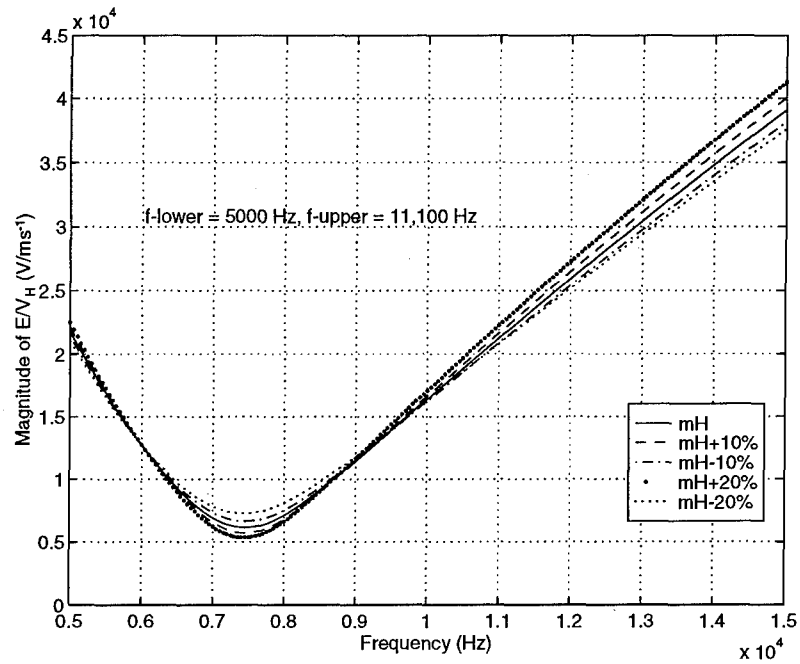

Fig. B.4-3 — STR-330A Model Results After Application of FEPA Case 2: In-water $|E/V_H|$ versus frequency for various m_H; fixed ω_L, ω_U, and m_T

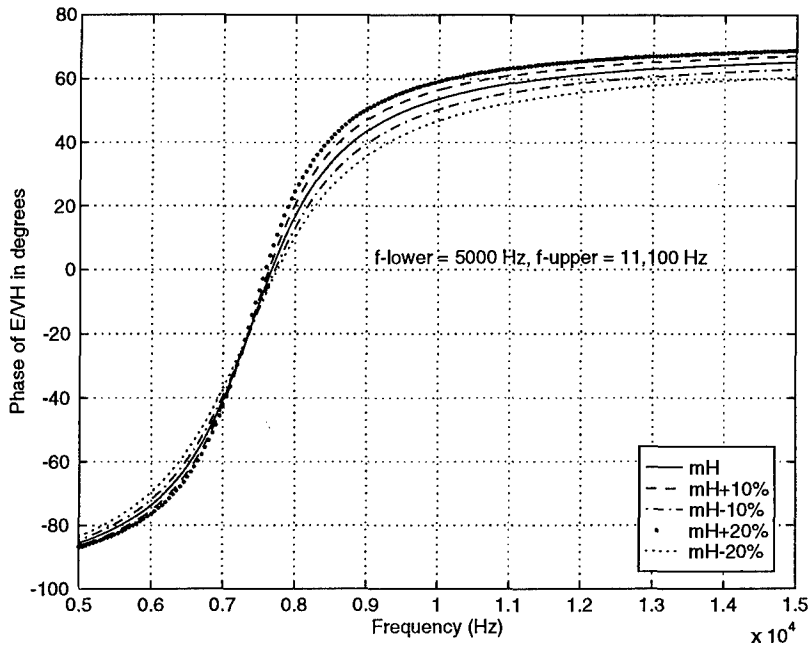

Fig. B.4-4 — STR-330A Model Results After Application of FEPA Case 2: In-water phase of E/V_H versus frequency for various m_H; fixed ω_L, ω_U, and m_T

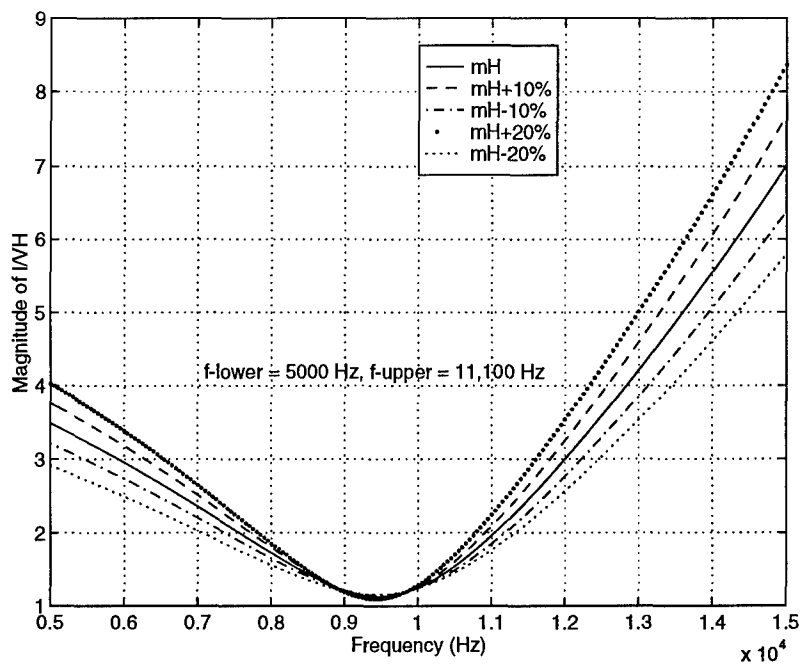

Fig. B.4-5 — STR-330A Model Results After Application of FEPA Case 2: In-water $|I/V_H|$ versus frequency for various m_H; fixed ω_L, ω_U, and m_T

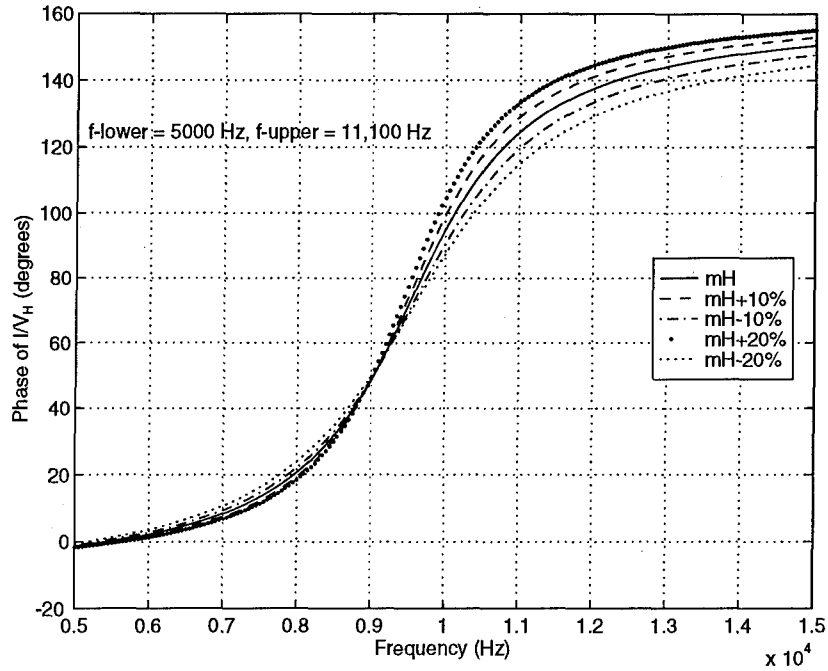

Fig. B.4-6 — STR-330A Model Results After Application of FEPA Case 2: In-water phase of I/V_H versus frequency for various m_H; fixed ω_L, ω_U, and m

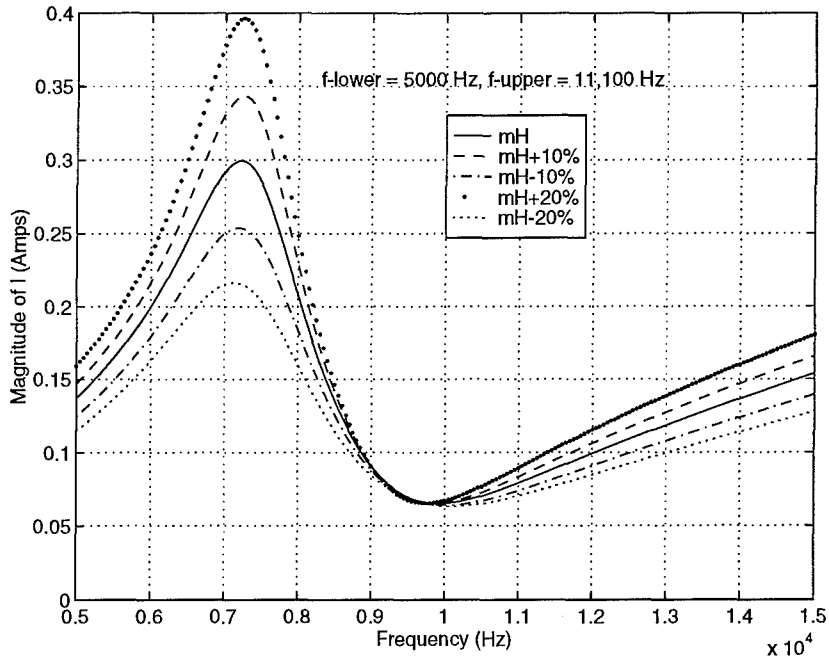

Fig. B.4-7 — STR-330A Model Results After Application of FEPA Case 2: In-water |I| versus frequency for various m_H; fixed ω_L, ω_U, and m_T

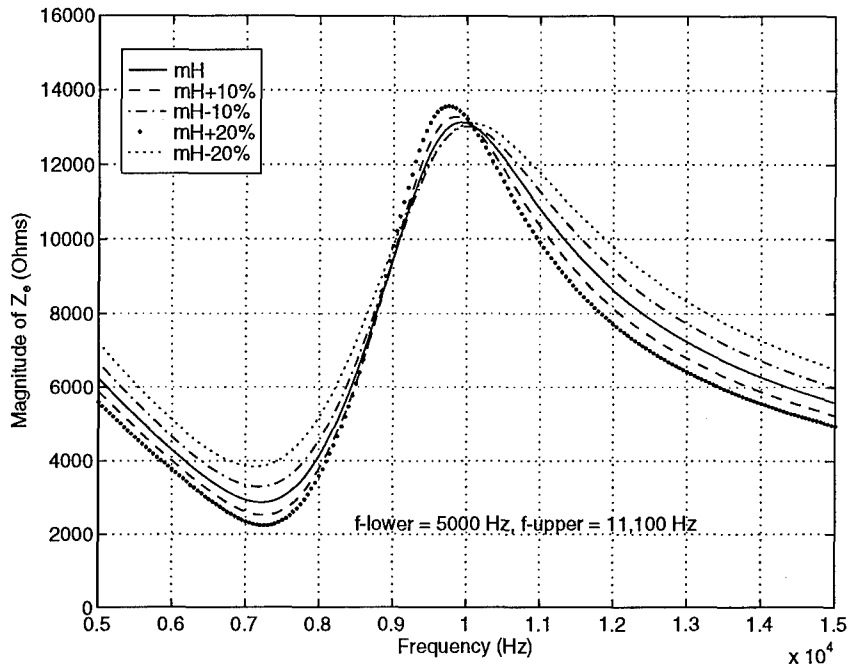

Fig. B.4-8 — STR-330A Model Results After Application of FEPA Case 2: In-water $|Z_e|$ versus frequency for various m_H; fixed ω_L, ω_U, and m_T

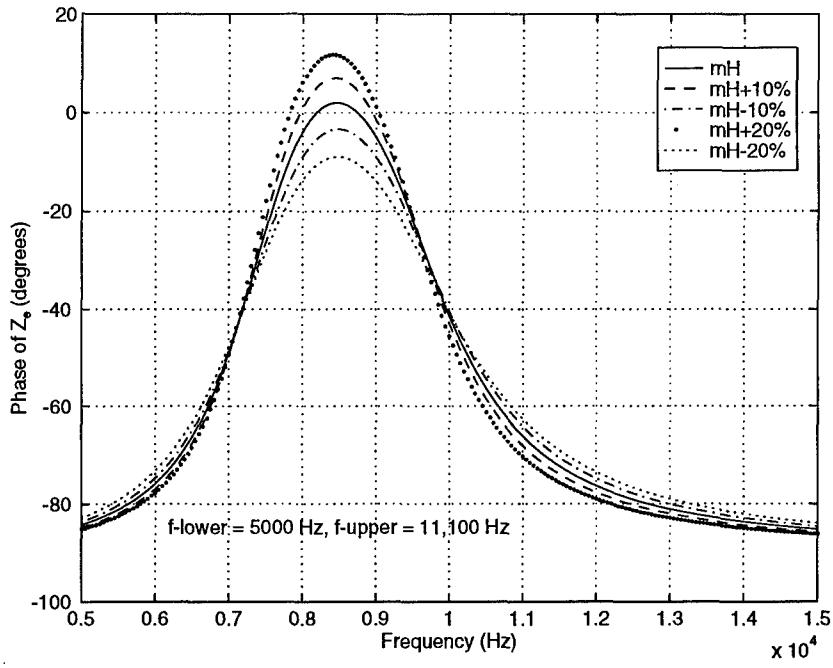

Fig. B.4-9 — STR-330A Model Results After Application of FEPA Case 2: In-water phase of Z_e versus frequency for various m_H; fixed ω_L, ω_U, and m_T

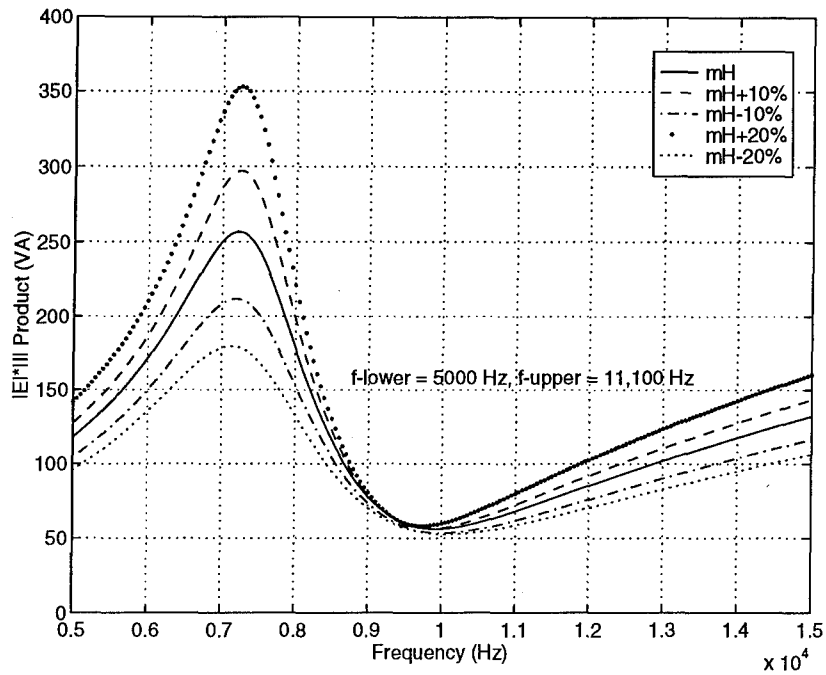

Fig. B.4-10 — STR-330A Model Results After Application of FEPA Case 2: In-water |E| • |I| product versus frequency for various m_H; fixed ω_L, ω_U, and m_T

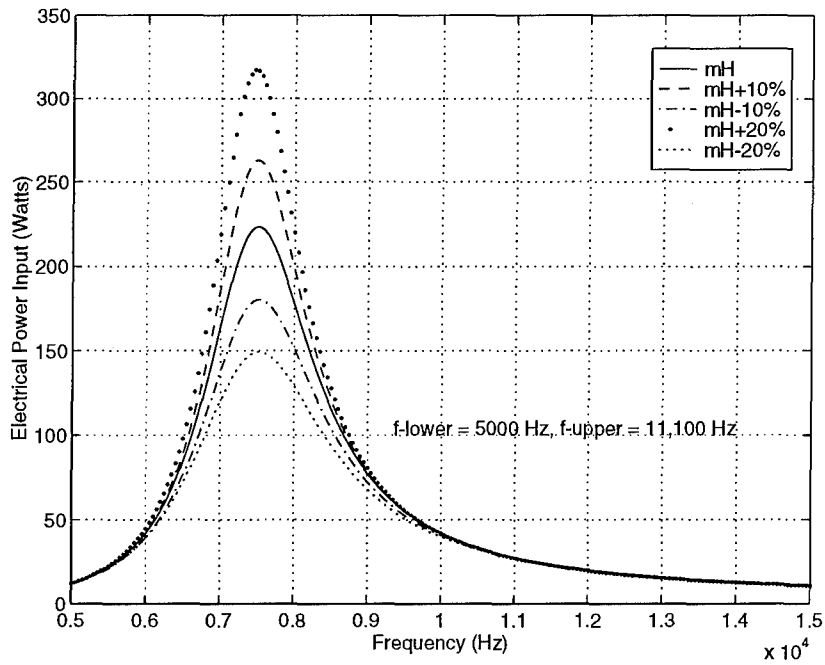

Fig. B.4-11 — STR-330A Model Results After Application of FEPA Case 2: In-water electrical power input versus frequency for various m_H; fixed ω_L, ω_U, and m_T

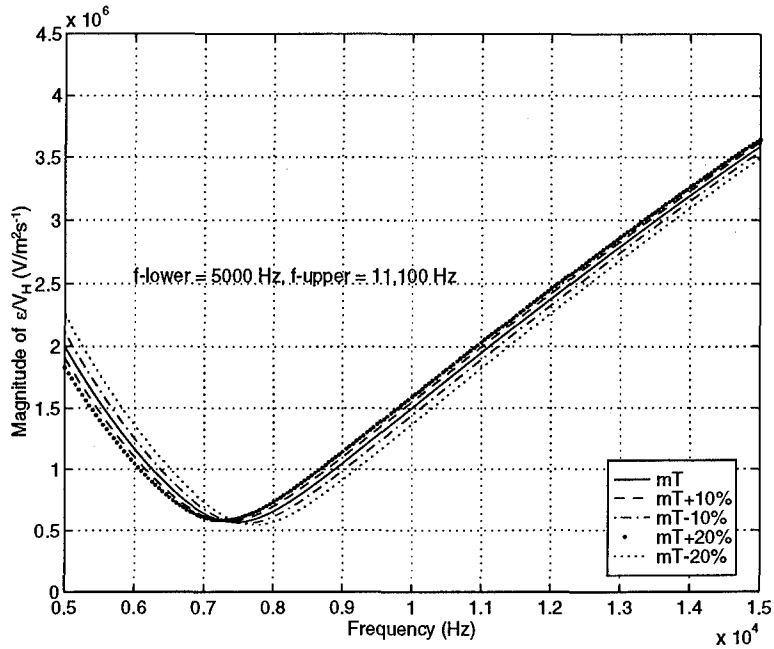

Fig. B.4-12 — STR-330A Model Results Before Application of FEPA Case 2: In-water $|\epsilon/V_H|$ versus frequency for various m_T; fixed ω_L, ω_U, and m_H

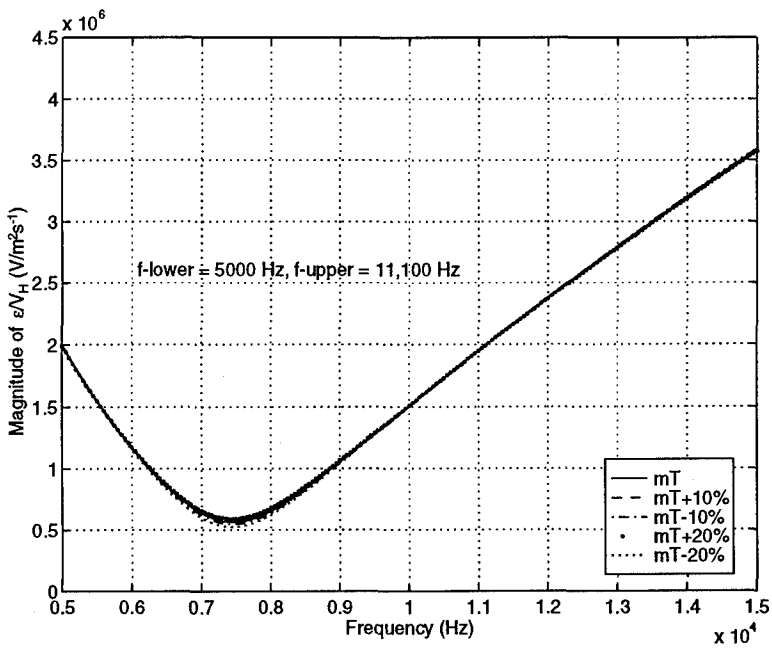

Fig. B.4-13 — STR-330A Model Results After Application of FEPA Case 2: In-water $|\epsilon/V_H|$ versus frequency for various m_T; fixed ω_L, ω_U, and m_H

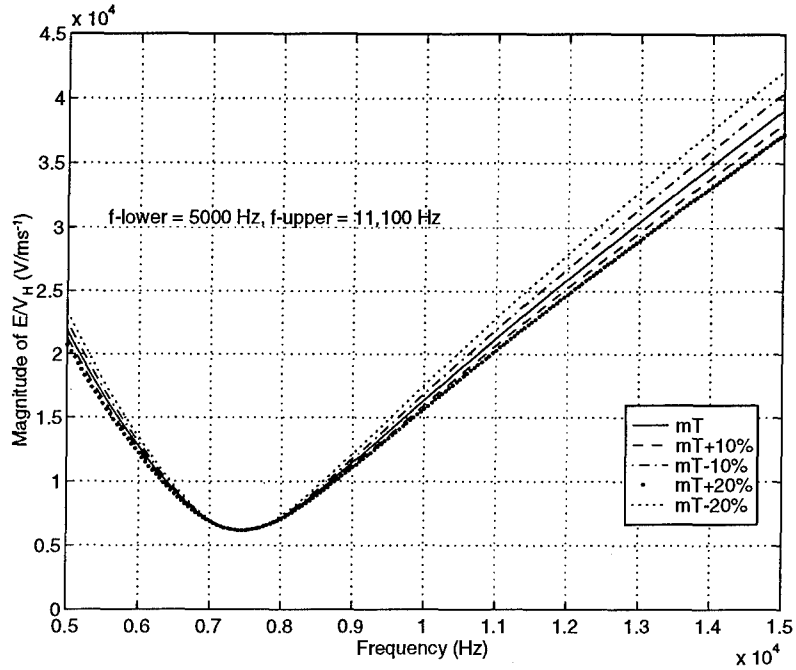

Fig. B.4-14 — STR-330A Model Results After Application of FEPA Case 2: In-water $|E/V_H|$ versus frequency for various m_T; fixed ω_L, ω_U, and m_H

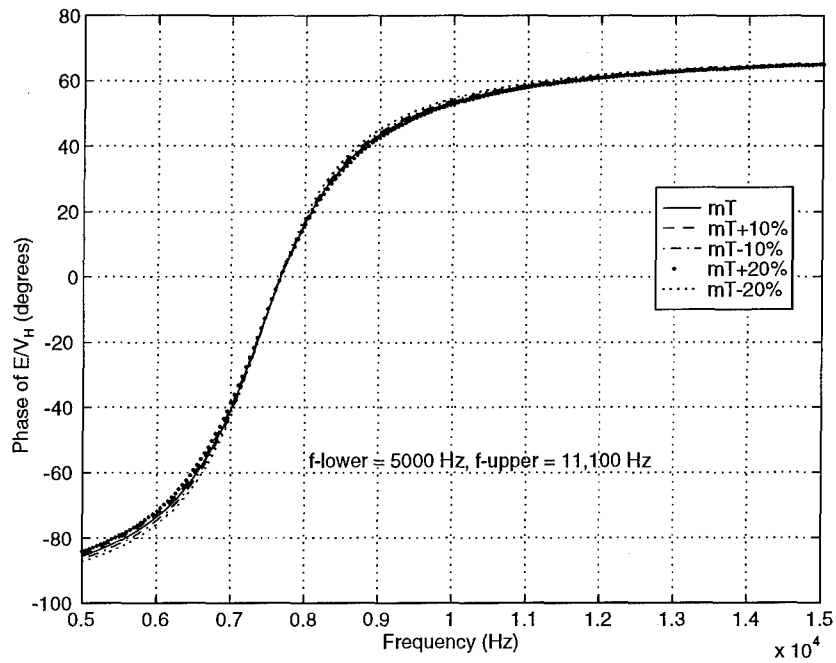

Fig. B.4-15 — STR-330A Model Results After Application of FEPA Case 2: In-water phase of E/V_H versus frequency for various m_T; fixed ω_L, ω_U, and m_H

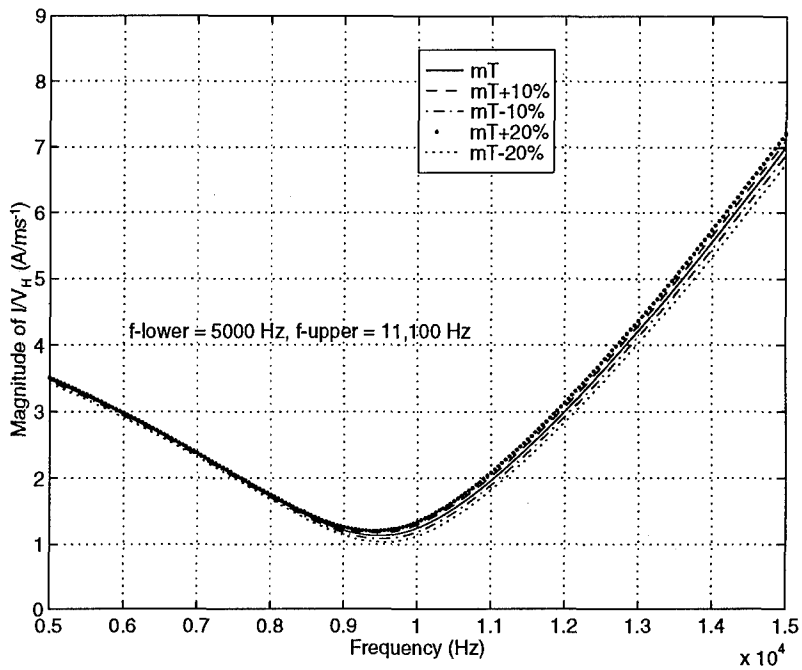

Fig. B.4-16 — STR-330A Model Results After Application of FEPA Case 2: In-water $|I/V_H|$ versus frequency for various m_T; fixed ω_L, ω_U, and m_H

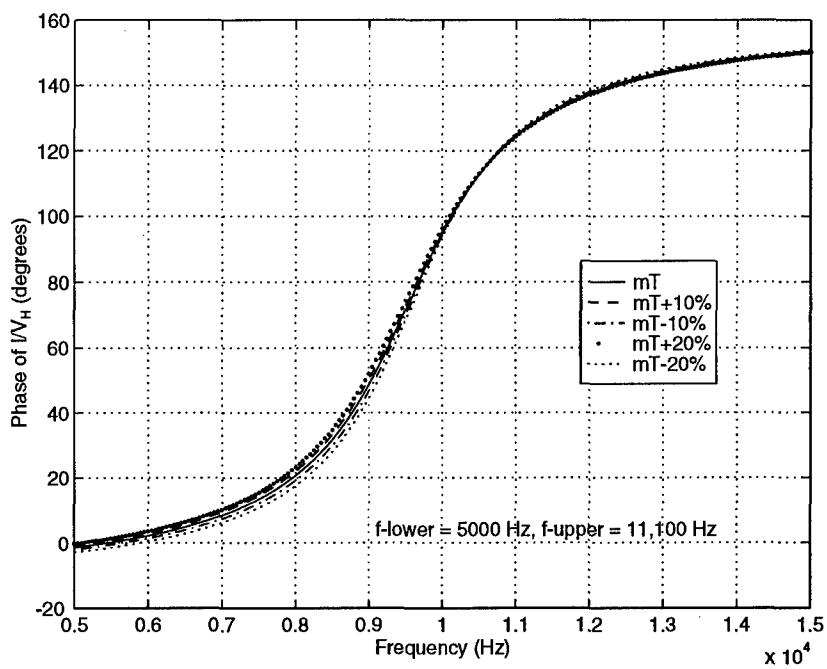

Fig. B.4-17 — STR-330A Model Results After Application of FEPA Case 2: In-water phase of I/V_H versus frequency for various m_T; fixed ω_L, ω_U, and m_H

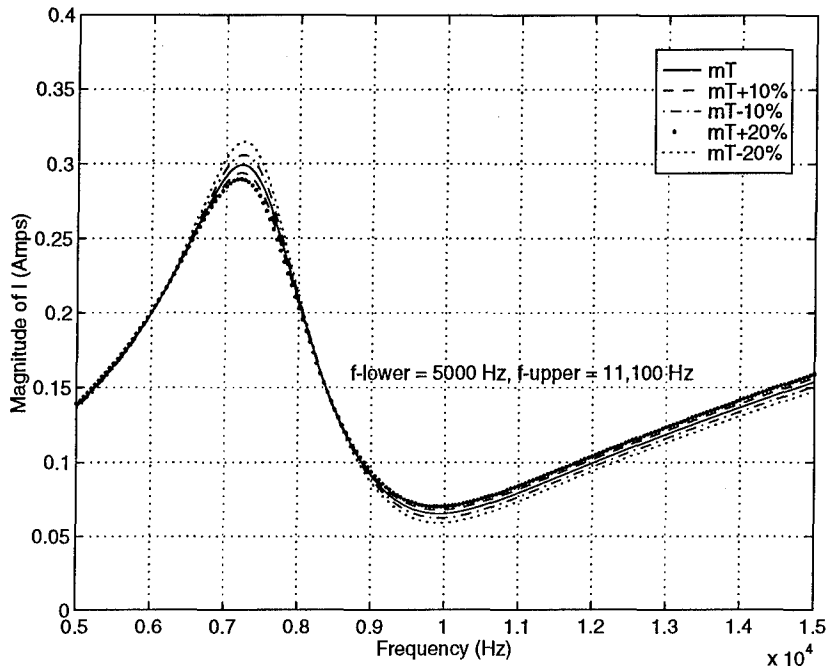

Fig. B.4-18 — STR-330A Model Results After Application of FEPA Case 2: In-water |I| versus frequency for various m_T; fixed ω_L, ω_U, and m_H

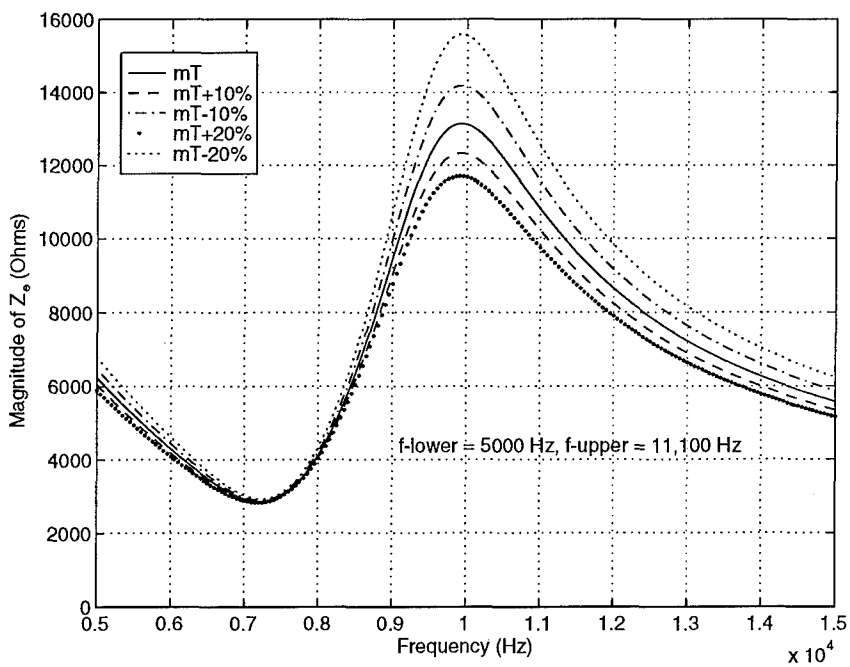

Fig. B.4-19 — STR-330A Model Results After Application of FEPA Case 2: In-water $|Z_e|$ versus frequency for various m_T; fixed ω_L, ω_U, and m_H

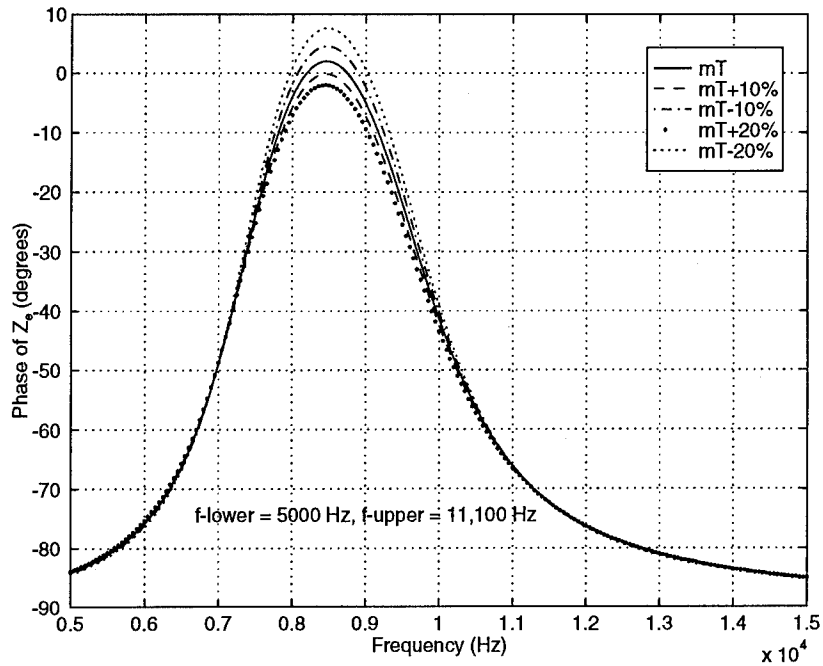

Fig. B.4-20 — STR-330A Model Results After Application of FEPA Case 2: In-water phase of Z_e versus frequency for various m_T; fixed ω_L, ω_U, and m_H

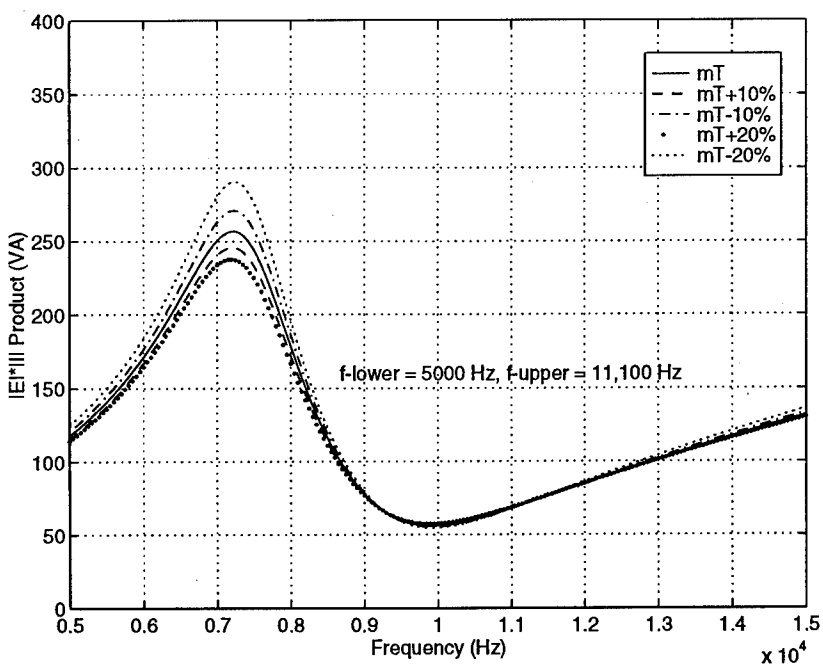

Fig. B.4-21 — STR-330A Model Results After Application of FEPA Case 2: In-water |E|•|I| product versus frequency for various m_T; fixed ω_L, ω_U, and m_H

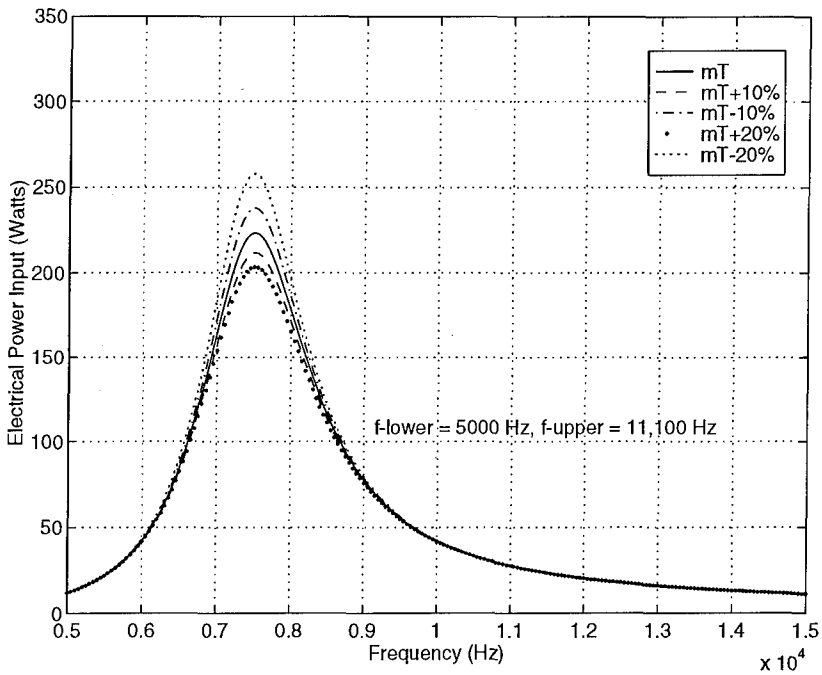

Fig. B.4-22 — STR-330A Model Results After Application of FEPA Case 2: In-water electrical power input versus frequency for various m_T; fixed ω_L, ω_U, and m_H